Assessing methane emission from dairy cows

Modeling and experimental approaches on rumen microbial metabolism

Henk J. van Lingen

Thesis committee

Promotor
Prof. Dr W.H. Hendriks
Professor of Animal Nutrition
Wageningen University & Research

Co-promotors
Dr J. Dijkstra
Associate professor, Animal Nutrition Group
Wageningen University & Research

Dr A. Bannink
Senior researcher, Wageningen Livestock Research
Wageningen University & Research

Dr C.M. Plugge
Associate professor, Laboratory of Microbiology
Wageningen University & Research

Other members
Prof. Dr G. Zeeman, Wageningen University & Research
Dr J.A.D.R.N. Appuhamy, Iowa State University, United States of America
Dr R. Kleerebezem, Technische Universiteit Delft, the Netherlands
Dr J.T. Schonewille, Universiteit Utrecht, the Netherlands

This research was conducted under the auspices of the Graduate School of Wageningen Institute of Animal Science (WIAS).

Assessing methane emission from dairy cows

Modeling and experimental approaches on rumen microbial metabolism

Henk J. van Lingen

Thesis

submitted in fulfillment of the requirements for the degree of doctor
at Wageningen University
by the authority of the Rector Magnificus
Prof. Dr A.P.J. Mol,
in the presence of the
Thesis Committee appointed by the Academic Board
to be defended in public
on Friday 28 April 2017
at 11.00 a.m. in the Aula

Henk J. van Lingen
Assessing methane emission from dairy cows.
Modeling and experimental approaches on rumen microbial metabolism, 207 pages.

PhD thesis, Wageningen University, Wageningen, the Netherlands (2017)
With references, with summary in Dutch and English

ISBN 978-94-6343-159-0
DOI 10.18174/411612

Contents

Chapter 1

General Introduction

1.1 Enteric methane from cattle emitted into the environment

Methane is a greenhouse gas (GHG) with a global warming potential of 28 CO_2 equivalents (Myhre et al., 2013). After long eras of constant environmental CH_4 concentration of approximately 0.650 ppm, the CH_4 concentration has increased to 1.775 ppm over the last few centuries. Currently, CH_4 is the second most abundant GHG in the environment after CO_2 which has a concentration of about 380 ppm. CH_4 is emitted from anthropogenic sources such as agriculture, natural gas distribution and landfills, and from natural sources of which wetlands contribute most (Forster et al., 2007).

The livestock sector was estimated to emit 7.1 gigatonnes of CO_2 equivalents, which is approximately 14.5% of total global anthropogenic GHG emissions (Gerber et al., 2013). Enteric fermentation is the main source of GHG emissions from dairy cattle, with CH_4 amounting to 1.1 gigatonnes per year, representing 46% of the global GHG emissions in dairy supply chains (Hristov et al., 2013b). From 1990 to 2014, an 11% decrease in CH_4 emission from enteric fermentation in cattle occurred in The Netherlands (Coenen et al., 2016). This decrease was largely the result of decreasing numbers of livestock, while product output did not decrease, indicating an increase in dairy production efficiency. The relative contribution of cattle to the Dutch national CH_4 emission from enteric fermentation remained constant at 89%. Based on expected farming and consumer lifestyle practices, global CH_4 emissions from enteric fermentation, compared with 1995, are predicted to increase by 70% in 2055 (Popp et al., 2010). This increase can, however, be partly offset by altered feeding strategies, increasing animal production through feeding and breeding, and other farm management practices (Hristov et al., 2013a; Montes et al., 2013; Hristov et al., 2013c; Knapp et al., 2014).

Ruminant production significantly contributes to a healthy diet for people, for example proteins and essential micronutrients in milk and meat (Biesalski, 2005; Huth et al., 2006; Elwood et al., 2010). In view of the ability of ruminants to effectively turn human inedible biomass into human edible food and to produce food from non-arable land (Gerber et al., 2015), there is an urgent need to develop strategies to decrease GHG emissions, in particular enteric CH_4. Evaluation of these strategies requires meticulous quantification and increased understanding of the formation of the GHG emitted. The research reported in this thesis will contribute to more knowledge about the relationship between feed degradation and enteric CH_4 formation from the microbial metabolism in the rumen of dairy cows. Furthermore, the modeling efforts reported in this thesis enable quantification of CH_4 emissions from (dairy)

cattle for policy makers, the dairy industry, and farmers to meet national and state regulatory standards in decreasing CH_4 emission.

1.2 Physiology of ruminal feed degradation and CH_4 production

1.2.1 Volatile fatty acid fermentation pathways

Complex carbohydrate polymers in the rumen are hydrolyzed to soluble sugar molecules such as hexose by microbial enzymes (Baldwin and Allison, 1983). Bacterial genera such as *Fibrobacter*, *Bacteroides* and *Ruminococcus* species degrade cellulose and are abundant in forage-fed animals; genera such as *Prevotella* and *Succinivibrio* are more abundant in concentrate-fed animals and may degrade amylose (Henderson et al., 2015). After polymer hydrolysis, hexoses are primarily converted to pyruvate via the Embden-Meyerhof-Parnas pathway (e.g., Melville et al., 1988; McSweeney et al., 1994). In this pathway, glucose is phosphorylated and then cleaved into two triose phosphate moieties that in turn are converted to 2 pyruvate, which yields 2 equivalents of ATP and reduces 2 NAD^+ to 2 NADH.

Besides the Embden-Meyerhof-Parnas pathway of hexose utilization, pathways of pentose utilization have been described as well (Baldwin and Allison, 1983). Pentoses are primarily derived from hemicelluloses and their fermentation proceeds by the transketolase and transaldolase reaction in which 3 pentoses are converted to 2 hexose phosphate and one triose phosphate (Russell and Wallace, 1997). These two chemical species are then further metabolized as in the Emden-Meyerhof-Parnas pathway yielding pyruvate (overall conversion shown in Fig. 1.1). Per amount of carbon atoms, the metabolism of pentose and hexose then yields the same amount of both ATP and NADH. Alternatively, pentose is metabolized into pyruvate plus acetate yielding two ATP (Baldwin and Allison, 1983).

The carbohydrate metabolism in the rumen diverges at pyruvate (Fig. 1.1). Acetate producers such as *Fibrobacter succinogenes* (Miller, 1978) and *Ruminococcus albus* (Glass et al., 1977) convert pyruvate to acetyl-CoA by a pyruvate-ferredoxin oxidoreductase, after which acetyl-CoA is converted into acetate and ATP (Michel and Macy, 1990). Besides pyruvate being metabolized to acetate, bacteria such as *Streptococcus bovis* may convert pyruvate into either lactate or formate plus acetyl-CoA (Asanuma et al., 1998), where lactate production appeares to outcompete formate production at increasing outflow rates from the rumen (Asanuma et al., 1999). Furthermore, Wolin (1979) suggested that the conversion of pyruvate into acetyl-CoA plus formate is not typical in the rumen.

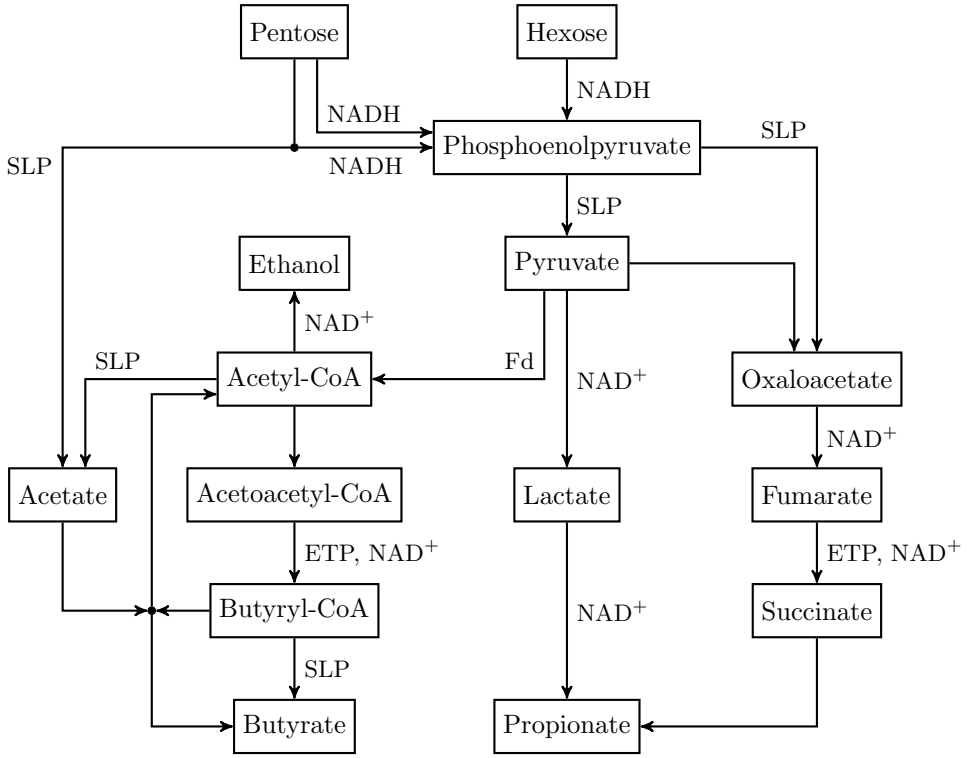

Figure 1.1: Major metabolites of hexose and pentose catabolism in rumen bacteria. Metabolic steps may be associated with energy conservation via substrate-level phosphorylation (SLP) or electron transport phosphorylation (ETP), the reduction of NAD^+ to NADH (NADH), the oxidation of NADH to NAD^+ (NAD^+), or the reduction of ferredoxin (Fd).

To maintain the metabolic conversion of hexose to pyruvate, the associated NADH that is formed needs to be oxidized back to NAD^+. This oxidation reaction may be achieved with the release of H_2. If this H_2 accumulates in the rumen environment, the oxidation of NADH may be thermodynamically unfeasible. The microbial metabolism may then oxidize NADH by producing more reduced fermentation products instead of producing H_2 (Baldwin and Allison, 1983). This is, for example, achieved by metabolizing acetyl-CoA to either butyrate or ethanol instead of acetate (Fig. 1.1). *Butyruvibrio fibrisolvens* is a predominant butyrate-producing bacterium in the rumen, which synthesizes butyrate from acetyl-CoA via acetoacetyl-CoA, β-hydroxybutyryl-CoA, crotonyl-CoA and butyryl-CoA (Miller and Jenesel, 1979; Buckel and Thauer, 2013). This butyrate yielding metabolic pathway is known as the kinase route, as butyryl-CoA is metabolized to butyrate via butyryl phosphate

with the conversion of butyryl phosphate to butyrate being catalyzed by butyrate kinase enzyme. Butyryl-CoA may alternatively be converted into butyrate by the butyryl-CoA:acetate CoA-transferase enzyme, present in for example *Clostridium* species (Pryde et al., 2002; Louis and Flint, 2009). For this conversion, external acetate is required and acetyl-CoA is formed. Species such as *R. albus* are able to reduce acetyl-CoA to ethanol, but significant concentrations were only observed in monoculture (Pavlostathis et al., 1990) and substantial ethanol yield may, therefore, not be expected in the rumen.

Besides the reduction of acetyl-CoA, metabolizing pyruvate to propionate also results in the oxidation of NADH to NAD^+ (Fig. 1.1). One pathway via which this can be achieved proceeds via succinate, another via lactate and acrylate. An estimated 70 to 100% of the propionate is produced via the succinate pathway, with the contribution of the lactate pathway generally increasing with higher carbohydrate availability in the diet (Baldwin et al., 1963). Among the known species of ruminal bacteria, *Megasphaera elsdenii* and *Prevotella* species produce propionate from lactate via the acrylate pathway (Marounek et al., 1989; Stewart et al., 1997). Bacteria such as *S. ruminantium* and *Succinimonas amylolytica* are known to use the succinate pathway (Hungate, 1966; Wolin et al., 1997). *P. ruminicola* and *Ruminobacter amylophilus* only produce succinate as a fermentation product, after which species such as *S. ruminantium* may rapidly decarboxylate succinate to propionate next to the direct synthesis of propionate from carbohydrate monomers. Production of propionate via the succinate pathway, however, may not always proceed via pyruvate. Glucose is also catabolized to propionate via phosphoenolpyruvate, oxaloacetate, malate, fumarate and succinate, as found for *S. ruminantium* (Melville et al., 1988) and relatives of *R. flavefaciens* (Kettle et al., 2015).

Volatile fatty acids (VFA) with more than three carbon atoms such as valerate and caproate are formed by the condensation of acetyl-CoA and/or propionyl-CoA. This condensation represents another means of reducing equivalent disposal (Russell and Wallace, 1997). Bacteria reported to substantially contribute to valerate and caproate production in the rumen are *M. elsdenii* (Rogosa, 1971), *Eubacterium pyruvativorans* (Wallace et al., 2004) and *Clostridium kluyveri* (Angenent et al., 2016) species. Branched-chain VFA are mainly derived from branched-chain amino acids, with the observed ruminal concentrations of isobutyrate, isovalerate and valerate being relatively similar. Differences in the molar proportions of these branched-chain VFA among various nitrogenous compounds represent the fermentation of different types of amino acids (Griswold et al., 1996).

Although the metabolism of rumen bacteria has been relatively well identified, the metabolism of rumen protozoa has in general received less attention (Newbold

et al., 2015). In addition, it is uncertain to what proportion bacteria and protozoa quantitatively contribute to feed degradation in the rumen. Like the bacterial community, protozoa also utilize both soluble and particulate carbohydrates yielding VFA, and may functionally overlap with the rumen bacteria.

1.2.2 Methanogenesis

Although various bacteria have the ability to oxidize NADH coupled to the production of more reduced fermentation products, bacteria also depend on NADH oxidation that is stimulated by the H_2 removal by other anaerobes. In the rumen, archaea facilitate this by utilizing small carbon-containing substrates for methanogenesis. The predominant methanogenic reaction in the rumen is (Thauer et al., 2008):

$$HCO_3^- + H^+ + 4\,H_2 \longrightarrow CH_4 + 3\,H_2O, \tag{1.1}$$

which shows the H_2 supply to be essential for methanogenesis. This conversion proceeds via a cascade of steps, of which the conversion of N^5-methyl-tetrahydromethanopterin into methyl coenzyme-M is associated with energy conservation. In this step two cations of either $2\,Na^+$ (Thauer et al., 2008), $2\,H^+$ or one of both (Schlegel et al., 2012) are translocated by a membrane bound ATPase generating ATP.

The presence or absence of cytochromes (i.e., membrane-bound proteins involved in electron transport) in archaea is an appropriate trait to classify methanogens. Methanogens with cytochromes that can grow on H_2 and CO_2 generally have a higher ATP and growth yield than methanogens without cytochromes (Thauer et al., 2008). Furthermore, methanogens with a higher ATP gain require a higher H_2 partial pressure (p_{H_2}) to keep the methanogenesis thermodynamically favorable. Threshold p_{H_2} for methanogens without cytochromes is equal to 10^{-5} to 10^{-4} bar, whereas this is at least tenfold higher for methanogens with cytochromes. These different thresholds also explain why methanogens with cytochromes hardly exist in the rumen environment where the p_{H_2} varies from approximately 10^{-4} to 10^{-2} bar.

Various methanogens exist in the rumen, which may depend on the uptake of their own specific substrate. Many of the previously mentioned hydrogenotrophic methanogenes without cytochromes are also able to grow on formate (Thauer et al., 2008). Henderson et al. (2015) found that across various geographical locations and ruminant species the hydrogenotrophic *Methanobrevibacter gottschalkii* and *Methanobrevibacter ruminantium* species accounted for 74% of all archaea in the rumen. They assigned 78% of the methanogens to be hydrogenotrophic and 22% to be methylotrophic using methanol and methylamine as a substrate. Acetoclastic

methanogens that produce CH_4 with acetate as a substrate contributed less than 0.015%.

Methanogens are found to be present in the fluid fraction and the solid fraction and attached to the rumen epithelium (Shin et al., 2004). Adherence of rumen microbes to particles allows a lower growth rate to maintain themselves in the rumen since the fractional passage rate for particles is lower than that for liquids (McAllister et al., 1994). Adherence to particles may explain why *Methanobrevibacter ruminantium* and *Methanobrevibacter gottschalkii* co-occurred with the Fibrobacteraceae and Ruminococcaceae, respectively (Kittelmann et al., 2013). Both bacterium families are cellulose degraders and waste CO_2/formate and H_2, respectively, which are used as a substrate by the methanogens. Methanogens may also live endosymbiotically in protozoal cells (Fenchel and Finlay, 2010), as protozoa are important sources of H_2, in particular for cows fed starch-rich diets (Hegarty, 1999). However, abundance of protozoa and methanogens may not be strongly correlated (Henderson et al., 2015).

1.3 Kinetics and thermodynamics of (bio)chemical conversions

Chemical conversions are described by kinetics and thermodynamics. Kinetics is the area of chemistry that deals with reaction rates and also considers the mechanism of a reaction (i.e., the pathways from a reactant to a product) and the concentration of the reactants involved. Biochemical conversions may be enzyme catalyzed and their reaction rate therefore depends on both the concentration of a substrate and enzyme activity. Biochemical conversion rates (v) are commonly described by the Michaelis-Menten relationship:

$$v = \frac{v_{\max}}{1 + K_S/[S]}, \tag{1.2}$$

with maximum rate of reaction $v_{\max}$, the substrate concentration [S] and the half-saturation or affinity constant of an enzyme for a substrate K_S (e.g., Atkins and de Paula, 2006).

In contrast to kinetics, thermodynamics considers the initial and final states and does not require knowledge of the pathway between the reactants and products (Zumdahl, 2005). It basically deals with the question whether a reaction occurs or not and in which direction. Entropy is a common characteristic to determine the direction in which processes occur based on how energy is distributed among the energy levels in the particles in a given system. The larger the number of possibilities by which a

state (i.e., the distribution of energy over its levels) can be achieved, the greater the probability of the occurrence of the state.

Spontaneity of chemical reactions can be described by the concept of probability. A greatly simplified representation of how the ratio between reactants and products can be related to probability is illustrated in Fig. 1.2. All bullets in the left-hand bulbs represent reactants and all bullets in the right-hand bulbs represent products. The less equal the bullets are distributed over the two bulbs, the lower the number of possibilities by which a state can be achieved, the lower the probability of a state. In Fig. 1.2a bullets are mainly localized in the left-hand bulb, reflecting a state in which reactants dominate over products. In Fig. 1.2b, bullets are equally distributed over the two bulbs, reflecting a state in which reactants and products are equally abundant. The number of possibilities by which the state can be achieved is larger for Fig. 1.2a than for Fig. 1.2b. Nature spontaneously proceeds towards the state that has the highest probability, and therefore, a chemical reaction in non-equilibrium (resembled in Fig. 1.2a) will proceed until equilibrium is achieved and the entropy is at its maximum (resembled in Fig. 1.2b).

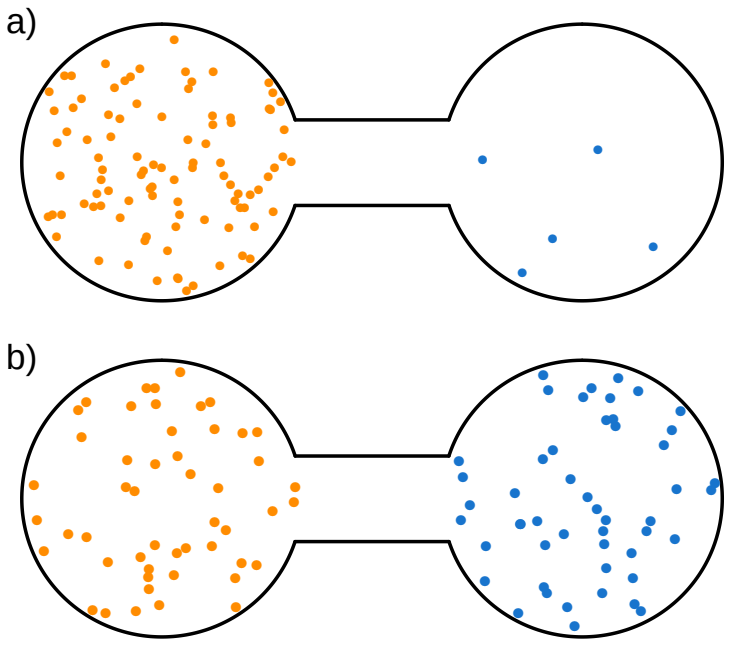

Figure 1.2: State of thermodynamic a) non-equilibrium and b) equilibrium. Left and right compartments of both states may represent reactants and products of a (bio)chemical conversion, respectively.

Besides an increase in entropy, spontaneity is also affected by temperature since every chemical reaction is associated with a temperature controlled heat flow (Zumdahl, 2005). To predict spontaneity of a chemical reaction based on entropy and temperature effect, the thermodynamic quantity of Gibbs energy has been developed (e.g., Atkins and de Paula, 2006). A chemical conversion is spontaneous in the direction in which the Gibbs energy decreases. It is convenient to define standard Gibbs energies of formation of a compound in a reference state. The Gibbs energy change of a reaction (ΔG) is given as:

$$\Delta G = \Delta G^o + RT \ \ln Q, \tag{1.3}$$

with the Gibbs energy change at standard temperature, pressure and concentrations ΔG^o, the universal gas constant R, the temperature T and the quotient of products to reactants Q. The appearance of the latter two in Eq. 1.3 clearly represents that spontaneity of chemical reactions is predicted by temperature and the probability of a state calculated as the ratio between reactants and products.

1.4 Milk fatty acid composition as a metabolic reprint of rumen fermentation and CH_4 production

Various methods have been used to estimate CH_4 production from ruminants. Methane production can be measured in respiration chambers, which are airtight compartments from which the gases flowing in and out are monitored. The respiration chamber technique is accurate but expensive and, therefore, unsuitable for large scale application, and does not allow measurements of grazing animals. Other methods, including the sulfur hexafluoride (SF_6) marker and CH_4/CO_2 ratio techniques, enable CH_4 emissions to be determined in a larger number of animals, but with higher between and within animal variation (Hammond et al., 2016).

The VFA formed in the rumen are potentially metabolized to milk fatty acids (FA) in the mammary gland. Milk FA composition is, therefore, a potential biomarker of rumen fermentation and CH_4 production (e.g., Mohammed et al., 2011). Cellulose and related feed components are converted to acetate, propionate and butyrate, which enter the blood circulation, with butyrate largely changed to β-hydroxybutyrate in the rumen wall (Jensen, 2002). Acetate and β-hydroxybutyrate are used for synthesis of the even-chain C4:0 to C16:0 FA in the mammary gland. Increased proportions of ruminal acetate and butyrate are positively associated with H_2 and CH_4 production

(Bannink et al., 2008), and increased proportion of even-chain FA in milk fat may, therefore, indicate elevated CH_4 production. Castro Montoya et al. (2011) found various milk odd- and branched-chain FA, which originate from rumen bacteria, to be related to VFA formation and CH_4 production. Several long-chain (unsaturated) FA and their biohydrogenation products end up in milk which originate from dietary oils (Chilliard et al., 2007; Shingfield et al., 2008). Elevated concentrations of long-chain unsaturated FA in dairy cattle diets decrease dry matter and fiber digestibility and in turn the yield of CH_4 (Patra, 2013). These relationships observed between milk even-chain, odd- and branched-chain and long-chain unsaturated FA concentrations, and ruminal CH_4 production may, therefore, be widely used as an easily accessible tool for the prediction of enteric CH_4 yield form dairy cows.

The predicted power of equations based on milk FA profile indicates good potential for CH_4 emission prediction, but the relationships between specific milk FA and CH_4 emission may well be diet specific (Van Gastelen and Dijkstra, 2016), hampering the use of general prediction equations for all dietary situations.

1.5 Modeling of enteric CH_4 production in dairy cattle

For inventory and prediction purposes, many empirical equations have been developed that relate CH_4 production per day or CH_4 yield per unit of feed to feed intake and composition. However, the prediction accuracy of these equations appears to be limited (Ellis et al., 2010). Mechanistic models on the contrary, are constructed to represent the underlying structure of a (biological) system or response variable. These models divide a system into components explaining whole-system behavior in terms of those components and their interactions. Mechanistic models represent biological causality but may have some degree of empiricism in the sense that a simplification of a biological process is incorporated. Mechanistic models describing the mechanism of enteric feed degradation provide, in general, more accurate predictions of CH_4 production than empirical models (Alemu et al., 2011). However, mechanistic models are more complex and require inputs that are not commonly measured. In addition, forcing functions used and inaccuracy of parameter values adopted may limit the meticulousness of model predictions.

1.5.1 Empirical approaches

Many relationships have been determined between feed intake and CH_4 output. Kriss (1930) and Blaxter and Clapperton (1965) developed a linear prediction equation

that relates dry matter intake (DMI) and CH_4 emission. Moe and Tyrrell (1979) developed a linear equation to predict CH_4 emission based on digestible cellulose, hemicellulose and soluble residue instead of DMI. This decomposition resulted in an improvement of the prediction accuracy. Mills et al. (2003) developed a non-linear dairy cattle CH_4 prediction equation that depended on DMI or metabolizable energy intake as input variable and had a smaller prediction error than the Kriss (1930) and Blaxter and Clapperton (1965) equations (Ellis et al., 2007). Studies by Moraes et al. (2014) and Appuhamy et al. (2016), in which rather extensive databases were used, confirmed the importance of feed intake to predict enteric CH_4 production and showed that also considering dietary fiber and fat contents often improves the prediction accuracy. Ellis et al. (2010) evaluated nine CH_4 prediction equations used in whole-farm GHG emission models. Their results show that the simple, more generalized equations performed worse than those that attempted to represent more details of diet composition and feed digestion.

Given that feed composition, and in particular diet digestibility, on commercial dairy farms are not easily determined, milk FA composition may be used alternatively to predict enteric CH_4 production. After studies demonstrating that diet composition affected both enteric CH_4 production and milk FA profile (Sauer et al., 1998; Johnson et al., 2002; Odongo et al., 2007), Chilliard et al. (2009) were the first to report direct relationships between milk FA concentrations and CH_4 production. Such relationships are based on the fact that CH_4 emission is related to the VFA profile produced in the rumen (Ellis et al., 2008) and the relationship of *de novo* FA synthesized in the mammary gland, odd- and branched-chains in particular, with their VFA precursors in the rumen (Vlaeminck et al., 2006a). Chilliard et al. (2009) obtained their results from cows assigned to four dietary treatments with a different linseed supply and availability. They quantified the CH_4 output (g/d) based on the forage intake (kg of DM/d) and the milk FA concentrations (g/100 g of FA) by performing a multiple regression analysis:

$$\begin{aligned} \mathrm{CH_4} &= 9.46 \cdot \mathrm{C16{:}0} - 97.6 \cdot (\textit{trans}\text{-}16{+}\textit{cis}\text{-}14)\text{-}\mathrm{C18{:}1} - 78.3 \cdot \textit{cis}\text{-}9\text{-}\mathrm{C14{:}1} \\ &\quad + 77.4 \cdot \textit{cis}\text{-}9{,}12\text{-}\mathrm{C18{:}2} + 13.3 \cdot \text{forage intake} - 21.2. \end{aligned} \tag{1.4}$$

The equation, with $R^2 = 0.95$, indicates that milk C16:0 and *cis*-9,12-C18:2 are positively related to CH_4 emission, while milk (*trans*-16+*cis*-14)-C18:1 and *cis*-9-C14:1 are negatively related to CH_4 emission. A simplified equation with $R^2 = 0.93$ was obtained by omitting the *cis*-9-C14:1 and *cis*-9,12-C18:2 terms and re-estimating the coefficients of the other terms.

The relationships between milk FA and CH_4 emission were determined based on

a limited range of diets and FA supply however. Dijkstra et al. (2011) evaluated the relationship between CH_4 production (g/kg DM) and milk FA concentrations (g/100 g of FA) from three experiments with a total of ten dietary treatments (mainly lipids). A multiple regression analysis resulted into the following equation:

$$\begin{aligned} CH_4 &= 24.6 + 8.74 \cdot \text{C17:0-}\textit{anteiso} - 1.97 \cdot (\textit{trans}\text{-10+}\textit{trans}\text{-11)-C18:1} \\ &\quad - 9.09 \cdot \textit{cis}\text{-11-C18:1} + 5.07 \cdot \textit{cis}\text{-13-C18:1}. \end{aligned} \tag{1.5}$$

Although equation 1.5 had a lower R^2 than equation 1.4 (0.73 *vs.* 0.95), equation 1.4 predicts CH_4 emission in absolute amount per day instead of per kg DM and requires forage intake as an input. In addition equation 1.4 was obtained by feeding diets only varying linolenic acid supply and availability.

The variables contributing to CH_4 in equations 1.4 and 1.5 were not the same suggesting that the applicability of these equations across various feeding conditions may be limited. Mohammed et al. (2011) evaluated the relationship between CH_4 production and milk FA composition by means of sunflower seed, canola seed and flax seed supplemented diets. Applying 3 different prediction equations (equation 1.4, a simpler equation of 1.4 in which no *cis*-9-C14:1 and *cis*-9,12-C18:2 were considered, and equation 1.5) to their diets resulted in an over-prediction of CH_4 by 61, 22 and 19%, respectively. Mohammed et al. (2011) concluded that this demonstrates that the scope for developing universal CH_4 prediction equations from milk FA composition alone appeared to be limited. A prediction equation based on a greater variety of dietary ingredients that also includes grass or corn can therefore be expected to be more generally applicable than the equations obtained hitherto. More importantly, the equation without inclusion of DMI had a smaller prediction error than the equation with inclusion of DMI, suggesting that the consideration of milk FA in their regression equation is relatively easy to improve.

1.5.2 Mechanistic approaches

Mechanistic models have been developed in order to describe processes in the GI-tract of animals and to simulate and predict the response in the animal (Dijkstra et al., 2007; Dumas et al., 2008). One of the first mechanistic models of rumen fermentation for dairy cattle that also included a representation of VFA formation was developed by Baldwin et al. (1987). Argyle and Baldwin (1988) added the effect of water kinetics and pH on VFA production to the model previously reported by Baldwin et al. (1987). Based on literature data, they determined an empirical equation which is dependent on pH that predicted hydrolysis and fermentation rate of cellulose.

Dijkstra et al. (1992) developed a model with a refined representation concerning microbial recycling, microbial substrate preference, energetic uncoupling related to N-availability, effect of pH on microbial activity and VFA and ammonia absorption as well as both amylolytic and fibrolytic microbes and the variation in microbial chemical composition. The total VFA synthesis appeared to be accurately predicted, but the VFA molar proportions were different from experimental values, which was attributed to the non-discriminating description of the microbes (Neal et al., 1992).

Benchaar et al. (1998) were the first to predict CH_4 formation with a mechanistic model and did this by means of updating the model of Baldwin et al. (1987). The amount of CH_4 formed was predicted from H_2 production associated with VFA formation, microbial uptake and biohydrogenation of unsaturated FA. Benchaar et al. (1998) also used this framework in combination with the Dijkstra et al. (1992) model to predict CH_4 production. It appeared that both mechanistic prediction efforts resulted in a more accurate CH_4 prediction than simple regression equations. Therein, the modified model of Dijkstra et al. (1992) underestimated the CH_4 production (root mean square prediction error (RMSPE) = 20% of the observed mean) whereas the updated model of Baldwin et al. (1987) overestimated the CH_4 production (RMSPE = 37% of the observed mean). Benchaar et al. (1998) attributed these deviations to overestimation and underestimation of the passage rate of structural carbohydrates, respectively, but also suggested to reconsider prediction of individual VFA produced because of their close relationship with CH_4 formed.

Mills et al. (2001) built on the model of Dijkstra et al. (1992) and updated the H_2 coefficients of Benchaar et al. (1998), for H_2 requirement for microbial growth on non-protein N and the H_2 yield of microbial growth on amino acids, the coefficients of the VFA molar proportions and added the concept of post-ruminal fermentation. The revision of the parameters regarding uptake and production of H_2 caused by microbial growth and the inclusion of post-ruminal fermentation increased the amount of CH_4 predicted being counteracted by the revised coefficients for molar proportions of VFA. Overall, the approach of Mills et al. (2001) resulted in a moderately decreased under-prediction of CH_4 (RMSPE = 12%) compared to the approach of Benchaar et al. (1998). This prediction error is comparable to another recent modeling effort with RMSPE = 13% (Gregorini et al., 2013), in which digestive and VFA production parameters were updated.

There has been much debate regarding the prediction of the molar proportions of the different VFA in the rumen. In the models of Baldwin et al. (1987) and Dijkstra et al. (1992), the molar proportions for either a concentrate- or roughage-rich diet were based on a statistical analysis of a wide variety of diets regarding source of carbohydrates or amino acids performed by Murphy et al. (1982). Bannink et al.

(2006) attempted to improve the prediction of individual VFA production for high roughage and high concentrate diets by means of a regression model that included observed rates of rumen digestion in lactating cows. Nozière et al. (2010, 2011) empirically determined the coefficients for the estimation of the individual VFA production for a wide variety of feeding situations based on rumen fermentable organic matter, further specified neutral detergent fiber, starch and crude protein. Alemu et al. (2011) evaluated VFA prediction parameters of both Bannink et al. (2006) and Nozière et al. (2010) and determined the RMSPE-values to be similar. The CH_4 prediction, however, was best when using the VFA prediction parameters of Bannink et al. (2006). Morvay et al. (2011), who evaluated various prediction models of rumen VFA molar proportions, indicated that the majority of variation among diets in acetate molar proportion was explained by the models. Furthermore, an adequate representation of additional rumen factors to improve model predictions of propionate, butyrate and branched-chain VFA molar proportions was advocated.

Aspects such as substrate degradation and microbial metabolism have been kinetically represented in the rumen models that was referred to in the previous paragraphs. The thermodynamic control of p_{H_2} on the cofactor dynamics, that in turn controls VFA formation, has not been elaborately explored for the rumen environment. Incorporation of these dynamics in rumen fermentation models may, therefore, lead to the desired improvement of the prediction of VFA molar proportions. Moreover, the models described previously all ignore the representation of methanogens. Therefore, representing p_{H_2} controlled cofactor fermentation dynamics as well as methanogenic micro-organisms enables to evaluate the effect of p_{H_2} on the type of VFA produced, and may improve prediction CH_4 production in dairy cows. Furthermore, both empirical and mechanistic approaches commonly ignore the diurnal dynamics of rumen microbial metabolism when assessing rumen fermentation end products, despite peaks in VFA (Hatew et al., 2015), H_2 and CH_4 occurring shortly after feed consumption (Rooke et al., 2014). Assessing diurnal dynamics may, therefore, also increase our understanding of CH_4 production in the rumen of cows.

1.6 Objectives and outline thesis

The research presented in this thesis was part of the TI Food and Nutrition project entitled "Reduced methane emissions of dairy cows" (see Textbox 1 for a brief program description). This program aimed to increase our understanding of nutrition, rumen microbiota and dairy cattle genetics and their interaction in relation to CH_4 production, and to explore how this knowledge can be used to decrease CH_4 emission from dairy cows. Research of this program will assessed CH_4 emission at three levels:

dairy cattle populations, the individual cow and the rumen. The emphasis of this PhD study was on the rumen and the overall objective was:

- to quantitatively evaluate enteric CH_4 emission from dairy cows as affected by feeding and rumen microbial metabolism.

To this end, the following specific objectives of this PhD project were:

1. to quantify relationships between CH_4 yield and individual milk FA concentrations in lactating dairy cattle, and to develop equations to predict CH_4 yield per unit of feed or milk based on milk FA concentrations.

2. to quantify the control of p_{H_2} on reaction rates of specific fermentation pathways, methanogenesis and NADH oxidation in rumen microbes.

3. to monitor diurnal patterns of: (i) gaseous and dissolved metabolite concentrations in the bovine rumen, (ii) H_2 and CH_4 emitted, and (iii) the rumen microbiota. Furthermore, the effect of dietary inclusion of linseed oil on these patterns was assessed.

4. to develop a dynamic mechanistic model that represents the thermodynamic control of p_{H_2} on VFA fermentation pathways, and on methanogenesis in the bovine rumen.

In Chapter 2 of this thesis, the relationship between milk FA composition and enteric CH_4 yield per amount of feed and fat- and protein-corrected milk is reported. For this study, a meta-analytic approach was applied making use of a database comprising eight different studies. In Chapter 3, a theoretical investigation of the thermodynamic control of p_{H_2} on rumen microbial metabolism is reported. The experimental study reported in Chapter 4, evaluated hypotheses that were formulated based on the theoretical investigation of Chapter 3. These hypotheses are related to the NAD^+ to NADH ratio, rather than p_{H_2} directly, as a key-controller of fermentation end products, and to this end the diurnal patterns of H_2 and CH_4, dissolved metabolites and microbiota in the rumen were quantified. Subsequently, the development of a dynamic mechanistic model is reported in Chapter 5. This model was developed based on recommendations made in Chapter 3, and evaluated using the diurnal patterns reported in Chapter 4. Chapter 6 of this thesis concludes with a general discussion of the results reported in the previous chapters.

Textbox 1: Top Institute Food and Nutrition project *Reduced methane emissions from dairy cows*

The work described in this thesis was part of the Top Institute Food and Nutrition (TIFN) project 'Reduced methane emissions from dairy cows'. This project aimed at increasing knowledge about methane emission from dairy cows in order to decrease the ecological footprint of dairy production. The project team had a multidisciplinary expertise, comprising experts in Animal Breeding and Genetics, Animal Nutrition, Dairy Science and Technology, and Microbiology. The project team consisted of four PhD candidates and three postdocs. The team was based at Wageningen University and collaborated with researchers from the industrial parties CRV, Lely Industries and Qlip. Financial support was obtained from Centraal Bureau Levensmiddelenhandel (CBL), Cooperative cattle improvement organization CRV, Federatie Nederlandse Levensmiddelen Industrie (FNLI), Lely Industries NV, Ministry of Economic Affairs, Qlip BV, Wageningen University and Research, and ZuivelNL.

The key objectives of the TIFN project were:

1. to develop and validate an indicator for methane emission in milk.
2. to quantify the variation in methane emission and relationships with milk composition, fertility and longevity.
3. to characterize of the composition and functionality of the rumen microbiota.
4. to unravel the interplay between cow, microbiota and feed.
5. to develop mathematical models of methane emission from dairy cows and dairy herds.

The research described in this thesis deals with objective 5: the development of mathematical models.

Chapter 2

Meta-analysis of relationships between enteric methane yield and milk fatty acid profile in dairy cattle

Henk J. van Lingen[1,2], Les A. Crompton[3], Wouter H. Hendriks[2,4], Christopher K. Reynolds[3], Jan Dijkstra[2]

1 TI Food and Nutrition, Wageningen, The Netherlands
2 Animal Nutrition Group, Wageningen University, Wageningen, The Netherlands
3 Division of Food Production and Quality, School of Agriculture, Policy and Development, University of Reading, Reading, United Kingdom
4 Faculty of Veterinary Medicine, Utrecht University, Utrecht, The Netherlands

Journal of Dairy Science, 97:7115-7132, 2014

Abstract

Various studies have indicated a relationship between enteric methane (CH_4) production and milk fatty acid (FA) profile of dairy cattle. However, the number of studies investigating such a relationship is limited and the direct relationships reported are mainly obtained by variation in CH_4 production and milk FA concentration induced by dietary lipid supplements. The aim of this study was to perform a meta-analysis to quantify relationships between CH_4 yield (per unit of feed and unit of milk) and milk FA profile in dairy cattle and to develop equations to predict CH_4 yield based on milk FA profile of cows fed a wide variety of diets. Data from eight experiments encompassing 30 different dietary treatments and 146 observations were included. CH_4 yield measured in these experiments was 21.5 ± 2.46 g per kg dry matter intake (DMI) and 13.9 ± 2.30 g per kg fat and protein corrected milk (FPCM). Correlation coefficients were chosen as effect size of the relationship between CH_4 yield and individual milk FA concentration (g/100 g FA). Average true correlation coefficients were estimated by a random-effects model. Milk FA concentrations of C6:0, C8:0, C10:0, C16:0 and C16:0-iso were significantly or tended to be positively related to CH_4 yield per unit of feed. Concentrations of *trans*-6+7+8+9-C18:1, *trans*-10+11-C18:1, *cis*-11-C18:1, *cis*-12-C18:1, *cis*-13-C18:1, *trans*-16+*cis*-14-C18:1 and *cis*-9,12-C18:2 in milk fat were significantly or tended to be negatively related to CH_4 yield per unit feed. Milk FA concentrations of C10:0, C12:0, C14:0-iso, C14:0, *cis*-9-C14:1, C15:0 and C16:0 were significantly or tended to be positively related to CH_4 yield per unit of milk. Concentrations of C4:0, C18:0, *trans*-10+11-C18:1, *cis*-9-C18:1, *cis*-11-C18:1, and *cis*-9,12-C18:2 in milk fat were significantly or tended to be negatively related to CH_4 yield per unit of milk. Mixed model multiple regression and a stepwise selection procedure of milk FA based on the Bayesian Information Criterion to predict CH_4 yield with milk FA as input (g/100 g FA) resulted in: CH_4 (g/kg DMI) = 23.39 + 9.74 · C16:0-*iso* – 1.06 · *trans*-10+11-C18:1 – 1.75 · *cis*-9,12-C18:2 ($R^2 = 0.54$), and CH_4 (g/kg FPCM) = 21.13 – 1.38 · C4:0 + 8.53 · C16:0-iso – 0.22 · *cis*-9-C18:1 – 0.59 · *trans*-10+11-C18:1 ($R^2 = 0.47$). This indicated milk FA profile to have a moderate potential for predicting CH_4 yield per unit of feed and a slightly lower potential for predicting CH_4 yield per unit of milk.

Keywords: Methane, Milk fatty acid profile, Meta-analysis, Dairy cow

2.1 Introduction

Enteric fermentation is the main source of greenhouse gas (GHG) emissions from dairy cattle, with enteric CH_4 amounting to 1.1 gigatonnes per year, representing 46% of the total GHG emissions in dairy supply chains (Gerber et al., 2013). Enteric CH_4 production is among the main targets of GHG mitigation practices for the dairy industry (Hristov et al., 2013a). In view of these emissions and various mitigation options, there is a clear need for simple and inexpensive measurement techniques to estimate CH_4 emissions from dairy cattle in commercial practice.

Various methods have been used to estimate CH_4 production from ruminants. CH_4 production can be measured in respiration chambers, which is an accurate but expensive technique, unsuitable for application on a large scale. Other methods, including the SF_6 marker and CH_4/CO_2 ratio techniques, enable CH_4 emissions to be determined in a larger number of animals, but with higher between and within animal variation (Storm et al., 2012). For inventory and prediction purposes, many empirical equations relating CH_4 production per day or yield per unit of feed to feed intake and composition have been developed. Such equations have major limitations in predicting effects of mitigation strategies at a whole farm level (Ellis et al., 2010). Mechanistic models describing the mechanism of enteric feed degradation provide more accurate predictions of CH_4 production than empirical models (Alemu et al., 2011). However, mechanistic models are more complex and require inputs that may not be commonly measured. In addition, forcing functions used and bias in parameter values adopted may limit the meticulousness of predicted model output. For these reasons, a simple and robust prediction equation of enteric CH_4 yield from dairy cattle based on characteristics of feed or milk would be of value for application on a large scale in GHG mitigation practices for the dairy industry.

Milk samples are frequently used in dairy farms to assess nutritional and health status of dairy cattle and to obtain information on losses to the environment. For example, milk urea content is used to assess protein status of the animal and to estimate N excretion (Spek et al., 2013). Several studies have related diet composition to both milk FA composition and enteric CH_4 production (e.g., Chilliard et al., 2009). Such relationships may be a result of lipid supplementation, which changes both CH_4 production and milk FA profile, or may be a result of changes in diet composition, in view of CH_4 production being associated with the VFA profile produced in the rumen (Ellis et al., 2008) and VFA in turn being precursors of milk FA synthesized *de novo* (Bernard et al., 2008). The odd- and branched-chain fatty acid (OBCFA) content of milk has also been shown to be related to rumen function (Vlaeminck et al., 2006b).

Chilliard et al. (2009) supplemented cattle diets with different physical forms

of linseed (crude, extruded and oil). The most positive correlations between CH_4 production (g/d) and milk FA concentrations were obtained for saturated FA (C6:0 to C16:0) and the most negative correlations for various *trans*-C18 FA. Milk OBCFA concentrations exhibited less strong correlations with CH_4 production. These relationships may only apply to linseed supplemented diets. Mohammed et al. (2011) using only dietary oilseed supplementation (sunflower seed, linseed and canola seed) best predicted CH_4 production (g/d) by milk FA concentration of C16:0-*iso* (positive relationship) and *cis*-9-C17:1 (negative relationship). Dijkstra et al. (2011) using a larger variety of diets (3 experiments, 10 dietary treatments) in which fat supplementation was a major source of dietary variation evaluated relationships between CH_4 yield per unit of feed and milk FA profile in dairy cattle. Their prediction equation included milk FA concentration of C17:0-*anteiso* and *cis*-13-C18:1 (positive relationship) and *trans*-10+11-C18:1 and *cis*-11-C18:1 (negative relationship). The various models to predict CH_4 emission in these three studies have only a few milk FA in common. This may be a result of the small number of experiments and the limited variation in dietary treatments, and analytical methods used to elucidate milk FA profile. Data from a greater number of experiments containing a wider variety of diets are required to firmly assess the potential of milk FA profile as an indicator of CH_4 yield. A greater number of experiments also allows the quantification of between-study variability or heterogeneity of the correlation between milk FA concentrations and CH_4 yield.

The aims of this study were to perform a meta-analysis to quantify relationships between CH_4 yield and individual milk FA concentrations in lactating dairy cattle while quantifying the heterogeneity of these relationships, and to develop equations to predict CH_4 yield (per unit feed and per unit milk) based on milk FA profile of cows fed a wide variety of diets. Such equations may ultimately be used to estimate CH_4 yield from dairy cattle under field conditions to fulfill the need for simple, inexpensive measurement techniques.

2.2 Materials and Methods

2.2.1 Data collection

For inclusion in the present meta-analysis, studies were required to have CH_4 production measured using respiration chambers and milk FA profile elucidated using gas chromatography. Four studies designed as 4 × 4 Latin squares from the University of Reading and four studies designed as randomized block experiments from Wageningen University met these requirements and were included (Table 2.1). The

procedures to determine CH_4 production and milk FA profile are described by Kliem et al. (2008) and Reynolds et al. (2014) for the Reading studies and by Van Knegsel et al. (2007) for the Wageningen studies. The eight studies represented 30 different dietary treatments and 146 individual observations encompassing a variety of diets. Studies 1, 3, 4, 7, 8 contained lipid treatments, whereas studies 2, 5 and 6 did not contain any lipid treatment. Studies 4 and 5 comprised diet treatments with different forage types and contents, and studies 2, 6, 7 and 8 contained various non-lipid additives. Animals were described by treatment diet composition, DMI, milk yield, milk composition, milk FA profile and CH_4 production (Table 2.2). Methane yield was expressed per unit of feed (g/kg DMI) and per unit of fat and protein corrected milk (g/kg FPCM; FPCM (kg/d) = [0.337 + 0.116 · milk fat (%) + 0.06 · milk protein (%)] · milk production (kg/d); CVB, 2008).

Some of the milk FA profile analyses did not allow the identification of certain individual milk FA but did identify certain FA together as one fraction. When these FA were individually identified in other studies, they were grouped together. Milk FA fractions were expressed in g/100 g total milk FA. FA fractions with an average study concentration < 0.1 g/100 g milk fat were excluded from the dataset.

2.2.2 Statistics

Random-effects model analysis

Relationships between CH_4 yield per unit of feed and per unit of milk, and individual milk FA concentrations for dairy cattle were meta-analyzed using the metafor package (version 1.6-0 Viechtbauer, 2010) in R statistical software. The effect size of these relationships for every of the eight studies was estimated by correlation coefficients (values in Supplementary Tables 1 and 2). The correlation coefficients were obtained by linear regression using individual animal data. In contrast to treatment mean data, individual animal data prevents from ignoring variation of CH_4 production and milk FA concentrations at animal level due to, for example, parity and DMI level. The correlation coefficients were transformed via Fisher's r-to-Z transformation, $Z = \tanh^{-1}(r)$, (Fisher, 1921). This transformation ensures more stable variance and normality. To obtain the average true effect, the meta-analytic model applied is given by:

$$y_i = \mu + u_i + e_i, \tag{2.1}$$

where y_i is the observed effect in the i-th study, μ is the average true effect, u_i is the variability among the true effect induced by study, e_i is the sampling error with $e_i \sim N(0, v_i)$. The sampling variance v_i, is known based on the number of

Table 2.1: Data sources and their characteristics used for meta-analysis, showing corresponding dietary treatments and basal diets

Study	Reference	Number of Observations	Number of Treatments	Diet composition/treatments description[a]
University of Reading, United Kingdom				
1	Crompton et al. (2010a)	16	4	Basal diet comprising 37.5% corn silage, 12.5% grass silage; treatments comprising 3.5% DM: control diet with calcium salts of palm oil fed once daily vs. control diet with calcium salts of palm oil fed twice daily vs. milled rapeseed diet fed twice daily vs. coconut oil diet fed twice daily.
2	Reynolds et al. (2010)	16	4	Basal diet comprising 37.5% grass silage, 12.5% corn silage; 50% concentrates vs. 50% concentrates + allicin vs. 40% concentrate + 10% glycerol vs. 20% concentrates + 30% naked oats
3	Crompton et al. (2011)[b]	16	4	Basal diet: 37.5% corn silage, 12.5% grass silage, 50% blend; 50:50 forage:concentrate ratio, no added lipid, diet fed twice daily vs. 50:50 forage:concentrate ratio, 3.5% lipid from milled rapeseed, diet fed twice daily vs. forage:concentrate ratio 50:50, 3.5% lipid from milled rapeseed, diet fed once daily vs. forage:concentrate ratio daily alternating 45:55 and 55:45, 3.5% lipid from milled rapeseed, diet fed once daily.
4	Livingstone et al. (2015)	16	4	Corn silage, grass silage, concentrates, extruded linseed (37.5:12.5:50.0:0.0 vs. 37.5:12.5:45.0:5.0 vs. 12.5:37.5:50.0:0.0 vs. 12.5:37.5:45.0:5.0)
Wageningen University, the Netherlands				
5	Van Gastelen et al. (2015)	32	4	80% (100:0 vs. 67:33 vs. 33:67 vs. 0:100 grass silage:corn silage), 20% concentrates
6	Van Zijderveld et al. (2011a)	20	4	4% grass silage, 26% corn silage, 34% concentrates; control vs. diallyldisulfide supplement vs. yucca plant powder supplement vs. calcium fumarate supplement
7	Van Zijderveld et al. (2011b)	10	2	29% grass silage, 22% corn silage, 2% wheat straw, 47% concentrates; supplemented with palm oil vs. supplemented with calcium fumarate plus mix of lauric acid, myristic acid and linseed oil
8	Van Zijderveld et al. (2011a)	20	4	41% grass silage, 35% corn silage and 24% concentrates; control vs. extruded

[a] Percentages on DM basis; [b] Experimental setup and description of diets in Relling et al. (2014).

Table 2.2: Descriptive statistics of dietary and animal characteristics, and milk fatty acid concentrations (g/100 g fatty acids)

Variable	**Mean**	**SD**	**Minimum**	**Maximum**
DMI (kg/d)	18.5	2.41	13.1	26.1
NDF (% of DM)	37.0	3.76	29.0	42.2
ADF (% of DM)[a]	21.7	2.05	17.9	27.6
Starch (% of DM)[b]	16.5	6.39	0.42	25.7
CFAT (% of DM)[c]	4.2	1.65	1.9	6.4
CP (% of DM)	16.0	1.12	13.3	19.1
Ash (% of DM)	7.3	0.92	5.0	9.4
Milk yield (kg/d)	28.9	6.40	16.8	44.4
FPCM (kg/d)	29.1	5.14	18.3	42.4
Milk fat (%)	4.20	0.679	2.28	6.24
Milk protein (%)	3.29	0.314	2.38	4.18
Milk lactose (%)[b]	4.53	0.203	3.81	5.06
CH_4 (g/d)	395	51.2	250	508
CH_4 (g/kg DMI)	21.5	2.46	15.9	27.9
CH_4 (g/kg FPCM)	13.9	2.30	8.8	20.3
C4:0	3.18	0.46	1.44	4.32
C6:0	2.10	0.35	0.73	2.73
C8:0	1.19	0.22	0.51	1.61
C10:0	2.67	0.57	1.12	3.77
C12:0	3.29	1.13	1.50	10.70
C14-*iso*[d]	0.10	0.04	0.03	0.22
C14:0	11.18	1.79	6.82	18.24
cis-9-C14:1	1.05	0.35	0.57	3.23
C15:0-*anteiso*	0.43	0.06	0.30	0.62
C15:0	0.99	0.25	0.64	2.25
C16:0-*iso*	0.22	0.07	0.01	0.37
C16:0	31.28	4.91	19.91	42.29
C17:0	0.55	0.12	0.27	0.82
C18:0	9.75	2.41	5.03	17.09
trans-6+7+8+9-C18:1[e]	0.57	0.32	0.25	1.63
trans-10+11-C18:1	1.46	1.01	0.51	9.00
cis-9-C18:1[e]	19.31	3.67	12.32	29.80
cis-11-C18:1[e]	0.60	0.21	0.30	1.37
cis-12-C18:1	0.28	0.13	0.07	0.81
cis-13-C18:1	0.17	0.11	0.04	0.65
cis-14+*trans*-16-C18:1[e]	0.33	0.19	0.10	0.90
cis-9,12-C18:2	1.54	0.37	0.57	2.94
cis-9,12,15-C18:3	0.45	0.17	0.14	1.02
C20:0	0.13	0.04	0.06	0.24

No data available for experiments 6, 7 and 8 (a), 6 and 8 (b), 4 (c), 8 (d), or 5 (e).

observations per study. The study effect, u_i, was taken into account as a random factor. This model is referred to as the random-effects model.

In the random-effects model, the variability among the true effect (or heterogeneity), which is regarded to be induced by experimental circumstances, is assumed to be normally distributed that has variance τ^2 such that $u_i \sim N(0, \tau^2)$. The model was fit with restricted maximum likelihood (REML). Heterogeneity (τ^2) was expressed as percentage of the total variability in the effect size (τ^2 plus sampling error), yielding the I^2 statistic (Higgins et al., 2003). In case of negative values of I^2, a value of 0% was adopted. I^2 greater than 50% indicates substantial heterogeneity. The transformed correlations were tested for homogeneity with the Q-statistic (Hedges and Olkin, 1985) which follows a χ^2 distribution. Average true correlation coefficients and their boundaries of the 95% confidence intervals were back transformed to raw correlation values for interpretation convenience. Estimates of average true correlations were declared significant at $P \leq 0.05$ and tendencies at $0.05 < P \leq 0.10$. The strength of the estimated average correlations is interpreted as small if $0.10 < |r| < 0.30$, moderate if $0.30 < |r| < 0.50$ and large if $|r| \geq 0.50$ (Cohen, 1988).

Mixed model analysis

To predict the actual CH_4 yield per unit of feed and per unit of milk, with milk FA concentrations as input, mixed model regression techniques (St-Pierre, 2001) were applied using PROC MIXED in SAS (SAS Institute Inc., Cary, NC). This enabled analysis of fixed effects of independent variables as well as the effect of study, which was taken into account as a random factor. The general model for single and multiple regression is represented as:

$$y_{ij} = b_0 + b_1 x_{ij} + s_i + b_i x_{ij} + e_{ij}, \tag{2.2}$$

where y_{ij} is the dependent variable (ith study 1, ..., 8, jth observation 1, ..., 146) and x_{ij} is the value of the kth explanatory variable (k = 1, 2, ..., p). The overall intercept b_0 and the overall regression coefficients of y on x across all studies comprise the fixed-effects part of the model for k different parameters. The random effect of the ith study on the overall intercept b_0, s_i, together with the unexplained residual error, e_{ij}, comprise the random-effects part of the model with both assumed to be normal. Random-effects were modeled with (co)variance matrices that were fitted with an unstructured approach, providing that matrices converged. In cases of non-convergence, (co-)variance matrices were fitted with a compounds symmetry. When matrices still did not converge, they were fitted with variance components. No

random effect on slope was included in the multiple regression analysis to prevent over-parameterization. A selection procedure for multiple regression was performed using a stepwise procedure (PROC GLMSELECT in SAS) retaining the experiment effect in every step, with CH_4 yield the dependent variable and stepwise selection of FA based on the Schwarz Bayesian Information Criterion, where lower values indicate better model adequacy. All available single FA or FA combinations, were included in the selection. For predicting CH_4 yield per unit of feed, milk fat, protein and contents were included in the selection as well. Parameter estimates for fixed effects were declared significant at $P \leq 0.05$. Adjusted dependent variable values were calculated based on regression parameters of the final model to determine r or R^2 corrected for experiment effect (St-Pierre, 2001). The residuals (predicted minus observed) were visually inspected for any patterns, as well as for any potentially confounding factors.

2.3 Results and Discussion

The studies used in this meta-analysis (see Table 2.1) comprises a significantly larger variety of diets compared with Chilliard et al. (2009) and Mohammed et al. (2011), and also compared with Dijkstra et al. (2011). In the present dataset, the forage proportion varied between 50 and 80% of total diet, with forage consisting of grass silage and corn silage in ratios ranging from 0:100 to 100:0 (all DM basis). It remains questionable though to what extent the present dataset represents the variety of diets supplied on commercial dairy farms. In particular, the large variation in forage proportion (fraction of total diet) and composition (type of forage and quality of forage) in practice is not completely represented in the eight studies included. As in the previous analyses cited above, the data used in the present study include measurements for diets that include supplemental lipids and other ingredients with potential to decrease CH_4 yield.

Study effect can be taken into account either as a fixed or a random factor in meta-analysis and leads to a fixed-effects model or a random-effects model, respectively. In contrast to fixed-effects models that make a conditional inference only about the number of studies included in the analysis, random-effects models estimate the unconditional inference about a larger set of studies of which the studies included in the analysis are assumed to be a normally distributed random sample (Viechtbauer, 2010). Therefore, including the study effect as a random factor and not as fixed factor instead, is in better agreement with the aim of this meta-analysis to search for a generally applicable prediction equation for CH_4 yield with milk FA concentration as input.

2.3.1 Random-effects model analysis

Correlation per unit of feed

The concentration of C16:0 in milk fat was moderately positively related to CH_4 yield (g/kg DMI), and concentrations of C6:0, C8:0, and C10:0 in milk fat tended to be weakly positively related to CH_4 yield (Table 2.3), which is largely in agreement with previous findings (Chilliard et al., 2009). These FA are synthesized *de novo* in the mammary gland from acetate and β-hydroxybutyrate, produced in the rumen (Bernard et al., 2008). Ruminal acetate production is positively associated with fiber intake (Bannink et al., 2008), which subsequently yields H_2 and ultimately CH_4 by methanogenic archaea. Milk C4:0 concentration was not significantly related to CH_4 yield. With the exception of C4:0, the *de novo* FA synthesis in the mammary gland of C16 and shorter FA is inhibited in the presence of unsaturated long-chain FA (Bernard et al., 2008; Shingfield et al., 2010). The fact that dietary unsaturated FA generally reduce CH_4 yield may explain why concentrations of C4:0 were not related to CH_4 yield, in contrast to other even-chain *de novo* synthesized FA. Moreover, C4:0 in milk fat does not require acetate for its production as it can be produced directly from β-hydroxybutyrate derived from the blood and is thus only partly originating from *de novo* FA synthesis using acetate.

As for milk FA concentration of C4:0, no significant relationship was found between CH_4 yield (g/kg DMI) and concentrations of C12:0 or C14:0. Based on genetic and herd clustering of milk FA, Heck et al. (2012) found that C4:0 and C12:0 differed from the general pattern of the other FA in the group of *de novo* synthesized even-chain FA. Milk FA C12:0 and C14:0 may not just be synthesized *de novo* in the mammary gland, but can also originate from dietary C12:0 and C14:0 (e.g., Van Zijderveld et al., 2011b). Ingredients including palm kernel expeller and extracted coconut with a relatively large proportion of C12:0 and C14:0 in fat are commonly included in dairy cattle diets and were also present in various diets in the current dataset. Dietary C12:0 and C14:0 inhibit CH_4 production (Patra, 2013), which might explain why no overall correlation of concentrations C12:0 and C14:0 in milk fat and CH_4 yield was found in this study. However, it should be noted that the levels of either C12:0 or C14:0 fed are not available for most of the studies included in this meta-analysis. A part of C14:0 is desaturated to *cis*-9-C14:1 by Δ9-desaturation in the mammary gland. This desaturation activity is regulated by genetics (Soyeurt et al., 2008) and may be stimulated by acetate from the rumen and inhibited by unsaturated FA from feed (Chilliard et al., 2007; Jacobs et al., 2011). These contrasting mechanisms together may result in milk *cis*-9-C14:1 not being related to CH_4 yield in the present study. In contrast with our study, Chilliard et al. (2009) found milk FA concentrations of all

Table 2.3: Estimated true correlation coefficients with standard errors and P-values, P-values for heterogeneity test statistic (Q-value P) , and heterogeneity as a fraction of total variability (I^2) for the correlation between CH_4 yield per unit of feed and per unit of milk (fat- and protein-corrected milk, FPCM) and milk FA concentration

	CH_4 yield (g/kg DMI) vs. milk FA concentration					**CH_4 yield (g/kg FPCM) vs. milk FA concentration**				
Milk FA	***r***	**SE**	**P-value**	**Q-value P**	**I^2(%)**	***r***	**SE**	**P-value**	**Q-value P**	**I^2(%)**
C4:0	0.07	0.147	0.647	0.016	60.7	–0.28	0.090	0.001	0.358	0.0
C6:0	0.19	0.103	0.056	0.265	21.0	0.02	0.090	0.830	0.837	0.0
C8:0	0.23	0.127	0.066	0.072	47.5	0.15	0.095	0.119	0.404	8.5
C10:0	0.18	0.096	0.057	0.381	10.7	0.24	0.105	0.021	0.258	23.7
C12:0	0.03	0.182	0.878	0.001	74.9	0.36	0.113	0.001	0.177	34.2
C14:0-*iso*[a]	0.26	0.173	0.131	<0.001	70.5	0.34	0.205	0.093	<0.001	79.1
C14:0	–0.02	0.194	0.902	0.001	77.8	0.26	0.115	0.021	0.152	36.3
cis-9-C14:1	–0.17	0.152	0.257	0.012	63.5	0.27	0.097	0.004	0.365	11.2
C15:0-*anteiso*	–0.19	0.185	0.316	0.001	75.6	0.10	0.151	0.526	0.010	62.9
C15:0	–0.16	0.190	0.414	<0.001	76.9	0.28	0.139	0.043	0.028	55.9
C16:0-*iso*	0.22	0.129	0.079	0.056	49.2	0.12	0.120	0.337	0.104	41.5
C16:0	0.34	0.112	0.001	0.080	33.1	0.29	0.090	0.001	0.904	0.0
C17:0	0.11	0.161	0.490	0.005	67.5	–0.09	0.114	0.454	0.139	35.5
C18:0	0.07	0.108	0.527	0.201	28.2	–0.24	0.090	0.006	0.530	0.0
trans-6+7+8+9-C18:1[b]	–0.27	0.103	0.008	0.557	0.0	–0.16	0.109	0.154	0.410	10.1
trans-10+11-C18:1	–0.56	0.157	<0.001	0.005	65.7	–0.16	0.090	0.068	0.869	0.0
cis-9-C18:1[c]	–0.13	0.157	0.412	0.007	65.7	–0.41	0.090	<0.001	0.896	0.0
cis-11-C18:1[b]	–0.52	0.151	<0.001	0.045	52.3	–0.45	0.155	0.002	0.037	55.0
cis-12-C18:1	–0.40	0.192	0.030	<0.001	77.5	–0.13	0.090	0.152	0.970	0.0
cis-13-C18:1	–0.26	0.141	0.057	0.024	57.3	–0.13	0.123	0.307	0.086	44.4
trans-16+*cis*-14-C18:1[b]	–0.35	0.214	0.088	0.001	76.7	–0.15	0.135	0.253	0.127	40.8
cis-9,12-C18:2	–0.25	0.143	0.082	0.021	58.9	–0.28	0.090	0.001	0.432	0.0
cis-9,12,15-C18:3	0.00	0.090	0.978	0.642	0.0	–0.12	0.113	0.300	0.145	34.3
C20:0	–0.02	0.148	0.871	0.020	57.4	–0.14	0.123	0.268	0.121	38.9

[a] No data available from experiment 7; [b] No data available from experiment 5;

[c] Co-eluted with *trans*-13+14-C18:1 in experiments 1 and 3, co-eluted with *trans*-12-C18:1 in experiment 5.

even-chain *de novo* synthesized FA between C4:0 and C16:0 to be positively related to CH_4 production. However, in the study of Chilliard et al. (2009), dietary treatments differed only in physical form of linseed.

Concentrations of OBCFA in milk FA are related to the molar proportions of VFA in the rumen and have potential to be used as rumen microbial markers as indicators of type of VFA formed and as predictors of CH_4 yield (Vlaeminck et al., 2006b,a). Of the various OBCFA concentrations in milk fat in the present study, only C16:0-*iso* tended to be weakly positive related ($r = 0.22$) with CH_4 yield (g/kg DMI). This weakly positive relationship is in line with Mohammed et al. (2011) and Castro Montoya et al. (2011) who attributed this to the fact that *iso*-FA are more abundant in cellulolytic bacteria (Vlaeminck et al., 2006a) which are associated with higher CH_4 yield. Milk C14:0-*iso* concentration was positively related to CH_4 yield in the study of Chilliard et al. (2009). Increased level of fiber in the diet generally results in increased CH_4 yield, and is associated with increased concentrations of C14:0-*iso* in milk fat (Boivin et al., 2013). This positive relationship was not confirmed in the current meta-analysis ($P = 0.131$). Vlaeminck et al. (2006b) reported a negative and positive correlation of milk C15:0-*anteiso* concentration with NDF and starch, respectively. These two feed components have counteracting effects on CH_4 yield (Ellis et al., 2008), which possibly explains why concentration C15:0-*anteiso* in milk fat was not significantly related to CH_4 yield in the present study. This result is in line with Fievez et al. (2012) who suggested the concentration of C15:0-*anteiso* to be only relevant in the prediction of butyrate proportions in the rumen that is associated with dietary sugars (Oba, 2011). Elevated sugar contents may not increase CH_4 yield (Staerfl et al., 2012) and may indicate CH_4 yield and milk C15:0-*anteiso* concentration not being related.

No significant relationships with CH_4 yield (g/kg DMI) were found for concentrations of C15:0 and C17:0 in milk fat (Table 4). Two different hypotheses on the relationship between diet composition and these odd-chain milk FA concentrations have been investigated. Patel et al. (2013) reported increased milk FA C15:0 concentration when feeding increased proportions of grass silage and dietary NDF levels, which was attributed to more abundant membrane lipids from rumen microbes. A high NDF content in the feed is associated with increased CH_4 yield (Ellis et al., 2008). This indicates a positive relationship between odd-chain milk FA concentrations and CH_4 yield. In contrast, Castro Montoya et al. (2011) reported milk FA concentrations C15:0 and the sum of C17:0 and *cis*-9-C17:1 to be positively related to propionate concentration in the rumen as these are synthesized from propionate *de novo* (French et al., 2012). Propionate production is negatively related to CH_4 production, suggesting a negative relationship between milk odd-chain

FA concentration and CH_4 yield. In the present meta-analysis, odd-chain FA concentrations in milk fat were not significantly related to CH_4 yield. It should be noted that the concentration of *cis*-9-C17:1, a desaturation product of C17:0 in the mammary gland, was not available in all experiments included in the present study. Grouping these two fractions together based on a broad database might shed new light on the relationship between CH_4 yield and odd-chain FA concentration in milk as also reported by Dijkstra et al. (2011), where the sum of milk FA concentrations C17:0 and *cis*-9-C17:1 was negatively related to CH_4 yield. Overall, in line with Chilliard et al. (2009) and Mohammed et al. (2011), relationships between concentrations of OBCFA in milk and CH_4 production were generally rather minor or absent, and also less than expected based on theoretical relationships between rumen fermentation products and CH_4 yield (e.g., Vlaeminck et al., 2006a,b; Castro Montoya et al., 2011).

A number of long-chain unsaturated FA in milk originate from dietary oils and their biohydrogenation products formed in the rumen. Higher concentrations of these FA in cattle diets, which are known to reduce DM and NDF digestibility, are negatively associated with CH_4 yield (e.g., Patra, 2013). Milk *cis*-9,12-C18:2 and *cis*-9,12,15-C18:3 directly originate from the corresponding FA in feed (Chilliard et al., 2007). Concentration of *cis*-9,12-C18:2 in milk fat tended to be negatively related to CH_4 yield (g/kg DMI), $r = -0.25$, and this is in line with expectations. In general, replacing grass silage with corn silage reduces CH_4 yield, and corn silage is rich in *cis*-9,12-C18:2 and increases the proportion of this FA in milk fat (Kliem et al., 2008). However, no relationship between milk *cis*-9,12,15-C18:3 concentration and CH_4 yield was found in the present meta-analysis. Chilliard et al. (2007) stated the potential to increase milk FA concentration *cis*-9,12,15-C18:3 to be limited, with some positive effects upon feeding protected oilseed supplements in particular. Oilseeds in protected form may not decrease methanogenesis (Dohme et al., 2000) and may not result in a significant negative correlation between CH_4 yield and milk *cis*-9,12,15-C18:3 concentration. The absence of a significant relationship between milk *cis*-9,12,15-C18:3 concentration and CH_4 yield is in line with Chilliard et al. (2009) for diets that differed in type of linseed supplemented. Nonetheless, the study of Mohammed et al. (2011) included a linseed treatment which is high in *cis*-9,12,15-C18:3 and indicated a moderate negative correlation which was observed between concentration of *cis*-9,12,15-C18:3 in milk fat and CH_4 production in (g/d). Additional evaluation of the rumen microbial metabolism of *cis*-9,12,15-C18:3 seems thus to be necessary to better understand these contrasting findings.

Various *trans*- and *cis*-C18:1 milk FA concentrations were negatively related to CH_4 yield (g/kg DMI), as shown in Table 4. In general, *trans*-11-C18:1 is the major monounsaturated biohydrogenation intermediate of both *cis*-9,12,15-C18:3 and

cis-9,12-C18:2 (e.g., Shingfield et al., 2010). These polyunsaturated FA inhibit CH_4 production and milk *trans*-11-C18:1 concentration is therefore expected to be negatively related to CH_4 yield. With reduced rumen pH values, the predominant biohydrogenation pathway of *cis*-9,12-C18:2 may shift to *trans*-10-C18:1 (Colman et al., 2012) and low rumen pH is negatively associated with CH_4 production (Ellis et al., 2008). Besides, diets rich in unsaturated FA often cause a shift to *trans*-10-C18:1 formation (Mohammed et al., 2011) also when 70% of the diet is roughage (Boeckaert et al., 2008). These observations explain the strong negative correlation (r = -0.56) obtained between milk *trans*-10+11-C18:1 concentration and CH_4 yield. *cis*-11-C18:1 and *cis*-12-C18:1 and the fraction *trans*-6+7+8+9-C18:1 also result from biohydrogenation of both *cis*-9,12-C18:2 and *cis*-9,12,15-C18:3 (e.g., Jouany et al., 2007; Shingfield et al., 2010) like *trans*-10+11-C18:1 and this explains their significantly negative strong (r = -0.53; *cis*-11-C18:1), moderate ($r = -0.40$; *cis*-12-C18:1) and weak ($r = -0.27$; *trans*-6+7+8+9-C18:1) relationship of concentrations of these FA with CH_4 yield.

Depending on their FA composition, different dietary lipids result in variable biohydrogenation products. Milk *trans*-16+*cis*-14-C18:1 concentration tended to be moderately negative related to CH_4 yield ($r = -0.35$). Elevated levels of *trans*-16-C18:1 have been found in duodenal digesta (Glasser et al., 2008) and in milk (Kliem et al., 2009) upon supplementing diets with feed ingredients rich in *cis*-9,12,15-C18:3. *trans*-16+*cis*-14-C18:1 also appeared as an in vitro rumen biohydrogenation product of *cis*-9,12,15-C18:3 (Jouany et al., 2007), which might suggest milk *cis*-14-C18:1 to be derived from *cis*-9,12,15-C18:3. *cis*-13-C18:1 was increased in milk when increased contents of corn silage were fed (Kliem et al., 2008) and was increased in vitro when *cis*-9,12-C18:2 or *cis*-9,12,15-C18:3 were used as a substrate (Jouany et al., 2007). In this meta-analysis, the relationship tended to be weakly negative ($r = -0.26$) and may suggest *cis*-13-C18:1 to be derived from both *cis*-9,12-C18:2 and *cis*-9,12,15-C18:3. The positive response of milk *cis*-13-C18:1 concentration to dietary linseed oil supplementation (Loor et al., 2004), further supports this.

Milk *cis*-9-C18:1 concentration was not significantly related to CH_4 yield in the present meta-analysis. The absence of a significant relationship is in line with the analysis of Mohammed et al. (2011), whereas Chilliard et al. (2009) did find a significantly negative relationship. *cis*-9-C18:1, which inhibits CH_4 production (e.g., Patra, 2013), is present in many feedstuffs and might be less sensitive to biohydrogenation than other unsaturated FA in high concentrate diets (Loor et al., 2004). Nonetheless, *cis*-9-C18:1 is converted into *trans*-C18:1 isomers in the rumen possibly contributing to the negative correlations between concentrations of several

milk *trans*-C18:1 isomers and CH_4 yield as obtained in this study and discussed earlier (e.g., Shingfield et al., 2010). Δ^9-desaturation of C18:0 in the mammary gland is another mechanism by which *cis*-9-C18:1 appears in milk. Furthermore, dietary C18:0, being a possible substrate for Δ^9-desaturase, was not observed to inhibit CH_4 production (Patra, 2013), so does not contribute to a relation of milk *cis*-9-C18:1 and C18:0 concentrations with CH_4 yield. In line with this and Mohammed et al. (2011), no relationship between milk C18:0 concentration and CH_4 yield was found in this meta-analysis. This is in contrast with Chilliard et al. (2009) who found a negative relationship, possibly coming from dietary linoleic and linolenic acid, which were biohydrogenated to C18:0 that was absorbed. Concentration of C20:0 in milk fat is an elongation product by action of elongase enzymes on C18:0 from the diet or body fat. The fact that milk C20:0 concentration and CH_4 yield were not related in the present meta-analysis is in line with C18:0 concentration not being related overall to CH_4 yield.

Evaluation of heterogeneity

Milk C6:0, C8:0, C10:0 and C16:0 concentrations were not substantially heterogeneously correlated to CH_4 yield per unit of feed (Table 2.3). These relatively low heterogeneity may indicate a good precision of the estimated relationships and the simplicity of the mechanism determining the relationship. Next to *de novo* FA synthesis and feed, body fat is another resource of milk C16:0 (Gross et al., 2011). Nonetheless, the *de novo* FA synthesis that regulates milk C16:0 concentration is positively associated with CH_4 yield. Milk C16:0 from body fat and feed may not induce heterogeneity among the relationship. Unlike other saturated even-chain FA, milk C12:0 and C14:0 concentration showed substantial heterogeneity among their true correlation with CH_4 yield. Variation in diet composition, in particular when ingredients relatively rich in C12:0 and C14:0 are supplied to cattle (discussed in a previous section), may explain such heterogeneity. The sum of all *de novo* synthesized even-chain FA concentrations (C4:0 to C16:0, including C12:0 and C14:0) did not show any heterogeneity among its true correlation (Table 2.4). The correlation of milk C14:0-*iso*, C15:0-*anteiso*, C15:0, C17:0 (Table 2.3) and of combined OBCFA concentrations, viz. C14:0-*iso*+C16:0-*iso* and C15:0+C17:0 (Table 2.4), were all substantially heterogeneous ($I^2 \geq 61.1\%$). The heterogeneity observed for these milk OBCFA concentrations might reflect the variation in microbial species and activities in the rumen. All concentrations of individual C18:1 fractions, appeared to be substantially heterogeneous $I^2 \geq 50\%$, except the fraction *trans*-6+7+8+9-C18:1 that was totally homogeneous (Table 2.3). The combination

Table 2.4: Estimated true correlation coefficient with standard error and P-values, P-values for heterogeneity test statistic (Q-value P), and heterogeneity as a fraction of total variability (I^2) for the correlation between CH_4 yield per unit of feed and milk FA concentration.

Milk FA combination	***r***	**SE**	**P-value**	**Q-value P**	I^2(%)
C6:0+C8:0+C10:0	0.22	0.11	0.050	0.173	34.0
C6:0+C8:0+C10:0+C16:0	0.34	0.10	<0.001	0.149	16.1
C12:0+C14:0	–0.02	0.20	0.919	<0.001	79.4
Even-chain C4:0 to C16:0	0.26	0.09	0.003	0.501	0.0
C16:0+C18:0	0.42	0.09	<0.001	0.128	5.6
C15:0+C17:0	–0.07	0.16	0.677	0.005	66.4
C14:0-*iso*+C16:0-*iso*[a]	0.24	0.15	0.108	0.012	61.1
trans-C18:1[b]	–0.52	0.18	<0.001	0.009	66.0
cis-C18:1[c]	–0.52	0.10	<0.001	0.570	0.0
C18:1[d]	–0.56	0.16	<0.001	0.003	68.5
C18:1[e]	–0.49	0.14	<0.001	0.079	42.1
C18:1[f]	–0.56	0.15	<0.001	0.045	52.5
C18:2+C18:3	–0.21	0.10	0.042	0.170	19.7

[a] No data for experiment 7;
[b] *trans*-6+7+8+9+10+11-C18:1, no data for experiment 5;
[c] *cis*-11+12+13-C18:1, no data for experiment 5;
[d] *trans*-10+11-C18:1+*cis*-12+13-C18:1;
[e] *trans*-6+7+8+9+16-C18:1+*cis*-11+12+13+14-C18:1, no data for experiment 5;
[f] *trans*-6+7+8+9+10+11+16-C18:1+*cis*-11+12+13+14-C18:1, no data for experiment 5.

of these four different FA may balance out all heterogeneity but does not indicate homogeneity for the correlation of the four individual FA concentrations. The correlation of the concentration of a combined fraction of milk *cis*-11+12+13-C18:1 with CH_4 yield also was homogeneous even though substantial heterogeneity was observed using the individual milk FA concentrations (Table 2.4). Substantial heterogeneity did appear for correlations between CH_4 yield and concentrations of all combined fractions of C18:1 isomers that contained *trans*-10+11-C18:1 and a tendency for heterogeneity when *trans*-16+*cis*-14-C18:1 was added to the fraction *trans*-6+7+8+9-*cis*-11+12+13-C18:1 (Table 2.4). Various concentrations of fractions with milk *trans*-C18:1 isomers and *cis*-9,12-C18:2 ($I^2 = 59.0\%$) did, therefore, not appear as precise indicators of CH_4 yield, whereas milk *cis*-11+12+13-C18:1 and *trans*-6+7+8+9-C18:1 concentration did. C18:1 isomers in milk other than isomers containing a *cis*-9 double bond mainly originate from the rumen, but micro-organisms and enzymes responsible for their production are not well characterized and candidate bacterial species have yet to be cultivated (Wallace et al., 2007; Lourenço et al., 2010). Isolation of bacterial species may help to better interpret heterogeneity and homogeneity observed.

Correlation per unit of milk

Positive relationships were obtained between CH_4 yield (g/kg FPCM) and the milk FA concentration of C10:0, C12:0, C14:0, *cis*-9-C14:1, C15:0 and C16:0. Concentration of C14:0-*iso* tended to be positively related to CH_4 yield. Negative relationships or a tendency for a negative relationship were obtained between CH_4 yield and the milk FA concentration of C18:0, *cis*-9-C18:1, *cis*-11-C18:1, *trans*-10+11-C18:1 and *cis*-9,12-C18:2. These relationships and the absence of significant relationships between CH_4 yield and milk FA concentration of C17:0, *cis*-9,12,15-C18:3 and C20:0 are largely in agreement with the correlations obtained when CH_4 yield was expressed per unit of feed. In contrast with CH_4 yield per unit of feed, no positive relationships were obtained between CH_4 yield per unit of milk and milk FA concentration of C6:0 and C8:0, and a negative relationship occurred for the concentration of C4:0. Moreover, no significant relationship was obtained between the milk FA concentrations of *trans*-6+7+8+9-C18:1, *cis*-12-C18:1, *cis*-13-C18:1 and *trans*-16+*cis*-14-C18:1 and CH_4 yield per unit of milk. This might be due to the fact that various biohydrogenation intermediates associated with a reduction in CH_4 yield per unit feed (Table 2.3) are associated with milk fat depression (e.g., Piperova et al., 2000), which negatively impacts on the amount of FPCM, thus yielding more CH_4 yield per unit of milk. A reduced correlation strength for *trans*-10+11-C18:1 per unit

of feed and milk ($r = -0.56$ vs. $r = -0.16$, respectively) is in line with this. The negative relationship between CH_4 yield per unit of milk and the concentration of C18:0 in milk fat may be explained by the concentration of C18:0 being decreased during lactation (Stoop et al., 2009) when milk yield decreases and next CH_4 yield per unit of milk increases. Milk FA concentration of the fraction odd-chain C5:0 to C15:0 and of *cis*-9-C18:1 are decreased and increased, respectively, during negative energy balance in early lactation (Stoop et al., 2009; Gross et al., 2011) when cows are high producing. High milk production is associated with lower CH_4 yield per unit of milk which may explain why milk FA concentrations of C15:0 and *cis*-9-C18:1 were positively and negatively related to CH_4 yield per unit of milk, as also obtained by Chilliard et al. (2009). Concentrations of C15:0-*anteiso* and C16:0-*iso* in milk fat were not significantly related to CH_4 yield per unit of milk, possibly attributed to the fact that the proportion of branched-chain FA does not vary during lactation (Stoop et al., 2009).

Most of the milk FA that were significantly correlated, or tended to be correlated, with CH_4 yield per unit of milk showed relatively low heterogeneity, with the exception of C14:0-*iso*, C15:0 and *cis*-11-C18:1 (Table 2.3). In general, milk FA concentrations may therefore be regarded as precise indicators of CH_4 yield per unit of milk.

Correlations between CH_4 yield (g/kg FPCM) and combined milk FA concentrations were significantly positive for C10:0+C12:0+C14:0, C10:0+C12:0+C14:0+C16:0, even-chain C4:0 to C16:0 and C16:0+C18:0 and significantly negative or tended to be negative for the various combined fractions consisting of C18:1 isomers and for the sum of C18:2 and C18:3 (Table 2.5). The strongest positive and negative correlations were not stronger than for correlations based on single FA fractions, 0.36 vs. 0.36 for C10:0+C12:0+C14:0+C16:0 and C12:0, and –0.43 vs. –0.45 for *trans*-10+11-C18:1+*cis*-9+11-C18:1 and *cis*-11-C18:1, respectively. The fractions of even-chain saturated FA and C18:1 isomers were not or not substantially heterogeneously correlated. Concentrations of combined fractions of milk OBCFA, viz. C15:0+C17:0 and C14:0-*iso*+C16:0-*iso*, were not related to CH_4 yield (g/kg FPCM), which is in line with absence of such relationships of CH_4 yield per unit feed. In general, most combined and single concentration of milk FA show less heterogeneity in the correlation with CH_4 yield per unit of milk than with CH_4 yield per unit of feed.

Table 2.5: Estimated true correlation coefficient with standard error and P-values, P-values for heterogeneity test statistic (Q-value P), and heterogeneity as a fraction of total variability (I^2) for the correlation between CH_4 yield per unit of milk and milk FA concentration.

Milk FA combination	r	**SE**	**P-value**	**Q-value P**	I^2(%)
C6:0+C8:0	0.08	0.090	0.384	0.753	0.0
C10:0+C12:0+C14:0	0.30	0.112	0.006	0.182	33.1
C10:0+C12:0+C14:0+C16:0	0.36	0.090	<0.001	0.982	0.0
Even-chain C4:0 to C16:0	0.34	0.090	<0.001	0.979	0.0
C16:0+C18:0	0.23	0.090	0.010	0.794	0.0
C15:0+C17:0	0.23	0.154	0.128	0.009	64.3
C14:0-*iso*+C16:0-*iso*[a]	0.22	0.183	0.233	0.002	73.6
trans-C18:1[b]	–0.17	0.103	0.092	0.720	0.0
cis-C18:1[c]	–0.41	0.103	<0.001	0.809	0.0
C18:1[d]	–0.43	0.090	<0.001	0.864	0.0
C18:1[e]	–0.43	0.103	<0.001	0.735	0.0
C18:1[f]	–0.42	0.103	<0.001	0.734	0.0
C18:2+C18:3	–0.24	0.090	0.007	0.516	0.0

[a] No data for experiment 7;
[b] *trans*-6+7+8+9+10+11-C18:1, no data for experiment 5;
[c] *cis*-9+11+12+13-C18:1, no data for experiment 5;
[d] *trans*-10+11-C18:1+cis-9+12+13-C18:1;
[e] *trans*-10+11-C18:1+cis-9+11-C18:1, no data for experiment 5;
[f] *trans*-6+7+8+9+10+11+16-C18:1+cis-9+11+12+13+14-C18:1, no data for experiment 5.

2.3.2 Mixed model regression analysis

CH_4 yield per unit of feed

Mixed model fits to evaluate the potential to predict CH_4 yield (g/kg DMI) using selected milk FA concentrations (g/100 g FA) resulted in R^2-values of 0.15 and 0.17 for the concentration of milk C16:0 and the fraction C6:0+C8:0+10:0+C16:0, respectively (Figure 2.1). Thus, the concentration of the fraction C6:0+C8:0+10:0+C16:0 did not show a substantially stronger positive relationship with CH_4 yield than the concentration of C16:0 alone. R^2-values were 0.20, 0.41, 0.31 and 0.41 for the prediction with milk FA concentrations of *trans*-6+7+8+9-C18:1, *cis*-11-C18:1, *cis*-11+12+13-C18:1 and C18:1 (*trans*-6+7+8+9+10+11+16-C18:1+*cis*-11+12+13+14-C18:1), respectively. Concentrations of C18:1 fractions that were grouped together did not result in a substantially stronger negative relationship with CH_4 yield than concentrations of single C18:1 fractions.

The best multiple regression to predict CH_4 yield using concentrations of milk FA is:

$$\begin{aligned} \text{CH}_4 \text{ (g/kg DMI)} \quad = \quad & 23.39 \pm 1.21 + 9.74 \pm 3.23 \cdot \text{C16:0-}\textit{iso} \\ & -1.06 \pm 0.17 \cdot \text{ (}\textit{trans}\text{-10+}\textit{trans}\text{11)-C18:1} \\ & -1.75 \pm 0.49 \cdot \textit{cis}\text{-9,12-C18:2}, \end{aligned} \tag{2.3}$$

where milk FA concentrations are in g/100 g total FA, $R^2 = 0.54$ after correction for experiment effect (St-Pierre, 2001) and $P \leq 0.003$ for all parameters. The model acceptably reproduced the CH_4 yield (Figure 2.2), as the slope and intercept of the regression between observed vs. predicted values did not differ from 1 and 0, respectively (results not shown). No clear patterns appear in the observed vs. predicted values of CH_4 yield and residual vs. predicted values of CH_4 yield (Figure 2.2), which does not indicate substantial bias or heteroscedasticity. The obtained R^2 is larger than for concentrations of single milk FA fractions but smaller than 0.73 that Dijkstra et al. (2011) obtained for their equation based on 3 experiments, and also lower than 0.82 Mohammed et al. (single experiment 2011, only FA concentrations included in prediction equation) and 0.95 Chilliard et al. (single experiment 2009, milk FA concentration and forage intake in prediction equation). The data used by Dijkstra et al. (2011) are also included in the present analysis. The larger number of studies included in our meta-analysis, including a wider variety of diet composition, may have caused the lower R^2 of Equation 2.3. A similar issue may hold when comparing the multiple regression analysis of Dijkstra et al. (2011) with the analyses of Mohammed

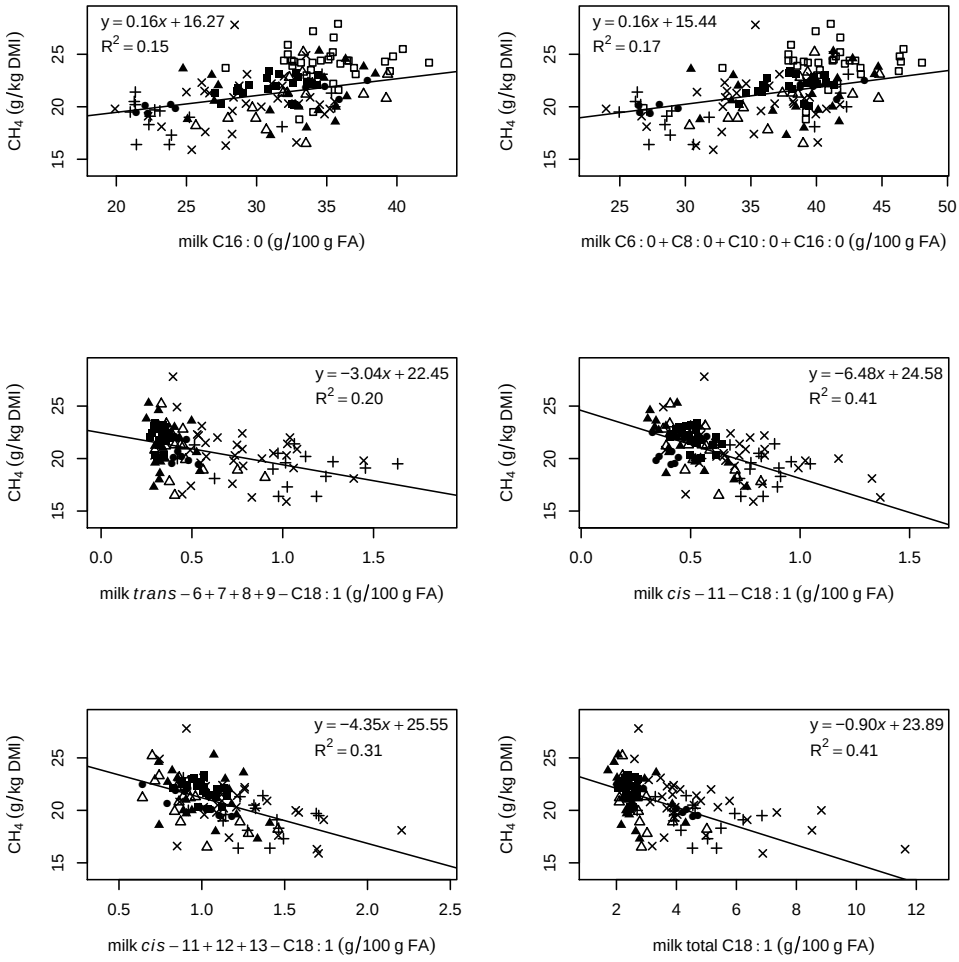

Figure 2.1: Relationships between CH_4 yield (g/kg DMI) and selected milk FA concentrations. Milk total C18:1 comprises trans-6+7+8+9-C18:1, trans-10+11-C18:1, cis-11-C18:1, cis-12-C18:1, cis-13-C18:1 and trans-16+cis-14-C18:1 from experiments 1 to 4 and 6 to 8. The different symbols identify the eight individual experiments (see Figure 2.2 for explanation).

et al. (2011) based on sunflower seed, linseed and canola seed supplemented diets and Chilliard et al. (2009) based on linseed supplements only. On the other hand, Dijkstra et al. (2011) did not include forage intake in their equation and expressed CH_4 yield in g/kg DMI whereas Chilliard et al. (2009) and Mohammed et al. (2011) expressed CH_4 production in g/d. Furthermore, the substantial heterogeneity of the correlation of CH_4 yield and milk FA concentrations of several C18:1 isomers found in the present analysis may limit a precise prediction of CH_4 yield (g/kg DMI) using milk FA profile.

Equation 2.3 of the present meta-analysis has various milk FA concentrations in common with previously reported equations. Milk C16:0-*iso* concentration did appear in the best equation of Mohammed et al. (2011). Milk *trans*-10+11-C18:1 concentration was also included by Dijkstra et al. (2011), and Mohammed et al. (2011) included all *trans*-C18:1 FA concentrations in their second best equation based on milk FA concentrations and DMI. Milk *cis*-9,12-C18:2 concentrations was also present in the best equation of Chilliard et al. (2009). However, milk *cis*-9,12-C18:2 concentration was positively related to CH_4 in that equation, whereas it was negatively related in Equation 2.3.

Different FA concentrations available for selection in different studies may hamper the development of a universally valid CH_4 prediction equation based on milk FA concentrations. A stepwise selection was also performed for concentrations of all milk FA that were available in seven experiments to extend the number of available FA with C14:0-*iso*, *trans*-6+7+8+9-C18:1, *cis*-11-C18:1 and *trans*-16+*cis*-14-C18:1. Methane yield was best predicted by the concentration of C16:0-*iso* (positively related) and the concentrations of *cis*-11-C18:1 and *trans*-16+*cis*-14-C18:1 (both negatively related), with $P \leq 0.02$ for all regressors and $R^2 = 0.55$. *cis*-11-C18:1 concentration was also present in the equation of Dijkstra et al. (2011) and in the second best equation of Mohammed et al. (2011), and *trans*-16+*cis*-14-C18:1 concentration also appeared in the best and second best equation of Chilliard et al. (2009). However, this equation is not preferred over Equation 2.3 because it is based on one less experiment and the coefficient of determination is just marginally higher.

Besides gas chromatography, Fourier transform infrared spectroscopy (FTIR) is often applied to quantify FA concentrations in milk. To achieve a reasonable accuracy of milk FA concentrations with FTIR, FA should have an average concentration of $\geq$ 2.45 g/100 g FA (Rutten et al., 2009). Restricting the selection of milk FA with this threshold concentration would have resulted in a best equation based on positive relationships of concentrations of C14:0, C16:0 and C18:0 and $R^2 = 0.29$. More recently, Soyeurt et al. (2011) found concentrations of milk C4:0, C6:0, C8:0, C10:0, C12:0, C14:0, C16:0, C18:0, all *trans*-C18:1, *cis*-9-C18:1, all *cis*-C18:1 and

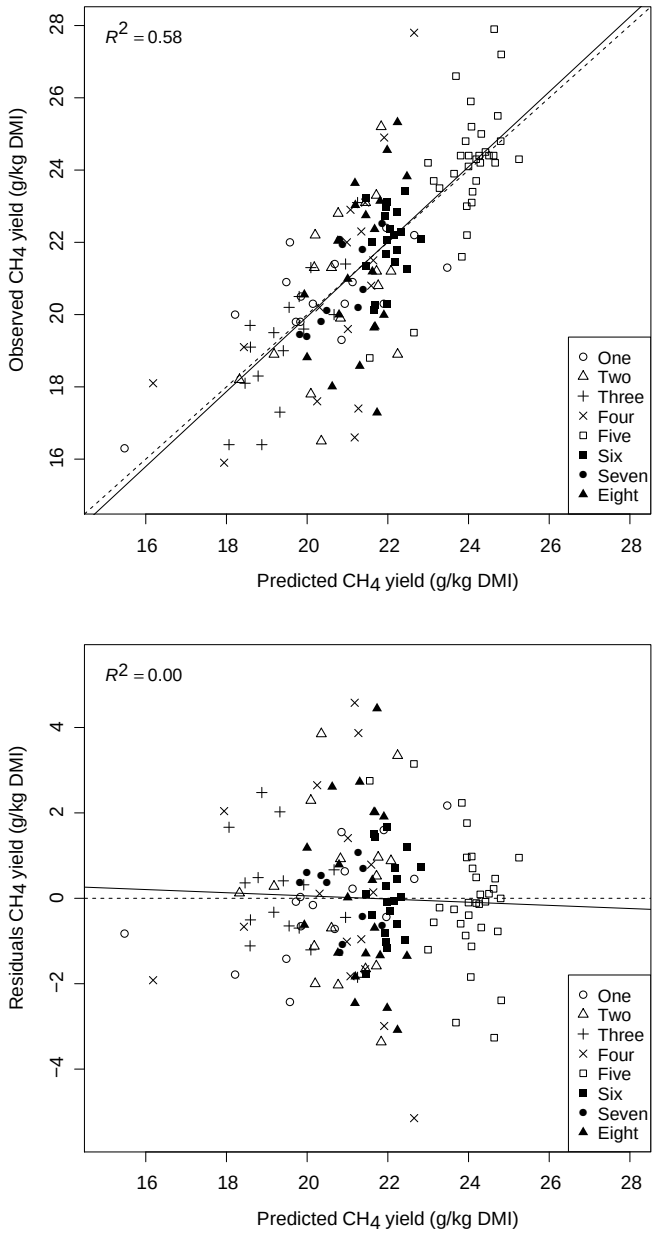

Figure 2.2: Observed vs. predicted (upper panel) and residuals (predicted minus observed) vs. predicted (lower panel) CH_4 yield per unit of feed from Equation 2.3 including experiment as a discrete class variable with experiment effect not shown. The different symbols identify the eight individual experiments. The line of unit slope (left panel) and the horizontal line (right panel) represent the line of equivalence.

some groups of FA in milk to be sufficiently accurate determined by FTIR to be used in milk payment systems. Including these FA concentrations mentioned by Soyeurt et al. (2011) in a selection procedure resulted in a best equation with a negative relationship of all *trans*-C18:1 concentration, where it is noted that the *trans*-C18:1 fraction consisted all *trans*-C18:1 available in studies 1 to 4 and 6 to 8. $R^2 = 0.43$ for this equation and is lower than R^2 obtained for Equation 2.3. Several milk FA with lower concentrations that appear in various equations published previously are not available when milk FA profile is determined with FTIR. Furthermore, concentrations of combined FA fractions, several of which are accurately determined with FTIR, did not substantially increase the potential for predicting CH_4 yield (Figure 2.1). Compared to gas chromatography, the current performance of FTIR therefore limits the potential for predicting CH_4 yield based on milk FA profile.

CH_4 yield per unit of milk

The best multiple regression to predict CH_4 yield using concentrations of milk FA is:

$$\begin{aligned} \text{CH}_4 \text{ (g/kg FPCM)} \quad = \quad & 21.13 \pm 1.72 - 1.38 \pm 0.38 \cdot \text{C4:0} \\ & +8.53 \pm 3.05 \cdot \text{C16:0-}\textit{iso} - 0.22 \pm \ 0.04 \cdot \textit{cis}\text{-9-C18:1} \\ & -0.59 \pm 0.18 \cdot \textit{trans}\text{-10+}\textit{trans}\text{11-C18:1}, \end{aligned} \tag{2.4}$$

where $R^2 = 0.47$ after correction for experiment effect (St-Pierre, 2001) and $P \leq 0.006$ for all parameters. The model acceptably reproduced the CH_4 yield (Figure 2.3), as the slope and intercept of the regression between observed vs. predicted values did not differ from 1 and 0, respectively (results not shown). No clear patterns appear in the observed vs. predicted values of CH_4 yield and residual vs. predicted values of CH_4 yield (Figure 2.3), which does not indicate substantial bias or heteroscedasticity. The obtained R^2 is somewhat smaller than for the prediction of CH_4 yield per unit of feed. Equation 2.4 also contains milk C16:0-*iso* and *trans*-10+11-C18:1 concentration like Equation 2.3 to predict CH_4 yield per unit of feed. Therefore, this may be regarded as further evidence for concentrations of milk C16:0-*iso* and *trans*-10+11-C18:1 to be appropriate predictors of CH_4 yield.

Restricting the selection of milk FA with a threshold concentration of 2.45 g/100 g FA for reasonable accuracy using FTIR would have resulted in a best prediction equation based on negative relationships of concentrations of C4:0 and *cis*-9-C18:1, and $R^2 = 0.28$. Including the FA concentrations mentioned by Soyeurt et al. (2011) in the selection procedure resulted in a best equation based on negative relationships of concentrations of C4:0, *cis*-9-C18:1 and total *trans*-C18:1, and $R^2 = 0.36$. It is

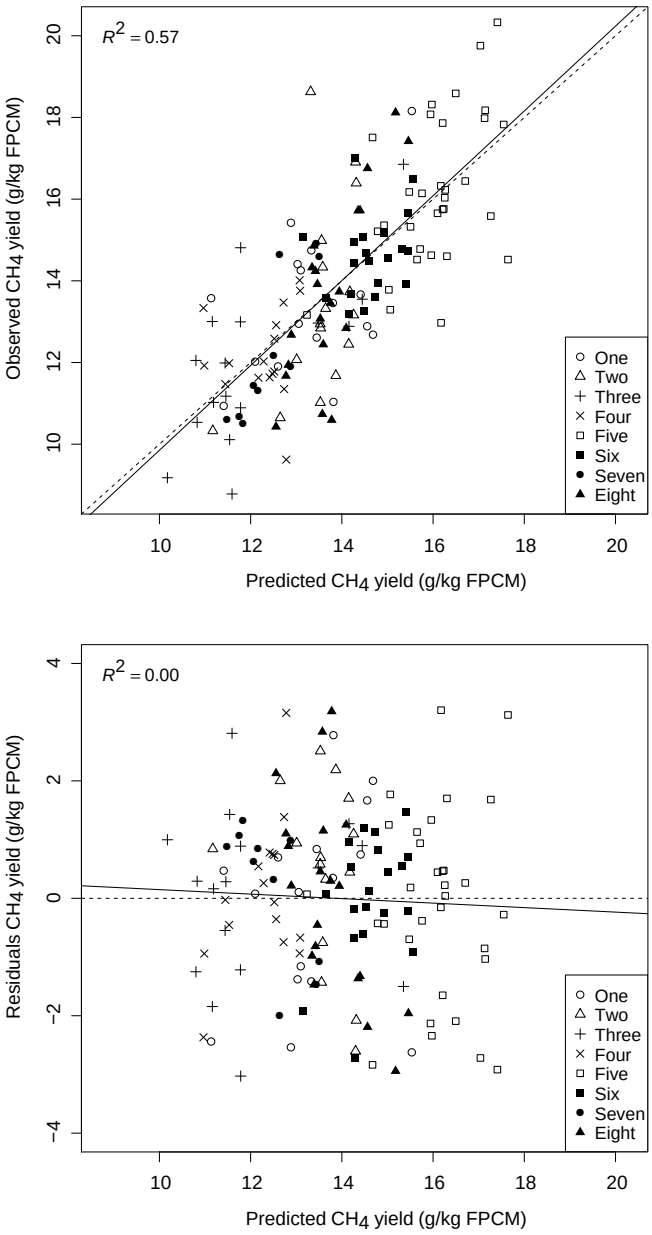

Figure 2.3: Observed vs. predicted (upper panel) and residuals (predicted minus observed) vs. predicted (lower panel) CH_4 yield per unit of milk from Equation 2.4 including experiment as a discrete class variable with experiment effect not shown. The different symbols identify the eight individual experiments. The line of unit slope (left panel) and the horizontal line (right panel) represent the line of equivalence.

noted that all FA available in studies 1 to 4 and 6 to 8 were included in the selection procedure because *trans*-10+11-C18:1 is the only *trans*-C18:1 fraction available in all eight studies. Similar to prediction of CH_4 yield per unit feed, these results indicate that current performance of FTIR limits the potential for predicting CH_4 yield per unit of milk based on milk FA profile, compared to gas chromatography.

The present meta-analysis showed that milk FA profile has a moderate potential to predict CH_4 yield. Further improvement in ability of milk FA based models to predict CH_4 yield may be achieved by distinguishing diets with or without lipid supplements and by including diet composition characteristics. The present dataset was too small to allow separate analyses of lipid-supplemented and non-lipid supplemented diets, and more data may be required to analyze possible effects of lipid supplements on the relationship. On diet composition, Mohammed et al. (2011) already indicated that the combination of milk FA profile and diet characteristics may improve prediction performance. For practical application, this requires knowledge of diet composition (including forage to concentrate ratio and chemical composition of feed consumed) which may not always be available.

2.4 Conclusion

Various FA concentrations in milk fat appeared to be weakly, moderately or strongly related to CH_4 yield per unit of feed. Milk C6:0, C8:0, C10:0, C16:0 and C16:0-*iso* concentrations showed positive relationships, whereas milk *cis*-9,12-C18:2, *trans*-10+11-C18:1, *cis*-11-C18:1, *cis*-12-C18:1, *cis*-13-C18:1 and *trans*-16+*cis*-14-C18:1 concentrations showed weak to strong negative relationships with CH_4 yield. Milk OBCFA concentrations C14:0-*iso*, C15:0-*anteiso*, C15:0, C17:0 as well as milk C4:0, C12:0, C14:0, *cis*-9-C14:1, C18:0, *cis*-9-C18:1, *cis*-9,12,15-C18:3 and C20:0 concentrations were not significantly related to CH_4 yield per unit of feed. When expressing CH_4 yield per unit of milk, relationships of milk C10:0, C15:0-*anteiso*, C16:0, C17:0, *trans*-10+11-C18:1, *cis*-11-C18:1, *cis*-9,12-C18:2, *cis*-9,12,15-C18:3 and C20:0 concentrations were in line with relationships expressing CH_4 yield per unit of feed. Concentrations of C18:1 isomers in milk fat showed more heterogeneity among the true correlation with CH_4 yield per unit of feed than concentrations of the saturated even-chain FA C6:0, C8:0, C10:0 and C16:0. Mixed model multiple regression resulted in various milk FA included in optimal equations to predict CH_4 yield per unit of feed and per unit of milk, with C16:0-*iso* and *trans*-10+11-C18:1 concentrations appearing in both equations. These regressions indicated a moderate potential for using milk FA profile to predict CH_4 yield per unit of feed and per unit of milk.

Supporting information

Table S1: Raw correlation coefficients between CH_4 yield (g/kg DMI) and for the resolved milk FA concentrations (g/100 g FA) for each separate experiment.

Milk FA	**Experiment**							
	1	2	3	4	5	6	7	8
C4:0	0.48	0.34	-0.22	0.62	-0.05	-0.26	0.05	-0.422
C6:0	0.40	0.57	-0.15	0.46	0.07	-0.17	0.25	0.218
C8:0	0.36	0.61	0.01	0.40	0.13	-0.39	0.24	0.466
C10:0	0.28	0.57	0.09	0.24	0.08	-0.26	0.18	0.349
C12:0	-0.37	0.43	0.19	0.18	0.05	-0.15	-0.82	0.640
C14:0	-0.24	0.40	0.22	0.30	-0.04	-0.10	-0.91	0.433
C14:0-*iso*[a]	0.19	0.62	0.60	0.21	-0.41	-0.04	NA	0.58
cis-9-C14:1	-0.47	-0.17	0.36	-0.40	-0.17	0.01	-0.82	0.33
C15:0-*anteiso*	0.26	0.11	0.35	-0.65	-0.09	-0.47	-0.86	0.19
C15:0	-0.79	0.36	0.41	-0.62	0.12	-0.22	-0.45	0.20
C16:0-*iso*	0.06	0.24	0.67	0.57	-0.18	0.05	0.49	-0.00
C16:0	0.13	0.464	0.39	0.30	0.10	0.38	0.91	0.15
C17:0	-0.06	-0.03	0.48	-0.43	0.34	-0.23	0.83	-0.14
C18:0	0.31	-0.21	-0.42	0.51	0.25	-0.09	0.04	0.02
trans-6+7+8+9-C18:1	-0.06	-0.49	-0.38	-0.52	NA	0.01	-0.42	-0.11
trans-10+11-C18:1	-0.74	-0.45	-0.51	-0.58	-0.73	0.14	-0.90	-0.38
cis-9-C18:1[b,c]	0.42	-0.63	-0.17	-0.22	0.04	-0.23	0.60	-0.56
cis-11-C18:1	-0.64	-0.72	-0.35	-0.49	NA	-0.47	0.37	-0.78
cis-12-C18:1	0.48	-0.41	-0.31	-0.55	-0.58	-0.45	-0.92	0.03
cis-13-C18:1	-0.29	-0.75	-0.22	-0.48	-0.38	0.16	-0.30	0.29
trans-16+*cis*-14-C18:1	0.36	-0.45	-0.54	-0.57	NA	-0.02	-0.91	0.06
cis-9,12-C18:2	0.27	-0.51	-0.02	-0.45	-0.42	-0.54	0.61	-0.45
cis-9,12,15-C18:3	0.03	-0.13	-0.09	-0.35	0.23	0.15	-0.37	0.02
C20:0[d,e]	0.17	0.22	-0.38	0.65	-0.41	-0.11	-0.12	-0.23

[a] 19 observations in experiment 8; [b] co-eluted with *trans*-13+14-C18:1 in experiments 1 and 3; [c] co-eluted with *trans*-12-C18:1 in experiment 5; [d] 8 observations in experiment 7; [e] 13 observations in experiment 8.

Chapter 3

Thermodynamic driving force of hydrogen on rumen microbial metabolism: a theoretical investigation

Henk J. van Lingen[1,2,*], Caroline M. Plugge[3], James G. Fadel[4], Ermias Kebreab[4], André Bannink[5], Jan Dijkstra[2]

1 TI Food and Nutrition, Wageningen, The Netherlands
2 Animal Nutrition Group, Wageningen University, Wageningen, The Netherlands
3 Laboratory of Microbiology, Wageningen University, Wageningen, The Netherlands
4 Department of Animal Sciences, University of California, Davis, California, United States of America
5 Animal Nutrition, Wageningen UR Livestock Research, Wageningen, the Netherlands

PLoS ONE 11:e0168052, 2016

Abstract

Hydrogen is a key product of rumen fermentation and has been suggested to thermodynamically control the production of the various volatile fatty acids (VFA). Previous studies, however, have not accounted for the fact that only thermodynamic near-equilibrium conditions control the magnitude of reaction rate. Furthermore, the role of NAD, which is affected by hydrogen partial pressure (p_{H_2}), has often not been considered. The aim of this study was to quantify the control of p_{H_2} on reaction rates of specific fermentation pathways, methanogenesis and NADH oxidation in rumen microbes. The control of p_{H_2} was quantified using the thermodynamic potential factor (F_T), which is a dimensionless factor that corrects a predicted kinetic reaction rate for the thermodynamic control exerted. Unity F_T was calculated for all glucose fermentation pathways considered, indicating no inhibition of p_{H_2} on the production of a specific type of VFA (e.g., acetate, propionate and butyrate) in the rumen. For NADH oxidation without ferredoxin oxidation, increasing p_{H_2} within the rumen physiological range decreased F_T from unity to zero for different NAD^+ to NADH ratios and pH of 6.2 and 7.0, which indicates thermodynamic control of p_{H_2}. For NADH oxidation with ferredoxin oxidation, increasing p_{H_2} within the rumen physiological range decreased F_T from unity at pH of 7.0 only. For the acetate to propionate conversion, F_T increased from 0.65 to unity with increasing p_{H_2}, which indicates thermodynamic control. For propionate to acetate and butyrate to acetate conversions, F_T decreased to zero below the rumen range of p_{H_2}, indicating full thermodynamic suppression. For methanogenesis by archaea without cytochromes, F_T differed from unity only below the rumen range of p_{H_2}, indicating no thermodynamic control. This theoretical investigation shows that thermodynamic control of p_{H_2} on individual VFA produced and associated yield of hydrogen and methane cannot be explained without considering NADH oxidation.

Keywords: Volatile fatty acids, Methane production, NADH oxidation, Fermentation

3.1 Introduction

Carbohydrates ingested by ruminants are degraded into monomers by action of rumen microbial enzymes and subsequently fermented to products such as volatile fatty acids (VFA) and alcohols. The most common pathway of hexose metabolism in rumen microbes is glycolysis, which yields two equivalents of pyruvate, ATP and NADH. The NADH, a cofactor carrying electrons, needs to be oxidized back to NAD^+ to keep the glycolysis possible and to maintain further metabolic steps of the overall microbial metabolism that depend on pyruvate (Baldwin and Allison, 1983; Hegarty and Gerdes, 1999). The oxidation of NADH to NAD^+ may be directly coupled to the product formation from pyruvate that follows glycolysis. Production of butyrate couples the oxidation of NADH to the reduction of acetoacetyl-CoA as well as crotonyl-CoA (Buckel and Thauer, 2013). Various fermentative micro-organisms are also able to convert pyruvate into ethanol, lactate or succinate (Stams and Plugge, 2009), which results in direct oxidation of NADH. Acetate is quantitatively the main VFA in the rumen, but its production from pyruvate is not directly coupled to the oxidation of NADH. In this case, NADH is oxidized via H_2 production, which is thermodynamically inhibited at elevated hydrogen partial pressure (p_{H_2}). Oxidation of NADH may be thermodynamically feasible by coupling it to the oxidation of reduced ferredoxin (Schut and Adams, 2009). Many methanogenic archaea utilize H_2 to reduce CO_2 to CH_4. This keeps p_{H_2} at a low level, which enables NADH oxidation in bacteria that are not able to directly couple NADH oxidation to reduction of metabolites (Stams and Plugge, 2009).

Multiple estimates of rumen VFA (e.g., acetate, propionate, butyrate and other) production from feed substrate have been reported in literature based on factors including type of organic matter fermented and type of diet (Bannink et al., 2006). Such estimates are required in rumen models to predict the amount and type of VFA entering the intermediary metabolism of ruminants. Another application of these estimates is the prediction of enteric CH_4 production, which is of interest in terms of the environment. Accuracy of predicted CH_4 emission by the model used by Bannink et al. (2011) appeared to be mostly affected by the error in the representation of the molar proportion at which individual VFA are produced. Reducing this error contributes to more adequate prediction of enteric CH_4 emission (Alemu et al., 2011). A recent metabolic model of mixed culture fermentation (Zhang et al., 2013) represents how incorporation of thermodynamically controlled cofactor dynamics may improve the prediction of end products such as VFA from glucose fermentation.

Thermodynamic control of rumen fermentation pathways by p_{H_2} has been investigated to explain variation in observed VFA concentrations (Ungerfeld and

Kohn, 2006). Thermodynamic control is often evaluated by Gibbs energy change (ΔG). Negative values of ΔG indicate a reaction to proceed in the forward direction, positive values in the reverse direction, and $\Delta G = 0$ indicates equilibrium. Using ΔG, it has been explained that increased concentrations of H_2 result in a shift to pathways forming propionate at the expense of acetate as an alternative way of accepting electrons to H_2-forming pathways because the latter become thermodynamically less favorable (Janssen, 2010). Reaction rates of fermentation pathways have been prescribed by setting the quotient of kinetic rate constants for the forward and reverse reaction equal to the thermodynamic equilibrium constant (Ungerfeld and Kohn, 2006; Ghimire et al., 2014). However, the quotient of the rate laws for reverse and forward reaction does not necessarily reflect the stoichiometry of a reaction and is not in general similar to the thermodynamic equilibrium constant. Besides, classical thermodynamic functions such as ΔG have no implications for the magnitude of reaction rate, except for near-equilibrium situations (Manes et al., 1950), and may not rigorously account for the thermodynamic driving force on reaction (Jin and Bethke, 2007). Furthermore, various investigations on the control of p_{H_2} on rumen fermentation have ignored the role of NAD, or have mentioned it without quantifying the redox state as affected by varying p_{H_2} (e.g., Baldwin and Allison, 1983; Hegarty and Gerdes, 1999; Janssen, 2010; Ghimire et al., 2014). The aim of the present study is to quantify the thermodynamic effect of p_{H_2} on the reaction rate of specific fermentation pathways, NADH oxidation and methanogenesis in the rumen.

3.2 Methods

3.2.1 Metabolic pathways

Glucose can be fermented via various pathways depending on the microbial diversity and the conditions in the rumen environment. To quantify the effect of p_{H_2} on reaction rates, five rumen glucose fermentation pathways each yielding different VFA, three H_2-dependent interconversions of VFA (viz. acetate to propionate, propionate to acetate and butyrate to acetate), oxidation of NADH with and without reduced ferredoxin oxidation, and methanogenesis were considered (Table 3.1). Selected reactions focus on formation of VFA and have been taken from Buckel and Thauer (2013) for reactions b, j and k; Stams and Plugge (2009) for reactions a, g, h and i; Laanbroek et al. (1982) for reaction f; Hackmann and Firkins (2015) for reaction c when butyrate is produced via the kinase route; and Kettle et al. (2015) for reactions c when butyrate is produced via the CoA-transferase route, and reactions d and e. Conversions of acetate to butyrate, butyrate to propionate and propionate to

butyrate are discussed, but the effect of p_{H_2} on reaction rate is not shown because these conversions do not yield any H_2 or have limited physiological significance. Glucose fermentation reactions in Table 3.1 are ordered following the stoichiometry of H_2 formation. The number of NADH oxidized with H_2 formation for the interconversion reactions were obtained considering reactions f and g as linear combinations of reactions a and d, and reaction h as a linear combination of reactions a and c. Various other cofactors are involved in the microbial degradation of glucose as well, but only NAD is involved in both the glycolysis and in further metabolic pathways of pyruvate to VFA or other fermentation products. The redox state of this cofactor explains the shift in pathways of glucose fermentation and therefore the focus is on oxidation of NADH. Besides being involved in NADH oxidation via confurcation, ferredoxin is involved in the production of acetate and butyrate, which explains why the H_2 yield reported for metabolic pathways in Table 3.1 may not be equal to the number of NADH oxidized with H_2 formation.

Moreover, as has been compared to the formation of propionate at the expense of acetate, reductive acetogenesis may be a potential alternative H_2 sink to methanogenesis in the rumen (Ungerfeld, 2013), but will not be considered in the present investigation. Although this conversion is associated with carbon turnover and is common in environments such as the human colon (Kettle et al., 2015) and foregut of kangaroos and wallabies (Gagen et al., 2010), acetogenic bacteria in the rumen have been hypothesized to be unable to compete for H_2 with the methanogens (e.g., Le Van et al., 1998). Unless mentioned otherwise, respiration was assumed not to be occurring within the rumen microbiome.

3.2.2 Thermodynamic potential factor

The thermodynamic control on rates of rumen fermentation pathways was quantified using the thermodynamic potential factor (F_T) as derived by Jin and Bethke (2007). This factor modifies commonly used rate laws and makes them thermodynamically consistent by accounting for the difference between the energy available through fermentation and the energy conserved. The energy available through fermentation is calculated from the ratio of reactants and products, which is associated with the progress of the forward and reverse direction of a reaction. A rate law that accounts for the forward as well as the reverse direction of a reaction is thermodynamically consistent and may be represented as:

$$r = k[\mathrm{X}]\frac{[\mathrm{S}]}{[\mathrm{S}] + K_S}F_T, \tag{3.1}$$

Table 3.1: Possible glucose fermentation pathways to VFA (Ac^-, Pr^- and Bu^- for acetate, propionate and butyrate, respectively), volatile fatty acid (VFA) interconversions, hydrogenase-catalyzed NADH oxidation and methanogenesis in the rumen and their yield of ATP (Y_{ATP}), number of NADH to be oxidized with H_2 formation (Y_{NADH}, mol per mol of glucose), the standard reaction Gibbs energy (ΔG^o in kJ·mol^{-1}, standardized to concentrations of 1 M, pH of 0, gas pressure of 1 bar) adjusted to 312K, and the average stoichiometric number (χ).

Microbial conversion				$\mathbf{Y_{ATP}}$	$\mathbf{Y_{NADH}}$	ΔG^o	χ
Glucose fermentation							
a)	$C_6H_{12}O_6 + 4\,H_2O$	$\longrightarrow$	$2\,Ac^- + 2\,HCO_3^- + 4\,H_2 + 4\,H^+$	4	2	-52	4
b)	$C_6H_{12}O_6 + 2.67\,H_2O$[a]	$\longrightarrow$	$0.67\,Ac^- + 0.67\,Bu^- + 2\,HCO_3^- + 3.33\,H^+ + 2.67\,H_2$	3.33	0.67	-111	3.33
c)	$C_6H_{12}O_6 + 2\,H_2O$[b]	$\longrightarrow$	$Bu^- + 2\,HCO_3^- + 2\,H_2 + 3\,H^+$	3	0	-138	3
d)	$C_6H_{12}O_6 + H_2O$[c]	$\longrightarrow$	$Ac^- + Pr^- + HCO_3^- + H_2 + 3\,H^+$	3.67	0	-159	3
e)	$C_6H_{12}O_6$[d]	$\longrightarrow$	$0.67\,Ac^- + 1.33\,Pr^- + 0.67\,HCO_3^- + 2.67\,H^+$	2.67	-0.67	-196	2.67
VFA interconversion							
f)	$Ac^- + HCO_3^- + H^+ + 3\,H_2$	$\longrightarrow$	$Pr^- + 3\,H_2O$	0	-2	-113	1
g)	$Pr^- + 3\,H_2O$	$\longrightarrow$	$Ac^- + HCO_3^- + H^+ + 3\,H_2$	0.33	2	113	2
h)	$Bu^- + 2\,H_2O$	$\longrightarrow$	$2\,Ac^- + H^+ + 2\,H_2$	0.33	2	86	2
Cofactor oxidation							
i)	$NADH + H^+$	$\longrightarrow$	$NAD^+ + H_2$	0	NA	-25	1
j)	$NADH + Fd^{2-}_{RED} + 3\,H^+$	$\longrightarrow$	$NAD^+ + Fd_{OX} + 2\,H_2$	0	NA	-102	2
Methanogenesis							
k)	$HCO_3^- + H^+ + 4\,H_2$	$\longrightarrow$	$CH_4 + 3\,H_2O$	1.5 or 0.5[e]	0	-172	2

[a] Butyrate production via the kinase route;

[b] Either for butyrate production via the kinase route, or a linear combination of reaction a) and $2\,Ac^- + 2\,C_6H_{12}O_6 + 2\,H_2O \longrightarrow 3\,Bu^- + 4\,HCO_3^- + 2\,H_2 + 5\,H^+$ for butyrate production via the CoA-transferase route;

[c] Propionate production via succinate;

[d] Propionate production via lactate;

[e] For archaeal species with and without cytochromes.

with the kinetic rate constant k, the microbial biomass concentration [X], the substrate concentration [S] and the half-saturation constant K_{S}. Kinetic rate laws, however, are often developed assuming that a large thermodynamic force drives a metabolic reaction forward. Under this condition, kinetic rate laws do not need to be corrected with any factor like F_{T}. This assumption is reasonable when the environment is rich in chemical energy, that is where the metabolic reaction is far from equilibrium. The F_{T} is mathematically represented as:

$$F_{\mathrm{T}} = 1 - \exp\left(-\frac{\Delta G_{\mathrm{A}} - \Delta G_{\mathrm{C}}}{\chi RT}\right), \tag{3.2}$$

where ΔG_{C} is the energy conserved ($\mathrm{J{\cdot}mol^{-1}}$), which is commonly determined from the number of ATP produced times the Gibbs energy of phosphorylation ($Y_{\mathrm{ATP}}{\cdot}\Delta G_{\mathrm{P}}$; ΔG_{P} is approximated by 44 $\mathrm{kJ{\cdot}(mol\ ATP)^{-1}}$ for rumen microbes in the present study); ΔG_{A} is the energy available through fermentation ($\mathrm{J{\cdot}mol^{-1}}$); χ is the average stoichiometric number representing the number of times elementary steps of product formation occurs relative to the main reactant; R the gas constant (8.31 $\mathrm{J{\cdot}mol^{-1}{\cdot}K^{-1}}$); T the temperature (312K in the rumen); this makes F_{T} dimensionless by definition. For $\Delta G_{\mathrm{A}} \gg \Delta G_{\mathrm{C}}$ and common values of T and χ, F_{T} approaches 1 (also designated as unity), and the net reaction rate is 100% of the forward rate, and F_{T} can be neglected in determining rates of reaction in microbial metabolism. When ΔG_{A} approaches ΔG_{C}, the forward and reverse reaction approach equilibrium, which is reflected in F_{T} approaching zero. For $\Delta G_{\mathrm{A}} < \Delta G_{\mathrm{C}}$, F_{T} becomes negative, suggesting that a reaction net proceeds in the reverse direction; for $\Delta G_{\mathrm{A}} \ll \Delta G_{\mathrm{C}}$, and common values of T and χ, F_{T} approaches $-\infty$ suggesting that the forward reaction is even negligibly small compared to the reverse reaction. Negative F_{T} may not be useful for prediction of reaction rate since common rate laws of such as the Monod equation are not used for reactions that overall proceed in the reverse direction. At a microbial level, a reverse reaction would consume energy rather than contribute to a cell's energy budget, which is not enzymatically supported and the metabolism may stop.

The ΔG_{A} is further specified as:

$$\Delta G_{\mathrm{A}} = -\Delta G^{\mathrm{o}} - RT \ln Q, \tag{3.3}$$

with ΔG^{o} the standard reaction Gibbs energy, and Q the reaction quotient, which is:

$$Q = \prod_{J} a_{\mathrm{J}}^{\nu_{\mathrm{J}}}, \tag{3.4}$$

where a_{J} denotes the concentration of substance J, and ν_{J} its corresponding stoichiometric number in the chemical equation, which is positive for products and

negative for reactants. Substituting Equations 3.3 and 3.4 into Equation 3.2 yields:

$$F_{\mathrm{T}} = 1 - Q^{\chi^{-1}} \exp\left(\frac{\Delta G^{\mathrm{o}} + \Delta G_{\mathrm{C}}}{\chi RT}\right). \tag{3.5}$$

Substances that are in the gaseous state under rumen conditions are represented in partial pressure instead of aqueous concentrations; water activity is assumed to be 1 and omitted from the reaction quotient in any case. To illustrate, F_{T} for the glucose to acetate conversion (reaction a, Table 3.1) by substituting into Equation 3.5 gives:

$$F_{\mathrm{T}} = 1 - [\mathrm{Ac}^-]^{0.5}[\mathrm{HCO}_3^-]^{0.5} P_{\mathrm{H}_2} [\mathrm{H}^+][\mathrm{C}_6\mathrm{H}_{12}\mathrm{O}_6]^{-0.25} \exp\left(\frac{-52 \cdot 10^3 + 4 \cdot 44 \cdot 10^3}{4 \cdot 8.31 \cdot 312}\right). \tag{3.6}$$

3.2.3 Reaction specific energy conservation and elementary reaction steps

In anaerobic fermentation, ATP is mostly produced by substrate level phosphorylation, but some electron transport phosphorylation may take place during fermentations (Müller, 2008; Hackmann and Firkins, 2015). Reaction steps associated with electron transport phosphorylation include fumarate reduction in the pathways of pyruvate to propionate, crotonyl-CoA reduction in the pathway of acetyl-CoA to butyrate, and the oxidations of succinate and butyryl-CoA in the syntrophic conversions of propionate to acetate and butyrate to acetate. Yield of ATP (shown in Table 3.1 for every reaction considered) was assumed to be 2 for the common pathway of glucose to 2 pyruvate, and 2, 1.33 and 1 for the conversion of 2 pyruvate into 2 acetate, 2 propionate and 1 butyrate, respectively (Stams and Plugge, 2009; Zhang et al., 2013); 0.33 for the oxidations of propionate and butyrate to acetate (Stams and Plugge, 2009); 0 for the reduction of acetate and HCO_3^- to propionate (Stams et al., 1984); and 1.5 or 0.5 per equivalent of CH_4 produced by archaeal species with and without cytochromes (Thauer et al., 2008; Buckel and Thauer, 2013). Since ATP was described to be generated by substrate level phosphorylation only for *Clostridium pasteurianum* (Buckel and Thauer, 2013), and uncertain ATP yield from electron transport phosphorylation was predicted for rumen *Butyrivibrios* (Hackmann and Firkins, 2015), reference values of ATP yield used in the present study may be subject to revision.

For microbial catabolism, likely rate-determining steps may be substrate level phosphorylation during fermentation, proton translocation, substrate activation or electron transfer to extracellular electron acceptors (Jin and Bethke, 2007). For

rumen glucose fermentation, the rate-determining step was chosen to be equal to the ATP yield from substrate level phosphorylation, which results in χ equal to 4, 3.33, 3, 3 and 2.67 for reactions a to e (Table 3.1). When assuming reactivity of NADH oxidation to be dominated by hydride transfer (Song et al., 2014), the rate-determining step occurs only once per equivalent of NADH oxidized, indicating $\chi = 1$ for NADH oxidation without ferredoxin oxidation. Although various aspects of hydrogenase-catalyzed cofactor oxdation require further clarification, a hydride intermediate may also be formed in the oxidation of reduced ferredoxin (Peters et al., 2015). NADH oxidation via electron confurcation (i.e., combining electrons from two dissimilar donors to generate a single product such as H_2) would then be associated with two hydrides intermediates, indicating $\chi = 2$ for NADH oxidation with ferredoxin oxidation. The rate-determining step for the reduction of acetate and HCO_3^- (reaction f, Table 3.1) was assumed to be the activation of acetate to acetyl phosphate. This activation occurs once per equivalent of acetate, which makes $\chi = 1$. The butyryl-CoA and succinate oxidations are the energetically most demanding steps in the overall pathways of butyrate and propionate fermentation (Stams and Plugge, 2009), where electron transfer was taken as the rate-determining step. Two electrons are transferred for both the oxidation of butyryl-CoA and succinate, which indicates $\chi = 2$ for both conversions. The rate-determining steps in methanogenesis, with and without the involvement of cytochromes, were assumed to be the methyltetrahydromethanopterin-coenzyme M methyltransferase and the reduction of the disulfide of coenzymes B and M, respectively. Both steps are coupled to the translocation of two sodium ions (Thauer et al., 2008), which occurs once per equivalent of CH_4 produced, indicating $\chi = 2$.

3.2.4 Continuous input variables and uncertainty of F_T

For reactions a to h and k, concentrations were 1 mM hexose, 60 mM acetate, 20 mM propionate, 12.5 mM butyrate and 40 mM bicarbonate, 0.25 bar partial pressure of CH_4 and pH was equal to 6.45; for reaction j, Fd^{2-}_{RED}/Fd_{OX} was equal to 9. Values for ΔG^o of fermentation pathways and standard redox potentials of cofactors were taken from Buckel and Thauer (2013) and Ungerfeld and Kohn (2006). Values of ΔG^o of metabolite formation were adjusted to rumen temperature using the Van 't Hoff equation (e.g., Atkins and de Paula, 2006).

The uncertainty of F_T to variation in inputs other than p_{H_2} was assessed for the five glucose fermentation pathways, the three VFA interconversions and methanogenesis (Table 3.1). Ten thousand different samples were drawn randomly from uniform distributions for glucose, acetate, propionate, butyrate concentrations, pH, p_{CO_2},

p_{CH_4} and ΔG_P ranging from 0.1 to 2.0 mM, 35 to 90 mM, 7 to 30 mM, 5 to 21 mM, 5.7 to 7.2, 0.35 to 0.80 bar, 0.15 to 0.35 bar and 35 to 50 kJ·mol^{-1}, respectively. For completeness, proton concentrations were calculated from pH and HCO_3^- concentrations were calculated using the Henderson-Hasselbalch equation (e.g., Kohn and Dunlap, 1998).

Uncertainty of F_T approaches zero when F_T approaches unity. If F_T of a specific reaction deviated from unity for the range of p_{H_2} considered, a 95% confidence interval of F_T was calculated for 10 values of p_{H_2} for which F_T was close to zero at the previously mentioned fixed concentrations. Values of p_{H_2} increased exponentially in steps according to $p_{H_2,n} = a \cdot b^{n-1}$, where a is the start value, b is the factor by which $p_{H_2,n}$ increases per step, and n runs from 1 to 10 for the number of steps. The exact values of a and b were chosen based on the visual representation of the uncertainty by the error bar. Applying this, the uncertainty of F_T was assessed for p_{H_2} at $\{2.00{\cdot}10^{-5}, 2.60 \cdot 10^{-5}, \ldots, 2.12 \cdot 10^{-4}\}$ bar for methanogenesis yielding 0.5 ATP, $\{6.00{\cdot}10^{-4}, 8.10 \cdot 10^{-4}, \ldots, 8.94 \cdot 10^{-3}\}$ bar for methanogenesis yielding 1.5 ATP, $\{7.70{\cdot}10^{-5}, 9.63 \cdot 10^{-5}, \ldots, 5.74 \cdot 10^{-4}\}$ bar for acetate to propionate conversion, $\{5.00{\cdot}10^{-6}, 6.50 \cdot 10^{-6}, \ldots, 5.30 \cdot 10^{-5}\}$ bar for propionate to acetate conversion, and $\{1.95{\cdot}10^{-6}, 2.93 \cdot 10^{-6}, \ldots, 7.50 \cdot 10^{-5}\}$ bar for butyrate to acetate conversion. The actual ranges of the 95% confidence intervals of F_T depends on metabolite concentrations and values of $\Delta G^o, \Delta G_C$ and χ, explicitly shown for the particular conversion of glucose into two equivalents of acetate (Equation 3.6). Equation 3.6 also shows the nonlinearity of F_T to its input, which makes the 95% confidence intervals asymmetric.

Calculation of the 95% confidence intervals of F_T at discrete values of p_{H_2} and plotting of F_T as a function of p_{H_2} was performed in R statistical software (R Core Team, 2016). Code is provided as supporting information (S1–S3 Files).

3.3 Results and Discussion

3.3.1 Glucose fermentation and NADH oxidation

The F_T for the fermentation pathways a to d (Table 3.1) did not deviate from unity for p_{H_2} between $2{\cdot}10^{-5}$ and $5{\cdot}10^{-2}$ bar and had zero uncertainty (Fig 3.1), which is inherent to F_T approaching unity. This indicates these fermentation reactions proceed far from thermodynamic equilibrium and implies no inhibition on reaction rates since p_{H_2} in the rumen varies between $2{\cdot}10^{-4}$ and $1{\cdot}10^{-2}$ bar (Hegarty and Gerdes, 1999). No F_T curve is shown for the conversion of glucose into 0.67 equivalents of acetate and 1.33 equivalents of propionate because it does not involve H_2. The actual value

of F_T for this conversion also yielded unity (result not shown) and indicates no thermodynamic inhibition of this fermentation pathway under the conditions assumed and range of p_{H_2} considered. In this investigation, we assumed an ATP yield of 3 per equivalent of butyrate if only substrate level phosphorylation takes place. Accounting for electron transport phosphorylation as well would predict an ATP yield of ~4.5 per equivalent of glucose (Hackmann and Firkins, 2015). Production of propionate via succinate has also been mentioned to yield 4 ATP per equivalent of glucose (Russell and Wallace, 1997). Adjusting ΔG_C of reactions associated with propionate and butyrate to these higher yields of ATP still did not make F_T deviate from unity for the considered range of p_{H_2} (result not shown).

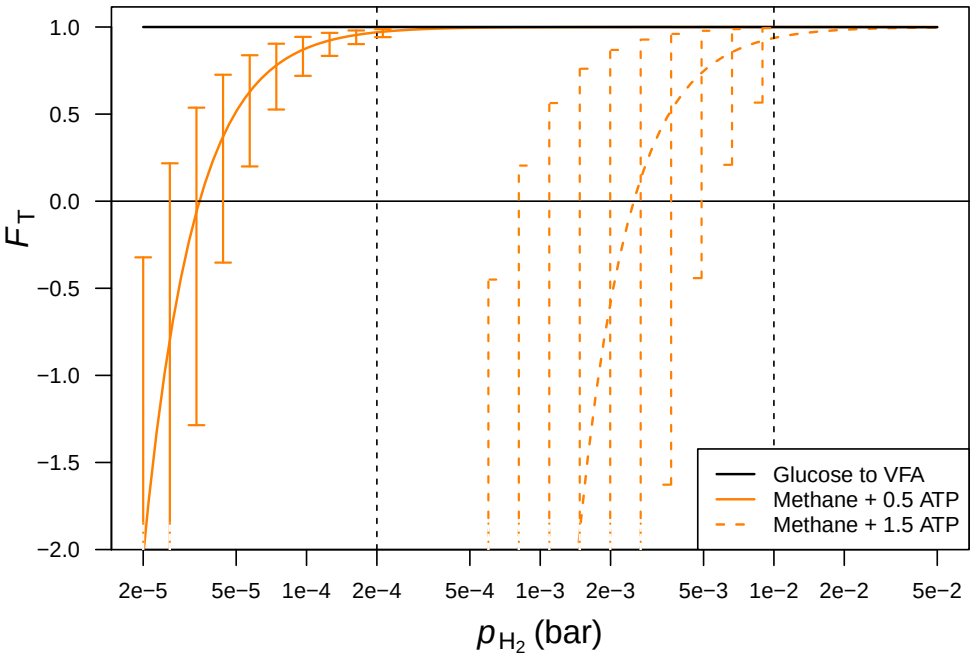

Figure 3.1: Thermodynamic potential factor (F_T) as a function of p_{H_2} for glucose fermentation pathways and methanogenesis. The black line for glucose to VFA is valid for the reactions a to d (yielding acetate, propionate or butyrate), the solid and dotted orange lines represent methanogenesis with 0.5 and 1.5 mol of ATP per mol of CH_4, respectively; a more detailed description of the glucose fermentation pathways to VFA and methanogenesis is given in Table 3.1. Confidence intervals represent uncertainty of F_T to variation in inputs other than p_{H_2}. Vertical lines demarcate the rumen physiological range of p_{H_2}. A log scale is used to plot the x-axis.

Absence of thermodynamic inhibition for any of the glucose fermentation pathways is not in line with conclusions drawn previously (Janssen, 2010), where the conversion of glucose into VFA was considered to be directly affected by the level of H_2. For common values of χ and T, F_T approaches unity when $\Delta G_A \gg \Delta G_C$, representing the far-from-equilibrium situation. This applies to the glucose fermentation pathways considered indicating that ΔG cannot be used as a measure of reaction rate for these reactions. This is in accordance with the fact that classical thermodynamic functions such as ΔG have no implications for magnitude of reaction rate, except for near-equilibrium situations (Manes et al., 1950). Only a difference between ΔG_A and ΔG_C closer to zero than approximately –20 kJ·mol^{-1}, which may be the cutoff for near-equilibrium, makes F_T deviate from unity. Additional evidence for $\Delta G \approx -20$ kJ·mol^{-1} as a cutoff value for inhibited progress of microbial metabolism is given by Schink (Schink, 1997) who assumed a heat loss of about 20 kJ·mol^{-1} for irreversible metabolic processes that generate ATP. However, it was experimentally shown that syntrophic bacteria metabolize up to a zero difference between ΔG_A and ΔG_C (Jackson and McInerney, 2002), which corresponds to $F_T = 0$.

The F_T for NADH oxidation without reduced ferredoxin oxidation decreased to zero upon an increase of p_{H_2} from $2{\cdot}10^{-4}$ to $1{\cdot}10^{-2}$ bar, whereas $F_T < 1$ may already be obtained at $P_{H_2} < 5{\cdot}10^{-5}$ bar for a high NAD^+ to NADH ratio and pH = 7.0 (Fig 3.2a). The F_T for NADH oxidation with reduced ferredoxin oxidation decreased to zero at $P_{H_2} > 1{\cdot}10^{-2}$ bar, whereas $F_T < 1$ may already be obtained at $P_{H_2} > 2{\cdot}10^{-4}$ bar when pH = 7.0 (Fig 3.2b). The actual value of F_T depends on pH and NAD^+ to NADH ratio. Partial pressure of H_2 and intracellular pH of microbes in the rumen are assumed to vary between $2{\cdot}10^{-4}$ and $1{\cdot}10^{-2}$ bar (Hegarty and Gerdes, 1999), and 6.2 and 7.0 (Russell, 1987), respectively. Shortly after new feed enters the rumen, the rate of fermentation will increase, which results in a high p_{H_2} (Van Zijderveld et al., 2011c) and a low pH; whereas during fasting, p_{H_2} will be low and pH high. In an experimental study in which the effects of starch type and level on rumen fermentation were evaluated (Hatew et al., 2015), the lowest acetate to propionate ratio was observed at 2 h after feeding, whereas the lowest pH was observed at 4 h after feeding. Achieving the lowest acetate to propionate ratio before the lowest pH may suggest that after feed consumption the increase in p_{H_2} occurs faster than the decrease in pH. This indicates that elevated p_{H_2} thermodynamically inhibits NADH oxidation shortly after feeding, but this is compensated by decreased pH later.

Although effects of the redox state of ferredoxin on the thermodynamic inhibition of NADH oxidation are not explicitly shown, ferredoxin is reduced during fermentation and the Fd^{2-}_{RED} to Fd_{OX} ratio, which was assumed to be 9, may increase in response to increased metabolism shortly after ingestion of feed. If an increased Fd^{2-}_{RED} to

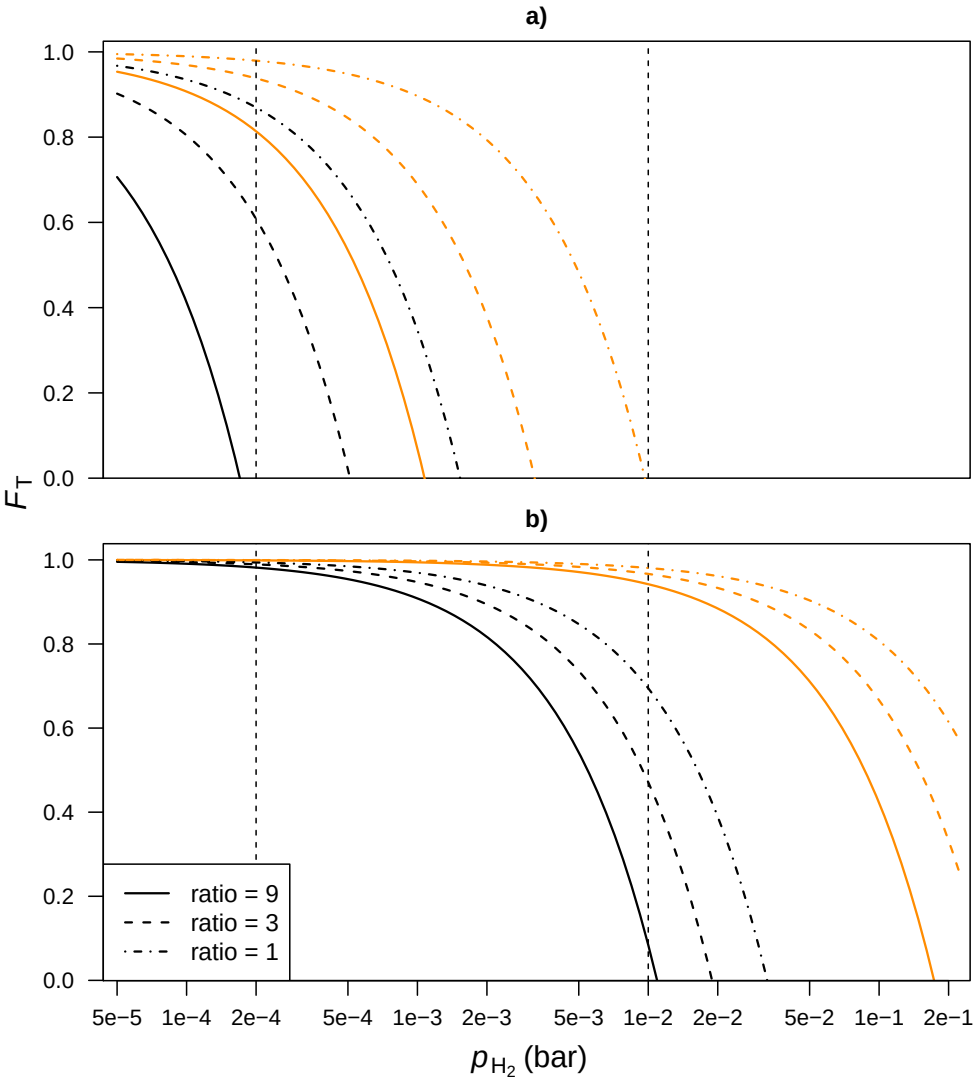

Figure 3.2: Thermodynamic potential factor (F_T) as a function of p_{H_2} for a) NADH oxidation without ferredoxin oxidation and b) NADH oxidation with ferredoxin oxidation and the Fd^{2-}_{RED} to Fd_{OX} ratio constant at 9. Line type represents NAD^+ to NADH ratio and line color represents intracellular pH equal to 6.2 (orange) and 7.0 (black). Vertical lines demarcate the rumen physiological range of p_{H_2}. A log scale is used to plot the x-axis.

Fd_{OX} ratio applies to rumen bacteria, the inhibition of NADH oxidation is potentially alleviated. To evaluate this alleviation, the solid, dashed and dot-dashed lines in Fig 3.2b may, alternative to keeping the Fd^{2-}_{RED} to Fd_{OX} constant at 9 and NAD^+ to NADH ratios of 9, 3 and 1, correspond to keeping the NAD^+ to NADH ratio

constant at 9 and Fd^{2-}_{RED} to Fd_{OX} ratios of 9, 27 and 81, respectively. This implies that the value of F_T is closer to 1 for more reduced ferredoxin, which weakens the thermodynamic force that inhibits NADH oxidation. Since ferredoxin is involved in the pathway from pyruvate to acetate and butyrate only and not in the glycolysis, whereas NAD may be involved in both pathways, the NAD^+ to NADH ratio may change more rapidly after feeding than the Fd^{2-}_{RED} to Fd_{OX} ratio. Inhibition of NADH oxidation may therefore occur shortly after feeding, but may be compensated later. Nonetheless, the present study demonstrates that the mechanism of NADH oxidation is critical for the magnitude of its inhibition; the inhibition of NADH oxidation is also determined by the thermodynamic state of the rumen with p_{H_2} and intracellular pH both being important determinants.

The NAD^+ to NADH ratio is sometimes assumed to be in thermodynamic equilibrium with p_{H_2} (Kleerebezem et al., 2008), or in other words, F_T is assumed zero for any value of p_{H_2}. For rumen bacteria incapable of confurcation this implies the NAD^+ to NADH ratio is ≥ 9 at $p_{H_2} = 2{\cdot}10^{-4}$ and ≤ 1 at $p_{H_2} = 1{\cdot}10^{-2}$ bar (Fig 3.2a); for rumen bacteria in which confurcation does take place this implies the NAD^+ to NADH ratio is ≥ 9 for $P_{H_2} \leq 1 \cdot 10^{-2}$ bar (Fig 3.2b). The NAD^+ to NADH ratio was reported to be 1.4 to 2.6 in rumen microbes (Hino and Russell, 1985), 1.1 to 2.7 for *Escherichia coli* (Berrios-Rivera et al., 2002), and was reported to be < 9 in living cells (Buckel and Thauer, 2013). These ratios largely fall within the range of our prediction but tend to be at the edge of physiological feasibility and the NAD^+ to NADH ratio in bacteria incapable of confurcation may be underestimated at elevated p_{H_2}. Although many anaerobic and syntrophic bacteria contain enzymes that catalyze electron confurcation, it is unclear whether many of the bacteria belonging to the core community in the rumen (e.g., *Prevotella*, *Fibrobacter*, *Ruminococcaceae*, *Bacteroidales*; Henderson et al., 2015) employ this mechanism. *Ruminococcus albus* 7 that is part of the rumen core community employs this mechanism (Zheng et al., 2014). In this strain, genes encoding for the hydrogenase enzyme involved in electron confurcation had a similar transcript abundance in mono- and biculture. In contrast, genes encoding for a different hydrogenase that reduces protons to molecular hydrogen using reduced ferredoxin only was 90-fold upregulated in mono- compared to biculture (Meier et al.). This suggests that the confurcating hydrogenase functions in central metabolism regardless of external p_{H_2}. Nonetheless, increased propionate to acetate ratios (Hatew et al., 2015) and production of lactate being reported in response to feeding (Counotte and Prins, 1981) may indicate these latter two ways of NADH oxidation are important alternatives for ferredoxin dependent oxidation of NADH. Direct evidence of how these mechanisms are applied by rumen bacteria is lacking, however.

Given that the NAD^+ to NADH ratio becomes less than or equal to 1 (Fig 3.2a), glycolytic reactions may be downregulated. Glycolytic activity of *Caldicellulosiruptor saccharolyticus* was found not to be completely inhibited at a NAD^+ to NADH ratio equal to 1 (Willquist et al., 2011), which may allow metabolic activity at ratios $<$ 1. Nonetheless, highly reduced NAD is reconditioned to more oxidized NAD by the upregulation of the production of metabolites such as lactate and ethanol, as explained for gut microbiota (Fischbach and Sonnenburg, 2011). This upregulation may take place in addition to increased proportions of propionate production. However, the production of lactate and ethanol is less favorable for microbial growth because conversion of pyruvate to either lactate or ethanol does not yield any ATP, unlike the conversion of pyruvate to acetate or butyrate, and to propionate via succinate. Another way in which bacteria may control p_{H_2} and the redox state of NAD in the rumen environment is the production of formate. Formate may be produced when pyruvate is converted to acetyl-CoA as an alternative for the oxidation of reduced ferredoxin (Stams and Plugge, 2009). Formate can be converted to H_2 and CO_2, but may also be directly used for CH_4-production by methanogens (Boone et al., 1989). In the latter case, no H_2 is produced and the synthesis of formate serves as a potential mechanism to maintain low p_{H_2} (Leng, 2014).

The present theoretical exercise indicates that, in the rumen, p_{H_2} does not directly control the glucose fermentation pathways. However, depending on mechanism and pH, p_{H_2} does thermodynamically control NADH oxidation, which influences VFA production. NAD^+ to NADH ratio as a key controller of fermentation end product formation is widely recognized in literature (e.g., Mosey, 1983; Rodríguez et al., 2006). When the NAD^+ to NADH ratio is low, the metabolism needs to yield more reduced products to oxidize NADH (Willquist et al., 2011; Fischbach and Sonnenburg, 2011). Production of butyrate and propionate from reactions c and d both oxidize all NADH obtained from glycolysis back to NAD^+ (Table 3.1) but does not explain why elevated propionate but no elevated butyrate is found at increased p_{H_2}. A difference between these pathways is the H_2 yield of 2 and 1 equivalents per equivalent of glucose from reaction c and d, respectively. The higher H_2 yield associated with butyrate production (reaction c) will inhibit NADH oxidation more than propionate production (reaction d), which explains why propionate production is more upregulated than butyrate production at increased p_{H_2}. Furthermore, production of butyrate yields only one VFA per equivalent of glucose (reaction c), whereas production of acetate and propionate (reaction d) yields two VFA per equivalent of glucose, which makes the rumen environment more acidic. Shortly after a meal, propionate may be produced via lactate production, via reaction e. Lactate is a stronger acid than propionate and makes the rumen environment even more acidic. In addition to the net 0.67 NADH

oxidized back to NAD^+, the acidic environment promotes the oxidation of NADH. Less inhibition of NADH oxidation at lower pH (Fig 3.2) explains why, at neutral or alkaline pH, propionate production is more effective in maintaining the NAD^+ to NADH ratio than butyrate production (Zhang et al., 2013).

Thermodynamic control of p_{H_2} on NADH oxidation but not on the glucose fermentation pathways, is also in line with the statement that the NAD^+ to NADH ratio determines the profile of VFA produced with rumen fermentation (Hegarty and Gerdes, 1999). One may designate this as the dynamic control of p_{H_2} on rumen fermentation pathways. Ghimire et al. (2014), building on the Molly cow model, which includes a representation of rumen fermentation processes, attempted to account for the effect of the thermodynamic state of the rumen environment on the interconversion between acetate and propionate. Besides keeping p_{H_2} constant in the calculation of these rate constants, they did not consider the NAD^+ to NADH ratio, which might have caused their model not to perform well in predicting observed variation in ruminal VFA production. Future modeling attempts might benefit from a representation of the NAD^+ to NADH ratio.

Even though an empirical relationship between p_{H_2} and proportion at which individual VFA are produced may appear from experimental data, the validity of a NAD-driven mechanistic prediction of metabolic end products is supported by the work of Salem et al. (2002). They used the NAD^+ to NADH ratio as a key controller of the type of glucose degradation products to be formed. Although their modeling effort deals with the myocardial energy metabolism, which partly differs from the energy metabolism of anaerobic bacteria, a similar approach may be applied for estimating rumen fermentation products. Oxygen concentration in blood, like p_{H_2} in anaerobic environments, dictates redox conditions and consequently the NAD^+ to NADH ratio. Therefore, predicting the production of individual VFA in the rumen might benefit from using the NAD^+ to NADH ratio as a controlling factor as was suggested from an evaluation of various VFA prediction models (Morvay et al., 2011). Future modeling attempts might benefit from a representation of the NAD^+ to NADH ratio.

The NAD^+ to NADH ratio as a key controller of the type of VFA produced explains why feeding rapidly degradable carbohydrates induces a shift from acetate to propionate production in the rumen. This shift has been confirmed by various studies, among which a regression analysis of molar proportions of VFA production (Bannink et al., 2006) and a metabolic model of mixed culture fermentations (Rodríguez et al., 2006; Zhang et al., 2013). Different carbohydrate polymers such as cellulose and amylose are broken down to the same monomers, and can be converted into the same fermentation end products. Degradation rate of carbohydrates, however, determines the magnitude of the increase in p_{H_2} and decrease in NAD^+ to NADH

ratio obtained via the glycolysis, which controls pathways of VFA production from pyruvate. The ability of specific microbial species to catalyze the breakdown of a certain type of carbohydrate polymer might be related to the production of specific VFA, like starch hydrolysis favors propionate production. Nonetheless, this may also be regarded as the NAD^+ to NADH ratio controls fermentation pathways, where the metabolic physiology of these species has been adapted to degrade specific carbohydrate polymers in the rumen.

3.3.2 VFA interconversion

Interconversion of VFA in the rumen has been discussed various times in the literature (Ungerfeld and Kohn, 2006; Ghimire et al., 2014). After measuring VFA production rates in the rumen of lactating dairy cows by infusion of ^{14}C labeled VFA, all six possible conversions between acetate, propionate and butyrate were confirmed to occur (Sutton et al., 2003). Of these conversions, acetate to propionate, propionate to acetate and butyrate to acetate are H_2-dependent.

Acetate to propionate conversion was observed at 2.0% and 2.6% of de novo synthesized acetate being converted into propionate at normal and low-roughage diets, respectively (Sutton et al., 2003). The higher conversion rate from the low-roughage diets may be attributed to higher p_{H_2} from the more rapidly degradable carbohydrates. To the authors' knowledge, there is only one study that has described this conversion (Laanbroek et al., 1982). Therein, H_2-dependent propionate production from acetate and CO_2 by a pure culture of *Desulfobulbus propionicus* was reported. This particular study focuses on freshwater sediments and other microbial species might be responsible for this conversion in the rumen. The F_T for this reaction increased from zero to unity for p_{H_2} between approximately $1.5{\cdot}10^{-4}$ and $5{\cdot}10^{-4}$ bar, and zero is no longer within the confidence interval of F_T for $p_{H_2} > 2.3{\cdot}10^{-4}$ bar (Fig 3.3a), implying the conversion of acetate to propionate to be controlled by p_{H_2} and thermodynamically feasible under common rumen conditions. However, Laanbroek et al. (1982) also reported not having observed any propionate from acetate and CO_2 in the presence of sulfate. Traces of sulfate may enter the rumen with regular feedstuffs and will be metabolized by the microbes (Gould et al., 1997). Especially when diets contain co-products from grain milling industries rumen sulfate concentrations may be high. Apart from p_{H_2}, also the sulfate concentration might control the rate of conversion of acetate to propionate. Besides, sulfate is an electron acceptor for respiration and will also compete for electrons and lower CH_4 production (Van Zijderveld et al., 2010).

The H_2-dependent conversions of propionate and butyrate into acetate yield multiple equivalents of H_2 (reactions g and h, Table 3.1) and require very low p_{H_2} to

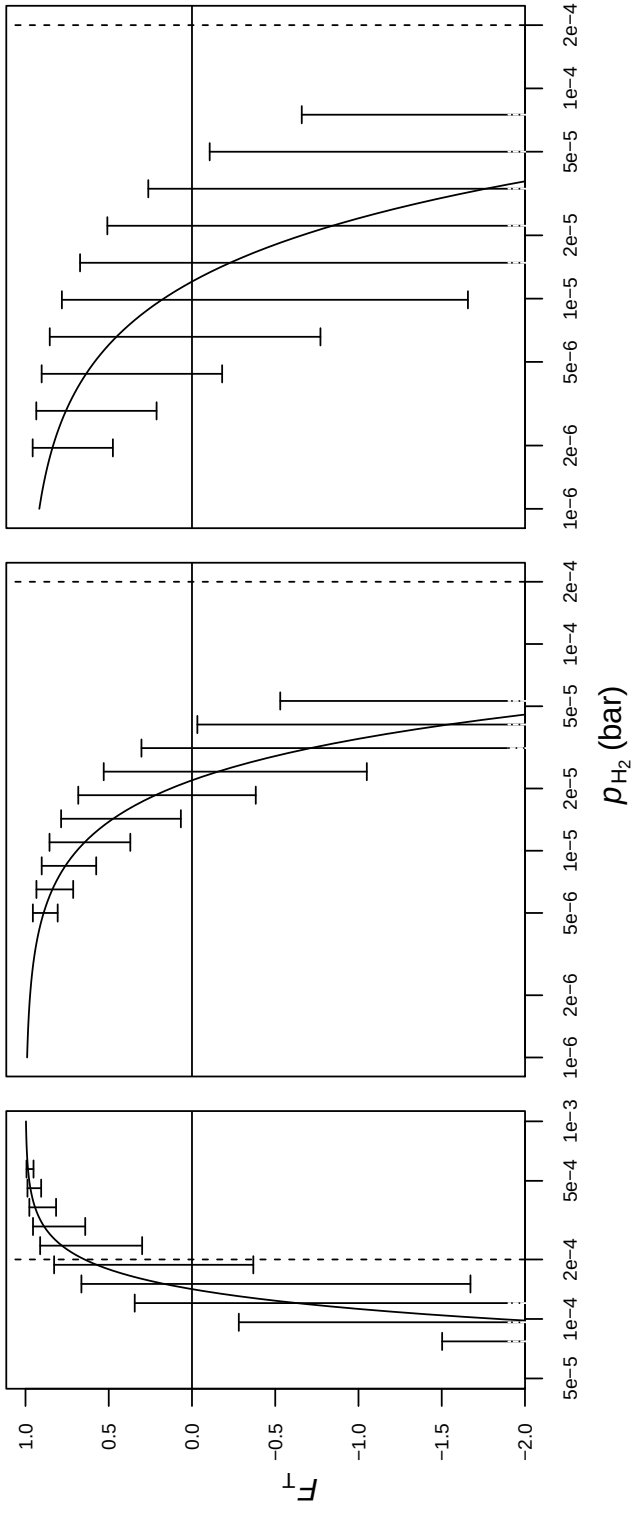

Figure 3.3: Thermodynamic potential factor (F_T) as a function of p_{H_2} for VFA interconversions. Conversions comprise a) acetate to propionate, b) propionate to acetate, c) butyrate to acetate. The 95% confidence intervals represent uncertainty of F_T to variation in inputs other than p_{H_2}. Vertical lines demarcate the rumen physiological lower bound of p_{H_2}. A log scale is used to plot the x-axis.

make them exergonic and proceed. For both reactions, values of $F_T \geq 0$ are within the 95% confidence interval for $p_{H_2} < 4 \cdot 10^{-5}$ bar (Figs 3.3b and 3.3c). This indicates these conversions do not occur under conditions that are common in the rumen where p_{H_2} is usually higher. However, propionate or butyrate degrading bacteria may aggregate with H_2-consuming methanogens in typical syntrophic associations. This association of cells enables interspecies H_2 transfer by diffusion, and its flux is enhanced when the intermicrobial distance decreases (McInerney et al., 2008; Stams and Plugge, 2009). If this local interspecies H_2 transfer occurs, p_{H_2} is lower than in other locations of the rumen, which makes the oxidation of propionate and butyrate exergonic. Furthermore, sulfate- and nitrate-reducing conditions have been reported to thermodynamically favor the degradation of propionate and butyrate (McInerney et al., 2008). Degradation of VFA under these conditions is H_2-independent, as was reported for propionate to acetate conversion in the presence of sulfate (Laanbroek et al., 1982). Therefore, the inhibition of p_{H_2} on the butyrate to acetate and propionate to acetate conversions might be counteracted in the presence of external electron acceptors. These conversions, though, require microbes capable of respiration.

Another pathway involving propionate to acetate conversion was described by de Bok et al. (2001). Using ^{13}C labeled compounds, they found *Smithella propionica* to convert propionate into acetate and butyrate via a six-carbon intermediate. This particular conversion of propionate also gives physiological evidence for the conversion of propionate into butyrate. Hydrogen is not directly involved in this pathway and indicates the conversion of propionate into either acetate or butyrate is not affected by p_{H_2}. Depending on the p_{H_2}, the concentrations of acetate, propionate and butyrate, and the abundance of microbial aggregates, this particular propionate conversion into acetate and butyrate may enable butyrate oxidation in methanogenic ecosystems in case the classical propionate oxidation pathway would be endergonic (Dolfing, 2013). In other words, this makes sense for the range of p_{H_2} with $F_T > 0$ for butyrate oxidation and $F_T < 0$ for propionate oxidation. This range is negligibly small and below $2 \cdot 10^{-4}$ bar (Figs 3.3b, 3.3c), explaining why this particular oxidation of propionate is not expected to occur under rumen conditions.

Besides the VFA interconversions discussed in the paragraphs above, the acetate to butyrate conversion is ecologically significant (Pryde et al., 2002) and seems to be more substantial than the other VFA interconversions in the rumen (Sutton et al., 2003). The final metabolic step of butyrate production, butyryl-CoA to butyrate, proceeds via butyrate kinase or via butyryl-CoA:acetate CoA-transferase (Pryde et al., 2002). Acetate to butyrate conversion may be described by the latter mechanism. For this conversion, apart from acetate, another substrate such as hexose is required to yield

butyryl-CoA. From human colon microbiota, genes encoding for enzymes for both pathways were detected in various *Butyrivibrio fibrisolvens* strains and *Clostridium* species that also reside in the rumen. The butyryl-CoA:acetate CoA-transferase step does not yield H_2 and will not be affected by p_{H_2}. The F_T for the conversion of glucose and acetate to butyrate did not deviate from unity for p_{H_2} between $2{\cdot}10^{-5}$ and $5{\cdot}10^{-2}$ bar. Furthermore, for butyrate formed via both butyryl-CoA:acetate CoA-transferase and butyrate kinase, butyryl-CoA is formed from pyruvate with the same metabolic steps. Hence, the two mechanisms of butyrate production yield the same H_2 balance and oxidize equal equivalents of NADH to NAD^+ per equivalent of glucose (reaction c, Table 3.1; Louis and Flint, 2009; Buckel and Thauer, 2013). Butyrate production via butyryl-CoA:acetate CoA-transferase and via butyryl kinase are therefore not controlled differently by the NAD^+ to NADH ratio and p_{H_2}. This would make a specific p_{H_2}-controlled flux of acetate to butyrate conversions in rumen dynamic modeling efforts redundant.

The ecological significance of the conversion of butyrate to propionate is low. Because ΔG^o for the propionate conversion into acetate and butyrate is nearly zero (Liu et al., 1999), the reverse reaction from butyrate to propionate might occur too. Furthermore, the metabolism of threonine fermentation in *Clostridium propionicum* has been described to yield both propionate and butyrate via 2-oxobutyrate (Hofmeister and Buckel, 1992). The conversion of butyrate into propionate might occur as a side reaction, albeit the actual occurrence via 2-oxobutyrate is questionable.

The different fluxes of rumen VFA in the three-pool model of Sutton et al. (2003) suggests that accounting for p_{H_2} controlled VFA interconversions in dynamic model predictions is compatible with the conversions of acetate to propionate, butyrate to acetate and propionate to acetate. Nonetheless, these VFA interconversions are still controlled by the NAD^+ to NADH ratio of which the dynamics, described in the present investigation, may already explain an important part of the observed variation in the proportion of individual VFA. Prediction of VFA interconversion would also require information such as intermicrobial distance in syntrophic aggregates and concentration of external electron acceptors such as nitrate and sulfate. Including this information in a model next to control by NAD^+ to NADH ratio increases the model complexity, and it needs to be further investigated whether it aids in explaining observed variation in the proportion of individual VFA. Furthermore, functions that microorganisms carry out in certain experimental settings may differ greatly, depending on the presence or absence of other community members (Fischbach and Sonnenburg, 2011). Applying this differing of functions to VFA interconversions makes dynamic predictions of rumen VFA concentrations uncertain.

3.3.3 Methanogenesis

The F_T for methanogenesis increased from zero to unity for p_{H_2} at $\sim 10^{-5}$ bar for archaea without cytochromes and $\sim 10^{-3}$ bar for archaea with cytochromes (Fig 3.1). This indicates a certain threshold of p_{H_2} to make methanogenesis proceed, depending on the physiology of the archaea. For methanogenesis by archaea with cytochromes, $F_T = 0$ for $p_{H_2} \approx 3 \cdot 10^{-3}$ bar and and based on the 95% confidence interval $F_T \leq 0$ for $p_{H_2} < 8 \cdot 10^{-4}$ bar (Fig 3.1). Rumen p_{H_2} may be as low as $2{\cdot}10^{-4}$ bar (Hegarty and Gerdes, 1999) which will yield a negative F_T and may explain why archaea with cytochromes are hardly found in the methanogenic community in the rumen (Janssen and Kirs, 2008; Thauer et al., 2008). Given that F_T approaches unity with rather minor uncertainty at p_{H_2} as low as $2{\cdot}10^{-4}$ bar (Fig 3.1), methanogenesis by archaea without cytochromes is hardly restricted by the thermodynamic state of the rumen environment.

The amount of H_2 present in the rumen has been expressed as dissolved H_2 concentration (Janssen, 2010). It is common to express gas contents in pressure, but the possible occurrence of supersaturation of dissolved H_2 (e.g., Kraemer and Bagley, 2006) would necessitate the use of dissolved H_2 concentration instead of p_{H_2}. Supersaturation, the violation of Henry's Law, is the non-equilibrium condition between dissolved H_2 concentration and p_{H_2} in the rumen headspace. The fact that archaea with cytochromes hardly exist in the rumen might suggest too low dissolved H_2 concentrations for their survival and negligible supersaturation of H_2. Furthermore, rumen contractions may prevent supersaturation of H_2 to occur. If supersaturation does occur in the rumen, archaea with cytochromes may survive and the NAD^+ to NADH ratio may become lower than indicated in the present study.

Several studies have recognized the importance of adequate coefficients of production rate of individual VFA to accurately predict CH_4 (Bannink et al., 2011; Alemu et al., 2011; Ghimire et al., 2014). The present finding that, under common rumen conditions, VFA dynamics rather than methanogenesis is controlled by p_{H_2}, confirms that the thermodynamic control on the type of VFA formed is significant and should be further elaborated. This finding corresponds with conclusions in previous publications (Ungerfeld and Kohn, 2006; Janssen, 2010). In contrast to these studies, however, it is argued here that the NAD^+ to NADH ratio should be considered as a key controller of the type of VFA produced and the associated amount of H_2 being formed available for methanogenesis, as also described in Hegarty and Gerdes (1999). The present theoretical effort, indicates that taking the NAD^+ to NADH ratio into account in dynamic rumen models is likely to improve prediction of type of VFA formed and CH_4 emissions.

3.4 Conclusion

Fermentation of glucose to various VFA proceeds far from thermodynamic equilibrium and is not controlled by p_{H_2} under rumen physiological conditions. However, oxidation of NADH does appear to be controlled by p_{H_2}, where the actual control also depends on the intracellular pH of microorganisms and the involvement of ferredoxin in NADH oxidation. The conversion of acetate to propionate is thermodynamic controlled by p_{H_2} and also depends on the NAD^+ to NADH ratio. Conversions of butyrate to acetate and propionate to acetate are thermodynamically suppressed by p_{H_2} and will not proceed without aggregation of rumen microbes. Rumen methanogenesis by archaea without cytochromes, which comprise most of the methanogenic population in the rumen, appears not to be thermodynamically restricted by p_{H_2}, implying the thermodynamic control of p_{H_2} to be negligible. Representation of the key role of the NAD^+ to NADH ratio in rumen fermentation models is required to improve the accuracy of prediction of VFA and CH_4 production by these models.

Supporting Information

S1 File: R code for calculating 95% confidence intervals of the thermodynamic potential factor (F_T) at discrete values of p_{H_2} and for plotting of F_T as a function of p_{H_2}, including the 95% confidence intervals, for glucose fermentation and methanogenesis (Fig 3.1). DOI:10.1371/journal.pone.0161362.s001.

S2 File: R code for plotting of the thermodynamic potential factor (F_T) as a function of p_{H_2} for NADH oxidation (Fig 3.2). DOI:10.1371/journal.pone.0161362.s002.

S3 File: R code for calculating 95% confidence intervals of the thermodynamic potential factor (F_T) at discrete values of p_{H_2} and for plotting of F_T as a function of p_{H_2}, including the 95% confidence intervals, for VFA interconversions (Fig 3.3). DOI:10.1371/journal.pone.0161362.s003.

Chapter 4

Diurnal dynamics of gaseous and dissolved metabolites and microbiota composition in the bovine rumen

Henk J. van Lingen[1,2], Joan E. Edwards[1,3], Jueeli D. Vaidya[1,3], Sanne van Gastelen[1,2], Bartholomeus van den Bogert[1,3], Edoardo Saccenti[4], André Bannink[5], Hauke Smidt[3], Caroline M. Plugge[3], Jan Dijkstra[2]

1 TI Food and Nutrition, Wageningen, The Netherlands
2 Animal Nutrition Group, Wageningen University & Research, Wageningen, The Netherlands
3 Laboratory of Microbiology, Wageningen University & Research, Wageningen, The Netherlands
4 Systems and Synthetic Biology, Wageningen University & Research, Wageningen, The Netherlands
5 Animal Nutrition, Wageningen UR Livestock Research, Wageningen, the Netherlands

Frontiers in Microbiology 8:425, 2017 (Accepted with minor revision)

Abstract

Diurnal patterns of ruminal fermentation metabolites and microbial communities are not commonly assessed when investigating variation in ruminal CH_4 production. The aims of this study were to monitor diurnal patterns of: (i) gaseous and dissolved metabolite concentrations in the bovine rumen, (ii) H_2 and CH_4 emitted, and (iii) the rumen microbiota. Furthermore, the effect of dietary inclusion of linseed oil on these patterns was assessed. Four multiparous rumen cannulated cows were used in a cross-over design with two 17-d periods and two dietary treatments: a control diet and a linseed oil supplemented diet (40% maize silage, 30% grass silage, 30% concentrate on dry matter (DM) basis for both diets; fat contents of 33 vs. 56 g/kg of DM). On day 11, rumen contents were sampled for 10 h after morning feeding to profile gaseous and dissolved metabolite concentrations and microbiota composition. H_2 and CH_4 emission was measured in respiration chambers from day 13 to 17. A 100-fold increase in ruminal H_2 partial pressure was observed at 0.5 h after feeding, followed by a decline. Qualitatively similar patterns after feeding were also observed for H_2 and CH_4 emission, ethanol and lactate concentrations, and propionate molar proportion, although the opposite pattern was seen for acetate molar proportion. Increased H_2 partial pressure may inhibit NADH oxidation, which shifts the fermentation to ethanol, lactate, and more propionate at the expense of acetate. Associated with this shift, a temporal biphasic change in the microbial composition was observed based on 16S ribosomal RNA with certain taxa specifically associated with each phase. Bacterial concentrations were affected by time, and were increased by linseed oil supplementation. Archaeal concentrations tended to be affected by time and were not affected by diet, despite linseed oil supplementation tending to decrease the partial pressure and emission of CH_4 and tending to increase propionate molar proportion. Linseed oil supplementation weakly affected microbiota composition, and was most associated with an uncultivated Bacteroidales taxon. In summary, our findings support the key role of the redox state of NAD in rumen fermentation and the importance of diurnal dynamics when understanding VFA, H_2 and CH_4 production.

Keywords: Volatile fatty acids, Hydrogen, Methane, Linseed oil, Dairy cow, Bacteria, Methanogenic archaea

4.1 Introduction

The rumen is home to a complex microbial ecosystem that enables ruminants to degrade a wide variety of feed components and metabolites. In this ecosystem, hydrolytic and fermentative bacteria convert carbohydrate polymers to saccharide monomers and ferment these monomers into metabolites such as volatile fatty acids (VFA), CO_2 and H_2. Methanogenic archaea then produce CH_4, primarily from CO_2 and H_2 (Morgavi et al., 2010). As CH_4 emitted into the environment contributes to global warming, abatement of the production of this gas in ruminants is one of the main targets of greenhouse gas mitigation practices for the livestock industry (Hristov et al., 2013a).

Variation in enteric CH_4 production has often been related to diet composition. Best fit empirical models reported by Moraes et al. (2014) identified fat content as one of the key dietary variables in predicting enteric CH_4 emissions of distinct cattle categories. In line with dietary fat content as a key predictor, Grainger and Beauchemin (2011) reported that a 10 g/kg dry matter (DM) increase in dietary fat decreased CH_4 yield from cattle by 1 g/kg DM ingested. Although Grainger and Beauchemin (2011) did not find an effect of the type of fatty acid in the diet on the decrease in CH_4 yield, Patra (2013) reported that C18:3 had marked inhibitory effect on CH_4 emission compared with other dietary fatty acids. Variation in enteric CH_4 production has also been predicted to vary with the type of dietary carbohydrates, the consequent molar proportions of VFA (primarily acetate, propionate and butyrate) produced and H_2 yield. Such effects have been included in several mechanistic models (e.g., Mills et al., 2001; Bannink et al., 2010). Nevertheless, with these empirical and mechanistic approaches, the diurnal dynamics of rumen microbial metabolism has commonly been ignored when assessing rumen fermentation end products, despite peaks in VFA (Hatew et al., 2015), H_2 and CH_4 occurring shortly after feed consumption (Rooke et al., 2014).

In a recent theoretical study, Van Lingen et al. (2016) investigated the sensitivity of the NAD^+/NADH ratio to H_2 partial pressure (p_{H_2}) in the rumen, and proposed the NAD^+/NADH ratio, rather than p_{H_2} directly, as a key-controller of fermentation end products, because it contributes to the redox homeostasis. Bannink et al. (2006), who estimated coefficients for VFA molar proportions based on substrate fermentation, previously suggested that incorporation of cofactor dynamics may be of importance for representing VFA molar proportions in non-steady state conditions. Model predictions of CH_4 produced, which is driven by the H_2 yield associated with the VFA molar proportions, may also benefit from the incorporation of cofactor dynamics. Similar to fermentation end products, the rumen microbiota itself is also affected by time

after feeding, with the concentration of viable rumen bacteria initially declining after feeding and then increasing (Leedle et al., 1982). Furthermore, the composition of metabolically active bacteria adherent to ruminally incubated forage has recently been shown to be biphasic in time (Huws et al., 2016). Little is known about how ruminal archaeal populations are affected by time after feeding, as in recent years more emphasis has been placed on the effect of diet composition and daily feed intake on ruminal archaea and CH_4 emission.

Studies of *in vivo* diurnal patterns that report simultaneously dissolved metabolite concentrations (e.g., ethanol, VFA and lactate) and partial pressures of H_2, CO_2 and CH_4 in the rumen along with emissions of H_2 and CH_4 are limited, particularly in combination with microbiota composition analysis. An integrated approach may provide additional insight into rumen metabolic dynamics, and factors influencing the production of CH_4. The aim of this study was therefore to monitor the diurnal patterns of H_2 and CH_4, dissolved metabolites and microbiota in the rumen, as well as H_2 and CH_4 emission, and assess whether the dietary inclusion of linseed oil affected these patterns.

4.2 Materials and Methods

4.2.1 Experimental design, cows, diets, sampling and measurements

The experiment was conducted at the animal research facilities of Wageningen University & Research & Research (Wageningen, the Netherlands). All experimental procedures were approved by the Institutional Animal Care and Use Committee of Wageningen University & Research & Research and carried out under the Dutch Law on Animal Experimentation.

Four rumen fistulated multiparous Holstein-Friesian cows (364 ± 20 days in milk, 22.0 ± 6.0 kg of milk/day, containing 4.54 ± 0.91% of fat and 4.03 ± 0.67% of protein; mean ± SD) were blocked in pairs according to lactation stage, parity and milk production. Blocks were balanced over treatment sequence in a 2 × 2 crossover design with repeated measurements within each period. Cows were fed either a control diet (CON; 40% corn silage, 30% grass silage and 30% concentrates on DM basis; crude fat content of 33 g/kg DM) or a diet for which the concentrate of the control diet was supplemented with linseed oil (LSO; proportions of corn silage, grass silage and concentrates unchanged, crude fat content of 56 g/kg DM; concentrate ingredient composition is presented in Table S1). There were two experimental periods of 17 days each, and a 28 day washout period between the two experimental periods to

prevent potential carryover effects. Cows were fed equal portions and milked twice daily (6 am and 4 pm). Concentrate was in meal form and manually mixed into the roughage mixture at the moment of feeding.

Diets were supplied ad libitum during the first 8 days of each period to let the cows adapt to the treatment diets and for recording of the individual feed intake. From day 9 to 17, dry matter intake (DMI) within a block was restricted to 95% of the ad libitum DMI of the animal consuming the lowest amount of feed during days 5 to 8, while ensuring that cows never received less than 80% of their voluntary DMI. Samples of grass and corn silage were obtained when fresh feed was prepared (i.e., twice weekly). One pooled sample of each of the concentrates was obtained and represented the whole experiment. These samples were stored at –20°C pending analyses. On day 11 of each period, 60 mL of rumen gas was sampled and feed left in the feeding bins was weighed at set time intervals (0, 0.5, 1, 1.5, 2, 2.5, 3, 4, 5, 6, 7, 8, 9 and 10 h after feeding), and 60 mL of rumen fluid was also sampled (0, 0.5, 1, 1.5, 2, 3, 4, 6, 8 and 10 h after feeding). Fistula lids were customized with a stopcock to sample rumen headspace gas, and a Teflon hose to sample rumen fluid. The Teflon hose was equipped with a perforated plastic tail that was wrapped in two layers of burlap with a pore size of 2 mm to separate fluid from particulate matter, and held at the ventral sac of the rumen with a 1.5 kg lead weight. Both gas and fluid samples were taken with a 60 mL BD Luer-Lok syringe. Gas samples were stored in N_2 flushed under-pressure serum bottles and analyzed within 72 h after collection. Fluid samples were stored at –20°C pending analysis, whereas pH was measured immediately after sampling.

4.2.2 Housing and respiration chambers

From the start of every experimental period cows were housed in tie-stalls, and then from 3 pm on day 13 until 9 am on day 17 the cows were housed in one of four respiration chambers for recording of gaseous emissions of H_2 and CH_4. In each chamber temperature was 16°C and relative humidity was 65%. The chambers were equipped with thin walls with windows, to allow audio-visual contact in order to minimize the effect of social isolation on cow behavior and performance. Cows were exposed to 16 hours of light per day, from 5.30 am to 9.30 pm. The ventilation rate within each chamber was 58 m^3/h to ensure that the H_2 peak after feeding was within reach of the H_2 analyzer (i.e., 0-100 ppm). Exhaust air of the four chambers was sampled at 12-min intervals. Every fifth interval was increased to 15 min for sampling of the inlet air. A H_2 gas analyzer with an electro chemical cell (MGA3000, ADC Gas Analysis Ltd, Hoddesdon, England, UK) was setup in series with the O_2-,

CO_2- and CH_4-analyzers to determine the H_2-concentration in sampled air. Gas concentrations and ventilation rates were corrected for pressure, temperature and humidity to arrive at standard temperature pressure dew point volumes of inlet and exhaust air. Calibration gases were sampled for analysis instead of the inlet air once per day. The analyzed and actual values of these calibration gases were used to correct the measured gas concentrations from the inlet air and exhaust air of all compartments. Before the present experiment started, chambers were checked by releasing known amounts of CO_2 in each compartment and comparing these values with the data from the gas analysis system to calculate the recovery, with recovered amounts being between 99 and 101%. All other aspects of the experimental setup of the respiration chambers were as previously described (Van Gastelen et al., 2015), except for the fact that gas measurements during milking and feeding were retained in the dataset.

4.2.3 Feed composition determination

Prior to analysis, feed samples were prepared as described by Hatew et al. (2015) and oven dried at 60°C, except for the ammonia analysis in the silages for which fresh samples were used. Dried feeds were analyzed for DM, neutral detergent fiber (NDF), acid detergent fiber (ADF), acid detergent lignin (ADL), ash, N (crude protein content calculated as N × 6.25), starch, sugars and gross energy (GE) as described by Hatew et al. (2015), and for crude fat based on NEN-ISO 1735 (2004) with modifications as described by Klop et al. (2017).

4.2.4 Analysis of concentrations of gaseous and dissolved metabolites

Gaseous metabolites were separated with a Compact GC gas chromatograph (Global Analyzer Solutions, Breda, The Netherlands) containing two lines. One line, which contained a Carboxen 1010 pre-column (Supelco, 3 m × 0.32 mm) followed by a Molsieve 5A column (Restek, 25 m × 0.32 mm), was used for H_2 analysis. The following settings were applied: He carrier gas, 200 kPa pressure, 20 mL/min split flow rate and an oven temperature of 90°C. A Pulsed Discharge Detector held at 110°C was used for quantification. The other line, which contained a single Carboxen 1010 column (Supelco, 15 m × 0.32 mm), was used for detection of CO_2 and CH_4. This column had the following settings: He carrier gas, 200 kPa pressure, 10 mL/min split flow rate and an oven temperature of 80°C. A thermal conductivity detector held at 110°C was used for quantification.

Rumen fluid samples were centrifuged (10,000 g for 14 min) after which the metabolites dissolved in the supernatants were separated by a Spectrasystem HPLC (Thermo Scientific, Breda) equipped with a Metacarb 67H column (Agilent, 300 × 65 mm). Column temperature was 45°C, except for the determination of ethanol that was performed at 25°C. A 5 mM sulfuric acid solution was used as an eluent. Flow rate was set at 0.8 mL/min. Metabolites were quantified with a Refractive Index detector. Minimum detectable concentrations of ethanol and lactate were 0.74 and 0.25 mM, respectively. Total VFA concentration was calculated as the sum of the concentrations of acetate, propionate, butyrate, valerate and isovalerate.

4.2.5 DNA extraction

For performing quantitative PCR (qPCR) analysis for the quantification of total bacterial and archaeal concentrations, total genomic DNA (gDNA) was extracted from rumen fluid samples using a protocol involving a combination of bead beating, Stool Transport and Recovery (STAR) buffer (Roche Diagnostics Nederland BV, Almere, The Netherlands) and the Maxwell®16 Instrument (Promega, Leiden, The Netherlands). The method was developed from the previously described method of Salonen et al. (2010) by (i) changing the repeated bead beating buffer to the STAR buffer and then (ii) proceeding with the lysate directly into a customized Maxwell®16 Tissue LEV Total RNA Purification Kit cartridge (XAS 1220). Briefly, cells were pelleted by centrifugation at 15,000 g for 10 min at 4°C from 1 mL of rumen fluid, resuspended in 700 μL of STAR buffer and transferred to a sterile screw-capped 2 mL tube (BIOplastics BV, Landgraaf, The Netherlands) containing 0.5 g of zirconium beads (0.1 mm; BioSpec Products, Inc., Oklahoma, USA) and 5 glass beads (2.5 mm; BioSpec Products). The sample was then treated in a bead beater (Precellys 24, Bertin technologies, Montigny-le-Bretonneux, France) at a speed of 5.5 m/s for 3 × 1 min, followed by incubation at 95°C with agitation (15 min and 300 rpm). The lysis tube was then centrifuged (13,000 g for 5 min at 4°C), and the supernatant transferred to a 2 mL microcentrifuge tube. STAR buffer (300 μL) was added to the remaining contents of the lysis tube, and all the previous steps starting with bead-beating repeated again. An aliquot (250 μL) of the combined supernatants from the sample lysis was then transferred into the custom Maxwell ®16 Tissue LEV Total RNA Purification Kit cartridge. The remainder of the extraction protocol was then carried out in the Maxwell ®16 Instrument according to the manufacturer's instructions. The quantity and purity of the resulting DNA was assessed using a NanoDrop ND-1000 spectrophotometer (NanoDrop®Technologies, Wilmington, DE, USA).

4.2.6 RNA extraction and cDNA synthesis

RNA was extracted for use as a template for rumen microbiota composition analysis, This was due to (i) its ability to reflect the more metabolically active microbes and (ii) its more rapid degradation, relative to DNA, increasing the ability to assess differences in community composition occurring between relatively short (<1 h) time point intervals. As with the DNA extracts, cells were pelleted by centrifugation at 15,000 g for 10 min at 4°C from 1 mL of rumen fluid. The cell pellet was resuspended in 500 μL Tris-EDTA buffer (Tris-HCl pH 7.6, EDTA pH 8.0). Total RNA was extracted from the resuspended pellet according to the Macaloid-based RNA isolation protocol (Zoetendal et al., 2006) with the use of Phase Lock Gel heavy (5 Prime GmbH, Hamburg, Germany) during phase separation. The aqueous phase was purified using the RNAeasy mini kit (QIAGEN Benelux BV, Venlo, The Netherlands), including an on-column DNAseI (Roche) treatment as described previously (Zoetendal et al, 2006). Total RNA was eluted in 30 μL Tris-EDTA buffer. RNA quantity and quality were assessed using a NanoDrop ND-1000 spectrophotometer and an Experion RNA StdSens analysis kit (Bio-Rad Laboratories BV, Veenendaal, The Netherlands) respectively. Absence of contaminating DNA was confirmed by performing a PCR directly on the RNA extract using the first step PCR of the Universal 16S rRNA gene MiSeq protocol (see section 4.2.8). Subsequently, total RNA (2.5 μg) was reverse transcribed using random hexamer primers with the Maxima H Minus First Strand cDNA synthesis kit (Fisher Scientific, Landsmeer, The Netherlands) following the manufacturer's guidelines. Non-template control reactions were also performed. cDNA preparations and control reactions were cleaned using a DNA Clean & Concentrator-5 kit (Zymo Research Europe GmbH, Freiburg, Germany) according to the manufacturer's protocol.

4.2.7 qPCR

For absolute quantification of bacteria and archaea, SYBR green qPCR assays were performed with sample DNA extracts using an iCycler iQ real-time detection system (Bio-Rad Laboratories BV). All qPCR analyses were carried out in triplicate with a reaction volume of 10 μL, using optical-grade PCR plates and sealing film. The reaction mixture contained 2× iQ SYBR green PCR mixture (Bio-Rad Laboratories B.V.), 200 nM (final concentration) of each primer (Table 4.1), and 2 μL of either the DNA template or PCR grade water. The bacterial amplification program consisted of an initial denaturation at 94°C for 10 min followed by 35 cycles of 94°C for 20 s, 60°C for 30 s and 72°C for 30 s. The archaeal amplification program consisted of an initial denaturation at 94°C for 10 min followed by 40 cycles of 94°C for 10 s, 60°C for 30

s and 72°C for 30 s. The fluorescent products were detected at the last step of each cycle. Following amplification, melting temperature analysis of PCR products was performed to determine the specificity of the PCR. The melting curves were obtained by slow heating at 0.5°C/s increments from 60 to 95°C, with continuous fluorescence collection. Standard curves (10^8 to 10^2 amplicon copies/μL) for the assays were prepared using purified PCR amplicons amplified from gDNA of *Ruminococcus albus* (bacterial qPCR standard) and *Methanosarcina mazei* (archaeal qPCR standard) with the primers and annealing temperatures indicated in Table 4.1.

4.2.8 Microbial composition analysis

For 16S rRNA based microbial composition profiling, barcoded amplicons from the V4 region of 16S rRNA genes were generated from cDNA using a 2-step PCR strategy. PCRs were performed with a SensoQuest Labcycler (Göttingen, Germany) using an adaptation of the cycling conditions of Walters et al. (2015) due to the use of the 2-step protocol (Tian et al., 2016) and the Phusion enzyme. The first PCR step was performed in a total volume of 50 μL containing 1× HF buffer (Finnzymes, Vantaa, Finland), 1 μL dNTP Mix (10 mM; Promega), 1 U of Phusion®Hot Start II High-Fidelity DNA polymerase (Finnzymes), 500 nM each of the primers UniTag1-515f and UniTag2-806rB (Table 4.1) and 10-20 ng of sample cDNA. The cycling conditions for the first step consisted of an initial denaturation at 98°C for 3 min, 25 cycles of: 98°C for 10 s, 50°C for 20 s and 72°C for 20 s, and a final extension at 72°C for 10 min. The size of the PCR products (∼330 bp) was confirmed by agarose gel electrophoresis on a 2% (w/v) agarose gel containing 1× SYBR®Safe (Invitrogen, Carlsbad, CA, USA).

The second PCR step was then employed to add an 8 nucleotide sample specific barcode to the 5'- and 3' -end of the PCR products. This step was performed as previously described by Tian et al. (2016). Incorporation of the sample specific barcodes, yielding a PCR product of ∼350 bp, was confirmed by agarose gel electrophoresis. Control PCR reactions were performed alongside each separate amplification with (i) the non-template control from the cDNA preparation and (ii) no addition of template, and consistently yielded no product. PCR products were then purified using HighPrep^{TM} (MagBio Europe Ltd, Kent, United Kingdom) and quantified using a Qubit in combination with the dsDNA BR Assay Kit (Invitrogen). Purified PCR products were mixed in equimolar amounts into pools together with defined synthetic mock communities which allow assessment of potential technical biases (Ramiro-Garcia et al., 2016). Pools then underwent adaptor ligation followed by sequencing on the HiSeq platform with addition of 20% PhiX (GATC-Biotech,

Table 4.1: 16S rRNA targeted primers and annealing temperatures (T_m) used in this study

Application	**Primer**[a]	**Primer sequence (5'-3')**[b]	**T_m(°C)**[c]	**Reference**
Bacterial qPCR standard	27F PROK1492R	AGATTTGATCCTGGCTCAG GGWTACCTTGTTACGACTT	55	Lane (1991) Suzuki et al. (2000)
Archaeal qPCR standard	25F PROK1492R	CYGGTTGATCCTGCCRG GGWTACCTTGTTACGACTT	52	Dojka et al. (1998) Suzuki et al. (2000)
Bacterial qPCR	Bact1369F PROK1492R	CGGTGAATACGTTCYCGG GGWTACCTTGTTACGACTT	60	Suzuki et al. (2000)
Archaeal qPCR	Arch-787f Arch-1059r	ATTAGATACCCSBGTAGTCC GCCATGCACCWCCTC	60	Yu et al. (2005)
Universal 16S Miseq	515f 806rB	GTGYCAGCMGCCGCGGTAA GGACTACNVGGGTWTCTAAT	-	Walters et al. (2015)
	UniTag1-515f UniTag2-806rB	GAGCCGTAGCCAGTCTGCGTGYCAGCMGCCGCGGTAA[d] GCCGTGACCGTGACATCGGGACTACNVGGGTWTCTAAT[d]		This study

[a] Primer names may not correspond to the original publication; [b] Degenerate nucleotides are described using the IUPAC nuleotide code; [c] Annealing temperature used with the respective primer pairs; [d] UniTag sequences are underlined.

Konstanz, Germany).

The 16S rRNA cDNA gene sequencing data was then analyzed using NG-tax, an in-house pipeline (Ramiro-Garcia et al., 2016). Paired end libraries were filtered to contain only read pairs with perfectly matching barcodes, which were used to demultiplex reads by sample. Operational taxonomic units (OTUs) were defined using an open reference approach, and taxonomy was assigned to those OTUs using a SILVA 16S rRNA gene reference database (Quast et al., 2013). The 16S rRNA sequence data generated in this study is deposited in the European Nucleotide Archive under the study accession number PRJEB17837.

4.2.9 Statistical analysis

Metabolites and microbes in the rumen

Prior to statistical analyses, values of lactate concentration, p_{H_2} and bacterial and archaeal concentrations and the ratio of archaeal to bacterial concentrations, were $\log_{10}$-transformed. If a boxplot identified an outlier that could be related to the feed intake pattern of a cow, data points were removed. Gaseous and dissolved metabolite and microbial concentrations and pH in the rumen were subjected to a repeated-measures ANOVA using the following model:

$$y_{ijkl} = \mu + \tau_i + \delta_j + \tau_i\delta_j + \pi_k + \gamma_l + e_{ijkl}, \tag{4.1}$$

where y_{ijkl} represents the measurement on cow l at sampling moment i given treatment j at period k; μ represents the overall mean; τ_i represents fixed effect of the ith sampling moment, $i = 1, 2, \ldots, 14$ for rumen gases and pH, $i = 3, 4, 5, 6$ for lactate concentration, $i = 1, 2, 3, \ldots, 6$ for ethanol concentration, and $i = 1, 2, \ldots, 10$ for all other dissolved metabolite and microbial concentrations; δ_j and π_k represents the fixed effect of diet, ($j = 1, 2$) and period ($\pi = 1, 2$), respectively; γ_l represents random effect of cow ($l = 1, 2, 3, 4$); e_{ijkl} represents the residual error. With this non-repeated crossover design, potential carryover or residual effects due to the diet fed in the preceding period cannot be identified (Tempelman, 2004), and no sequence effect was included in the model. Correlations of repeated measurements within period, fitted to a cow $\times$ period interaction, were modeled with a spatial power, exponential or spherical matrix structure. In case of non-positive definite random-effect or residual covariance matrix, either the random effect of cow and/or the spatial correlation structure were removed from the model. Matrix structure was evaluated using Akaike information criterion (AIC). Degrees of freedom were estimated using the Kenward-Roger approximation. Multiple comparisons were

performed according to the Tukey-Kramer method. Data from sampling times with less than five concentrations above the minimum detectable concentration were excluded from the analysis, which applied to lactate and ethanol concentrations. Analyses were carried out using PROC GLIMMIX in SAS (SAS Institute Inc., 2010). All results are reported as least squares means. Significance of effects was declared at $P \leq 0.05$ and tendencies to significance at $0.05 < P \leq 0.10$.

Gaseous emissions

Translocation of cows to chambers may affect the gas emission profile of that particular day and therefore only data obtained between morning feedings on day 14 and day 17 were evaluated. Since cows were fed at 10 and 14 h intervals every day, values of H_2 and CH_4 emission observed between morning and evening feeding, and evening and morning feeding were fitted to time separately. Values of H_2 emission rate were $\log_{10}$-transformed to stabilize variance. Gas emission rates were evaluated using the following double-exponential and hyperbolic nonlinear models:

$$y_{ijk} = \begin{cases} \phi_{1ij} + \phi_{2ij}(-\exp^{\phi_{3ij}t} + \exp^{\phi_{4ij}t}) + e_{ijk} \\ \phi_{1ij} + \dfrac{\phi_{2ij}t^{\phi_{4ij}}}{1 + \phi_{3ij}t^{1+\phi_{4ij}}} + e_{ijk} \end{cases},$$

$$\boldsymbol{\phi}_{ij} = \begin{bmatrix} \phi_{1ij} \\ \phi_{2ij} \\ \phi_{3ij} \\ \phi_{4ij} \end{bmatrix} = \begin{bmatrix} \beta_1 \\ \beta_2 \\ \beta_3 \\ \beta_4 \end{bmatrix} + \begin{bmatrix} b_{1i} \\ b_{2i} \\ b_{3i} \\ b_{4i} \end{bmatrix} + \begin{bmatrix} b_{1i,j} \\ b_{2i,j} \\ b_{3i,j} \\ b_{4i,j} \end{bmatrix} = \boldsymbol{\beta} + \boldsymbol{b}_i + \boldsymbol{b}_{i,j},$$

$$\text{with } \boldsymbol{b}_i \sim N(\mathbf{0}, \boldsymbol{\Psi}_1), \boldsymbol{b}_{i,j} \sim N(\mathbf{0}, \boldsymbol{\Psi}_2) \text{ and } e_{ijk} = \begin{cases} N(0, \sigma^2) \\ N(0, \sigma^2|\nu_{ijk}|^{2\omega}) \\ N(0, \sigma^2 \exp^{2\omega\nu}) \end{cases}, \tag{4.2}$$

where $\boldsymbol{\beta}$ is the vector of fixed effects, where β_1 is the asymptote, β_2 is a linear multiplier, β_3 and β_4 represent the increase and decline of gas emission after feeding, respectively; $\boldsymbol{b}_i$ is the vector of random effects of the cow × period interaction, with $i = 1, \ldots, 8$ and its covariance matrix $\boldsymbol{\Psi}_1$; $\boldsymbol{b}_{i,j}$ is the vector of random effects of portion nested within the cow × period interaction, with $j = 1, 2, 3$ and its covariance matrix $\boldsymbol{\Psi}_2$; e_{ijk} is the residual error with variance covariate ν_{ijk} (gas emission rate for the power function, gas emission rate or time from feeding for the exponential function) and unrestricted parameter ω (i.e., may take any real value, the variance increases or decreases with the variance covariate). Effect of dietary treatment on emission profile was evaluated by stepwise replacement of the four fixed-effects parameters ($\beta_1, \ldots, \beta_4$)

according to:

$$\beta_n = \delta_{n1} x_{n1} + \delta_{n2} x_{n2}, \tag{4.3}$$

with $\begin{bmatrix} x_{n1} \\ x_{n2} \end{bmatrix} = \begin{bmatrix} 1 \\ 0 \end{bmatrix}$ if diet is control and $\begin{bmatrix} x_{n1} \\ x_{n2} \end{bmatrix} = \begin{bmatrix} 0 \\ 1 \end{bmatrix}$ if diet is linseed, and δ_{n1} and δ_{n2} the control and linseed diet main effects, respectively. Inclusion of treatment fixed effect and random effects, and random-effects covariance structure and residual variance were modelled using AIC. Model parameters for control and linseed diet were compared using Tukey's pairwise comparison. Analyses were carried out using nlme (Pinheiro and Bates, 2000) and multcomp (Hothorn et al., 2008) packages in R statistical software.

Microbiota composition

Microbial composition summary plots and Principal Coordinate Analysis (PCoA) of the weighted unifrac distance matrix of the OTU was performed using a workflow based on Quantitative Insights Into Microbial Ecology (QIIME) v1.2 (Caporaso et al., 2010). Permutational Multivariate Analysis of Variance (PERMANOVA) (Anderson, 2001) was used to assess the significance of changes in the rumen microbiota composition with respect to the factors: time (10 levels), diet (2 levels: CON and LSO) and the factor interaction period × diet (4 levels). PERMANOVA was also used to test the effect of time by categorizing time points based on the concentration of rumen metabolites being either 'high' (0.5-4 h; total concentration of VFA+lactate+ethanol $\leq$ 90 mM or a maximum in gas partial pressure) or 'low' (0, 6-10 h; every other case). PERMANOVA and Bonferroni corrected multiple comparisons were applied on the weighted unifrac distance matrix using the Matlab Fathom toolbox (Jones, 2015). Redundancy analysis (RDA) was performed using Canoco 5 (Šmilauer and Lepš, 2014) to assess the relationship between genus-level phylogenetic groupings of the OTU and time or diet.

4.3 Results

4.3.1 Composition of diets and feed intake

The composition of the grass silage, corn silage and the concentrates as well as total mixed ration is shown in Table 4.2. On day 11 of both experimental periods, cows started ingesting their portions immediately after morning feed delivery with the highest intake consistently occurring during the first 0.5 h after feeding (Figure S1). Small differences between cows in the time taken to finish their portions were observed,

Table 4.2: Analyzed composition of grass silage, corn silage and treatment concentrates (without linseed oil (CON) and with linseed oil (LSO)) and calculated composition of total mixed diets (g/kg dry matter (DM), unless stated otherwise)

	Silage		Concentrate[b]		Diet	
Item	**Grass**	**Corn**	**CON**	**LSO**	**CON**	**LSO**
DM (g/kg)	554	316	878	890	465	466
Crude Ash	91	41	120	111	79	77
Crude protein	140	80	394	361	192	182
Crude fat	30	35	33	108	33	56
NDF	542	333	203	178	357	349
ADF	322	202	101	91	208	205
Starch	ND[a]	373	18	14	154	153
Sugars	89	ND[a]	137	124	68	64
Gross Energy (MJ/kg of DM)	18.3	18.3	18.0	19.7	18.2	18.7

[a] Not determined; [b] For concentrate ingredient composition see Table S1.

particularly with cow 2 in period 1 which took longer to finish its portion (8 h) compared to the other cows (2-6 h). Portion size was 9.1 ± 0.2 kg of DM and no refusals were found from any of the cows. During the chamber measurement days, 9.0 ± 0.3 kg of DM of the portions were ingested and feed refusals (0.1 ± 0.2 kg of DM) only occurred with cow 2.

4.3.2 Headspace gases, dissolved metabolites and microbial numbers

In response to feeding, p_{H_2} increased from $2.4{\cdot}10^{-4}$ to $2.2{\cdot}10^{-2}$ bar in 0.5 h and then steadily decreased to and did not significantly differ from the 0 h level at 10 h (Figure 4.1). A similar pattern was observed for CO_2 partial pressure (p_{CO_2}) which increased from 0.54 to 0.69 bar during the first 0.5 h and then decreased and did not differ from the 0 h level from 3 h onwards, with the numerically lowest p_{CO_2} of 0.53 bar at 10 h. The profile of CH_4 partial pressure (p_{CH_4}), however, showed a decrease from 0.29 to 0.18 bar over the first 0.5 h and then increased to values not different from 0 h level at 2, 2.5, 3, 7 and 9 h. From 4 to 10 h, p_{CH_4} was between 0.22 and 0.25 bar and did not significantly differ from the values observed at 2, 2.5 and 3 h. In contrast to p_{H_2} and p_{CO_2}, which were not affected by diet (Table S2), p_{CH_4} tended to be lower for cows fed the linseed diet ($2.4{\cdot}10^{-1}{\pm}4.8{\cdot}10^{-3}$ bar for CON vs. $2.3{\cdot}10^{-1}{\pm}4.8{\cdot}10^{-3}$ bar for LSO; $P = 0.067$). No time × diet interaction was observed for any of the gaseous metabolites ($P > 0.567$). Rumen fluid pH was 7.0 at feeding, decreased to 6.3 by 2 h, remained relatively constant until 5 h and then increased to 6.7 at 10 h (Figure 4.1). The largest decrease was between 0.5 and 1 h and pH-values were significantly

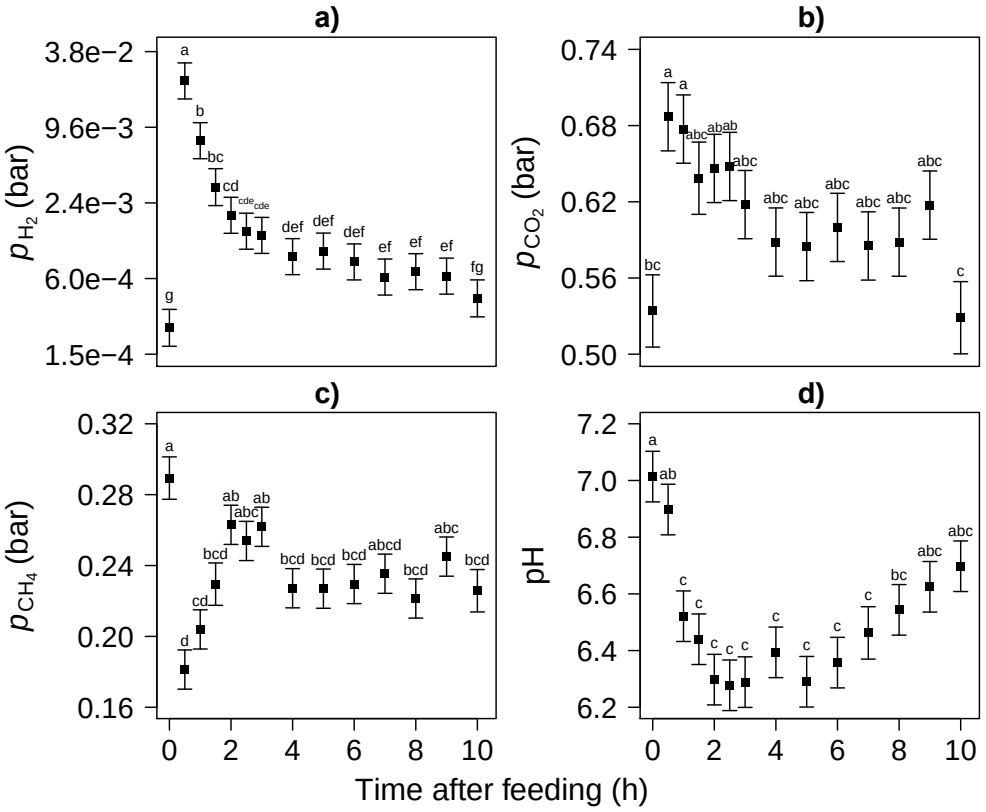

Figure 4.1: Partial pressure of a) H_2, b) CO_2, c) CH_4 in the rumen headspace and d) pH of rumen fluid over the first 10 h after feeding. Values represent least square mean (LSM) ± standard error, with different letters indicating significant differences in time ($P < 0.05$).

different from 0 h level from 1 to 8 h. Rumen fluid pH was not affected by diet ($P = 0.538$) and no time × diet interaction was observed ($P = 0.902$).

No ethanol was detected at 0 h after feeding but its concentration increased to a maximum of 5.4 mM at 1 h. After this maximum ethanol concentration steadily decreased, falling below the detection limit by 4 h (Figure 4.2a). No lactate was detectable at 0 and 0.5 h, and a numerical maximum of 2.7 mM was observed at 1 h, after which concentrations decreased to below the detection limit by 4 h (Figure 4.2b). After feeding, total VFA concentration increased from 69 mM at 0 h to its numerical maximum of 123 mM after 3 h with the values at 2 and 2.5 h not significantly differing from the numerical maximum (Figure 4.2c). The molar proportion of acetate decreased from 68 to 62% over the first 1.5 h post feeding and then recovered towards the 0 h level after 3 h from feeding (Figure 4.2d). Propionate proportion showed

the opposite pattern in time and significantly increased from 16% to its numerical maximum of 22% at 1.5 h, after which it declined to a proportion not significantly different from the 0 h level (Figure 4.2e). The proportion of butyrate showed a different pattern with a steady increase after feeding, from 11% at 0 h to a peak of 15% at 6 h after feeding (Figure 4.2f). Propionate proportion tended to be greater (0.61 ± 0.35%; $P = 0.098$) and ethanol concentration tended to be lower (–1.3 ± 0.6 mM; $P = 0.065$) for LSO compared to CON. No effects or tendencies for diet ($P > 0.536$) to affect the other dissolved metabolites assessed were observed and no time × diet interaction was observed for any of dissolved metabolites (Table S2).

In response to feeding the bacterial concentration ($\log_{10}$ 16S rDNA gene copies per mL rumen fluid) increased significantly from 0 to 0.5 h, and at 4 h was significantly lower than at 0.5, 1 and 3 h (Figure 4.3a). Linseed oil supplementation increased the bacterial concentration (10.4 vs. 10.3 $\log_{10}$ 16S rDNA gene copies/mL; $P < 0.001$); no time × diet interaction was observed ($P = 0.899$). The archaeal concentration ($\log_{10}$ 16S rDNA gene copies/mL) tended to be affected by time after feeding ($P = 0.077$), with the 3 and 4 h observations significantly different from each other ($P = 0.014$). No diet effect ($P = 0.385$) and time × diet interaction ($P = 0.941$) on the archaeal concentration were observed. The ratio of archaea to bacteria varied from 0.11 to 0.22 (Figure 4.3b) and tended to be affected by time from feeding ($P = 0.089$), with no significant differences between time points ($P \geq 0.138$). Neither a diet effect ($P = 0.611$) nor a time × diet interaction was observed ($P = 0.934$) for the archaea to bacteria ratio (Table S2).

4.3.3 Hydrogen and methane emission

Average emission rates of H_2 during daytime, which was from morning feeding at 6 am to afternoon feeding at 4 pm, were 33.0 and 34.3 mmol/h for CON and LSO fed cows, respectively (Table S3). Average emission rates of H_2 overnight, which was from afternoon feeding at 4 pm to morning feeding at 6 am, were 28.3 and 28.1 mmol/h for CON and LSO diets, respectively. Average daytime CH_4 emission rates were 1.12 and 1.07 mol/h and average overnight CH_4 emission rates 1.05 and 1.02 mol/h for CON and LSO diets, respectively.

The hyperbolic model fitted best to the $\log_{10}$ transformed H_2 emission rate on AIC (Table S4). The double exponential model appeared to be insufficiently capable of fitting the sharp peak in H_2 emission rate (result not shown). As substantial scattering of measurement points appeared after peak emission, modeling the H_2 emission rate of the daytime and overnight periods with residual variance functions improved the model fit. The selected hyperbolic model showed an increase in H_2 emission rate from

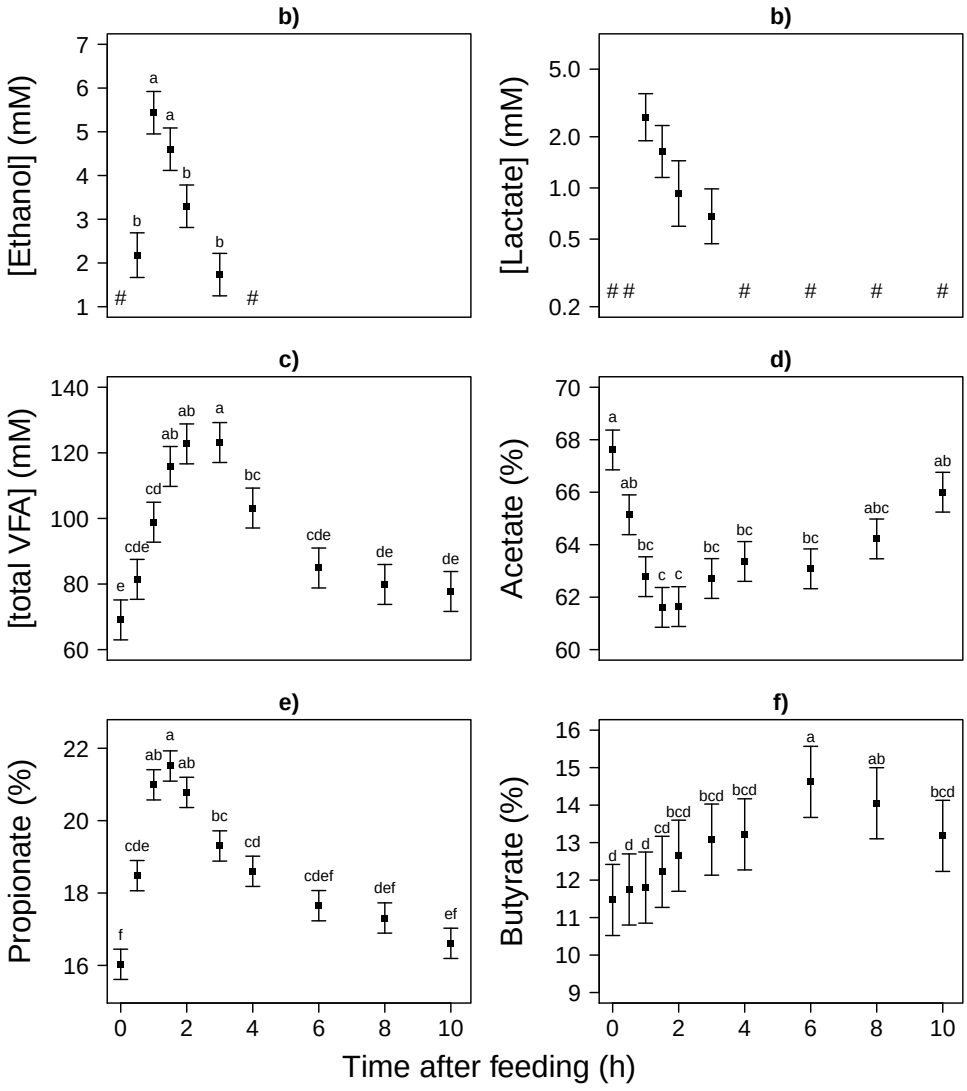

Figure 4.2: Concentrations of a) ethanol, b) lactate, c) total VFA, and proportions of d) acetate, e) propionate and f) butyrate in rumen fluid over the first 10 h after feeding. The "#" indicates that the metabolite concentration was non-detectable. Values represent least square mean (LSM) ± standard error, with different letters indicating significant differences in time ($P < 0.05$). Values of lactate concentration are back-transformed and plotted on a log scale.

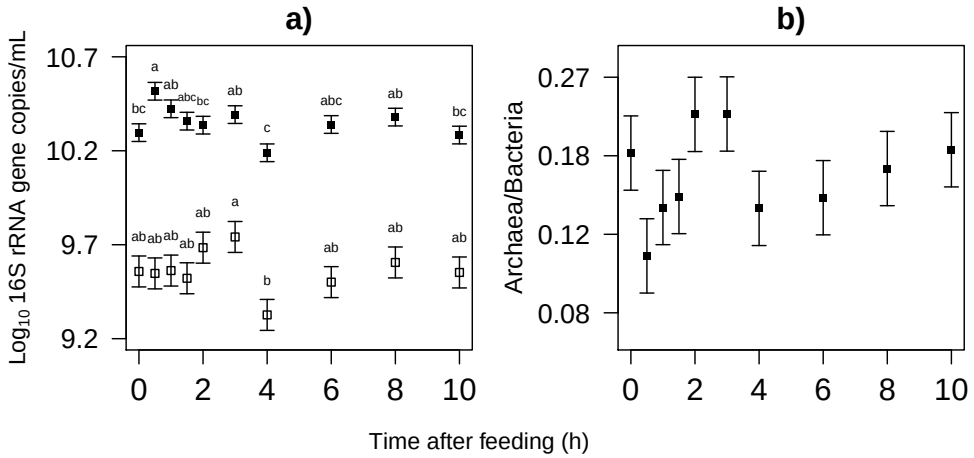

Figure 4.3: a) Log_{10} transformed bacterial (closed squares) and archaeal (open symbols) 16S rRNA gene concentration and b) back-transformed archaea to bacteria ratio in the rumen over the first 10 h after feeding with a y-axis that is plotted on a log scale. Values represent least square mean (LSM) ± standard error, with different letters indicating significant differences in time ($P < 0.05$).

approximately 5 to 200 mmol/h in 0.5 h after feeding and then decreased to basal level (Figures 4.4a and 4.4b). No diet effect was observed on any of the parameters of the best-fit models for daytime and overnight H_2 emission.

Based on AIC, daytime and overnight emission rate of CH_4 were best described by the double exponential model. The CH_4 emission rate increased by about a factor two from approximately 0.7 to 1.5 mol/h in 0.8 h after feeding (Figures 4.4c and 4.4d, Table S4). On AIC, best-fit models for CH_4 emission resulted in parameters that were significantly affected by diet, indicating decreased CH_4 emission from LSO fed cows. For daytime CH_4 emission, β_2 was affected by diet (difference CON – LSO, 0.08 ± 0.04, $P = 0.036$; Table S4), whereas for overnight CH_4 emission rate, β_4 was affected by diet (difference CON – LSO, 0.02 ± 0.01, $P = 0.015$; Table S4).

4.3.4 Microbial composition

Bacteria (80.8 ± 7.8% of the 16S rRNA sequences) were represented by 787 different OTU whereas the archaea (18.6 ± 7.7% of the 16S rRNA sequences) were represented by 68 different OTU. Of the 75 different genus-level phylogenetic groupings (72 for bacteria and 3 for archaea) that the 855 OTU could be summarized to, six dominant groupings represented a major proportion of the bacteria (71.1 ± 4.7% of the bacterial 16S rRNA sequences) and one grouping the archaea (93.5 ± 2.4% of the archaeal

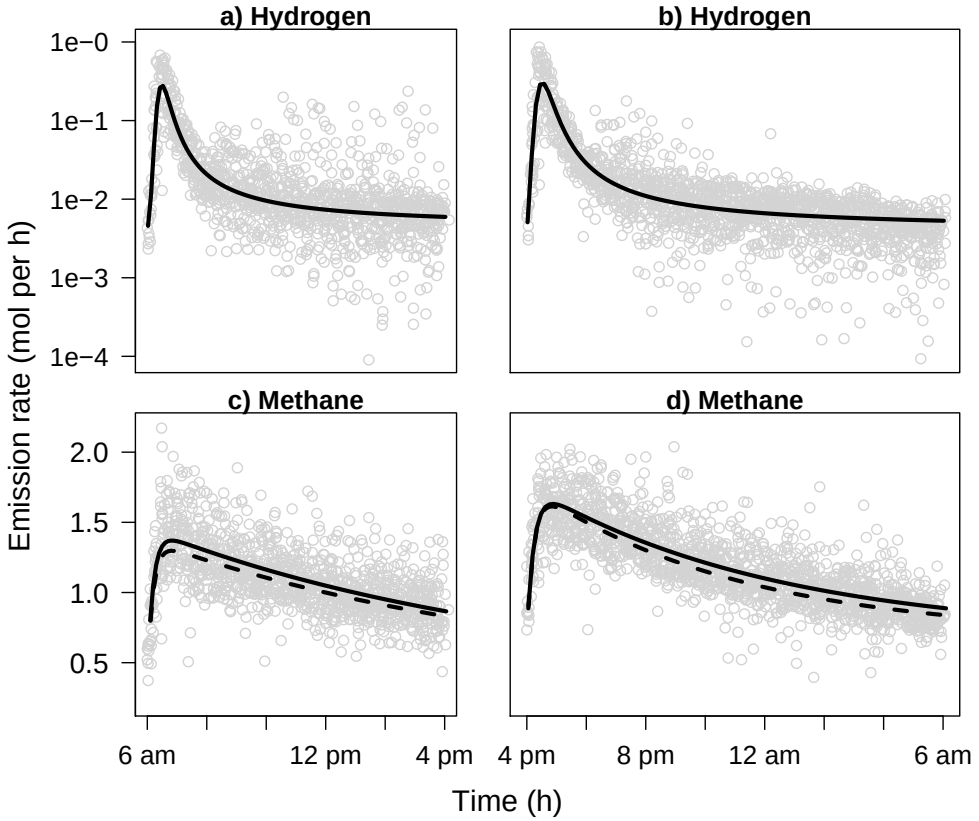

Figure 4.4: Gas emission rates as a function of time from feeding. The graph shows a) daytime (from morning feeding at 6 am to afternoon feeding at 4 pm) and b) overnight (from afternoon feeding at 4 pm to morning feeding at 6 am) back-transformed H_2 emission rate plotted on a log scale predicted with a hyperbolic model, and c) daytime and d) overnight CH_4 emission rate predicted with a double exponential model. H_2 emission rate was not affected by dietary treatment, CH_4 emission rate was affected by dietary treatment (solid line for control diet, dashed line for linseed oil diet). See Table S4 for model parameters.

16S rRNA sequences). These seven major genus-level phylogenetic groupings could be annotated to either the family (Succinivibrionaceae;genus-NotAnnotated (g-NA), Ruminococcaceae;g-NA and Christensenellaceae;g-NA) or genus level (*Ruminococcus*, *Butyrivibrio*, *Prevotella* and *Methanobrevibacter*). A summary of the relative abundances of the genus-level phylogenetic groupings is given with respect to both sampling time (Figure S2) and diet (Figure S3).

Principal Coordinate Analysis (PCoA) of the OTU-level data did not show any clear clustering of the samples with respect to either distinct time points or diet (Figure 4.5). The time points 0, 6, 8 and 10 h however were generally located to the bottom half of the PCoA-2 axis (18% of total variation), and the 1-4 h time points to the top. The 0.5 h time points were more centrally located along the PCoA-2 axis. No factors explaining variation could be identified for the separation of the samples on the PCoA-1 axis (31% of total variation). In line with the time point localization along the PCoA-2 axis, PERMANOVA indicated a difference in the microbial composition between the 'low' (0, 6-10 h) and 'high' (0.5-4 h) metabolite concentration categories ($P < 0.001$). Besides a few tendencies for significance, only the 1.0 and 1.5 h time points were significantly different from the 8 h time point (Table S5). PERMANOVA also indicated an effect of diet on microbial composition ($P = 0.024$), as well as a period $\times$ diet effect (Table S6). The period $\times$ diet as well as inherent cow variation in the rumen microbiota, may have limited the appearance of the diet effect in the PCoA plot.

Time points separated along the first canonical axis of the RDA by the 'low' and 'high' time point categories (Figure 4.6). *Pseudobutyrivibrio*, *Lactobacillus*, *Selenomonas*, *Succiniclasticum*, *Streptococcus* and *Prevotella* genera appeared to be associated with the 'high' time point category, along with some genus-level phylogenetic groupings that could only be annotated to the family (Prevotellaceae and Erysipelotrichaceae Incertae Sedis) or order level (Lentisphaeria RFP12 gut group). Ruminococcaceae Incertae Sedis, *Succinivibrio* and *Ruminobacter* genera appeared to be associated with the 'low' time point category, along with some genus-level phylogenetic groupings that could only be annotated to the family (Succinivibrionaceae), order (Aeromonadales) or class level (Cyanobacteria SHA-109). Many of the genus-level phylogenetic groupings also differed further in terms of the time points where their relative abundance was highest (Figure 4.6). The nine genus-level phylogenetic groupings for the 'high' time point category had high relative abundances at the following times after feeding: *Pseudobutyrivibrio* (0.5-1.5 h), *Lactobacillus* (1-2 h), *Selenomonas* (1.5 h), *Succiniclasticum* (1.5 h), Erysipelotrichaceae Incertae Sedis (1.5 h), *Streptococcus* (1.5 h), *Prevotella* (1.5 h), Prevotellaceae;g-NA (1.5-3 h) and Lentisphaeria RFP12 gut group (4 h). The six

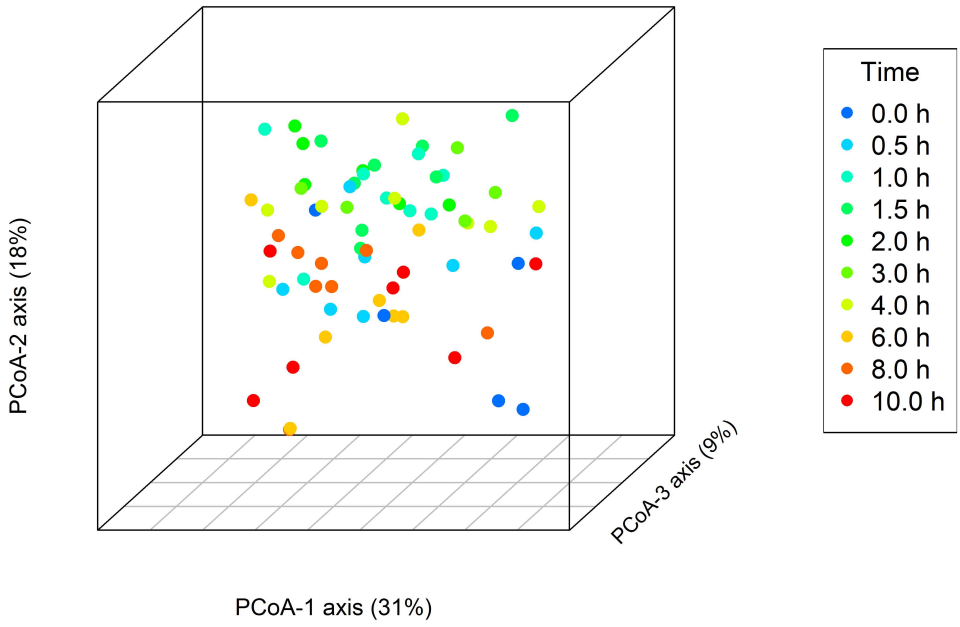

Figure 4.5: Principal Coordinate Analysis of samples at the OTU level using weighted unifrac distances, with samples labelled by time point as indicated by the key.

genus-level phylogenetic groupings for the 'low' time point category had high relative abundances at the following times after feeding: Cyanobacteria SHA-109;ofg-NA (0-0.5 h), Aeromonadales;fg-NA (8 h), *Ruminobacter* (8 h), *Succinivibrio* (8 h), Succinivibrionaceae:g-NA (8-10 and 0 h) and Rumincoccaceae Incertae Sedis (10 and 0 h). Of the variation in the relative abundance of genus-level phylogenetic groupings that were best explained by diet, only two groupings appeared to have high relative abundance associated with one of the diets (Figure 4.7). The Bacteroidales BS11 gut group and the Rikenellaceae RC9 gut group had a positive association with CON, and were therefore negatively associated with the LSO.

4.4 Discussion

To our knowledge, this is the first comprehensive study that has identified the diurnal profiles of gaseous and dissolved metabolites (including lactate and ethanol) and the microbiota in the rumen, along with associated respiration chamber measured H_2 and CH_4 emission rates. It is unique that these diurnal profiles were mapped with at least ten time points during the first 10 h after feeding, and the obtained data illustrated the importance of frequent sampling during the first few hours after feeding. This insight is important when developing an integrated understanding of the dynamics of rumen microbial fermentation, and its implications for the production of H_2 and CH_4.

4.4.1 Gaseous metabolites

In this study the lowest value of p_{H_2}, observed at the moment of feeding (0 h), is similar to the lower bound values of 0.1-0.6 μM ($1{\cdot}10^{-4}$-$8{\cdot}10^{-4}$ bar of p_{H_2} according to Henry's law) reported in the review of Janssen (2010). Hegarty and Gerdes (1999) suspected p_{H_2} to be rarely higher than $1{\cdot}10^{-2}$ bar, which applies to all our observations except for the one at 0.5 h after feeding. The $2.2{\cdot}10^{-2}$ maximum of p_{H_2} however is still in line with Smolenski and Robinson (1988) who reported a H_2 spike of 10-20 μM ($1\text{-}3{\cdot}10^{-2}$ bar of p_{H_2}) that lasted for 30 min after feeding. Moate et al. (1997) reported 0.66 and 0.76 bar of p_{CO_2} and 0.31 and 0.22 bar of p_{CH_4} before and after an hour of active grazing, respectively. These absolute values are higher than observed in the present study, but the increased p_{CO_2} and decreased p_{CH_4} in response to feed consumption is similar.

The increase in H_2 emission rate, of which the magnitude reflects the increase observed in ruminal p_{H_2}, is similar to the profile shown by Rooke et al. (2014) where a H_2 emission peak from a forage-concentrate fed steer appeared shortly after feeding.

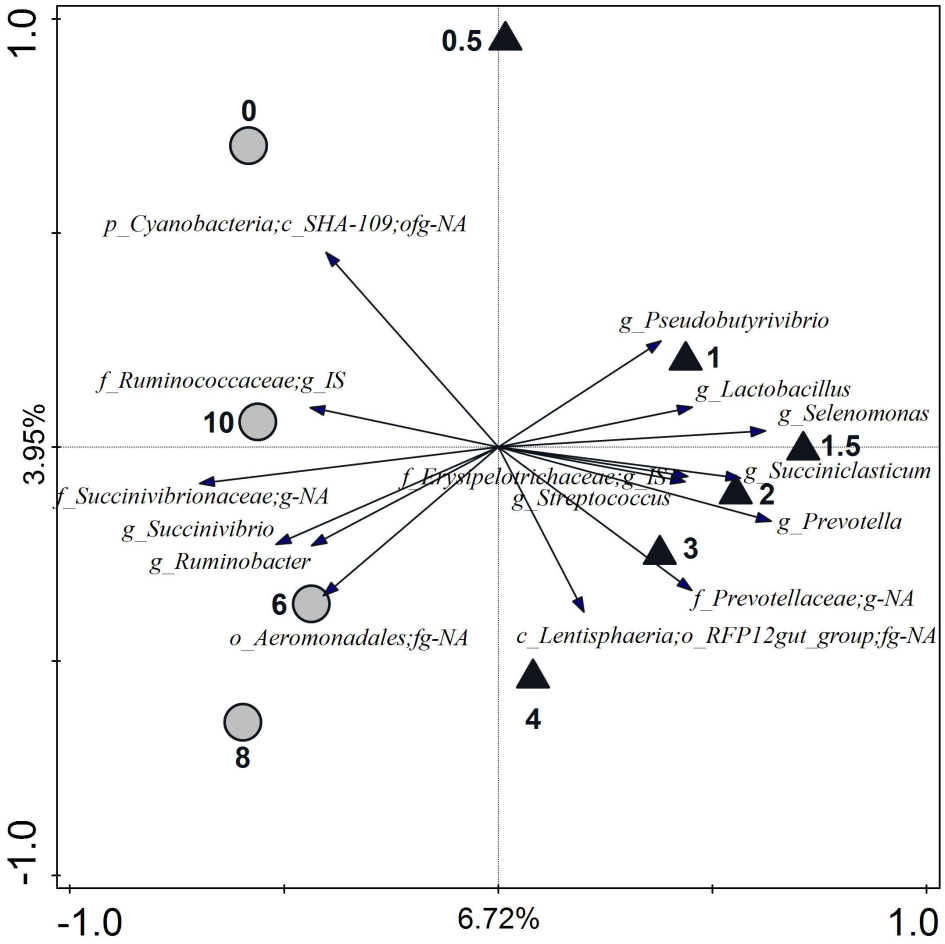

Figure 4.6: Redundancy analysis triplot showing the relationship between the top fifteen genus-level phylogenetic groupings of the OTUs explaining the variance with time. Time points (0-10 h) are indicated relative to the ruminal concentration of metabolites being either high (total VFA + lactate + ethanol > 90 mM or peaks in p_{H_2} and p_{CO_2}, triangles) or low (all other concentrations, circles). Arrow length indicates the variance that can be explained by the parameter time, with the perpendicular distance of the time points to the arrow indicating the relative abundance of the genus-level phylogenetic grouping. Arrow labels indicate the taxonomic affiliation of genus-level phylogenetic groups, with the level (i.e., kingdom (k), phylum (p), class (c), order (o), family (f) or genus (g)) and taxon (as defined by the Silva 16S rRNA database) that the groups could be reliably assigned to. For example ' *g_Prevotella*' represents an OTU reliably assigned to the *Prevotella* genus, whereas 'p_Cyanobacteria;c_SHA-109;ofg-NA' was reliably assigned to the class SHA-109 but the order, family and genus could not be annotated (NA). IS = Incertae Sedis.

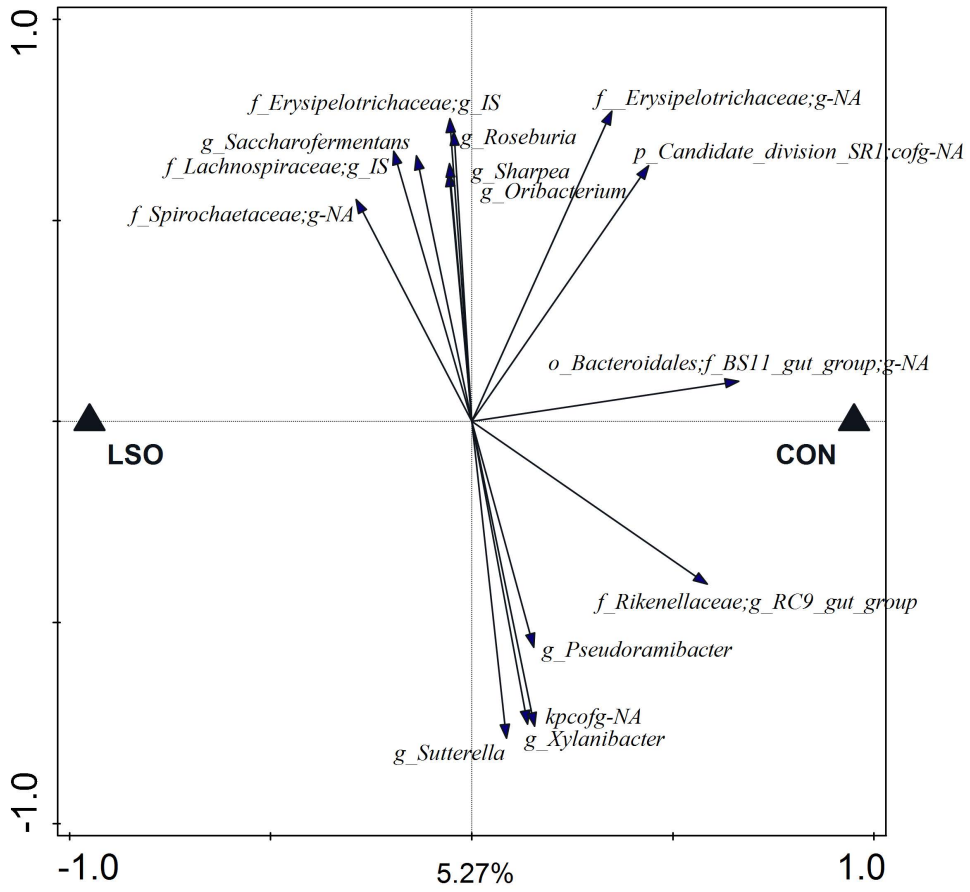

Figure 4.7: Redundancy analysis triplot showing the relationship between the top fifteen genus-level phylogenetic groupings of the OTU explaining the variance with diet (control (CON) or linseed oil (LSO)). Arrow length indicates the variance that can be explained by diet; distance and labels are as previously described in Figure 4.6. IS = Incertae Sedis.

The H_2 yield in Rooke et al. (2014), however, appeared to be higher (0.11 mol/kg DM) than observed in the present study (0.04 mol/kg DM). Olijhoek et al. (2016) observed the lowest average H_2 emission of 6 mmol/h over the hour before feeding, and the highest average H_2 emission of 134 mmol/h over the first hour after feeding for their control diet. Veneman et al. (2015) observed maximum H_2 emission rate of about 125 mmol/h during the first hour after feeding for control and linseed diets. These hourly averages are generally in line with the results in this study (minimum 5 mmol/h; maximum 200 mmol/h; peak at 0.5 h). The fitted CH_4 emission profiles in the present study are in line with Brask et al. (2015) who reported the highest average hourly emission in the second hour after feeding, whereas the highest average hourly emission was observed in the third hour after feeding by Olijhoek et al. (2016). Rooke et al. (2014) and Olijhoek et al. (2016) observed an increase in CH_4 emission by a factor of two after feeding, which is similar to the increase observed in the present study. Given the CH_4 emission rate and DMI, the CH_4 yield in the present study is 22.6 g/kg of DM, which is comparable to the CH_4 yields reported by Veneman et al. (2015) for control and linseed oil diets, Van Gastelen et al. (2015) and the mixed diet of Rooke et al. (2014) ranging from 21.4 to 25.0 g/kg of DM.

The fitted emission rate of both gases showed a rapid increase after feeding, whereas residual variance of the H_2 emission rate increased after the peak emission, in particular for the daytime period (Figure 4.4). Upward scattering may have been caused by delayed feed intake as not all cows ingested their feed within the same period of time (Figure S1), while downward scattering might have resulted from decreased activity of cows. Although the selected non-linear model visually appears to properly estimate the average emission rate in time, in future experiments on rumen fermentation dynamics it might be useful to give cows access to feed only during the first few hours after feed delivery. Data following a non-skewed distribution would be particularly helpful when making inference on effects such as diet.

The increase of ruminal p_{H_2} and p_{CO_2} at the expense of p_{CH_4}, and the peak in H_2 emission rate shortly after feeding can be explained by microbial fermentation of rapidly degradable feed components, yielding H_2 and CO_2. Archaea in turn use the H_2 and CO_2 released from fermentation to produce CH_4, which is reflected in the peak in CH_4 emission rate that follows the peak in H_2 emission rate (at 0.8 and 0.5 h, respectively). Increased archaeal production of CH_4 relative to microbial fermentation in response to feed intake may have caused the recovery of p_{H_2}, p_{CO_2} and p_{CH_4} towards the basal level, as observed from 1 h after feeding. The coincidence of a sharp peak in H_2 emission and a relatively weak increase in CH_4 emission, followed by a steeper decline in H_2 emission compared with CH_4 emission after the peak emission, is in line with Olijhoek et al. (2016). These patterns suggest that for the observed range

of p_{H_2}, the archaeal enzymes available became saturated with H_2 as a methanogenic substrate and operated at their maximum rate.

4.4.2 Fermentation dynamics and microbiota

The sharp peak in H_2 emission shortly after feeding is associated with the microbial degradation of rapidly fermentable feed contents such as sugars (e.g., Leedle et al., 1982) as many different rumen micro-organisms swiftly utilize these. Apart from the Cyanobacteria, no genus-level phylogenetic grouping of OTU had a high relative abundance at the 0.5 h time point. The lack of further specific association with the 0.5 h time point might indicate that almost all micro-organisms can swiftly use rapidly degradable soluble substrates, resulting in no single species being more abundant than the others at this time.

Several of the genus-level phylogenetic groups in the rumen were positively associated with the time points that were within 1-3 h after feeding: *Pseudobutyrivibrio*, *Lactobacillus*, *Selenomonas*, *Succiniclasticum*, Erysipelotrichaceae Incertae Sedis, *Streptococcus*, *Prevotella* and Prevotellaceae;g-NA (Figure 4.6). The majority of these genera are known for their ability to promptly utilize non-structural carbohydrates. *Lactobacillus* was most abundant between 1-2 h after feeding, which coincided with the appearance of their major fermentation end product lactate.

Species of *Ruminobacter* and *Succinivibrio* are involved in starch degradation (Anderson, 1995; Bryant and Small, 1956), and their abundance between 6-10 h suggests that starch utilization is a key activity of the planktonic rumen bacteria at this stage (Figure 4.6). This may occur at this time due to release of (or increased access to) internal plant cell components as the structural carbohydrates are broken down by fibrolytic microbes. Bacteria degrading complex structural carbohydrates however were probably under-represented in our study as only rumen fluid was sampled.

The ecological role of the Aeromonadales;fg-NA and Ruminococcaceae *Incertae Sedis* genus-level phylogenetic groups (which were positively associated with the 4-10 h, and the 6-10 and 0-0.5 h time points, respectively) could not be identified due to the limited functional annotation of these groups. It is possible though that these phylogenetic groups are involved in cross-feeding of secondary metabolites released by the action of other microbes that colonize the feed particles. In line with this, Leedle et al. (1986) reported that the changes in time that occurred in the carbohydrate composition were not always consistent with the predicted scheme of fermentation of carbohydrates such as cellulose/hemicellulose, pectin, starch and soluble sugars.

In line with an early increase in metabolic activity, reflected by the H_2 production spike shortly after feeding, bacterial concentration increased to its highest value at 0.5 h (Figure 4.4). As bacterial proliferation may not occur rapidly enough to solely explain this increase, microbes might have migrated from the rumen particulate matter to rumen fluid in response to the freshly ingested feed, which temporarily increased the bacterial concentration in the fluid. The significant decline observed at 4 h is in line with the previous findings of Leedle et al. (1982), who also observed a minimum in direct bacterial counts at 4 h after feeding a 77% forage diet. The bacterial decline from 3 to 4 h is likely to be associated with decreased metabolic activity, as evidenced by the significant decrease in total VFA concentration also from 3 to 4 h after feeding (Figure 4.2). Since the bacterial concentration did not consistently increase until 2 h after feeding (whereas the total VFA concentration did) other processes may have been counteracting an increase in the bacterial concentration in the rumen fluid, such as adherence of bacteria to feed particles.

Rumen methanogenic archaea do not directly utilize feed but only fermentation product such as H_2, which explains why the peak in emission of CH_4 appeared after the peak in H_2 emission (0.8 vs. 0.5 h). The less steep decline of CH_4 emission after its peak compared to H_2 emission suggests that the archaeal enzymes are saturated with H_2 producing CH_4 still close to their maximum rate. The increased bacterial concentration and unaffected archaeal concentration at 0.5 h after feeding resulted also in a numerically decreased archaea to bacteria ratio. Wallace et al. (2014) found that the archaea to bacteria ratio may be an indicator of CH_4 yield per amount of feed. In the present study, the dynamics of the archaea to bacteria ratio and p_{CH_4} were qualitatively similar, both having a minimum at 0.5 h after feeding (Figures 4.3 and 4.1). This would imply that the archaea to bacteria ratio is associated with the amount of CH_4 produced relative to the total active metabolism, or in other words resembling the CH_4 yield per amount of feed degraded.

The p_{H_2} up to $2.2 \cdot 10^{-2}$ bar may thermodynamically inhibit hydrogenase catalyzed NADH oxidation in rumen bacteria (e.g., Van Lingen et al., 2016). In this thermodynamic state, the metabolism oxidizes NADH back to NAD^+ by generating more reduced fermentation products (e.g., Counotte and Prins, 1981; McSweeney et al., 1994; Fischbach and Sonnenburg, 2011). This explains why increased proportions of propionate at the expense of acetate were observed, and why lactate and ethanol appeared in response to feeding (Figure 4.2). These findings are therefore consistent with such a shift in metabolism being driven by a decreased NAD^+ to NADH ratio.

Increased propionate and decreased acetate proportion in response to feeding is in line with several reports (e.g., Hatew et al., 2015; Brask et al., 2015) that observed

the lowest acetate to propionate ratio at 2 h after feeding. The peak in lactate concentration appeared to be lower and later in response to feeding than in Counotte and Prins (1981), who observed 16, 29 and 16 mM of lactate at 15, 30 and 60 min after feeding 6 kg of concentrates. The lower amount of rapidly degradable carbohydrates in the 70:30 roughage to concentrate ratio diets used in this study may explain this difference.

Ethanol concentration in the rumen has not been widely measured *in vivo*, but was found to accumulate in the rumen of cattle and sheep after overfeeding with readily fermentable carbohydrates (Allison et al., 1964). The highest ethanol concentration occurred 1 h after feeding and was associated with among others the genus *Pseudobutyrivibrio* (Figure 4.6), which has been reported to include a species capable of producing ethanol (Kopečnỳ et al., 2003). The decrease in ethanol and lactate concentrations after 1 h, combined with the decrease of the propionate proportion in favor of acetate from 1.5 h, suggest that NADH oxidation was no longer strongly inhibited. This is also consistent with the observation that the p_{H_2} declined in combination with a decreased pH. Besides elevated concentrations of VFA, lactate will also contribute to a decrease in pH despite its relatively low concentration. This is because it is a stronger acid than acetate, propionate or butyrate. From 1 h after feeding, the pH in the rumen remained significantly decreased for several hours. The decrease in pH until 2-3 h after feeding followed the increase in total VFA concentration (Figures 4.1 and 4.2). Decreased pH counteracts the inhibition of NADH oxidation caused by increased p_{H_2} (Van Lingen et al., 2016), which alleviates the inhibition of NADH oxidation from 1 h after feeding.

4.4.3 Effects of linseed oil supplementation

The lack of effect of LSO on emission of H_2 is in line with Veneman et al. (2015), who also did not observe a difference in H_2 emitted from control and linseed treated cows with 2.2 and 6.2% crude fat, respectively. Similarly, Troy et al. (2015) did not observe an effect on H_2 emitted when feeding a control and rapeseed cake treated diet with 2.7 and 5.4% crude fat, respectively. In the present study, linseed oil decreased CH_4 emission rate and tended to decrease ruminal p_{CH_4}. This is consistent with the study of Martin et al. (2016) where decreased CH_4 emission was observed in response to increasing linseed supply with hay and corn silage based diets. In contrast Veneman et al. (2015) did not observe a significant effect of linseed treatment on emission of CH_4 in the two experiments they performed. Patra (2013) indicated CH_4 emission to be affected by the amount of C18:3, a major component in linseed oil, but demonstrated that the CH_4-suppressing effect might be more marked with high concentrations of

non-fiber carbohydrates in diets. However, Livingstone et al. (2015) did not find a decrease in CH_4 emission upon linseed supplementation regardless of the ratio of grass silage to corn silage in the diet. Various non-fiber carbohydrates may yield different VFA proportions, which makes it difficult to explain the CH_4-suppressing effect of C18:3 in detail. Biohydrogenation of unsaturated fatty acids also serves as a H_2 sink, but only has a minor contribution to the decrease in CH_4 production (Czerkawski, 1986). Furthermore, decreased CH_4 production may have resulted from decreased H_2 production, because oils are not fermented and their degradation does not yield H_2.

A tendency for an increased molar proportion of propionate for the LSO diets, is in line with the study of Li et al. (2015) who observed a decreased acetate to propionate ratio 3 and 6 h after feeding in steers fed linseed compared with control diets. Moreover, Martin et al. (2016) reported an increased propionate proportion with increased linseed supply. Changes in the proportion of VFA may therefore be a component of the C18:3 mode of action, as propionate proportion tended to be increased in the present study. The archaea concentration was unaffected by diet but bacterial concentration increased. The biological significance of this increase is not clear however as no corresponding increase of total VFA occurred in LSO fed animals.

Other studies, however, differ in their reports of the effect of linseed oil on microbial concentrations. Veneman et al. (2015) reported that the bacterial concentration associated with the solid phase tended to be decreased upon linseed oil supplementation, whereas the bacteria concentration in the fluid was not significantly affected. Yang et al. (2009) found that increased proteolytic bacteria at the expense of cellulolytic bacteria occurred rather than increased total viable bacteria concentration upon linseed oil supplementation. Differences observed in results from the present study may be related to the ruminal site of sampling as the rumen is not a completely homogeneous environment. The cranial ventral sac, which was the sampling site in this study, is known to have a higher total VFA concentration, lower pH and differ in its microbiota and activity compared to the central rumen sacs (Martin et al., 1999; Wang et al., 2016a). Another possible explanation is that the increased concentration of planktonic bacteria with linseed oil was caused by a decreased number of bacteria able to colonize the feed particles (Duval et al., 2004). This would also partly explain the lack of a concurrent increase in total VFA concentration. Sampling of the rumen solid contents should be considered to investigate a possible reduction in fiber colonization. In the present study, however, this was not possible as the required opening of the fistula would have abolished the possibility to determine detailed headspace gas profiles after feeding.

The linseed oil supplementation appeared to have a limited impact on the rumen microbiota composition and the metabolite concentrations in our study,

consistent with other studies (Li et al., 2015; Veneman et al., 2015). For both the metabolite concentrations and the microbiota composition, time from feeding clearly explained more variation than diet. Differences in the degradation rates of various types of carbohydrates may explain the observed temporal variation in metabolite concentration (Leedle et al., 1982) and microbiota composition (e.g., Rooke et al., 2014; Li et al., 2015; Wang et al., 2016b). Therefore, an experimental approach with contrasts in carbohydrate degradation rate, rather than contrasts in the amount of dietary fat, might have revealed even more about the microbial metabolic dynamics in the rumen.

Despite the limited effect of the linseed oil on the rumen microbiota, the linseed oil still decreased ruminal CH_4 emission. The variation in the rumen microbiota associated with the period × diet, might be due to the various grass silage batches used in this experiment. The crude fat and WSC fractions of the grass silage were 32 and 95 g/kg of DM in period 1 and 26 and 81 g/kg of DM in period 2, respectively, which might explain the period × diet effect. It may have also prevented diet specific effects in the rumen microbiota composition analysis from being detected. This is evidenced by the various genus-level phylogenetic groupings in the RDA triplot that had no substantial association with either of the experimental diets. The Bacteroidales BS11 gut group was most clearly negatively associated with the LSO diet. As no cultured representative is available for this taxon, it is not clear by which mechanism the linseed oil supplementation would decrease their relative abundance. C18:3 may be toxic to this taxon, as has been previously reported for various other rumen bacteria (Maia et al., 2007).

4.5 Conclusion

Time after feeding appeared to explain more variation in diurnal pattern of rumen metabolite concentrations and microbial composition than the CON and LSO diets. The large variation observed in diurnal patterns of rumen metabolites, the substantial increase of p_{H_2} rapidly after feeding followed by the occurrence of shifts in fermentation towards ethanol, lactate, and propionate at the expense of acetate, supports the key role of the redox state of NAD in rumen fermentation. This also highlights the importance of including diurnal dynamics in rumen fermentation studies to improve understanding of VFA and CH_4 production. The findings of this study also give insight into the key control points of rumen microbial metabolism, providing future opportunities to develop novel sustainable approaches to reduce the ecological footprint of ruminant livestock production.

Acknowledgments

We thank the staff of the experimental facilities "Carus" (Wageningen, the Netherlands) for their assistance during the implementation of the experiment, Sven Alferink (Wageningen University & Research, the Netherlands) for his assistance during sampling, and the laboratory staff of the Animal Nutrition Group (Wageningen, the Netherlands) for conducting the feed composition analysis. Additionally, we thank Ton van Gelder (Wageningen University & Research, the Netherlands) for his assistance with the GC and HPLC analyses.

Supporting information

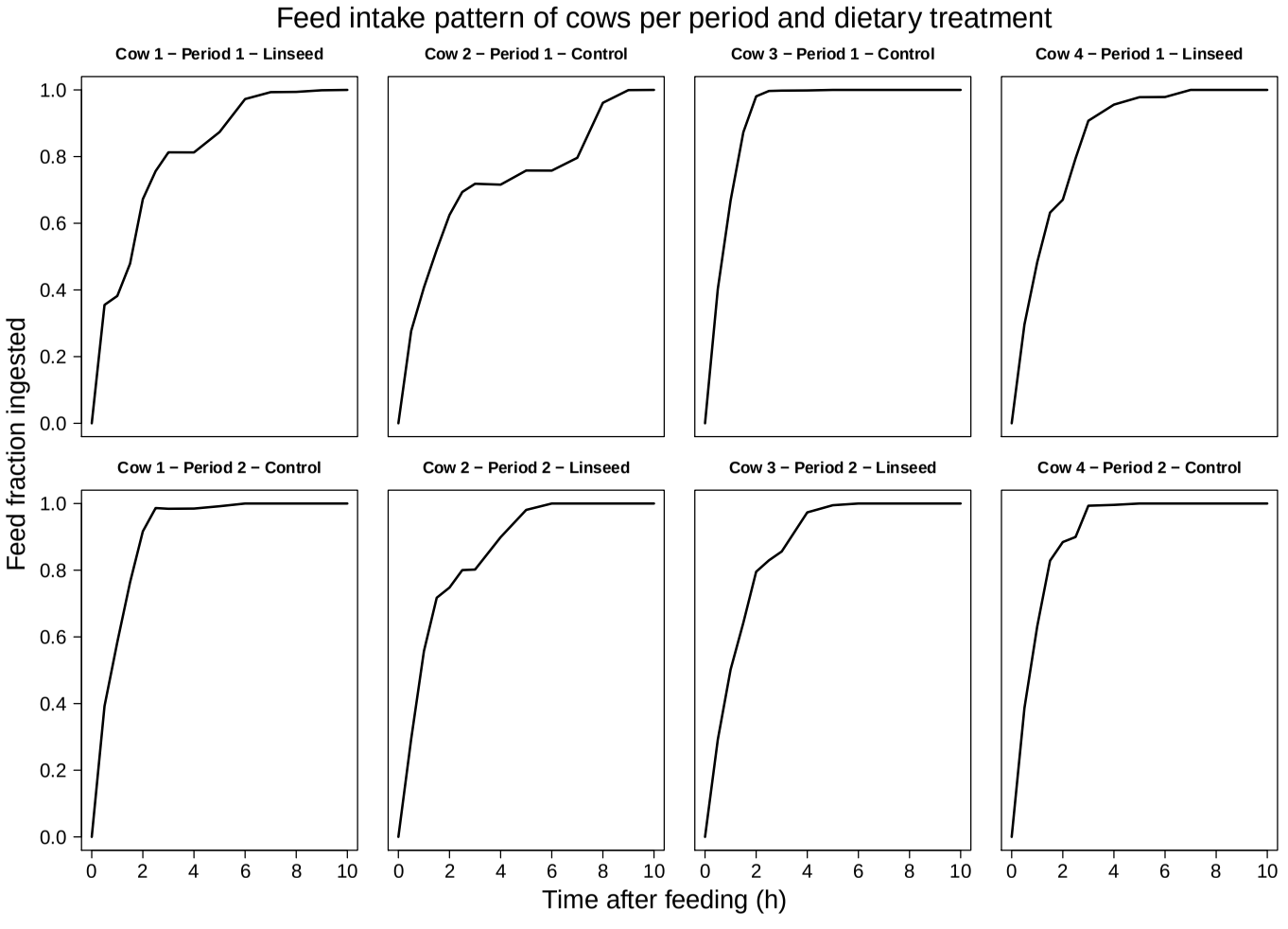

Figure S1: Feed intake pattern per cow, diet and/or period on experimental day 11 after morning feeding.

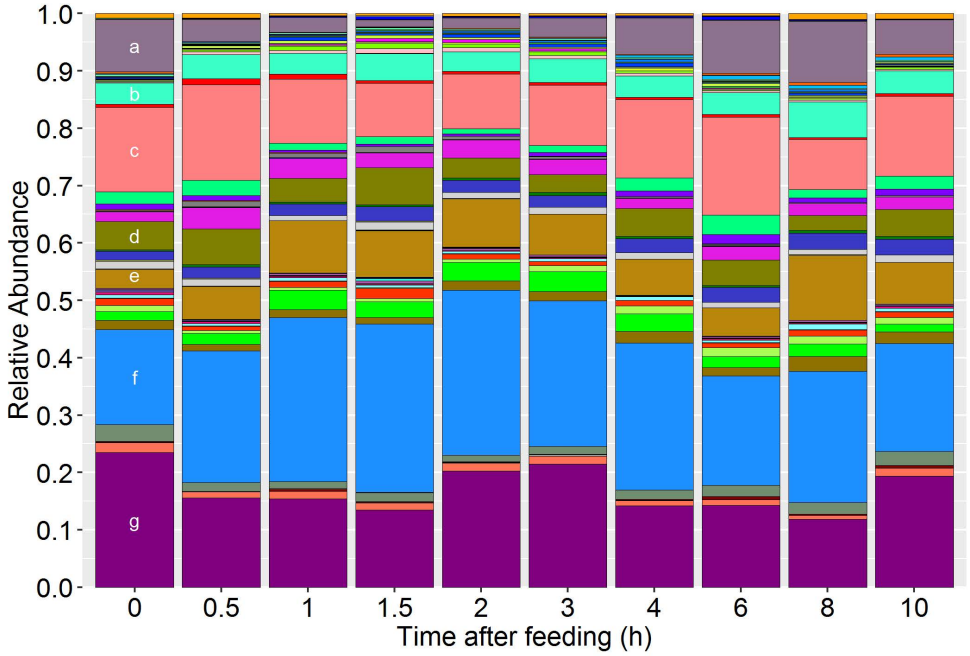

Figure S2: Taxonomic summary of the samples by time with the major phylogenetic groupings (annotated to the closest possible taxonomic level (family or genus)), indicated as follows: a) Succinivibrionaceae b) Ruminococcaceae c) *Ruminococcus* d) *Butyrivibrio* e) Christensenellaceae f) *Prevotella* and g) *Methanobrevibacter*.

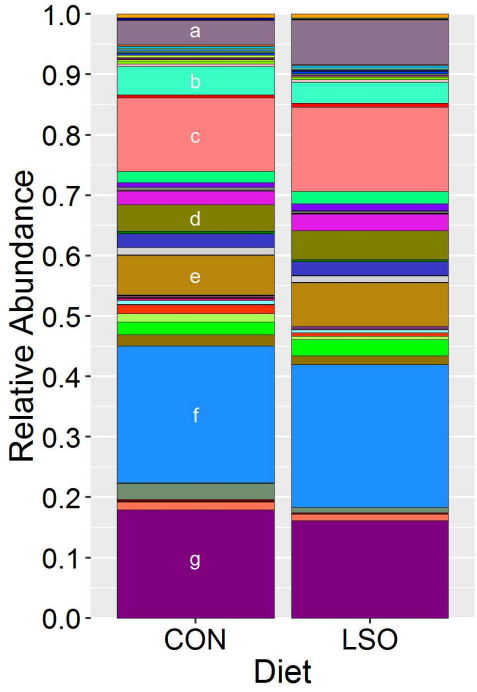

Figure S3: Taxonomic summary of the samples by diet with the major phylogenetic groupings (annotated to the closest possible taxonomic level (family or genus)), indicated as follows: a) Succinivibrionaceae b) Ruminococcaceae c) *Ruminococcus* d) *Butyrivibrio* e) Christensenellaceae f) *Prevotella* and g) *Methanobrevibacter*.

Table S1: Ingredient composition (g/kg DM) of experimental concentrates without linseed oil (CON) and with linseed oil (LSO).

Item	**CON**	**LSO**
Soybean meal	400	369
Soybean meal, formaldehyde treated	200	184
Rapeseed meal	100	92
Rapeseed meal, formaldehyde treated	100	92
Sugar beet pulp	119	109
Sugarcane molasses	40	37
$CaCO_3$	15	15
NaCl	8	8
$NaHCO_3$	2	2
Trace mineral and vitamin mix[a]	8	8
MgO	7	7
Cr_2O_3	2	2
Linseed oil[b]	0	76

[a] Research Diet Services, Wijk bij Duurstede, The Netherlands;

[b] Linagro, Lichtervelde, Belgium.

Table S2: Repeated-measures ANOVA P-values of time, diet, time × diet (T × D) and period fixed effects, and diet least square differences (LSD) for control diet minus linseed oil diet for partial pressure of gases in the headspace, pH, dissolved metabolite concentrations and 16S rRNA gene based microbial numbers in rumen fluid.

Metabolite	**Time**	**Diet**	**T × D**	**Period**	**LSD ± SE[a]**
p_{H_2}	<0.001	0.285	0.209	0.566	$4.6{\cdot}10^{-2} \pm 4.2{\cdot}10^{-2}$
p_{CO_2}	<0.001	0.932	0.433	0.791	$1.2{\cdot}10^{-3} \pm 1.4{\cdot}10^{-2}$
p_{CH_4}	<0.001	0.067	0.567	0.005	$1.3{\cdot}10^{-2} \pm 6.8{\cdot}10^{-3}$
pH	<0.001	0.538	0.902	<0.001	0.06 ± 0.09
Total VFA (mM)	<0.001	0.536	0.811	0.126	–2.6 ± 4.1
Acetate (% of VFA)	<0.001	0.604	0.808	0.076	0.56 ± 1.00
Propionate (% of VFA)	<0.001	0.057	0.783	0.038	–0.61 ± 0.34
Butyrate (% of VFA)	<0.001	0.970	0.536	0.255	0.02 ± 0.55
Lactate (mM)	0.089	0.804	0.732	0.771	0.1 ± 0.2
Ethanol (mM)[b]	<0.001	0.065	0.184	0.832	1.3 ± 0.6
Bacteria (copies/mL)	<0.001	<0.001	0.899	0.564	–0.09 ± 0.02
Archaea (copies/mL)	0.077	0.385	0.941	0.165	–0.06 ± 0.06
Archaea:Bacteria	0.089	0.611	0.934	0.272	0.03 ± 0.06

[a] $\log_{10}$-transformed values for p_{H_2}, lactate concentration and quantities of bacteria and archaea are shown; [b] results for best model, without random effect of cow, are shown; when data were fitted to the model that included both random effect of cow and a spatial correlation structure (Eq. 4.1) a second-best fit was obtained where the repeated measures covariance matrix converged to zero, P-values were < 0.001 (time), 0.003 (diet), 0.313 (time × diet) and 0.205 (period).

Table S3: Descriptive statistics of daytime (D; from morning feeding at 6 am to afternoon feeding at 4 pm) and overnight (N; from afternoon feeding at 4 pm to morning feeding at 6 am) average dry matter intake during chamber period (DMI; kg/portion) and hydrogen and methane emission rates (mmol/h and mol/h) for control (CON) and linseed (LSO) fed cows.

Item	**Time**	**Mean**	**SD**	**Min**	**Max**
DMI - CON	D	8.9	0.2	8.7	9.3
DMI - LSO	D	9.0	0.4	8.0	9.3
DMI - CON	N	9.1	0.2	8.7	9.3
DMI - LSO	N	9.1	0.2	8.7	9.3
H_2 - CON	D	33.0	76.4	$1.53 \cdot 10^{-1}$	624
H_2 - LSO	D	34.3	76.9	$9.02 \cdot 10^{-2}$	680
H_2 - CON	N	28.3	80.7	$9.32 \cdot 10^{-2}$	746
H_2 - LSO	N	28.1	75.8	$1.53 \cdot 10^{-1}$	864
CH_4 - CON	D	1.12	0.27	0.44	2.17
CH_4 - LSO	D	1.07	0.24	0.37	1.89
CH_4 - CON	N	1.05	0.30	0.38	1.93
CH_4 - LSO	N	1.02	0.30	0.21	1.85

Table S4: Parameter estimates (± SE), peak emission time (t_{peak} in h) and fit statistic of selected double-exponential (DE) and hyperbolic (HB) models for daytime (D; from morning feeding at 6 am to afternoon feeding at 4 pm) and overnight (N; from afternoon feeding at 4 pm to morning feeding at 6 am) log10-transformed hydrogen and methane emission rates (mol/h). β_1 is the asymptote, β_2 is a dimensionless linear multiplier, β_3 and β_4 determine the increase and decline of gas emission after feeding, respectively; if applicable, $\beta_n = \delta_{n1}x_{n1} + \delta_{n1}x_{n1}$, with $\begin{bmatrix} x_{n1} \\ x_{n2} \end{bmatrix} = \begin{bmatrix} 1 \\ 0 \end{bmatrix}$ if diet is control and $\beta_n = \delta_{n1}x_{n1} + \delta_{n1}x_{n1}$, with $\begin{bmatrix} x_{n1} \\ x_{n2} \end{bmatrix} = \begin{bmatrix} 0 \\ 1 \end{bmatrix}$ if diet is linseed, $\delta_{n1} - \delta_{n2}$ is the least square difference of the control and linseed diet effects parameters associated with β_n.

Model	**Time**	β_1	β_2	β_3	β_4	**AIC**	t_{peak}
Hydrogen							
DE[a]	D	-2.13 ± 0.09	2.94 ± 0.29	-3.98 ± 0.45	-0.87 ± 0.10	907	0.49
DE	N	-2.31 ± 0.07	2.22 ± 0.08	-5.74 ± 0.34	-0.47 ± 0.07	203	0.48
HB	D	-2.36 ± 0.06	18.80 ± 3.10	13.70 ± 2.57	1.82 ± 0.14	789	0.49
HB	N	-2.40 ± 0.06	9.19 ± 0.69	5.14 ± 0.47	1.20 ± 0.08	52	0.52
Methane							
DE[b]	D	0.38 ± 0.05	1.08 ± 0.08	-5.15 ± 0.55	-0.08 ± 0.01	-772	0.82
			1.00 ± 0.08				
DE[c]	N	0.52 ± 0.04	1.13 ± 0.04	-4.18 ± 0.57	-0.12 ± 0.01	-1173	0.87
					-0.14 ± 0.01		0.84
HB	D	0.65 ± 0.06	0.98 ± 0.15	0.42 ± 0.04	0.55 ± 0.06	-698	1.19
HB	N	0.25 ± 0.04	1.39 ± 0.03	0.19 ± 0.02	0.25 ± 0.03	-1159	1.25
			2.46 ± 0.22				

[a] $\delta_{21} - \delta_{22} = 0.48 \pm 0.20$, P-value = 0.015; [b] $\delta_{21} - \delta_{22} = 0.08 \pm 0.04$, P-value = 0.036; [c] $\delta_{41} - \delta_{42} = 0.02 \pm 0.01$, P-value = 0.015.

Table S5: Bonferroni corrected P-values from PERMANOVA pairwise comparisons applied on the weighted unifrac distance matrix to evaluate the effect of time on rumen microbiota composition. P-values < 0.05 (bold) are considered as significant, and P-values < 0.10 (underlined) indicate a tendency.

Time	0 h	0.5 h	1 h	1.5 h	2 h	3 h	4 h	6 h	8 h
0.5 h	1								
1 h	0.081	1							
1.5 h	0.081	0.207							
2 h	0.540	1	1	1					
3 h	0.540	1	1	1					
4 h	0.297	1	1	1					
6 h	1	1	1	0.351	1	1	1		
8 h	0.162	0.072	**0.009**	**0.018**	0.198	0.090	0.684	1	
10 h	1	1	0.468	0.117	1	1	1	1	1

Table S6: Bonferroni corrected P-values from PERMANOVA pairwise comparisons applied on the weighted unifrac distance matrix to evaluate the effect of diet × period on rumen microbiota composition. P-values < 0.05 (bold) are considered as significant, and P-values < 0.10 (underlined) indicate a tendency.

Diet × period	CON × P1	CON × P2	LSO × P1
CON × P2	0.097		
LSO × P1	**0.020**	0.170	
LSO × P2	0.196	0.232	0.124

Chapter 5

Dynamics of volatile fatty acids, hydrogen and methane in dairy cattle: a model of rumen metabolic pathways

Henk J. van Lingen[1,2], André Bannink[3], Jan Dijkstra[2]

1 TI Food and Nutrition, Wageningen, The Netherlands
2 Animal Nutrition Group, Wageningen University & Research, Wageningen, The Netherlands
3 Animal Nutrition, Wageningen UR Livestock Research, Wageningen, the Netherlands

To be submitted

Abstract

A dynamic mechanistic model that represents the thermodynamic control of hydrogen partial pressure (p_{H_2}) on volatile fatty acid (VFA) fermentation pathways, and methanogenesis in the bovine rumen was developed. The model represents substrate degradation, microbial fermentation and methanogenesis in the rumen. The type of VFA formed is controlled by the NAD^+ to NADH ratio, which in turn is controlled by p_{H_2}. Feed composition and intake rate (twice daily feeding regime) were used as model input. Model parameters were estimated to experimental data using a Bayesian calibration procedure, after which the uncertainty of the parameter distribution on the model output was assessed. The model predicted a marked peak in p_{H_2} after feeding that rapidly declined in time. This peak in p_{H_2} caused a decrease in NAD^+ to NADH ratio followed by an increased propionate molar proportion at the expense of acetate molar proportion. In response to feeding, the model predicted an increase in methane (CH_4) production that steadily decreased in time. The pattern of CH_4 emission rate followed the patterns of p_{H_2} and H_2 emission rate, but its magnitude of increase in response to feeding was less pronounced. A global sensitivity analysis was performed to determine the impact of parameters on daily CH_4 production. The parameter that determines the NADH oxidation rate explained 41% of the variation in predicted daily CH_4 emission. Model evaluation indicated under-prediction of experimental total CH_4 emission with a root mean square prediction error of 15%. The present modeling effort provides the integration of more detailed knowledge than in previous rumen fermentation models. Diurnal dynamics of rumen metabolic pathways yielding VFA, H_2 and CH_4 can herewith be assessed.

Keywords: Bayesian calibration, Dairy cow, Global sensitivity analysis, Mechanistic modeling, Enteric fermentation, Methanogenesis

5.1 Introduction

Since the first attempt of Baldwin et al. (1970), various mechanistic rumen fermentation models have been developed to describe nutrient digestion, substrate fermentation to volatile fatty acids (VFA), and hydrogen (H_2) and methane (CH_4) production in the gastrointestinal tract of cattle. For example, Dijkstra et al. (1992) developed a rumen model representing microbial growth and nutrient degradation to end products including VFA. This model predicted the total VFA concentration better than the rumen molar proportions of individual VFA (Neal et al., 1992). Other mechanistic rumen fermentation models (e.g., Gregorini et al., 2013; Huhtanen et al., 2015) pointed to the importance of accurate digestion parameters for the prediction of CH_4 production, and in a recent review the need to improve prediction of VFA molar proportion was emphasized (Bannink et al., 2016). Analyzing various approaches, Morvay et al. (2011) advocated that the move toward feed evaluation systems based on animal response might necessitate an improved representation of rumen fermentation, in particular that of type of VFA formed. Benchaar et al. (1998) used the metabolic balance equations of Baldwin (1995) to predict CH_4 production from the H_2 yield from, among others, the type and amount of VFA produced.

The inability to accurately predict individual VFA responses to changes in diet composition may be due to the representation in current rumen models being limited to type of substrate fermented and to rumen pH (Ghimire et al., 2014). In the previously mentioned rumen modeling efforts, mechanisms in microbial metabolism such as the thermodynamic control of H_2 partial pressure (p_{H_2}) on the cofactor dynamics, that in turn controls VFA formation, have not yet been well represented. Van Lingen et al. (2016) stated that the thermodynamic control of p_{H_2} on the type of VFA formed and associated yield of H_2 and CH_4 is profound and should be further elaborated, but cannot be explained without considering the dynamics of NADH oxidation. They argued the NAD^+ to NADH ratio to be a key controller of the type of VFA produced and of the associated formation of H_2 that drives methanogenesis. Besides lack of representation of H_2 dynamics and p_{H_2} controlled cofactor driven fermentation dynamics, the rumen models also ignore the representation of methanogen metabolism. Both empirical and mechanistic approaches commonly adopt a steady-state approach and ignore the diurnal dynamics of rumen microbial metabolism when assessing rumen fermentation end products, despite peaks in VFA (Hatew et al., 2015), H_2 and CH_4 occurring shortly after feed consumption (Rooke et al., 2014). Assessing diurnal dynamics may increase our understanding of CH_4 production in the rumen.

A mechanistic representation may be used to understand underlying metabolic

processes and to predict a system response to external input. Although this type of modeling is detailed, both the model representation and parameters may be associated with substantial uncertainty and bias. Estimating model parameters using experimental data may then be an essential step to streamline these model representation matters. This procedure is usually performed by minimizing a measure of goodness of fit using a least square function or a weighted sum of squared residuals (e.g., Appuhamy et al., 2014). The conventional approach of model parameterization by tuning model parameters until the modeler obtains satisfactory fit (Beven and Binley, 1992) does not properly address the poor parameter identifiability issue, in which the same model outputs are obtained for different inputs. Bayesian parameter estimation is a convenient means to incorporate existing knowledge and determine the joint parameter distribution to data (Arhonditsis et al., 2007). Such a modeling approach may help to accurately estimate parameters of mechanistic models that predict microbial fermentation and production of individual VFA in the rumen.

The objective of this study was to develop a dynamic mechanistic model that represents the thermodynamic control of p_{H_2} on VFA fermentation pathways, and methanogenesis in the bovine rumen, in which model parameters are estimated using a Bayesian approach.

5.2 Materials and Methods

5.2.1 General model description

The model represents the rumen microbial ecosystem. It is assumed that all carbohydrate polymers are hydrolyzed to hexose. Fermentative microbes (in the present study all micro-organisms except methanogens) utilize the hexose yield from fiber, starch and sugar hydrolysis, which results in the production of volatile fatty acids and H_2. Methanogens utilize H_2, which yields CH_4. The model emphasizes a representation of the thermodynamic control of p_{H_2} on carbohydrate metabolism via NAD as described by Van Lingen et al. (2016). The mechanistic model is diagrammatically represented in Fig. 5.1 and includes state variables for degradable fiber (F_g), degradable starch (S_g), water soluble carbohydrates (W_r), hexose (He), fermentative microbes (Mi), acetate (Ac), propionate (Pr), butyrate (Bu), hydrogen (H_2) and methanogens (Me). Also NAD, which is subdivided in NAD^+ and NADH, is considered; of these three entities, only NADH is explicitly represented as a state variable in the model. The model focuses on the carbon metabolism and to limit the model complexity, no pools representing N-compounds such as ammonia and soluble protein are included. The F_g, S_g, W_r and Mi pools are expressed in [g], all other pools

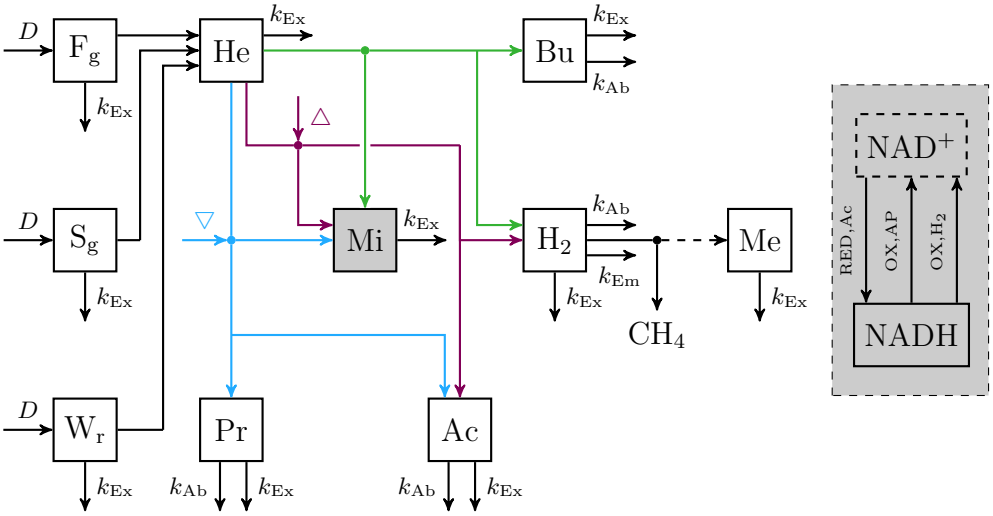

Figure 5.1: Flow chart that conceptually represents the rumen model. Boxes enclosed by solid lines represent state variables (with F_g for degradable fiber [g], S_g for degradable starch [g], W_r for soluble carbohydrates [g], He for hexose [mol], Mi for fermentative microbes [g], Ac for acetate [mol], Pr for propionate [mol], Bu for butyrate [mol], H_2 for hydrogen [mol], Me for methanogens [g]. The sum of NAD^+ and NADH [mol] is a fraction of Mi and a gray fill is used to visualize this), arrows represent fluxes with the dashed arrow indicating H_2 is not incorporated but its conversion to CH_4 is required for growth (with D for dietary input, k_{Ex} for fractional exit from the rumen to the lower tract, k_{Ab} fractional absorption, k_{Em} for fractional emission, RED,Ac for NAD^+ reduction associated with hexose converted into 2 Ac, {OX,AP} for NADH oxidation associated with hexose converted into $\frac{2}{3}$ Ac + $\frac{4}{3}$ Pr, and $\{OX,H_2\}$ for hydrogenase catalyzed NADH oxidation; △ and ▽ indicate that at increased NAD^+ to NADH ratio the microbial conversion is promoted and inhibited, respectively; fluxes may be unique per pool and are further specified in section 5.2.2), dots indicate microbial conversions.

are expressed in [mol]; as time is expressed in [h], all fluxes are in [mol·h^{-1}] or [g·h^{-1}]. Fluxes are mathematically represented by Michaelis-Menten and mass-action forms given in the Appendix. Notation of influxes and outfluxes of pools is $P_{i,jm}$ and $U_{i,jm,n}$, respectively, where the subscript represents the uptake or production of i by j-to-m transaction (generating n). To illustrate this, P_{F_g,InF_g} represents the increase in F_g as a result of the inflow of F_g. All abbreviations and general notation used are provided in Tables S1 and S2. Microbial composition and nutrients required for growth are provided in Table 5.1, yields and fractions associated with microbial transactions in Table 5.2, (bio)physical constants in Table 5.3, and parameters in Table 5.4.

Table 5.1: Microbial composition of polysaccharide (PS) free mass [g·(100 g dry matter)$^{-1}$] and nutrients required for biosynthesis [mmol·g^{-1}], with hexose to acetate for energy ($HeAc_{ATP}$), hexose to butyrate for energy ($HeBu_{ATP}$) hexose to acetate + propionate for energy ($HeAP_{ATP}$), hexose incorporated (He_{inc}), amino acids incorporated (AA_{inc}) and ammonia incorporated (Am_{inc})

Cell	**PS-**	**growth on AA**					**growth on Am**				
part	**free DM**	**$HeAc_{ATP}$**	**$HeBu_{ATP}$**	**$HeAP_{ATP}$**	**He_{inc}**	**AA_{inc}**	**$HeAc_{ATP}$**	**$HeBu_{ATP}$**	**$HeAP_{ATP}$**	**He_{inc}**	**Am_{inc}**
Protein	53.0	6.02	8.03	6.76	-	4.81	6.44	8.58	7.23	4.08	6.07
DNA	3.4	0.18	0.24	0.20	0.15	0.37	0.64	0.86	0.72	0.23	0.46
RNA	12.3	0.51	0.68	0.57	0.51	1.22	1.67	2.22	1.87	0.77	1.54
Lipid	14.3	0.06	0.08	0.06	1.80	-	0.06	0.08	0.06	1.80	-
Cell wall	4.2	0.15	0.20	0.16	0.04	0.29	0.12	0.17	0.14	0.27	0.34
Ash	12.9	-	-	-	-	-	-	-	-	-	-
Total[a]	100	6.91	9.21	7.76	2.50	6.69	8.92	11.90	10.02	7.15	8.41

[a] Content of NAD (c_{NAD}) is 7.0·10^{-6} mol (g DM)$^{-1}$.

Table 5.2: Yields ($Y_{i,jm}$ and $Y_{i,jm,n}$) and fractions ($f_{i,jm}$) associated with microbial transactions in the rumen. For notation of $Y_{i,jm}$ and $Y_{i,jm,n}$ and $f_{i,jm}$, see Tables S1 and S2

Conversion	$f_{i,jm}$	$Y_{i,jm,n}$	**Unit**
Ac,HeAc		2	$mol \cdot mol^{-1}$
Ac,HeAP		0.67	$mol \cdot mol^{-1}$
Pr,HeAP		1.33	$mol \cdot mol^{-1}$
Bu,HeBu		1	$mol \cdot mol^{-1}$
Mi,HeMi,Ac		84.25	$g \cdot mol^{-1}$
Mi,HeMi,AP		68.95	$g \cdot mol^{-1}$
Mi,HeMi,Bu		77.86	$g \cdot mol^{-1}$
He,HeAc	0.65		-
He,HeAP	0.67		-
He,HeBu	0.71		-
He,LaHe		$2.5 \cdot 10^{-3}$	$mol \cdot g^{-1}$
H_2,HeAc		4	$mol \cdot mol^{-1}$
H_2,HeBu		2	$mol \cdot mol^{-1}$
Me,H_2CH_4		2	$g \cdot mol^{-1}$
CH_4,H_2CH_4		0.25	$mol \cdot mol^{-1}$

5.2.2 Detailed model description

Degradable fiber pool, $\mathbf{Q_{F_g}}$ [g]. This pool has one input, which is from the feed (Eq. 5.4). There are two outputs, hydrolysis to He (Eq. 5.5) and outflow to the duodenum with the solid material (Eq. 5.6). All fractional hydrolysis rates considered in this model depend on the digestion turnover time of the particular dietary component (for Fg and Sg presented in Table 5.5) and the concentration of fermentative microbes present. Note that C^*_{Mi} [$g \cdot L^{-1}$] is a reference value of the concentration of microbial DM in the rumen (Table 5.3), as described by Dijkstra et al. (1996).

Degradable starch pool, Q_{S_g} [g]. Like Q_{F_g}, this pool receives input from the feed. The potentially degradable starch fraction and half of the soluble starch fraction of the feed flow into Q_{S_g} (Eq. 5.8). S_g is hydrolyzed to He (Eq. 5.9) or washed out with the solid material (Eq. 5.10).

Water soluble carbohydrate pool, Q_{W_r} [g]. Like Q_{F_g} and Q_{S_g}, this pool receives input from the feed. The water soluble carbohydrate fraction and half of the soluble starch fraction of the feed flow into Q_{W_r} (Eq. 5.12). Q_{W_r} contains di- and oligosaccharides that are hydrolyzed to He, which is represented by Eq. 5.13. The

Table 5.3: (Bio)physical constants in the model

Notation	Description	Value
C^*_{Mi}	Reference concentration of microbes	12.5 g·L^{-1}
F_{b}	Blood flow to the rumen	703 L·h^{-1}
ΔG^{o}	Gibbs energy change of NADH oxidation	-102 kJ·mol^{-1}
$H_{\mathrm{H_2}}$	Henry's constant for H_2	1382 L·atm·mol^{-1}
p_0	Standard atmospheric pressure	101 kPa
q_{GM}	Growth-maintenance relationship	3
R	Universal gas constant	8.31 J·mol^{-1}·K^{-1}
T	Temperature	312 K
χ	Average stoichiometric number for NADH oxidation via confurcation	2
$V_{\mathrm{headspace}}$	Rumen headspace volume	40 L
V_{mol}	Molar volume at T = 312 K and p_0	25 L

Table 5.4: Values of parameters representing microbial metabolism and VFA absorption. Notation is explained in Tables S1 and S2.

Transaction	k_{jm}	v_{jm}	$M_{\mathrm{i,jm}}$	$J_{\mathrm{i,jm}}$	$J_{\mathrm{pH,jm}}$	Φ_{jm}	$\Theta_{\mathrm{pH,jm}}$
W_rHe	14						
He,HeMi			0.02				
He,HeVf			0.055				
NAD,HeAc			9				
NAD,HeAP				1			
Am,HeVf				$8.61{\cdot}10^{-3}$			
P_s,HeVf				$1.465{\cdot}10^{-2}$			
Ac,AcAb		0.0808	0.0791		6.02	1.17	3.91
Ac,PrAb		0.249	0.112		6.02	0.95	4.61
Bu,BuAb		1.279	0.4934		6.02	0.99	5.13
NADH,$Fd_{\mathrm{RED}}Fd_{\mathrm{OX}}$	202						

fractional hydrolysis rate of sucrose reported by Weisbjerg et al. (1998) was taken as the fractional hydrolysis rate of the water soluble carbohydrates (k_{WrHe} [h^{-1}]; Table 5.4). Washout with the fluid is represented by Eq. 5.14.

Hexose pool, Q_{He} [mol]. This pool receives input from lactate (Eq. 5.17), and hydrolysis of F_g, S_g and W_r (Eq. 5.18). The outputs are the growth and non-growth functions of fermentative microbes, yielding either 2 mol acetate (Eq. 5.19, 5.22), 1 mol butyrate (Eq. 5.20, 5.23) or $\frac{2}{3}$ mol acetate + $\frac{4}{3}$ mol propionate (Eq. 5.21, 5.24).

Although several other fermentation pathways exist, including these three pathways in the present study suffices to represent the production of the three major VFA and achieve the study objectives. The dimensionless parameter q_{GM}

is introduced to relate the maximum hexose uptake rate for microbial growth to the maximum hexose uptake rate for non-growth functions (Eq. 5.19–5.21). Based on the maximum hexose uptake rates for growth and non-growth in Dijkstra et al. (1992), this parameter was set at 3. The introduction of this parameter decreased the total number of parameters to be estimated as only one parameter per fermentation pathway needs to be evaluated. The inhibition constants of ammonia and soluble protein with respect to hexose fermentation to VFA for non-growth functions, and the $M_{\mathrm{He,HeMi}}$ and $M_{\mathrm{He,HeVf}}$ saturation constants were taken from Dijkstra et al. (1992). Fermentation end product formation dependent on the NAD^+ to NADH ratio (r_{NAD}), has been discussed previously (Mosey, 1983; Fischbach and Sonnenburg, 2011). The conversion of hexose into 2 acetate is stimulated at elevated r_{NAD}, the conversion of hexose into $\frac{2}{3}$ acetate + $\frac{4}{3}$ propionate is inhibited at elevated r_{NAD}. The value of the affinity constant for hexose fermented into 2 acetate with respect to r_{NAD} ($M_{\mathrm{NAD,HeAc}}$ [dimensionless]; Table 5.4) was set at 9, the r_{NAD} common in living cells (Buckel and Thauer, 2013). The inhibition constant for hexose fermented into $\frac{2}{3}$ acetate + $\frac{4}{3}$ propionate with respect to r_{NAD} ($J_{\mathrm{NAD,HeAP}}$ [dimensionless]; Table 5.4) was set 1, the lower bound of r_{NAD} observed in rumen bacteria (Hino and Russell, 1985). Hexose is washed out with the fluid (Eq. 5.25).

Fermentative microbes pool, Q_{Mi} [g]. The input to the fermentative microbes (i.e., bacteria and protozoa) is associated with hexose fermentation to 2 acetate, 1 butyrate or $\frac{2}{3}$ acetate + $\frac{4}{3}$ propionate, where the microbial growth rate is related to the ATP yield associated with the specific fermentation pathway used (Eq. 5.28). The washout is related to particulate matter as well as fluid including selective retention of protozoa, described by Dijkstra et al. (1996) and given by (Eq. 5.29).

Acetate pool, Q_{Ac} [mol]. Input to acetate is from feed (Eq. 5.32), and from microbial growth and non-growth functions associated with production of 2 acetate and $\frac{2}{3}$ acetate + $\frac{4}{3}$ propionate (Eq. 5.33). Output was represented by the VFA absorption rate equations from Dijkstra et al. (1993), where the maximum absorption rate parameter was substituted by $q_{\mathrm{VfAb}} \cdot v_{\mathrm{AcAb}}$ (Eq. 5.34). v_{AcAb} is the acetate specific maximum absorption rate, where the multiplication by q_{VfAb} enables to further optimize absorption rates of all three VFA with the fewest number of parameters. Rumen fluid pH was calculated as in Tamminga and Van Vuuren (1988) (Eq. 5.35). The washout of acetate is with the fluid fraction (Eq. 5.36).

Propionate pool, Q_{Pr} [mol]. Input to propionate is from feed (Eq. 5.39), and from microbial growth and non-growth functions associated with production of $\frac{2}{3}$

acetate + $\frac{4}{3}$ propionate (Eq. 5.40). Output represents absorption (Eq. 5.41), with $q_{\mathrm{VfAb}} \cdot v_{\mathrm{PrAb}}$ as the maximum absorption rate, and v_{PrAb} as the propionate specific maximum absorption parameter. The washout is with the fluid fraction (Eq. 5.42).

Butyrate pool, Q_{Bu} [mol]. Input to butyrate is from feed (Eq. 5.45), and from microbial growth and non-growth functions associated with production of butyrate (Eq. 5.46). Output represents absorption (Eq. 5.47), with $q_{\mathrm{VfAb}} \cdot v_{\mathrm{BuAb}}$ as the maximum absorption rate, and v_{BuAb} as the butyrate specific maximum absorption parameter. The washout is with the fluid fraction (Eq. 5.48).

H_2 pool, Q_{H_2} [mol]. Input to the H_2 pool is from the hexose fermentation pathways that yield 2 acetate (Eq. 5.59) and 1 butyrate (Eq. 5.60). Note that hexose fermentation yielding $\frac{2}{3}$ acetate + $\frac{4}{3}$ propionate does not result in net H_2 production. Output represents H_2 used for methanogenic growth (Eq. 5.61; the CH_4 production rate is represented by Eq. 5.67), eructation of gaseous H_2 (Eq. 5.63), absorption (Eq. 5.64) and fluid washout of dissolved H_2 (Eq. 5.65). The representation of H_2 output via eructation, exhalation, absorption and washout was based on the model of Berends et al. (2014).

NADH pool, Q_{NADH} [mol]. The sum of NAD^+ and NADH was calculated using its content in microbes (c_{NAD}; $7.0{\cdot}10^{-6}$ mol·(g DM)$^{-1}$), which was taken from Agrimi et al. (2011). Depending on the fermentation rate, NAD is net oxidized from NADH to NAD^+ or net reduced from NAD^+ to NADH. NAD^+ is reduced when hexose is fermented to 2 acetate (Eq. 5.50); NADH is oxidized by hexose fermentation yielding $\frac{2}{3}$ acetate + $\frac{4}{3}$ propionate (Eq. 5.51), or by means of a confurcating hydrogenase enzyme (also called bifurcation, see Schut and Adams, 2009). The hydrogenase catalyzed oxidation rate of NADH is calculated based on the instantaneous absolute quantity of NADH, corrected for the thermodynamic state of the intracellular environment (Eq. 5.52, with f_{NADH} defined as $\frac{\mathrm{NADH}}{\mathrm{NAD^+ + NADH}}$). The thermodynamic state was determined using the thermodynamic potential factor (F_{T} [dimensionless]; Jin and Bethke, 2007). Similar to the approach of Salem et al. (2002), the fractional rate constant for this hydrogenase catalyzed NADH oxidation flux was set such that, at fermentation rates and proportions of VFA formation approaching their diurnal average, the redox state of NAD remained constant. The F_{T} was calculated based on the instantaneous r_{NAD}, p_{H_2}, the intracellular pH, and the reduced ferredoxin to oxidized ferredoxin ratio (r_{Fd}) taken to be constant and set at 9 (Buckel and Thauer, 2013). The relationship between fluid pH ($\mathrm{pH_{Fl}}$) and intracellular pH ($\mathrm{pH_{Cell}}$) (Eq. 5.54), which is valid for fluid pH > 5.7, was obtained by applying

non-linear regression on data taken from Russell (1987). The f_{NADH} is discretely updated with every numerical integration step (Δt), with every updated fraction of NADH ($f_{\mathrm{NADH}_{t+\Delta t}}$) calculated based on its initial fraction of NADH (f_{NADH_t}) times the quantity of NAD, plus the net reduction of NAD^+ to NADH per integration step (i.e., ΔQ_{NADH} is the solution of the numerical integration of Eq. 5.55) divided by the quantity of NAD (Eq. 5.56).

Methanogen pool, Q_{Me} [g]. Input to the methanogen pool is from growth using hydrogenotrophic methanogenesis (Eq. 5.68); no other methanogenic pathways are considered in the present model. The only outflow represents the average washout (Eq. 5.69), where it was assumed that methanogens flow out with the solid and fluid fraction or stay in the rumen when they are adhered to the rumen epithelium or are associated with protozoa. The adherence of methanogens explains why the fractional outflow rate of methanogens is less than the average of the outflow rates of fluid and solid material. The growth yield of methanogens without cytochromes (2 g·(mol of $\mathrm{CH_4}$)$^{-1}$) was taken from Thauer et al. (2008). Growth of methanogens with cytochromes was not considered in the present study.

5.2.3 Constants and parameters

Rumen fluid volume (V_{Fl}) and fractional outflow rates of the solid (k_{SoEx}) and fluid material (k_{FlEx}) from the rumen to the lower gastrointestinal tract, which was assumed to depend on total daily dry matter intake (DMI [kg·d^{-1}]) as adopted by Mills et al. (2001) and given by V_{Fl} [L] = 47.86 + 1.759 · DMI, k_{SoEx} [h^{-1}] = (0.57 + 0.017 · DMI)/24 and k_{FlEx} [h^{-1}] = (0.97 + 0.116 · DMI)/24. Concentrations of ammonia (C_{Am}) and soluble protein ($C_{\mathrm{P_s}}$) were arbitrarily set at $5{\cdot}10^{-3}$ and $3{\cdot}10^{-3}$ M, respectively, assuming no diurnal changes.

The microbial growth requirements are taken from Dijkstra et al. (1992), who assumed a yield of 4.5 moles of ATP per mol of hexose fermented, and updated according to the number of ATP produced per pathway, which was 4, 3 and 3.56 mol per mol of hexose fermented to 2 acetate, 1 butyrate and $\frac{2}{3}$ acetate + $\frac{4}{3}$ propionate, respectively (Zhang et al., 2013). For the latter pathway, it was assumed that 90% of propionate is generated via the succinate pathway and the remainding 10% via the lactate pathway. The smaller ATP production assumed in the present model results in greater $f_{\mathrm{He,HeAc}}$, $f_{\mathrm{He,HePr}}$ and $f_{\mathrm{He,HeBu}}$ values compared with Dijkstra et al. (1992). All fraction and yield parameters regarding growth of fermentative microbes used in this modeling effort were obtained by taking the means of parameters for growth on ammonia and amino acids.

5.2.4 Data sources for model calibration and evaluation

Data representing rumen diurnal dynamics were used for estimation of model parameters. These data were taken from a 2 × 2 crossover experiment with four lactating rumen cannulated Holstein cows. Cows were fed a control diet and a linseed oil supplemented diet. Feed intake patterns (twice daily feeding regime) were obtained by weighing the feed that was left in the feed bins every 0.5 h between 0 and 3 after feeding and every h between 3 and 10 h after feeding. At these time points, headspace gas was sampled for determination of p_{H_2}. At 0, 0.5, 1, 1.5, 2, 3, 4, 6, 8 and 10 h after feeding, rumen fluid was sampled for determination of VFA concentrations and molar proportions, respectively. In addition, emission of H_2 and CH_4 were continuously measured in climate respiration chambers. A more detailed description of this calibration experiment is reported in Chapter 4. Data from three other in-house experiments (Hatew et al., 2015; Van Gastelen et al., 2015; Warner et al., 2015) representing 40 observations and 12 treatments from cannulated lactating dairy cows, were used to evaluate the average daily CH_4 output predicted by the model. Because of the similarities of the experimental design (i.e., twice daily feeding; restricted to 95% of ad lib intake), the same feed intake pattern model input as in Chapter 4 was used to perform simulations for these three evaluation experiments.

5.2.5 Model simulation: input and numerical integration

Inputs to the model were intake rate (shown in Fig. 5.2) and composition of DM (Table 5.5). Of the eight feed intake patterns obtained from the calibration experiment, one comprised a period of zero intake before the cow consumed the whole portion and this pattern was excluded from the data and the seven others were averaged and used as model input. As the DMI was recorded for a 10 h period, 2 h of zero intake were appended to the average DMI pattern, which provides a sequential DMI rate with 12 h periods. The average DMI pattern corresponds to a DMI of 17.9 kg·d^{-1}. The k_{SgHe} hydrolysis rate constant was only available for the Hatew et al. (2015) data. The dietary fractions and k_{FgHe} and k_{SgHe} for the other studies were set per dietary treatment and taken from previous experiments with rumen in situ incubations of similar forages and feed ingredients. Non-identified fractions such as pectin and fructans were assigned to Fg and Sg. An overview of all degradation characteristics is given in Table 5.5. The differential equations of all state variables were numerically integrated for a given set of initial conditions and parameter values. To simulate the dynamic responses, the equations were solved using the lsoda numerical integration method (Petzold, 1983), a robust implicit integrator for stiff and non-stiff systems. This numerical integrator changes step size automatically to

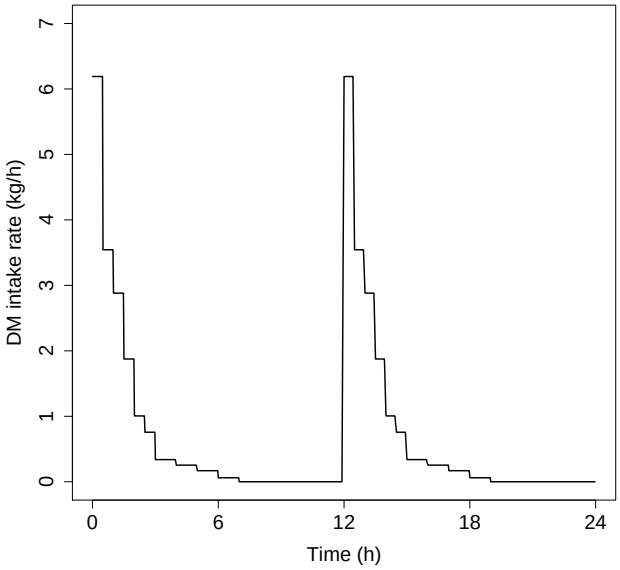

Figure 5.2: Diurnal pattern of dry matter intake

minimize computation time while maintaining calculation accuracy. The DM intake profile caused dramatic changes in Q_{H_2} shortly after feeding, which is why integration steps sizes were $2{\cdot}10^{-4}$ h during the first 1.2 h and 10^{-3} h during the remaining hours of every consecutive 12 h period.

5.2.6 Parameter optimization and uncertainty analysis

The periodic input makes that the model dynamics approaches quasi steady-state. A 48 h run of the model was considered to be converged to quasi steady-state. The sum of squared residuals, which were weighted to the mean of every observed variable, of the model output of the final 12 h versus the experimental data were calculated to assess the model performance given the model parameter values. The parameters v_{HeAc}, v_{HeAP}, v_{HeBu}, $k_{\mathrm{H_2Em}}$, $v_{\mathrm{H_2CH_4}}$, $M_{\mathrm{H_2,H_2CH_4}}$, q_{VfAb} were selected for optimization to the diurnal patterns observed for $p_{\mathrm{H_2}}$, H_2 emission rate, CH_4 emission rate, total volatile fatty acid concentration, and proportions of acetate, propionate and butyrate. Before the parameter optimization was run, the identifiability of all possible parameter combinations was investigated. This investigation was performed based on the approximate linear dependence of parameter sets, γ, also called collinearity (Brun et al., 2001). Parameters were regarded to be jointly identifiable for $\gamma < 10$. The

Table 5.5: Degradable fiber (Fg), degradable starch (Sg), soluble sugars (Wr), acetate (Ac), propionate (Pr), butyrate (Bu) and lactate (La) feed contents [g·kg^{-1}], and fractional hydrolysis rates [h^{-1}] of degradable fiber and degradable starch per experiment and/or treatment assigned (ExpTr) for data from Chapter 4 (VL; average of control and linseed oil supplemented diets), Van Gastelen et al. (2015) (VG1-VG4), Warner et al. (2015) (W1-W4), and Hatew et al. (2015) (H1-H4).

ExpTr	**Fg**	**Sg**	**Wr**	**Ac**	**Pr**	**Bu**	**La**	k_{FgHe}	k_{SgHe}
VL	293	168	102	11	2	2	21	0.036	0.075
VG1	403	4	207	12	2	2	24	0.042	0.080
VG2	350	91	171	11	2	2	22	0.038	0.099
VG3	297	179	135	10	2	2	19	0.033	0.100
VG4	245	267	100	8	1	1	17	0.025	0.100
W1	360	51	317	0	0	0	0	0.061	0.100
W2	374	51	336	0	0	0	0	0.061	0.100
W3	377	50	241	0	0	0	0	0.061	0.100
W4	401	51	276	0	0	0	0	0.061	0.100
H1	422	108	85	9	2	2	18	0.050	0.054
H2	348	198	86	9	2	2	18	0.046	0.054
H3	399	116	105	9	2	2	18	0.051	0.173
H4	332	187	108	9	2	2	18	0.046	0.137

aforementioned set of parameters that was found to be identifiable was optimized to the sum of squared residuals using the BFGS algorithm (Conn et al., 1991).

Although the deterministic BFGS algorithm provides an optimal set of parameters to the experimental data used, the parameter uncertainty may be high and needs to be estimated as well. A Bayesian calibration method that uses Markov chain Monte Carlo (MCMC) simulation combined with the delayed rejection and adaptive Metropolis (DRAM) sampling procedure was applied to assess the parameter uncertainty. The model for this calibration was defined as:

$$y_{ij} = f(x(t_j), c, \theta)_i + e_{ij}, \tag{5.1}$$

$$e_{ij} \sim N(0, \sigma^2), \tag{5.2}$$

where y_{ij} is the observed value of the ith entity ($i = 1, \ldots, 7$, for $p_{\mathrm{H_2}}$, $\mathrm{H_2}$ emission rate, $\mathrm{CH_4}$ emission rate, total volatile fatty acid concentration, and proportions of acetate, propionate and butyrate in rumen fluid) at the jth time point ($j = 1, \ldots, 10$); $f(t_j, c, \theta)$ represents model output of i variables at j time points, for model input $x(t)$ representing (periodic) DM intake rate, c represents the diet composition, and θ is a vector of the parameters to be optimized; e_{ij} the independent gaussian error with unknown variance σ^2. Based on the increase in $p_{\mathrm{H_2}}$ and $\mathrm{H_2}$ emission rate by about 2

orders of magnitude in response to feeding, a log transformation was applied on these two entities, which changed the calibration model to:

$$\log y_{ij} = \log(f(x(t_j), c, \theta)_i) + e_{ij}. \tag{5.3}$$

The posterior of the parameters was then obtained by applying Bayes' theorem. The likelihood function was based on the parameter dependent sum of squares of predicted versus experimental data. A non-informative prior distribution was used for the parameter vector θ, and a gamma prior distribution for the reciprocal of the error variance, σ^{-2}. The MCMC simulation was started with the best solution parameter set that returned from the BFGS algorithm, while the prior error variance was chosen to be the mean of the unweighted squared residuals for every observed variable. The weight added to this prior was 0.1. The proposal distribution to generate new parameter values was updated every 50 iterations, and the covariance at the start of the simulation was the approximated covariance that returned from the BFGS optimization, and was scaled with $2.4^2/n$, with n the number of parameters evaluated. The length of the MCMC simulation was 4000 iterations, where the first 1000 iterations were taken to be the burnin period.

5.2.7 Global sensitivity analysis

The effect of the parameter uncertainty on the model output was identified by model simulations for which parameters were randomly sampled from the parameter probability density function that was generated by the MCMC simulation. This procedure determines the sensitivity of time series of model output variables as a function of the parameter probability density. In addition to this procedure, the effect of distinct parameters on the average daily CH_4 production was evaluated. In this evaluation, parameters simultaneously varied from 0.75 to 1.25 times their optimum value, and were randomly sampled from a uniform distribution. The average daily CH_4 production was calculated for 500 samples of parameter sets. The relative impact of a parameter on CH_4 production output was quantified by the top marginal variance (TMV) (Jansen et al., 1994). TMV quantifies the variance decrease that occurs in the output if the input was fully known, and can be obtained from regressing model output against parameter set input. Multiple linear regression was used for assessing sensitivity of average daily CH_4 production model output to parameters with its applicability evaluated based on the adjusted R^2. Values of adjusted $R^2 > 0.90$ are regarded acceptable for using multiple linear regression to identify the sensitivity of model output to parameters. All analyses were performed using the base (R Core Team, 2016) and FME packages (Soetaert and Petzoldt, 2010) in R statistical software.

5.3 Results and Discussion

This model is unique in that it provides a mechanistic understanding of diurnal dynamics of VFA, H_2 and CH_4 production in the bovine rumen, where the type of VFA formed is controlled by NAD homeostasis. Such a mechanistic understanding of diurnal patterns in rumen fermentation may be the ultimate tool to further improve the quantification of daily production of enteric CH_4. This modeling effort provides a framework in which proportions of VFA depend on fermentation rate and p_{H_2}.

Janssen (2010) and Ungerfeld (2013) evaluated the thermodynamic effect of the H_2 concentration on various fermentation pathways ΔG. These thermodynamic investigations determine the energetic favorability of fermentation pathways at different p_{H_2}. However, ΔG is not a direct measure of reaction rate and does not quantify to what extent changed rumen conditions affect VFA production rates. Initially by Ungerfeld and Kohn (2006), and later by Ghimire et al. (2014), interconversion rates of VFA were predicted using aspects of kinetic rate laws and reaction quotients of chemical equilibria. These approaches may not be consistent with both kinetic and thermodynamic control of reaction rates. Thermodynamic control on a reaction may be realistically assessed by correcting a kinetic rate law for thermodynamic effects as applied in the present modeling study and suggested by Van Lingen et al. (2016).

Ghimire et al. (2014) fitted rate constants for VFA interconversion from *in vivo* observations of rumen VFA interconversion and assumed a fixed value of p_{H_2}. They concluded that the model did not perform well in predicting ruminal VFA production rates due to lack of data on thermodynamic control factors other than pH and rumen VFA concentration. Also, for an evaluation of thermodynamic control of rumen fermentation pathways, p_{H_2} is best varied, as opposed to being kept constant. The prediction inaccuracy may be associated with their model structure as cofactor redox state such as r_{NAD} was not considered. Offner and Sauvant (2006) introduced the dynamics of reduced cofactors in their model to predict end products of rumen fermentation but with a kinetically and thermodynamically similar approach as Ghimire et al. (2014). The uniqueness of the present modeling effort is the methodology accordance with principles of reaction kinetics and thermodynamics and the dynamic evaluation of the effect of p_{H_2} on rumen fermentation, which is mechanistically assessed via r_{NAD}. Furthermore, the mechanistic representation of methanogenic archaea and their metabolism has hardly been applied in rumen fermentation models.

The use of a Bayesian calibrated mechanistic model in the field of ruminant nutrition is not entirely novel, but only a limited number of studies in which this

approach was applied has been published (e.g., Reed et al., 2016). Bayesian inference facilitated the identification of a joint distribution of parameters sets and provided the basis for estimating model prediction error. Mechanistic prediction of total daily CH_4 production based on diurnal profiles has also not widely been applied.

5.3.1 Parameter estimates

Parameter estimates and their standard deviation as obtained from the MCMC simulation, along with the coefficient of variation are provided in Table 5.6. The k_{H_2Em}, representing the fractional output of H_2 from the rumen, was estimated to be 7.59 ± 1.21 h^{-1}, which is substantially higher than in Berends et al. (2014) where it was set at 2.36 h^{-1}. Maximum utilization rate and affinity for dissolved H_2 concentration of archaea were estimated to be 0.27 ± $8.50{\cdot}10^{-3}$ $mol{\cdot}g^{-1}{\cdot}h^{-1}$ and $6.21{\cdot}10^{-7}$ ± $1.03{\cdot}10^{-7}$ M. This corresponds to a maximum fractional growth rate of 0.13 h^{-1}. Fractional growth rates of 0.03 and 0.17 h^{-1} have been reported for *Methanobacterium bryantii* M.o.H. (Karadagli and Rittmann, 2005) and *Methanobrevibacter smithii* (Pavlostathis et al., 1990), respectively. A maximum fractional growth rate of 0.13 h^{-1} may then be a reasonable average for the various methanogenic archaea in the rumen.

The v_{HeAc}, v_{HeAP} and v_{HeBu} parameters were estimated to be $6.16{\cdot}10^{-2}$ ± $1.70{\cdot}10^{-2}$, $1.18{\cdot}10^{-2}$ ± $3.28{\cdot}10^{-3}$ and $4.87{\cdot}10^{-3}$ ± $1.33{\cdot}10^{-3}$ $mol{\cdot}g^{-1}{\cdot}h^{-1}$, which corresponds to maximum fractional growth rates of 1.73, 0.27 and 0.13 h^{-1}, respectively. In this model, the production of acetate is stimulated at high r_{NAD}, the production of $\frac{2}{3}$ acetate + $\frac{4}{3}$ propionate is inhibited at high r_{NAD} and the production of butyrate is not controlled by r_{NAD}. The hexose dependent maximum fractional growth rate of bacteria would then be 1.0 h^{-1} for $r_{NAD} = 9$, and 0.44 h^{-1} for $r_{NAD} = 1$. The latter two maximum fractional growth rates are in the range of 0.39 to 2.04 h^{-1}, which was reported for different rumen bacteria growing on glucose substrate in continuous culture (Russell and Baldwin, 1978).

The maximum absorption rate correction parameter, q_{VfAb}, was estimated to be 0.71 ± $4.83{\cdot}10^{-2}$, resulting into average daily fractional absorption rates of 0.27,

Table 5.6: Estimated mean, standard deviation (SD) of the v_{HeAc} [mol· $g^{-1}{\cdot}h^{-1}$], v_{HeAP} [$mol{\cdot}g^{-1}{\cdot}h^{-1}$], v_{HeBu} [$mol{\cdot}g^{-1}{\cdot}h^{-1}$], k_{H_2Em} [h^{-1}], $v_{H_2CH_4}$ [$mol{\cdot}g^{-1}{\cdot}h^{-1}$], M_{H_2,H_2CH_4} [M] and q_{VfAb} parameters obtained from the Markov chain Monte Carlo (MCMC) simulation.

	k_{H_2Em}	v_{HeAc}	v_{HeAP}	v_{HeBu}	$v_{H_2CH_4}$	M_{H_2,H_2CH_4}	q_{VfAb}
mean	7.59	$6.16{\cdot}10^{-2}$	$1.18{\cdot}10^{-2}$	$4.87{\cdot}10^{-3}$	0.27	$6.21{\cdot}10^{-7}$	0.71
SD	1.21	$1.70{\cdot}10^{-2}$	$3.28{\cdot}10^{-3}$	$1.33{\cdot}10^{-3}$	$8.50{\cdot}10^{-3}$	$1.03{\cdot}10^{-7}$	$4.83{\cdot}10^{-2}$

0.29 and 0.24 h^{-1} for acetate, propionate and butyrate, respectively. Dieho et al. (2016) observed fractional absorption rates of 0.40, 0.47 and 0.28 h^{-1}, respectively. Production and concentration of the VFA in that study are higher than in the present modeling effort, which may have caused the higher fractional absorption rates. Estimating maximum absorption rate parameters for acetate, propionate and butyrate separately may further improve the VFA absorption dynamics. Data of both VFA production and concentrations may then be needed to make a larger set of parameters identifiable.

5.3.2 Effect of parameter uncertainty on model output

Model predictions showed that in response to feeding, p_{H_2} increased from $3{\cdot}10^{-4}$ to $1.3{\cdot}10^{-2}$ bar in 0.5 h and then steadily decreased to basal level (Fig. 5.3). The posterior parameter set seems to qualitatively predict the pattern obtained from the experiment, but under-predicts the peak p_{H_2} at 0.5 h. Other observations were within the predicted range of p_{H_2}, relatively close to the predicted minimum of p_{H_2} at 1.5-4 h, or marginally higher than the predicted range at 8 h. Similar to the pattern of p_{H_2}, the increase of the total VFA concentration in response to feeding followed by a decline was qualitatively well simulated by the model. Although the peak concentration of total VFA appeared to be fairly well predicted predicted, the model underpredicts the basal total VFA concentration. The 0 and 10 h observations, and 6 h observation appeared above and below the predicted range of total VFA concentration, respectively, which suggests over-prediction of VFA absorption rate at lower concentrations of VFA. The affinity for absorption of VFA may be smaller than assumed in this model.

Diurnal patterns of acetate and propionate molar proportions are qualitatively well represented, but the model predictions appear to be more extreme in peak and basal proportions than the observed data. The observed basal butyrate proportion of 0.125 is within the predicted range, whereas the peak in butyrate proportion was predicted at 1 h after feeding, occurred more rapidly than the peak observed at 6 h. Therefore, the predictive performance of the butyrate proportion diurnal dynamics is relatively weak. Increased butyrate proportions were predicted together with decreased pH and decreased r_{NAD} (Zhang et al., 2013), and a more refined modeling of butyrate production controlled by these two factors may, therefore, improve the prediction of its diurnal profile. The predicted H_2 emission rate closely reflected the p_{H_2}, although the peak H_2 emission rate observed at 0.5 h was under-predicted. In addition, the model under-predicted the basal H_2 emission rate. The CH_4 emission rate observed from 0 to 3 h after feeding was lower than the range predicted by the model, whereas the CH_4 emission rate was underpredicted from 3 to 10 h after feeding, with the latter

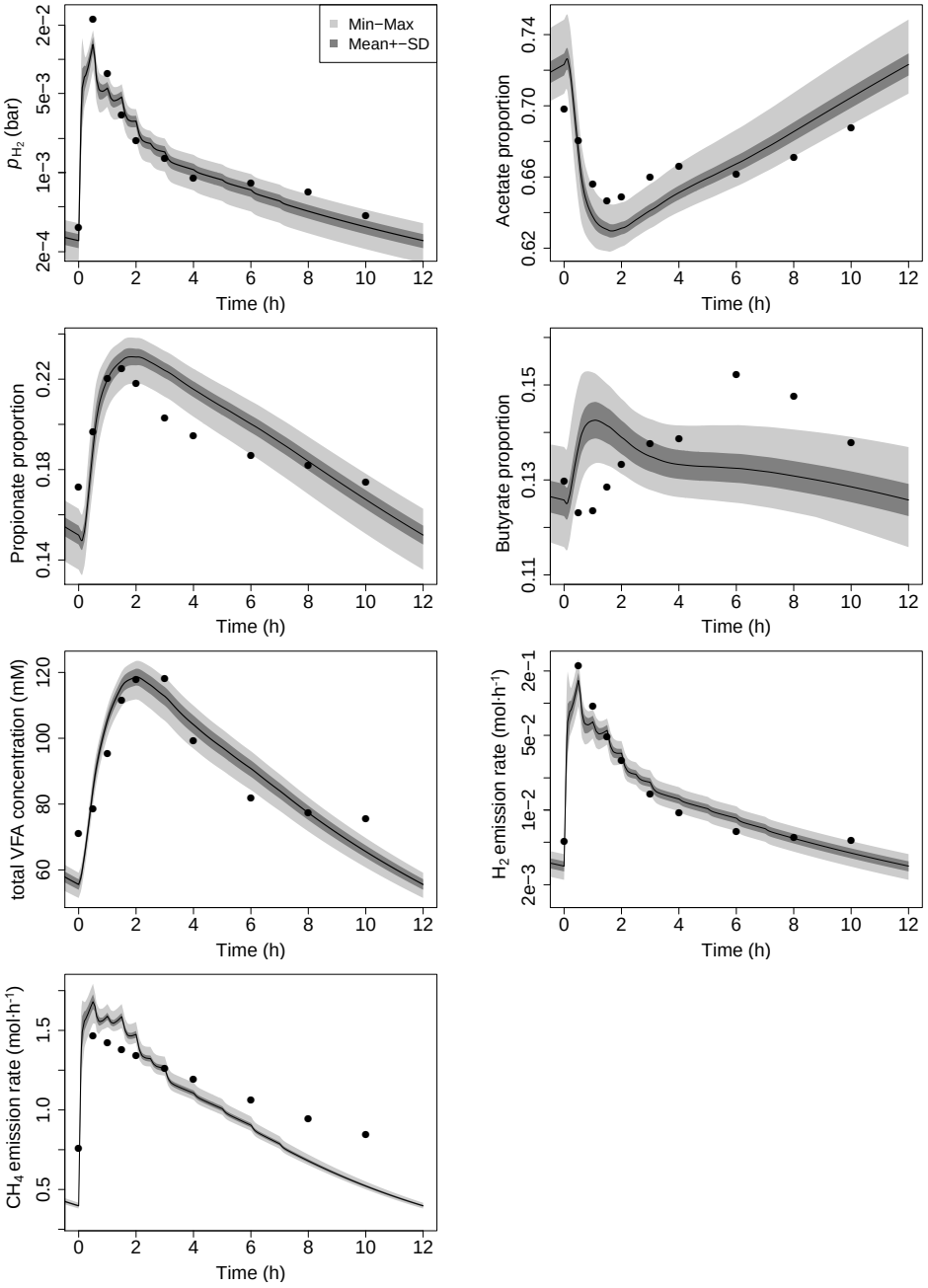

Figure 5.3: Model solutions with standard deviation, minimum and maximum to the MCMC generated parameter probability plotted against time, along with the observed data used to fit the model for p_{H_2} [bar], VFA concentration [mM], acetate, propionate and butyrate proportions [%], H_2 and CH_4 emission rates [mol·h^{-1}].

possibly due to ignoring the concept of hindgut fermentation in the model.

Experimental data points outside the prediction range of the model might suggest either the data or the model structure including the parameters that were not estimated to these data to be inadequate, rather than the joint parameter distribution. A potential limitation of the experimental data used to fit model parameters is that all data points belong to one experiment and represent the average of seven diurnal profiles that were fed two diets on a twice daily feeding regime, as the computational cost of the model did not allow a more detailed parameter estimation procedure. Data representing a broad variety of diets and feeding regimes, however, may improve the parameter estimates and will potentially enhance the general feasibility of the model. The model input reflects the average feed intake of cows during time intervals and may not accurately approach the instantaneous feed intake rate that occurred in reality. Forcing functions used to mathematically represent biological processes and inclusion or exclusion of key biological processes can also be a source of error (Ramin and Arhonditsis, 2013). A different mathematical representation of VFA production might therefore improve the model fit of the basal and peak VFA molar proportions. Under-prediction of the H_2 and CH_4 emission rates may disappear after inclusion of hindgut fermentation, which was previously predicted to contribute about 9% of the daily enteric CH_4 production in cows (Mills et al., 2001). Inclusion of methylotrophic methanogenesis (Lang et al., 2015) as a key biological process may also affect H_2 and CH_4 emission rates based on its higher CH_4 yield per equivalent of H_2 compared to purely hydrogenotrophic methanogenesis assumed in the present model.

Hexose concentration was predicted to increase from 1 to 7 mM in 0.6 h after feeding, to decline to basal level at 12 h (Fig. 5.4). Prediction uncertainty of hexose concentration appeared to be positively associated with its mean concentration, with peak hexose concentration varying from 3 to 11 mM. These diurnal dynamics of hexose concentration are largely in line with previous studies where a spike in soluble carbohydrate and free sugar concentrations in the rumen of sheep was observed rapidly after feeding (Clapperton and Czerkawski, 1969; Takahashi and Nakamura, 1969). The fluid and intracellular pH ranged from 6.1 to 6.9 and 6.5 to 7.0, respectively, and showed the opposite pattern of the total VFA concentration with some degree of uncertainty. The r_{NAD} was predicted to decrease from 3.2 to 0.8 in 0.6 h after feeding, followed by a recovery to its basal ratio at 12 h. Model predictions showed uncertainty to the parameter probability density, with the minimum and maximum values of r_{NAD} ranging from 0.6 to 0.9 and 2.8 to 3.6, respectively.

The thermodynamic potential factor (F_{T}), the quantity used to corrects a kinetic rate law for the thermodynamic effects exerted on reaction, was simulated to decrease from 0.95 to 0.55 in less than 0.5 h after feeding. The F_{T} adopting 0 and approaching

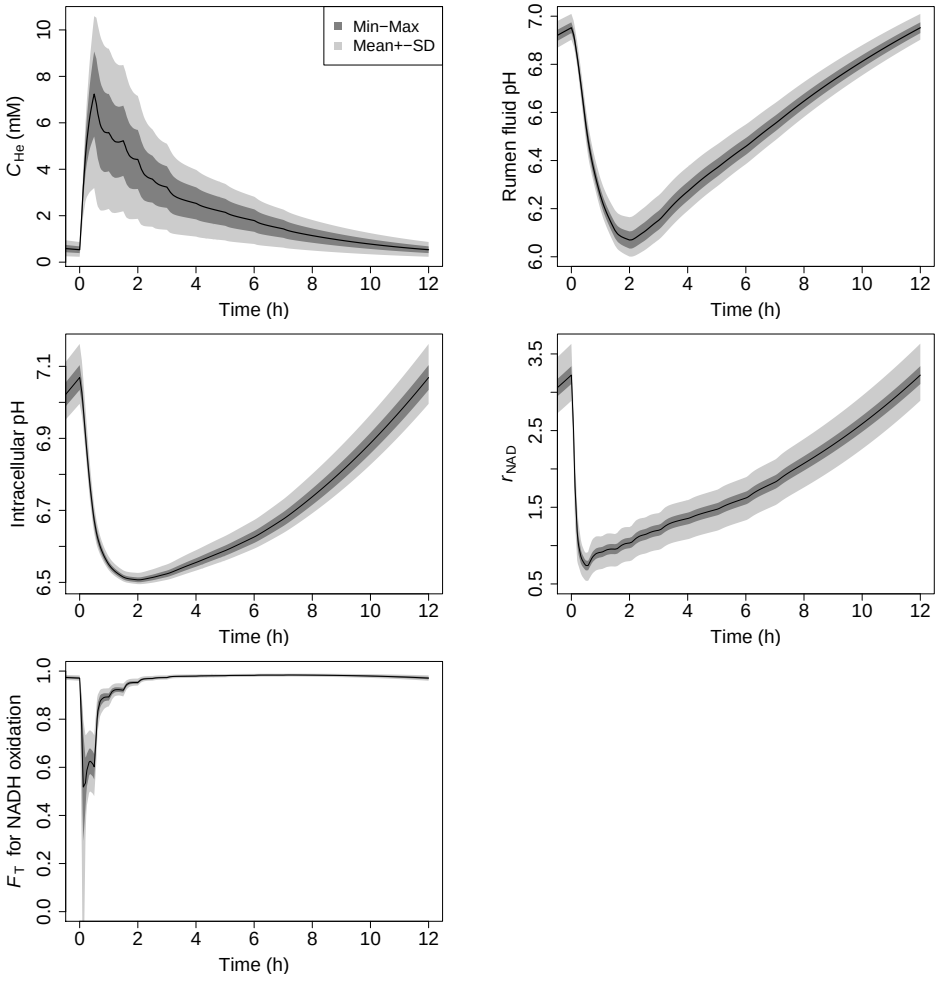

Figure 5.4: Model solutions with standard deviation, minimum and maximum to parameter probability as generated with the MCMC application plotted against time for hexose concentration [mM], rumen fluid pH, intracellular pH, NAD^+ to NADH ratio (r_{NAD}) and F_{T}

1 indicate full and no thermodynamic inhibition exerted on a reaction, respectively. The simulated decrease in F_T therefore indicates a transition from weak to moderate inhibition of NADH oxidation in response to feeding. The increase of F_T from 0.55 to 0.98 over the 0.5 to 4 h period indicates that the inhibition of NADH oxidation has vanished. A small decrease of F_T from 0.98 to 0.95 was predicted between 8 to 12 h after feeding. Inhibition of NADH oxidation is also determined by pH with greater F_T values when intracellular pH decreases. The emerging inhibition of NADH oxidation may be less *in vivo* as the basal total VFA concentration appears to be under-predicted causing the pH to be too high. The larger uncertainty shown for lower values of F_T is intrinsic to its definition, which states F_T to asymptotically approach 1 when changing to states that are not associated with any thermodynamic inhibition on a certain chemical reaction. The r_{NAD} was reported to be 1.4 to 2.6 in rumen microbes (Hino and Russell, 1985) and 1.1 to 2.7 for *Escherichia coli* (Berrios-Rivera et al., 2002), which is within the predicted range throughout the day and in line with $r_{NAD} < 9$ that was reported for living cells (Buckel and Thauer, 2013).

Overall, simulation shows that the hexose concentration in rumen fluid increases substantially after feeding. This stimulates the fermentation as reflected by the large increase in p_{H_2} and H_2 emission rate that immediately follows the increase in hexose concentration. The increase in p_{H_2} inhibits NADH oxidation, causing a decrease in r_{NAD}, which shifts the fermentation towards more propionate production at the expense of acetate production. Proportions of acetate and propionate then recondition to basal values when p_{H_2} decreases and r_{NAD} increases, with also the decreased pH also contributing to this. The CH_4 emission rate follows the patterns of p_{H_2} and H_2 emission rate, but its magnitude of increase in response to feeding is less substantial. The CH_4 production is, therefore, predicted to be relatively low at elevated p_{H_2} and H_2 emission rate. Model simulation shows that the rumen diurnal dynamics is qualitatively well predicted, but the quantitative behavior is somewhat inaccurate.

5.3.3 Global sensitivity analysis

The adjusted R^2 was 0.94, indicating that nearly all variance in CH_4 production output was explained using multiple linear regression, and that there was no indication of interaction between the parameters. The $k_{NADH,Fd_{RED}Fd_{OX}}$ parameter, which (together with the yield factors; Eq 5.52) determines the NADH oxidation rate, appeared to be most influential on predicted daily CH_4 production with a TMV of 41% (Fig. 5.5). The v_{H_2Me} parameter, which determines the maximum methanogenesis rate, also appeared to be rather influential and accounted for 16% of the variation in predicted CH_4 output. The TMV of the k_{F_gHe}, k_{S_gHe} and k_{WrHe} parameters that

determine the fermentability of the feed were 16, 0 and 0%, respectively. The TMV of v_{HeAc}, v_{HeAP}, $M_{\mathrm{NAD,HeAc}}$ and $J_{\mathrm{NAD,HeAP}}$, which are parameters that determine the production of acetate and propionate, were 7.6, 4.2, 4.1 and 3.6%, respectively. The $k_{\mathrm{H_2Em}}$, v_{HeBu}, q_{VfAb}, and $M_{\mathrm{H_2,H_2Me}}$ parameters all had negligible effect on daily CH_4 production with TMV $\leq 1.1\%$.

The positive relationship between CH_4 production output and $k_{\mathrm{NADH,Fd_{RED}Fd_{OX}}}$ (Fig. 5.5) indicates the more rapidly NADH is oxidized to NAD^+, the higher the acetate and H_2 yield and in turn the CH_4 production. The positive relationship between between CH_4 production output and $v_{\mathrm{H_2CH_4}}$ indicates that a larger maximum utilization rate of H_2 to form CH_4 by archaea increases CH_4 production. The positive and negative relationships that appear between the CH_4 production output and the v_{HeAc} and v_{HeAP} parameters, respectively, can be traced back to the higher and lower H_2 yields associated with acetate and propionate production pathways available for methanogenesis. The fact that v_{HeBu} does not contribute to variation in CH_4 output was somewhat unexpected, and is likely the result of considering v_{HeBu} relative to all other parameters included in this global sensitivity analysis. If only the estimated parameters were considered in the sensitivity analysis, v_{HeBu} would be positively related with CH_4 output and contributes to 6% of its variation, which is in line with the conversion of one hexose into one butyrate yielding two equivalents of H_2 that are potentially converted to CH_4. The biological feasibility of this very weak relationship needs to be taken with caution in view of the relatively inaccurate butyrate proportion diurnal profile generated by the model.

The positive relationship obtained for the $k_{\mathrm{F_gHe}}$ parameter with CH_4 output indicates the that increased fibrous substrate available for fermentation increases CH_4 production. The relatively large TMV associated with this parameter is in line with Gregorini et al. (2013) who pointed to the importance of accurate rumen digestive parameters for predicting CH_4 production. Although most CH_4 prediction equations reported in the literature are based on feed content rather than feed fermentability, the positive relationship for $k_{\mathrm{F_gHe}}$ together with the lack of relationship for $k_{\mathrm{S_gHe}}$ and k_{WrHe} obtained in the present study is in line with the fact that fibrous fractions rather than starch and sugars fraction appear in CH_4 prediction equations (e.g., Moraes et al., 2014; Appuhamy et al., 2016). The small TMV for the $k_{\mathrm{H_2Em}}$ parameter, which determines the H_2 emission rate, may be explained by the fact that only 0.6% of H_2 produced is emitted. Varying $k_{\mathrm{H_2Em}}$ from 75 to 125% of its mean value will hardly have an effect on the daily CH_4 output. Utilization of H_2 for CH_4 production is the predominant fate of H_2, as also indicated by the large TMV for the $v_{\mathrm{H_2CH_4}}$ parameter discussed previously.

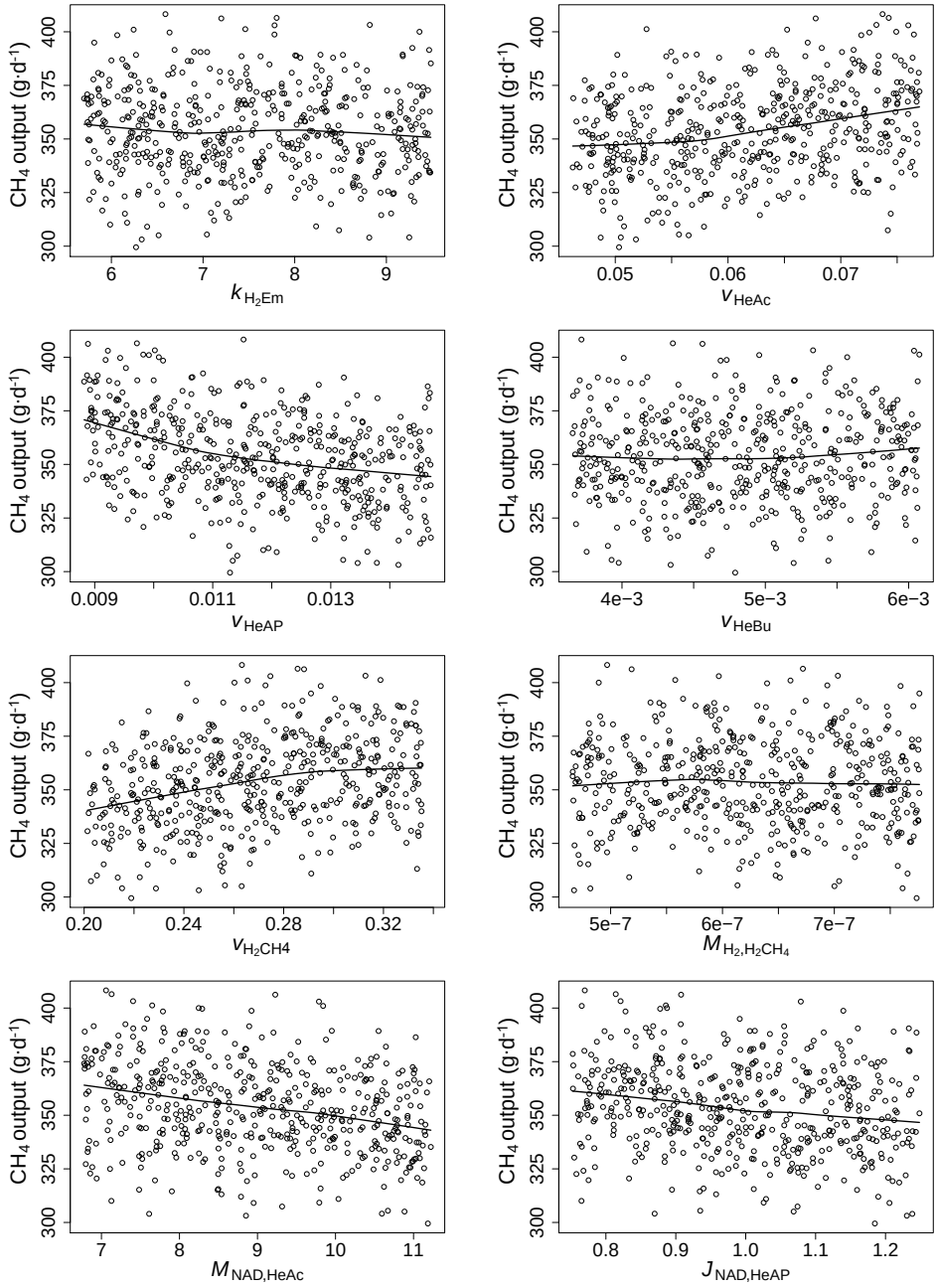

Figure 5.5: Global sensitivity of predicted daily methane production to model parameters sampled from a uniform distribution and varying from 0.75 to 1.25 times their estimated value.

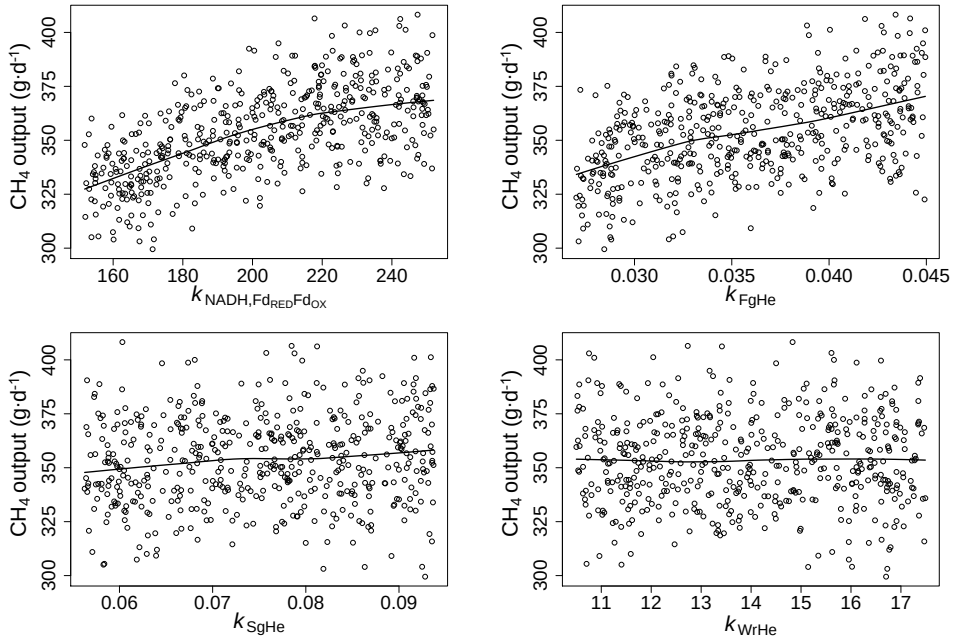

Figure 5.5: (continued)

5.3.4 Evaluation of model concept

The root mean square prediction error of the average daily CH_4 output from the three experiments used for model evaluation was 15%, with the model under-predicting the observations (351 ± 56 vs. 388 ± 28 g·d^{-1}). This model performance is in the range of 9.8 to 17% as obtained for four different models evaluated by Alemu et al. (2011), similar to the 15% of Mills et al. (2001), but less than 4.3–8.6% and 10% as reported by Gregorini et al. (2013) and Ramin and Huhtanen (2015), respectively. Unlike Mills et al. (2001), the present model did not represent H_2 utilization and production associated with microbial growth on non-protein nitrogen and amino acids, respectively, H_2 utilization for biohydrogenation of unsaturated fatty acids, and hindgut methanogenesis. Incorporation of these mechanisms may decrease the model prediction error. Furthermore, only one methanogenic pathway has been considered in the present model. For example, in comparison to hydrogenotrophic methanogenesis, methylotrophic methanogenesis yields more CH_4 per amount of H_2 (Lang et al., 2015), and incorporating this pathway in the present model would increase the predicted methanogenesis.

Fermentative microbes are represented by only one state variable in the present model. Dijkstra et al. (1992) discriminated between cellulolytic and amylolytic

bacteria, where the amylolytic bacteria also contained storage polysaccharides. This biomass fraction may, after lysis of bacteria, re-enter the substrate pool (i.e., hexose) and hence affect the rumen fermentation diurnal profiles. Next, discriminating between cellulolytic and amylolytic bacteria may more accurately predict degradation characteristics and affect the amount of hexose substrate available for fermentation and in turn the H_2 and CH_4 yield per amount of feed. Based on the various TMV obtained in the present study, this may in particular be the case for fiber degradation. The simplified representation of fermentative microbes may therefore have caused prediction inaccuracy within the present modeling effort.

Oxidation of NADH was represented via the confurcation mechanism only. The large TMV of the NADH oxidation parameter indicates the substantial impact of this mechanism on the predicted CH_4 and emphasizes the need for an accurate estimate of this parameter. Therefore, evaluation of a dynamic representation of the redox state of ferredoxin, instead of the static representation that was incorporated in the present model, is recommended. Moreover, the way in which NADH oxidation is incorporated in the model may need to be reconsidered. Zhang et al. (2013) developed a mixed culture fermentation model that included both confurcation and classical hydrogenase catalyzed NADH oxidation. This model was demonstrated to be more realistic than the mixed culture fermentation model of Rodríguez et al. (2006) in which only the classical NADH oxidation was represented. The performance of these mixed culture modeling efforts therefore supports the incorporation of the confurcation mechanism in addition to the classical mechanism. Nonetheless, it does not evaluate the need for incorporating the classical mechanism in addition to the confurcation mechanism. Hence, the value of incorporating the classical mechanism in the present model remains unclear.

The present dynamic mechanistic modeling effort provides a prediction tool of time-variant rumen fermentation and CH_4 production. Crompton et al. (2010b) examined CH_4 emission of dairy cattle as affected by feeding a total mixed ration in one, two or four portions throughout a day. They found a consistent numerical decrease in the daily average CH_4 yield per amount of feed with a reduced feeding frequency. The fermentation mechanism incorporated in the present model may, therefore, be an ultimate evaluation tool for the combined effect of feeding frequency and feed composition on rumen fermentation dynamics.

5.4 Conclusion

This modeling effort provides the integration of more detailed knowledge on rumen metabolic pathways yielding VFA, H_2 and CH_4 compared to whole rumen models

reported in the literature. The mechanistic approach to evaluate the effect of p_{H_2} on fermentation via r_{NAD} is based on principles of reaction kinetics and thermodynamics is rather unique in rumen modeling. Furthermore, the mechanistic representation of methanogenic archaea and their metabolism has not been widely applied. Model simulations qualitatively reproduce diurnal patterns of rumen metabolite concentrations. Quantitative evaluation of model predictions suggests the need for further parameter fine-tuning and reconsideration of the model structure. Global sensitivity analysis indicated the relatively large impact of the NADH oxidation parameter on prediction of average daily CH_4 output. In conclusion, this modeling effort can be regarded as a promising tool for further development of the mechanistic prediction of diurnal dynamics of rumen microbial metabolism, substrate fermentation and methanogenesis based on various feeding regimes.

Acknowledgments

Dr James G Fadel (University of California, Davis) is greatly acknowledged for valuable discussions.

Supporting information

Table S1: Abbreviations used in mathematical expressions in the model

Symbol	Entity	Symbol	Entity
Ab	Absorption	La	Lactate
Ac	Acetate	Me	Methanogens
Am	Ammonia	Mi	Fermentative microbes
AP	Acetate + propionate	NAD	General NAD^+ and/or NADH
Bu	Butyrate	Pr	Propionate
DM	Dry matter	Ps	Soluble protein
Em	Emission (from the rumen)	Ru	Rumen
Ex	Exit to lower tract	Sg	Degradable starch
F_g	Degradable fiber	So	Solid
Fd	Ferredoxin	Sr	Soluble starch
Fl	Fluid	Vf	Volatile fatty acids
GM	Growth-maintenance	Wr	Water soluble carbohydrates
He	Hexose	Xg	Degradable carbohydrates
In	Intake		

Table S2: General notation used in the model

Notation	Description	Unit
c_{i}	Content of i in feed or microbial dry matter	$\mathrm{g{\cdot}kg^{-1}}$
C_{i}	Concentration of i	M or $\mathrm{g{\cdot}L^{-1}}$
C_{i}^{*}	Reference concentration of i	M or $\mathrm{g{\cdot}L^{-1}}$
D_{DM}	DM ingestion rate	$\mathrm{kg{\cdot}h^{-1}}$
F_{T}	Thermodynamic potential factor	-
$f_{\mathrm{i,j}}$; $f_{\mathrm{i,jm}}$	Fraction of i or i in j-to-m transaction	-
$J_{\mathrm{i,jm}}$	Inhibition constant for i associated with the j-to-m transaction	M or -
k_{jm}	Mass action rate constant for j-to-m transaction	$\mathrm{h^{-1}}$
$M_{\mathrm{i,jm}}$	Affinity constant for i associated with the j-to-m transaction	M or -
$P_{\mathrm{i,jm}}$	Production of i by j-to-m transaction	$\mathrm{mol{\cdot}h^{-1}}$ or $\mathrm{g{\cdot}h^{-1}}$
p_i	Partial pressure of gas i	atm
pH_i	pH of medium i	-
$\Phi_{\mathrm{Vf,jm}}$	Steepness variable for the j to m transaction with respect to C_{VFA}	-
$\Theta_{\mathrm{pH,jm}}$	Steepness variable for the j to m transaction with respect to pH	-
Q_{i}	Quantity of i	mol or g
q_{jm}	Proportion of j with respect to m	-
r_{NAD}	$\mathrm{NAD^{+}}$ to NADH ratio	-
r_{Fd}	Reduced ferredoxin to oxidized ferredoxin ratio	-
$U_{\mathrm{i,jm}}$; $U_{\mathrm{i,jm,n}}$	Utilization/outflow of i by j-to-m transaction (generating m)	$\mathrm{mol{\cdot}h^{-1}}$ or $\mathrm{g{\cdot}h^{-1}}$
v_{jm}	Maximum uptake rate of j converted to m	$\mathrm{mol{\cdot}g^{-1}{\cdot}h^{-1}}$ or $\mathrm{h^{-1}}$ or $\mathrm{h^{-1}{\cdot}L^{-0.75}}$
V_{i}	Volume of i	L
W_{i}	Molecular weight of i	$\mathrm{g{\cdot}mol^{-1}}$
$Y_{\mathrm{i,jm}}$, $Y_{\mathrm{i,jm,n}}$	Yield of i from j-to-m transaction (generating n)	$\mathrm{mol{\cdot}mol^{-1}}$ or $\mathrm{g{\cdot}mol^{-1}}$ or $\mathrm{mol{\cdot}g^{-1}}$

Model Equations Appendix

Degradable fiber pool, $Q_{\mathrm{F_g}}$ [g]

Degradable fiber inflow :

$$P_{\mathrm{F_g,InF_g}}\ [\mathrm{g{\cdot}h^{-1}}] = D_{\mathrm{DM}} \cdot c_{\mathrm{F_g}} \tag{5.4}$$

Microbial fiber hydrolysis to hexose:

$$U_{\mathrm{F_g,F_gHe}}\ [\mathrm{g{\cdot}h^{-1}}] = k_{\mathrm{F_gHe}} \cdot C_{\mathrm{Mi}}/C^*_{\mathrm{Mi}} \cdot Q_{\mathrm{F_g}} \tag{5.5}$$

Outflow of $\mathrm{F_g}$ from the rumen to the lower tract:

$$U_{\mathrm{F_g,F_gEx}}\ [\mathrm{g{\cdot}h^{-1}}] = k_{\mathrm{SoEx}} \cdot Q_{\mathrm{F_g}} \tag{5.6}$$

Differential equation:

$$\frac{\mathrm{d}Q_{\mathrm{F_g}}}{\mathrm{d}t}\ [\mathrm{g{\cdot}h^{-1}}] = P_{\mathrm{F_g,InF_g}} - U_{\mathrm{F_g,F_gHe}} - U_{\mathrm{F_g,F_gEx}} \tag{5.7}$$

Degradable starch pool, $Q_{\mathrm{S_g}}$ [g]

Degradable starch (soluble+insoluble) inflow:

$$P_{\mathrm{S_g,InS_g}}\ [\mathrm{g{\cdot}h^{-1}}] = D_{\mathrm{DM}} \cdot (c_{\mathrm{S_g}} + \frac{1}{2} c_{\mathrm{S_r}}) \tag{5.8}$$

Microbial starch hydrolysis to hexose:

$$U_{\mathrm{S_g,S_gHe}}\ [\mathrm{g{\cdot}h^{-1}}] = k_{\mathrm{S_gHe}} \cdot C_{\mathrm{Mi}}/C^*_{\mathrm{Mi}} \cdot Q_{\mathrm{S_g}} \tag{5.9}$$

Outflow of starch from the rumen to the lower tract:

$$U_{\mathrm{S_g,S_gEx}}\ [\mathrm{g{\cdot}h^{-1}}] = k_{\mathrm{SoEx}} \cdot Q_{\mathrm{S_g}} \tag{5.10}$$

Differential equation:

$$\frac{\mathrm{d}Q_{\mathrm{S_g}}}{\mathrm{d}t}\ [\mathrm{g{\cdot}h^{-1}}] = P_{\mathrm{S_g,InS_g}} - U_{\mathrm{S_g,S_gHe}} - U_{\mathrm{S_g,S_gEx}} \tag{5.11}$$

Soluble sugar pool, $Q_{\mathrm{W_r}}$ [g]

Soluble sugar inflow:

$$P_{\mathrm{W_r,InW_r}}\ [\mathrm{g{\cdot}h^{-1}}] = D_{\mathrm{DM}} \cdot (c_{\mathrm{W_r}} + \frac{1}{2} c_{\mathrm{S_r}}) \tag{5.12}$$

Hydrolysis to hexose:

$$U_{\mathrm{W_r,W_rHe}}\ [\mathrm{g{\cdot}h^{-1}}] = k_{\mathrm{W_rHe}} \cdot C_{\mathrm{Mi}} / C^*_{\mathrm{Mi}} \cdot Q_{\mathrm{W_r}} \tag{5.13}$$

Outflow of soluble sugars from the rumen to the lower tract:

$$U_{\mathrm{W_r,W_rEx}}\ [\mathrm{g{\cdot}h^{-1}}] = k_{\mathrm{FlEx}} \cdot Q_{\mathrm{W_r}} \tag{5.14}$$

Differential equation:

$$\frac{\mathrm{d}Q_{\mathrm{W_r}}}{\mathrm{d}t}\ [\mathrm{g{\cdot}h^{-1}}] = P_{\mathrm{W_r,InW_r}} - U_{\mathrm{W_r,W_rHe}} - U_{\mathrm{W_r,W_rEx}} \tag{5.15}$$

Hexose pool, Q_{He} [mol]

Concentration of hexose:

$$C_{\mathrm{He}}\ [\mathrm{M}] = \frac{Q_{\mathrm{He}}}{V_{\mathrm{Fl}}} \tag{5.16}$$

Hexose inflow from feed lactate:

$$P_{\mathrm{He,LaHe}}\ [\mathrm{mol{\cdot}h^{-1}}] = D_{\mathrm{DM}} \cdot Y_{\mathrm{He,LaHe}} \cdot c_{\mathrm{La}} / W_{\mathrm{La}} \tag{5.17}$$

Hexose inflow from hydrolysis of $\mathrm{F_g}$, $\mathrm{S_g}$ and $\mathrm{W_r}$:

$$P_{\mathrm{He,X_gHe}}\ [\mathrm{mol{\cdot}h^{-1}}] = (U_{\mathrm{F_g,F_gHe}} + U_{\mathrm{S_g,S_gHe}} + U_{\mathrm{W_r,W_rHe}}) / W_{\mathrm{He}} \tag{5.18}$$

Hexose uptake for microbial growth yielding 2 acetate:

$$U_{\mathrm{He,HeMi,Ac}}\ [\mathrm{mol{\cdot}h^{-1}}] = \frac{(v_{\mathrm{HeAc}} / q_{\mathrm{GM}}) \cdot Q_{\mathrm{Mi}}}{\left(1 + \frac{M_{\mathrm{He,HeMi}}}{C_{\mathrm{He}}}\right)\left(1 + \frac{M_{\mathrm{NAD,HeAc}}}{r_{\mathrm{NAD}}}\right)} \tag{5.19}$$

Hexose uptake for microbial growth yielding 1 butyrate:

$$U_{\mathrm{He,HeMi,Bu}}\ [\mathrm{mol{\cdot}h^{-1}}] = \frac{(v_{\mathrm{HeBu}} / q_{\mathrm{GM}}) \cdot Q_{\mathrm{Mi}}}{1 + \frac{M_{\mathrm{He,HeMi}}}{C_{\mathrm{He}}}} \tag{5.20}$$

Hexose uptake for microbial growth yielding $\frac{2}{3}$ acetate + $\frac{4}{3}$ propionate:

$$U_{\mathrm{He,HeMi,AP}}\ [\mathrm{mol{\cdot}h^{-1}}] = \frac{(v_{\mathrm{HeAP}}/q_{\mathrm{GM}}) \cdot Q_{\mathrm{Mi}}}{\left(1 + \frac{M_{\mathrm{He,HeMi}}}{C_{\mathrm{He}}}\right)\left(1 + \frac{r_{\mathrm{NAD}}}{J_{\mathrm{NAD,HeAP}}}\right)} \tag{5.21}$$

He uptake for non-growth functions yielding 2 acetate:

$$U_{\mathrm{He,HeAc}}\ [\mathrm{mol{\cdot}h^{-1}}] = \frac{v_{\mathrm{HeAc}} \cdot Q_{\mathrm{Mi}}}{\left(1 + \frac{M_{\mathrm{He,HeVf}}}{C_{\mathrm{He}}}\right)\left(1 + \frac{C_{\mathrm{Am}}}{J_{\mathrm{Am,HeVf}}} + \frac{C_{\mathrm{P_s}}}{J_{\mathrm{P_s,HeVf}}}\right)\left(1 + \frac{M_{\mathrm{NAD,HeAc}}}{r_{\mathrm{NAD}}}\right)} \tag{5.22}$$

He uptake for non-growth functions yielding 1 butyrate:

$$U_{\mathrm{He,HeBu}}\ [\mathrm{mol{\cdot}h^{-1}}] = \frac{v_{\mathrm{HeBu}} \cdot Q_{\mathrm{Mi}}}{\left(1 + \frac{M_{\mathrm{He,HeVf}}}{C_{\mathrm{He}}}\right)\left(1 + \frac{C_{\mathrm{Am}}}{J_{\mathrm{Am,HeVf}}} + \frac{C_{\mathrm{Ps}}}{J_{\mathrm{PsHeVf}}}\right)} \tag{5.23}$$

He uptake for non-growth functions yielding $\frac{2}{3}$ acetate + $\frac{4}{3}$ propionate:

$$U_{\mathrm{He,HeAP}}\ [\mathrm{mol{\cdot}h^{-1}}] = \frac{v_{\mathrm{HeAP}} \cdot Q_{\mathrm{Mi}}}{\left(1 + \frac{M_{\mathrm{He,HeVf}}}{C_{\mathrm{He}}}\right)\left(1 + \frac{C_{\mathrm{Am}}}{J_{\mathrm{Am,HeVf}}} + \frac{C_{\mathrm{P_s}}}{J_{\mathrm{P_s,HeVf}}}\right)\left(1 + \frac{r_{\mathrm{NAD}}}{J_{\mathrm{NAD,HeAP}}}\right)} \tag{5.24}$$

Outflow of hexose from the rumen to the lower tract:

$$U_{\mathrm{He,HeEx}}\ [\mathrm{mol{\cdot}h^{-1}}] = k_{\mathrm{FlEx}} \cdot Q_{\mathrm{He}} \tag{5.25}$$

Differential equation:

$$\begin{aligned} \frac{\mathrm{d}Q_{\mathrm{He}}}{\mathrm{d}t}\ [\mathrm{mol{\cdot}h^{-1}}] \quad = \quad & P_{\mathrm{He,LaHe}} + P_{\mathrm{He,X_gHe}} - U_{\mathrm{He,HeMi,Ac}} - U_{\mathrm{He,HeMi,Bu}} \\ & - U_{\mathrm{He,HeMi,AP}} - U_{\mathrm{He,HeAc}} - U_{\mathrm{He,HeBu}} - U_{\mathrm{He,HeAP}} \\ & - U_{\mathrm{He,HeEx}} \end{aligned} \tag{5.26}$$

Microbes pool, Q_{Mi} [g]

Concentration of microbes:

$$C_{\mathrm{Mi}}\ [\mathrm{g{\cdot}L^{-1}}] = \frac{Q_{\mathrm{Mi}}}{V_{\mathrm{Fl}}} \tag{5.27}$$

Microbial growth associated with hexose fermentation to 2 acetate, 1 butyrate and

$\frac{2}{3}$ acetate + $\frac{4}{3}$ propionate:

$$\begin{aligned} P_{\mathrm{Mi,HeMi}}\ [\mathrm{g{\cdot}h^{-1}}] &= Y_{\mathrm{Mi,HeMi,Ac}} \cdot U_{\mathrm{He,HeMi,Ac}} + Y_{\mathrm{Mi,HeMi,Bu}} \cdot U_{\mathrm{He,HeMi,Bu}} \\ &\quad + Y_{\mathrm{Mi,HeMi,AP}} \cdot U_{\mathrm{He,HeMi,AP}} \end{aligned} \tag{5.28}$$

Outflow of microbes from the rumen to the lower tract:

$$U_{\mathrm{Mi,MiEx}}\ [\mathrm{g{\cdot}h^{-1}}] = (0.65 \cdot k_{\mathrm{SoEx}} + 0.15 \cdot k_{\mathrm{FlEx}}) \cdot Q_{\mathrm{Mi}} \tag{5.29}$$

Differential equation:

$$\frac{\mathrm{d}Q_{\mathrm{Mi}}}{\mathrm{d}t}\ [\mathrm{g{\cdot}h^{-1}}] = P_{\mathrm{Mi,HeMi}} - U_{\mathrm{Mi,MiEx}} \tag{5.30}$$

Acetate pool, Q_{Ac} [mol]

Concentration of acetate:

$$C_{\mathrm{Ac}}\ [\mathrm{M}] = \frac{Q_{\mathrm{Ac}}}{V_{\mathrm{Fl}}} \tag{5.31}$$

Acetate from feed input:

$$P_{\mathrm{Ac,InAc}}\ [\mathrm{mol{\cdot}h^{-1}}] = D_{\mathrm{DM}} \cdot c_{\mathrm{Ac}} / W_{\mathrm{Ac}} \tag{5.32}$$

Acetate from hexose fermentation for microbial maintenance and growth:

$$\begin{aligned} P_{\mathrm{Ac,HeAc}}\ [\mathrm{mol{\cdot}h^{-1}}] &= Y_{\mathrm{Ac,HeAc}} \cdot (f_{\mathrm{He,HeAc}} \cdot U_{\mathrm{He,HeMi,Ac}} + U_{\mathrm{He,HeAc}}) + \\ &\quad Y_{\mathrm{Ac,HeAP}} \cdot (f_{\mathrm{He,HeAP}} \cdot U_{\mathrm{He,HeMi,AP}} + U_{\mathrm{He,HeAP}}) \end{aligned} \tag{5.33}$$

Absorption of acetate across the rumen wall:

$$U_{\mathrm{Ac,AcAb}}\ [\mathrm{mol{\cdot}h^{-1}}] = \frac{q_{\mathrm{VfAb}} \cdot v_{\mathrm{AcAb}} \cdot V_{\mathrm{Fl}}^{0.75}}{\left[1 + \left(\frac{M_{\mathrm{Ac,AcAb}}}{C_{\mathrm{Ac}}}\right)^{\Phi_{\mathrm{Ac,AcAb}}}\right]\left[1 + \left(\frac{p\mathrm{H}}{J_{\mathrm{pH,AcAb}}}\right)^{\Theta_{\mathrm{pH,AcAb}}}\right]} \cdot Q_{\mathrm{Ac}} \tag{5.34}$$

with:

$$\mathrm{pH} = 7.73 - 14 C_{\mathrm{Vf}} \tag{5.35}$$

Outflow of acetate to the lower tract:

$$U_{\mathrm{Ac,AcEx}}\ [\mathrm{mol{\cdot}h^{-1}}] = k_{\mathrm{FlEx}} \cdot Q_{\mathrm{Ac}} \tag{5.36}$$

Differential equation:

$$\frac{\mathrm{d}Q_{\mathrm{Ac}}}{\mathrm{d}t}\ [\mathrm{mol{\cdot}h^{-1}}] = P_{\mathrm{Ac,InAc}} + P_{\mathrm{Ac,HeAc}} - U_{\mathrm{Ac,AcAb}} - U_{\mathrm{Ac,AcEx}} \tag{5.37}$$

Propionate pool, Q_{Pr} [mol]

Concentration of propionate:

$$C_{\mathrm{Pr}}\ [\mathrm{M}] = \frac{Q_{\mathrm{Pr}}}{V_{\mathrm{Fl}}} \tag{5.38}$$

Propionate from feed input:

$$P_{\mathrm{Pr,InPr}}\ [\mathrm{mol{\cdot}h^{-1}}] = D_{\mathrm{DM}} \cdot c_{\mathrm{Pr}}/W_{\mathrm{Pr}} \tag{5.39}$$

Propionate from hexose fermentation for microbial maintenance and growth:

$$P_{\mathrm{Pr,HeAP}}\ [\mathrm{mol{\cdot}h^{-1}}] \quad = \quad Y_{\mathrm{Pr,HeAP}} \cdot (f_{\mathrm{He,HeAP}} \cdot U_{\mathrm{He,HeMi,AP}} + U_{\mathrm{He,HeAP}}) \tag{5.40}$$

Absorption of propionate across the rumen wall:

$$U_{\mathrm{Pr,PrAb}}\ [\mathrm{mol{\cdot}h^{-1}}] = \frac{q_{\mathrm{VfAb}} \cdot v_{\mathrm{PrAb}} \cdot V_{\mathrm{Fl}}^{0.75}}{\left[1 + \left(\frac{M_{\mathrm{Pr,PrAb}}}{C_{\mathrm{Pr}}}\right)^{\Phi_{\mathrm{Pr,PrAb}}}\right]\left[1 + \left(\frac{p\mathrm{H}}{J_{\mathrm{pH,PrAb}}}\right)^{\Theta_{\mathrm{pH,PrAb}}}\right]} \cdot Q_{\mathrm{Pr}} \tag{5.41}$$

Outflow of propionate to the lower tract:

$$U_{\mathrm{Pr,PrEx}}\ [\mathrm{mol{\cdot}h^{-1}}] = k_{\mathrm{FlEx}} \cdot Q_{\mathrm{Pr}} \tag{5.42}$$

Differential equation:

$$\frac{\mathrm{d}Q_{\mathrm{Pr}}}{\mathrm{d}t}\ [\mathrm{mol{\cdot}h^{-1}}] = P_{\mathrm{Pr,InPr}} + P_{\mathrm{Pr,HePr}} - U_{\mathrm{Pr,PrAb}} - U_{\mathrm{Pr,PrEx}} \tag{5.43}$$

Butyrate pool, Q_{Bu} [mol]

Concentration of butyrate:

$$C_{\mathrm{Bu}}\ [\mathrm{M}] = \frac{Q_{\mathrm{Bu}}}{V_{\mathrm{Fl}}} \tag{5.44}$$

Butyrate from feed input:

$$P_{\mathrm{Bu,InBu}}\ [\mathrm{mol{\cdot}h^{-1}}] = D_{\mathrm{DM}} \cdot c_{\mathrm{Bu}} / W_{\mathrm{Bu}} \tag{5.45}$$

Butyrate from hexose fermentation for microbial maintenance and growth:

$$P_{\mathrm{Bu,HeBu}}\ [\mathrm{mol{\cdot}h^{-1}}] \quad = \quad Y_{\mathrm{Bu,HeBu}} \cdot (f_{\mathrm{He,HeBu}} \cdot U_{\mathrm{He,HeMi,Bu}} + U_{\mathrm{He,HeBu}}) \tag{5.46}$$

Absorption of butyrate across the rumen wall:

$$U_{\mathrm{Bu,BuAb}}\ [\mathrm{mol{\cdot}h^{-1}}] = \frac{q_{\mathrm{VfAb}} \cdot v_{\mathrm{BuAb}} \cdot V_{\mathrm{Fl}}^{0.75}}{\left[1 + \left(\frac{M_{\mathrm{Bu,BuAb}}}{C_{\mathrm{Bu}}}\right)^{\Phi_{\mathrm{Bu,BuAb}}}\right]\left[1 + \left(\frac{p\mathrm{H}}{J_{\mathrm{pH,BuAb}}}\right)^{\Theta_{\mathrm{pH,BuAb}}}\right]} \cdot Q_{\mathrm{Bu}} \tag{5.47}$$

Outflow of butyrate to the lower tract:

$$U_{\mathrm{Bu,BuEx}}\ [\mathrm{mol{\cdot}h^{-1}}] = k_{\mathrm{FlEx}} \cdot Q_{\mathrm{Bu}} \tag{5.48}$$

Differential equation:

$$\frac{\mathrm{d}Q_{\mathrm{Bu}}}{\mathrm{d}t}\ [\mathrm{mol{\cdot}h^{-1}}] = P_{\mathrm{Bu,InBu}} + P_{\mathrm{Bu,HeBu}} - U_{\mathrm{Bu,BuAb}} - U_{\mathrm{Bu,BuEx}} \tag{5.49}$$

NADH pool, Q_{NADH} [mol]

NAD^+ reduction by hexose fermentation to 2 acetate:

$$P_{\mathrm{NADH,HeAc}}\ [\mathrm{mol{\cdot}h^{-1}}] = 2 \cdot (f_{\mathrm{He,HeAc}} \cdot U_{\mathrm{He,HeMi,Ac}} + U_{\mathrm{He,HeAc}}) \tag{5.50}$$

NADH oxidation by hexose fermentation to $\frac{2}{3}$ acetate + $\frac{4}{3}$ propionate:

$$U_{\mathrm{NADH,HeAP}}\ [\mathrm{mol{\cdot}h^{-1}}] = 0.67 \cdot (f_{\mathrm{He,HeAP}} \cdot U_{\mathrm{He,HeMi,AP}} + U_{\mathrm{He,HeAP}}) \tag{5.51}$$

NADH oxidation by H_2 production:

$$U_{\mathrm{NADH,Fd_{RED}Fd_{OX}}}\ [\mathrm{mol{\cdot}h^{-1}}] = k_{\mathrm{NADH,Fd_{RED}Fd_{OX}}} \cdot f_{\mathrm{NADH}} \cdot c_{\mathrm{NAD}} \cdot Q_{\mathrm{Mi}} \cdot F_{\mathrm{T}} \tag{5.52}$$

with F_{T}:

$$1 - \left(r_{\mathrm{NAD}} \cdot r_{\mathrm{Fd}} \cdot \frac{p_{\mathrm{H_2}}^2}{10^{-3 \cdot p\mathrm{H_{cell}}}}\right)^{1/\chi} \cdot \exp\left(\frac{\Delta G^o}{\chi RT}\right) \tag{5.53}$$

and

$$\mathrm{pH_{cell}} = 6.43 + 3.62 \cdot 10^{-8} \exp(2.4\mathrm{pH_{Fl}}) \tag{5.54}$$

Differential equation:

$$\frac{\mathrm{d}Q_{\mathrm{NADH}}}{\mathrm{d}t}\ [\mathrm{mol{\cdot}h^{-1}}] = P_{\mathrm{NADH,HeAc}} - U_{\mathrm{NADH,HeAP}} - U_{\mathrm{NADH,Fd_{RED}Fd_{OX}}} \tag{5.55}$$

The discretized update of the fraction of NADH per numerical integration step:

$$f_{\mathrm{NADH}_{t+\Delta t}} = \frac{f_{\mathrm{NADH}_t} \cdot c_{\mathrm{NAD}} \cdot Q_{\mathrm{Mi}} + \Delta Q_{\mathrm{NADH}}}{c_{\mathrm{NAD}} \cdot Q_{\mathrm{Mi}}} \tag{5.56}$$

and the $\mathrm{NAD^+}$ to NADH ratio:

$$r_{\mathrm{NAD}} = \frac{1 - f_{\mathrm{NADH}}}{f_{\mathrm{NADH}}} \tag{5.57}$$

H_2 pool, Q_{H_2} [mol]

H_2 partial pressure in the rumen headspace according to the ideal gas law:

$$p_{H_2}\ [\text{atm}] = \frac{10^3 \cdot Q_{H_2} \cdot RT}{p_0 \cdot V_{\text{headspace}}} \tag{5.58}$$

H_2 yield from hexose fermentation to 2 acetate:

$$P_{H_2,\text{HeAc}}\ [\text{mol}\cdot\text{h}^{-1}] = Y_{H_2,\text{HeAc}} \cdot (f_{\text{He,HeAc}} \cdot U_{\text{He,HeMi,Ac}} + U_{\text{He,HeAc}}) \tag{5.59}$$

H_2 yield from hexose fermentation to 1 butyrate:

$$P_{H_2,\text{HeBu}}\ [\text{mol}\cdot\text{h}^{-1}] = Y_{H_2,\text{HeBu}} \cdot (f_{\text{He,HeBu}} \cdot U_{\text{He,HeMi,Bu}} + U_{\text{He,HeBu}}) \tag{5.60}$$

H_2 for methanogenic growth:

$$U_{H_2,H_2CH_4}\ [\text{mol}\cdot\text{h}^{-1}] = \frac{v_{H_2CH_4} \cdot Q_{\text{Me}}}{1 + \frac{M_{H_2,H_2CH_4}}{C_{H_2}}} \tag{5.61}$$

With dissolved H_2 concentration calculated using the ideal gas law and Henry's law:

$$C_{H_2}\ [\text{M}] = \frac{Q_{H_2} \cdot RT}{H_{H_2} \cdot p_0 \cdot V_{\text{Fl}}} \tag{5.62}$$

H_2 emitted via eructation and exhalation:

$$U_{H_2,H_2\text{Em}}\ [\text{mol}\cdot\text{h}^{-1}] = k_{H_2\text{Em}} \cdot Q_{H_2} \tag{5.63}$$

H_2 absorbed across the rumen wall:

$$U_{H_2,H_2\text{Ab}}\ [\text{mol}\cdot\text{h}^{-1}] = \left(\frac{F_{\text{b}} \cdot V_{\text{mol}}}{V_{\text{headspace}} \cdot H_{H_2}}\right) \cdot Q_{H_2} \tag{5.64}$$

H_2 to the lower tract:

$$U_{H_2,H_2\text{Ex}}\ [\text{mol}\cdot\text{h}^{-1}] = \frac{V_{\text{Fl}} \cdot k_{\text{FlEx}} \cdot V_{\text{mol}}}{V_{\text{headspace}} \cdot H_{H_2}} \cdot Q_{H_2} \tag{5.65}$$

Differential equation:

$$\begin{aligned} \frac{\text{d}Q_{H_2}}{\text{d}t}\ [\text{mol}\cdot\text{h}^{-1}] \quad = \quad & P_{H_2,\text{HeAc}} - P_{H_2,\text{HeBu}} - U_{H_2,H_2CH_4} - U_{H_2,H_2\text{Em}} \\ & - U_{H_2,H_2\text{Ab}} - U_{H_2,H_2\text{Ex}} \end{aligned} \tag{5.66}$$

Production rate of CH_4 is calculated as:

$$P_{CH_4,H_2CH_4}\ [\text{mol}\cdot\text{h}^{-1}] = Y_{CH_4,H_2CH_4} \cdot U_{H_2,H_2CH_4} \tag{5.67}$$

Methanogens pool, Q_{Me} [g]

Methanogenic growth from methanogenesis:

$$P_{Me,H_2CH_4}\ [\text{g}\cdot\text{h}^{-1}] = Y_{Me,H_2CH_4} \cdot Y_{CH_4,H_2CH_4} \cdot U_{H_2,H_2CH_4} \tag{5.68}$$

Methanogenic outflow from the rumen to the lower tract:

$$U_{Me,MeEx}\ [\text{g}\cdot\text{h}^{-1}] = (0.4 \cdot k_{SoEx} + 0.4 \cdot k_{FlEx}) \cdot Q_{Me} \tag{5.69}$$

Differential equation:

$$\frac{\mathrm{d}Q_{Me}}{\mathrm{d}t}\ [\text{g}\cdot\text{h}^{-1}] = P_{Me,H_2CH_4} - U_{Me,MeEx} \tag{5.70}$$

Chapter 6

General discussion

Modeling of enteric CH_4 production in dairy cows contributes to the understanding of the rumen as a (micro)biological system, and helps to quantify global greenhouse gas (GHG) emissions from livestock production. Increased understanding obtained from modeling aids to develop abatement strategies of livestock enteric CH_4 emissions. The livestock sector was estimated to emit 7.1 gigatonnes of CO_2 equivalents, which is about 14.5% of total global anthropogenic GHG emissions (Gerber et al., 2013). Enteric methanogenesis was the main source of GHG emissions from dairy cattle, with amounting to 1.1 gigatonnes per year, representing 46% of the global GHG emissions in dairy supply chains (Hristov et al., 2013b). The research reported in this thesis contributes to increased understanding of rumen fermentation and microbial metabolism, and has provided a basis to further improve prediction models of enteric CH_4 emissions from cattle.

The main objective of this thesis was to quantitatively evaluate enteric CH_4 emission from dairy cows as affected by feeding and rumen microbial metabolism. An empirical prediction model for CH_4 emissions from dairy cows based on milk FA concentrations, in which rumen microbial metabolism is assessed indirectly, is reported in Chapter 2. Chapters 3 and 4 contain a theoretical and experimental investigation of rumen fermentation and CH_4 production. The thermodynamic control of p_{H_2} on the carbohydrate catabolism examined in these two chapters formed the conceptual basis for the mechanistic modeling framework reported in Chapter 5. Modeling is applied for the purpose of prediction and evaluation of hypotheses. The experimental results provide evidence for the applicability of mechanisms described and incorporated in the mechanistic model. In this thesis, the enhanced understanding of the fermentative and methanogenic metabolisms tend to be more important than the development of a prediction model with the highest achievable predictive performance.

The combination of a meta-analysis, a theoretical investigation, an experimental study and a mechanistic modeling effort enables a solid and robust evaluation of rumen fermentation and methanogenesis. The theoretical investigation reported in Chapter 3 explores the control of p_{H_2} on rumen fermentation in the light of classical thermodynamic functions, where the *in vivo* results of Chapter 4 provide experimental evidence for hypotheses discussed in Chapter 3. Moreover, experimental results obtained in the experiment are used for parameter estimation in the model development effort reported in Chapter 5. Results from the experiment that comprised a linseed oil dietary treatment may also be used to increase our understanding of the milk FA based CH_4 prediction equations reported in Chapter 2. The data used for developing these equations comprised a substantial number of experiments with lipid treatments.

The integration of concepts of microbial physiology and dairy cattle nutrition is

another strength of this PhD study. Microbial physiologists commonly describe the anaerobic metabolism in a relatively static manner and often use standardized values when quantitatively assessing microbial conversions. For example, thermodynamic feasibility of conversions are assessed using the standardized ΔG^o rather than the more specific ΔG (see section 1.3 for more information about Gibbs energy). In both the theoretical investigation on thermodynamic control of rumen fermentation (Chapter 3) and the mechanistic modeling effort (Chapter 5) the more specific concept is used in a dynamic manner for the range of conditions occurring in the rumen. In Chapter 4, the diurnal dynamics of rumen fermentation have been experimentally assessed. Dynamic approaches are more common in cattle nutrition modeling than in microbial physiology. Compared to mechanistic models reported previously where VFA molar proportions are estimated based on feed composition and rumen pH (Bannink et al., 2011; Gregorini et al., 2013), microbial physiology concepts have decreased the 'degree of empiricism' of the mechanistic model reported in Chapter 5. Some systematic approaches are reported for predicting anaerobic digestion and fermentation of biomass in tank reactors (e.g., Vavilin et al., 2007). These studies often apply steady-state modeling to describe a system. The dynamic modeling approach describing diurnal variation of rumen fermentation (Chapter 5) is, therefore, a rather unique approach.

6.1 Feasibility of predicting CH_4 yield using milk FA concentrations

The suitability for the large scale application is a major motivation for predicting dairy cattle CH_4 emission using milk FA concentrations. Although the potential to predict CH_4 emission based on milk FA concentrations appeared to be moderate (Chapter 2), further exploration of the relationships, including the underlying putative mechanisms is needed. In the meantime, Dijkstra et al. (2016) have evaluated the CH_4 prediction equations reported in Chapter 2 using grass herbage and grass silage based data. They obtained concordance correlation coefficients of 0.13 and 0.22 for CH_4 yield per unit of feed and milk, respectively, and concluded the predicted performance of these equations not to be accurate. This rather weak performance of equations regressed on data that comprised various FA supplemented dietary treatments, on data for grass- and grass silage-based diets is not promising, but does not disprove the applicability of these equations within certain diet categories. Castro-Montoya et al. (2017) reported that milk FA are not yet reliable predictors of specific amounts of CH_4 emitted by a cow, while holding a modest potential to differentiate cases of high or low emissions.

It may therefore be worthwhile to explore the predictive potential of CH_4 emission regression equations for distinct diet categories (Van Gastelen and Dijkstra, 2016).

Regardless of the correlation strength of relationships between CH_4 yield and milk FA concentrations obtained so far, one may reconsider the potential of predicting CH_4 production per group of milk FA, viz., C4:0 to C16:0 even-chain saturated FA that are mostly synthesized *de novo* from acetate and β-hydroxybutyrate in the mammary gland (with also a substantial proportion of C16:0 originating from body fat mobilization and a minor proportion from the diet), odd- and branched-chain fatty acids (OBCFA) originating from microbial FA and possibly rumen odd- and branched-chain VFA, and unsaturated long-chain fatty acids (LCFA) originating from the diet. These three groups of milk FA may reflect the metabolism employed in fermentative micro-organisms, the cell membrane anatomy of fermentative micro-organisms or dietary amino acids fermented in the rumen, or the control of LCFA on the metabolism of fermentative micro-organisms, respectively.

Interestingly, even-chain FA concentrations did not appear in the prediction equation for CH_4 yield per unit of feed, while only C4:0 concentration appeared in the prediction equation for CH_4 yield per unit of milk. Milk C4:0 is the only milk FA that is synthesized *de novo* in the mammary gland and of which its synthesis may not be inhibited by unsaturated LCFA (Bernard et al., 2008). This leaves room for stating that, based on the database used in Chapter 2, *de novo* synthesized milk FA originating from ruminal acetate and butyrate are not clearly associated with enteric CH_4 production. Even-chain FA in milk therefore appeared to have only limited potential to predict CH_4 yield from dairy cows, despite the fact that their precursors, in contrast to OBCFA and LCFA, are end- products of fermentation pathways that yield H_2. This indicates that either the precursors of these FA are not associated with CH_4 yield or even-chain milk FA do not accurately reflect acetate and butyrate production in the rumen in the database, where 5 out of 8 studies comprised FA treatments. In Chapter 4 of this thesis, linseed oil supplementation did not significantly affect H_2 emission and acetate and butyrate molar proportions in the rumen but tended to decrease CH_4 emission. This gives evidence that linseed oil supplementation does not substantially affect fermentation patterns, but tends to affect CH_4 production. In that case no relationship between milk even-chain FA (derived from ruminal acetate and butyrate) concentrations and CH_4 yield may be expected. This also suggests that at the dosage applied in the experiment reported in Chapter 4, and the experiments used for development of the empirical equations reported in Chapter 2, linseed oil inhibits methanogenic archaea more than fermentative micro-organisms. The tendency for increased propionate proportion suggests, however, that the effect of linseed oil on bacteria is not completely negligible.

If linseed oil affects archaea rather than fermentative micro-organisms, significant relationships between milk unsaturated LCFA concentrations and CH_4 may be expected. However, only a tendency for decreased CH_4 production was observed (experiment Chapter 4; absolute decrease of 3.7%), which may explain the relatively weak relationship between enteric CH_4 and the concentration of a milk unsaturated LCFA concentration. Furthermore, the depressive effect of fat on enteric CH_4 emissions varies with the type of forage of the basal diet (Benchaar et al., 2015) and indicates milk unsaturated LCFA concentrations are not in general correlated to enteric CH_4 emissions. The finding that linseed oil supplementation appeared to have only a limited impact on the rumen microbiota composition (Chapter 4) explains why most of the milk OBCFA concentrations did not appear to be correlated to enteric CH_4 yield. It may also explain Dijkstra et al. (2016) the equations reported in Chapter 2 that also comprised C16:0-*iso* did not accurately predict CH_4 yield.

As Dijkstra et al. (2016) showed the prediction equations of Chapter 2 not to perform well for grass and grass-silage-based diets, Van Gastelen and Dijkstra (2016) advocated the development of dietary category specific CH_4 prediction equations. There is, however, still no evidence that this will result in equations with high predictive performance within to be defined specific dietary categories. In addition, our understanding of the relatively bad performance of the equations developed in this thesis, as well as the descriptive identification of metabolic stages between milk FA and rumen metabolites can be largely improved. A way to achieve this may be the identification of blood metabolites originating in the rumen that are candidate precursors of milk FA. Although blood samples are not as easily obtained as milk samples, which may hamper its large scale applicability, many OBCFA and LCFA can be identified in blood (Jacobs et al., 2011; Sterk et al., 2012). Furthermore, if milk FA concentration based CH_4 prediction equations also do not perform well for various diets other than grass- and grass silage-based, it may be worth to investigate the potential for predict enteric CH_4 using blood FA. Blood FA composition is not affected by the *de novo* FA synthesis in the mammary gland, and thus a metabolic step closer to rumen fermentation and might therefore be stronger associated with CH_4 production than milk FA composition.

6.2 Cofactor controlled fermentation dynamics

In this thesis, the control of cofactor NAD on rumen fermentation pathways has been evaluated using a methodology that is in accordance with principles of reaction kinetics and thermodynamics. Main characteristics of the rumen model presented in Chapter 5 are the diurnal dynamics in the feed intake rate input, the representation

of H_2 emission and p_{H_2}, and the redox state of NAD controlling the acetate and propionate formation pathways where the oxidation of NADH is affected by both p_{H_2} and pH. The modeling effort of Chapter 5 may also be relevant for anaerobic digester modeling (e.g., Yu et al., 2013) given the fact that those models often contain many stoichiometric equations instead of a dynamic regulation mechanism.

Modeling of cofactor control has been applied for both anaerobic and aerobic systems. Mosey (1983) presented a cofactor controlled model for laboratory digestion of waste water. Salem et al. (2002) presented a myocardial energy metabolism model that also included the redox state of NAD. Rodríguez et al. (2006) and Zhang et al. (2013) presented a modeling framework based on mixed culture glucose fermentation in a continuously stirred tank reactor under stable environmental conditions. In contrast to the latter two studies, in the model presented in Chapter 5 of this thesis, the H_2 produced is calculated based on the fermentation pathways instead of cofactor regeneration (NAD or ferredoxin (Fd). This is not fundamentally different because H_2 yield and the net NAD reduction are the same with respect to glucose. It might, however, affect the predicted instantaneous microbial activity and metabolite concentrations of the fermentative environment.

Besides the evidence for the NAD^+ to NADH ratio controlling anaerobic fermentation, elevated p_{H_2} was not always found to be correlated with a decreased NAD^+ to NADH ratio. This indicates that NADH oxidation could occur. Therefore, De Kok et al. (2013) suggested that additional electron carriers associated with NADH oxidation, such as Fd and formate, should be included in models predicting product formation by mixed cultures. Regardless of the correctness of this suggestion, the pH in their mixed culture fermentation chemostat study was kept constant at a relatively low value of 5.5, at which NADH oxidation is more thermodynamically favorable. Chapter 3 of this thesis illustrates the thermodynamic feasibility of NADH oxidation at decreased pH and more reduced Fd. Either of these two mechanisms may explain why a decreased NAD^+ to NADH ratio does not occur at increased p_{H_2}.

Ren et al. (1997), observed negligible amounts of propionate, but substantial amounts of ethanol, after increasing the organic loading rate of molasses of the reactor system with pH < 5.5. This study therefore indicates that high p_{H_2} does not in general induce more propionate production, and that ethanol production is also a mechanism to oxidize NADH. Nonetheless, in Chapter 4 of this thesis, ethanol was found to appear in rumen fluid in response to feeding, and was accompanied with the appearance of lactate and an increase in propionate molar proportion at the expense of acetate molar proportion. Hence, multiple mechanisms that stimulate NADH oxidation seem to apply to the rumen environment.

Although the redox state of NAD has been elaborated most in this thesis, various

other mechanism are known to control anaerobic fermentation. Hoelzle et al. (2014) listed various regulatory mechanisms that apply to pure and mixed culture microbial fermentation, including pH and organic loading rate. Butyrate production will not induce the dissociation of more than one proton per equivalent of glucose and has less impact on pH than acetate and propionate production (Hoelzle et al., 2014). It therefore decreases active transport energy expenditure and more energy is then retained in cells, which explains the benefit of butyrate production at low pH in particular. Ions other than protons such as sodium are also used for active transport and it might be questionable whether the decreased energy expenditure applies for all conditions. The increased butyrate production at decreased pH might also contribute to more energy generation than propionate production, as the ATP yield per equivalent of butyrate has been postulated to be up to 4.5 (Hackmann and Firkins, 2015). The energy generation from pyruvate to propionate and butyrate has not been consistently quantified, however. At higher pH-values, butyrate production may still retain more ATP, but at increased pH propionate production can be more favorable as it may result into lower pH due to its yield of acid per amount of glucose, which favors NADH oxidation. If propionate production proceeds via lactate, a stronger acid is formed and NADH oxidation is favored even more, in addition to the net oxidation of NADH associated with this pathway (Table 3.1). Lactate production will, however, result into lower yields of ATP and hence relatively less energy retained in cells.

Besides pH, Hoelzle et al. (2014) listed organic loading rate as a regulatory mechanism of microbial fermentation. The organic loading rate of reactors and mixed cultures, i.e., the influent substrate mass rate per unit of reactor volume, is conceptually similar to feed intake rate to the rumen. In mixed culture studies organic loading rate is often evaluated together with retention time. The reciprocal retention time is called passage rate in ruminant nutrition. From mixed culture studies it appears that an increased organic loading rate and decreased retention time are accompanied with higher VFA production and in some cases with increased lactate and propionate levels (Hoelzle et al., 2014). For the rumen, higher VFA production, increased lactate concentrations and propionate proportions are then expected after feeding (e.g., Counotte and Prins, 1981; Hatew et al., 2015). Observations reported in Chapter 4 of this thesis, indicate that appearance of lactate and increase of propionate molar proportions indeed occurred in response to feeding. In a biohydrogen reactor study (Hafez et al., 2010), shorter retention was associated with a lower H_2 yield per mol of glucose, which was more drastically affected than the absolute H_2 production rate. No putative mechanism was proposed in the biohydrogen reactor study, but Van Ginkel and Logan (2005) also explained this fact via NAD-controlled fermentation. Increased organic loading induces greater p_{H_2} and the microbial

metabolism starts producing more reduced compounds to regenerate NAD^+, which results in a lower H_2 yield per mole of glucose.

In the present thesis, the occurrence of thermodynamic inhibition of NADH oxidation has not been strictly evaluated. Chapter 3 evaluates the thermodynamic feasibility of NADH oxidation given the NADH oxidation mechanisms and metabolite concentrations assumed. Chapter 4 maps the diurnal profile of metabolites that are indicative of the redox state of NAD. From those profiles, it turns out that the appearance of lactate and ethanol, as well as the increase in propionate molar proportion at the expense of acetate molar proportion, follows a substantial increase in p_{H_2}. The modeling effort presented in Chapter 5 simulates rumen fermentation pathways with the redox state of NAD controlling the acetate and propionate formation pathways, with the oxidation of NADH via confurcation being affected by both p_{H_2} and pH. In Chapter 3 and 5, known mechanisms and common metabolite concentrations are used to predict the thermodynamic control on NADH oxidation, while in Chapter 4 extracellular metabolite diurnal profiles indicative for thermodynamically inhibited NADH oxidation have been found. Experimental determination of the microbial intracellular NAD^+ to NADH ratio in response to feed intake and/or metabolic activity may further clarify the physiological mechanisms employed in fermentative microbes.

6.3 General applicability of developed models for quantifying dairy cattle enteric CH_4 emission

The International Panel of Climate Change (IPCC) uses tiered approaches for the quantification of enteric CH_4 from livestock production (Dong et al., 2006). In the Tier 1 approach, the most basic estimate is made by predicting enteric CH_4 emission based on the number of animals within a livestock category (e.g., dairy and/or beef cattle, buffalo, sheep, goats, swine, horses, camels, mules/asses, and poultry) and assuming a fixed CH_4 emission for every category. In the Tier 2 approach, 'enhanced' characterization of animals is needed for a more accurate prediction of enteric CH_4 emission. Such an enhanced characterization comprises animal productivity, diet quality and management circumstances. Prediction of livestock enteric CH_4 emission may tier down to a more complex third category of models. This Tier 3 approach for predicting enteric CH_4 emission from livestock is more potent to identify causes of variation in CH_4 emissions. Tier 2 and Tier 3 are in general recommended to be used for the various subcategories of cattle.

Prediction of dairy cattle CH_4 emission using milk FA concentrations may be an

alternative to the Tier approaches. Milk FA composition may be determined at herd or animal level and may discriminate between cows, groups of cows, herds of cows, or types of farms. Given the inaccuracy of predictions of enteric CH_4 emission from milk FA as established in the evaluation study of Dijkstra et al. (2016), predicting CH_4 emission using feed intake level and feed composition data may be more accurate when a prediction equation is developed for a specific geographical region or continent (e.g., Appuhamy et al., 2016). However, with the aim to predict CH_4 emission at animal or herd level, data on feed intake and feed composition may not be easily obtained and application of milk FA composition based equations would be more convenient. If diet specific CH_4 prediction equations using milk FA concentrations perform well, they may not be less useful than feed intake level- and composition-based equations. Milk FA concentration based CH_4 prediction equations may then be limited to certain diet categories, feed intake level- and composition-based equations to geographical regions.

Although Appuhamy et al. (2016) concluded that enteric CH_4 emissions from dairy cows can be predicted successfully, they also suggested that predictions should be made on a regional rather than global basis. The equations they considered have also not yet been evaluated for tropical conditions, whereas Kouazounde et al. (2015) reported that IPCC Tier 2 estimates of enteric CH_4 from dairy cattle in Benin can be considerably inaccurate and recommended to improve emissions from African cattle. Moreover, Kaewpila and Sommart (2016) who also applied the IPCC Tier 2 approach recommended the development of a specific enteric CH_4 conversion factor model for estimating Zebu beef cattle production in tropical developing countries. The general performance of feed intake level- and composition-based equations has therefore been demonstrated to be limited.

A rather conceptual representation of the anaerobic metabolism in mechanistic models of rumen fermentation (i.e., low degree of empiricism) may identify causes of variation in CH_4 emissions. The mechanistic model presented in Chapter 5 including the parameter uncertainty analysis provides a profound basis for studying the model applicability as a Tier 3 approach. The modeling effort in this thesis has a level of detail far beyond the Tier 3 approach reported by Jo et al. (2016) who empirically estimated CH_4 emission from steers based on feed intake, body weight and average daily gain. The present modeling effort also provides a more conceptual representation of fermentation mechanisms compared to the Tier 3 approach by Bannink et al. (2011). In this approach the prediction of VFA production is based on feed intake, feed composition and feed degradation characteristics in the rumen, where propionate molar proportion increases at decreased pH. In the model discussed in Chapter 5, however, decreased pH stimulates NADH oxidation, which results in a higher NAD^+ to NADH ratio and hence the formation of more acetate and less propionate. Increased

proportions of propionate with decreased pH, as adopted in the Tier approach 3 of Bannink et al. (2011), may also be predicted with the present model in response to elevated p_{H_2} normally caused by increased feed intake. The microbial metabolism will then generate more reduced products such as propionate or lactate, which is a propionate precursor. At increased feed intake, the microbial fermentative activity will also increase and results into a higher VFA concentration which is associated with a drop in pH. The coincidence of a decreased pH and an increased propionate molar proportion is then expected. It is questionable, however, to what extent this difference between the model approaches affects the predicted CH_4 production. An elaborate evaluation of the model presented in Chapter 5 is required to assess its CH_4 prediction accuracy. Nevertheless, the representation of the effects of type and level of feed intake, feed substrate fermentation rate, microbial and archaeal population size and growth rate, p_{H_2}, pH and intracellular NAD^+ to NADH ratio in the Chapter 5 model, provides a solid basis for predicting CH_4 emission rate at a wide range of rumen fermentation conditions.

6.4 General conclusion

The combination of a meta-analysis, a theoretical investigation, an experimental study and a mechanistic modeling effort strengthened the evaluation of the backgrounds of variation in rumen fermentation and methanogenesis. Also, the integration of concepts of microbial physiology and dairy cattle nutrition has strengthened the research presented in this thesis. The potential for predicting enteric CH_4 emission from dairy cattle based on milk FA profile appeared to be moderate, but the general feasibility of predicting CH_4 yield using milk FA concentrations needs to be further assessed. The concept of NAD-controlled fermentation increases the understanding of rumen diurnal dynamics including CH_4. The mechanistic model developed predicts the rumen diurnal dynamics fairly well and provides a profound basis to continue modeling of CH_4 production based on feeding regime, feed composition and feed intake level.

Bibliography

G. Agrimi, L. Brambilla, G. Frascotti, I. Pisano, D. Porro, M. Vai, and L. Palmieri. Deletion or overexpression of mitochondrial NAD^+ carriers in *Saccharomyces cerevisiae* alters cellular NAD and ATP contents and affects mitochondrial metabolism and the rate of glycolysis. *Applied and Environmental Microbiology*, 77:2239–2246, 2011.

A.W. Alemu, J. Dijkstra, A. Bannink, J. France, and E. Kebreab. Rumen stoichiometric models and their contribution and challenges in predicting enteric methane production. *Animal Feed Science and Technology*, 166:761–778, 2011.

M.J. Allison, R.W. Dougherty, J.A. Bucklin, and E.E. Snyder. Ethanol accumulation in the rumen after overfeeding with readily fermentable carbohydrate. *Science*, 144: 54–55, 1964.

K.L. Anderson. Biochemical analysis of starch degradation by *Ruminobacter amylophilus* 70. *Applied and Environmental Microbiology*, 61:1488–1491, 1995.

M.J. Anderson. A new method for non-parametric multivariate analysis of variance. *Austral Ecology*, 26:32–46, 2001.

L.T. Angenent, H. Richter, W. Buckel, C.M. Spirito, K.J.J. Steinbusch, C.M. Plugge, D.P.B.T.B. Strik, T.I.M. Grootscholten, C.J.N. Buisman, and H.V.M. Hamelers. Chain elongation with reactor microbiomes: open-culture biotechnology to produce biochemicals. *Environmental Science & Technology*, 50:2796–2810, 2016.

J.A.D.R.N. Appuhamy, C. Wagner-Riddle, D.P. Casper, J. France, and E. Kebreab. Quantifying body water kinetics and fecal and urinary water output from lactating Holstein dairy cows. *Journal of Dairy Science*, 97:6177–6195, 2014.

J.A.D.R.N. Appuhamy, J. France, and E. Kebreab. Models for predicting enteric methane emissions from dairy cows in North America, Europe, and Australia and New Zealand. *Global Change Biology*, 22:3039–3056, 2016.

J.L. Argyle and R.L. Baldwin. Modeling of rumen water kinetics and effects of rumen pH changes. *Journal of Dairy Science*, 71:1178–1188, 1988.

G.B. Arhonditsis, S.S. Qian, C.A. Stow, E.C. Lamon, and K.H. Reckhow. Eutrophication risk assessment using Bayesian calibration of process-based models: application to a mesotrophic lake. *Ecological Modelling*, 208:215–229, 2007.

N. Asanuma, M. Iwamoto, and T. Hino. Formate metabolism by ruminal microorganisms in relation to methanogenesis. *Animal Science and Technology*, 69:576–584, 1998.

N. Asanuma, M. Iwamoto, and T. Hino. Structure and transcriptional regulation of the gene encoding pyruvate formate-lyase of a ruminal bacterium, *Streptococcus bovis*. *Microbiology*, 145:151–157, 1999.

P. Atkins and J. de Paula. *Atkins' Physical Chemistry, 8th Edition*. Oxford University Press, 2006.

R. L. Baldwin and M. J. Allison. Rumen metabolism. *Journal of Animal Science*, 57: 461–477, 1983.

R.L. Baldwin. *Modeling ruminant digestion and metabolism*. Chapman & Hall, London, 1995.

R.L. Baldwin, W.A. Wood, and R.S. Emery. Conversion of glucose-^{14}C to propionate by the rumen microbiota. *Journal of Bacteriology*, 85:1346–1349, 1963.

R.L. Baldwin, H.L. Lucas, and R. Cabrera. Energetic relationships in the formation and utilization of fermentation end-products. In A. T. Phillipson, E. F. Annison, D. G. Armstrong, C. C. Balch, R. S. Comline, R. S. Hardy, P. N. Hobson, and R. D Keynes, editors, *Physiology of Digestion and Metabolism in the Ruminant*, pages 319–334. Oriel Press Newcastle-upon-Tyne, 1970.

R.L. Baldwin, J.H. Thornley, and D.E. Beever. Digestive elements of a mechanistic model. *Journal of Dairy Research*, 54:107–131, 1987.

A. Bannink, J. Kogut, J. Dijkstra, J. France, E. Kebreab, A.M. Van Vuuren, and S. Tamminga. Estimation of the stoichiometry of volatile fatty acid production in the rumen of lactating cows. *Journal of Theoretical Biology*, 238:36–51, 2006.

A. Bannink, J. France, S. Lopez, W.J.J. Gerrits, E. Kebreab, S. Tamminga, and J. Dijkstra. Modelling the implications of feeding strategy on rumen fermentation and functioning of the rumen wall. *Animal Feed Science and Technology*, 143:3–26, 2008.

A. Bannink, M.C.J. Smits, E. Kebreab, J.A.N. Mills, J.L. Ellis, A. Klop, J. France, and J. Dijkstra. Simulating the effects of grassland management and grass ensiling on methane emission from lactating cows. *Journal of Agricultural Science*, 148: 55–72, 2010.

A. Bannink, M.W. Van Schijndel, and J. Dijkstra. A model of enteric fermentation in dairy cows to estimate methane emission for the Dutch National Inventory Report using the IPCC Tier 3 approach. *Animal Feed Science and Technology*, 166:603–618, 2011.

A. Bannink, H.J. Van Lingen, J.L. Ellis, J. France, and J. Dijkstra. The contribution of mathematical modeling to understanding dynamic aspects of rumen metabolism. *Frontiers in Microbiology*, 7:1820, 2016.

C. Benchaar, J. Rivest, C. Pomar, and J. Chiquette. Prediction of methane production from dairy cows using existing mechanistic models and regression equations. *Journal of Animal Science*, 76:617–627, 1998.

C. Benchaar, F. Hassanat, R. Martineau, and R. Gervais. Linseed oil supplementation to dairy cows fed diets based on red clover silage or corn silage: Effects on methane production, rumen fermentation, nutrient digestibility, N balance, and milk production. *Journal of Dairy Science*, 98:7993–8008, 2015.

H. Berends, W.J.J. Gerrits, J. France, J.L. Ellis, S.M. Van Zijderveld, and J. Dijkstra. Evaluation of the SF_6 tracer technique for estimating methane emission rates with reference to dairy cows using a mechanistic model. *Journal of Theoretical Biology*, 353:1–8, 2014.

L. Bernard, C. Leroux, and Y. Chilliard. Expression and nutritional regulation of lipogenic genes in the ruminant lactating mammary gland. In *Advances in Experimental Medicine and Biology*, volume 606, pages 67–108. Springer New York, 2008.

S.J. Berrios-Rivera, G.N. Bennett, and K.Y. San. The effect of increasing NADH availability on the redistribution of metabolic fluxes in *Escherichia coli* chemostat cultures. *Metabolic Engineering*, 4:230–237, 2002.

K. Beven and A. Binley. The future of distributed models: model calibration and uncertainty prediction. *Hydrological Processes*, 6:279–298, 1992.

H-K. Biesalski. Meat as a component of a healthy diet–are there any risks or benefits if meat is avoided in the diet? *Meat Science*, 70:509–524, 2005.

K.L. Blaxter and J.L. Clapperton. Prediction of the amount of methane produced by ruminants. *British Journal of Nutrition*, 19:511–522, 1965.

C. Boeckaert, B. Vlaeminck, J. Dijkstra, A. Issa-Zacharia, T. Van Nespen, W. Van Straalen, and V. Fievez. Effect of dietary starch or micro algae supplementation on rumen fermentation and milk fatty acid composition of dairy cows. *Journal of Dairy Science*, 91:4714–4727, 2008.

M. Boivin, R. Gervais, and P.Y. Chouinard. Effect of grain and forage fractions of corn silage on milk production and composition in dairy cows. *Animal*, 7:1–10, 2013.

D.R. Boone, R.L. Johnson, and Y. Liu. Diffusion of the interspecies electron carriers H_2 and formate in methanogenic ecosystems and its implications in the measurement of k_m for H_2 or formate uptake. *Applied and Environmental Microbiology*, 55:1735–1741, 1989.

M. Brask, M.R. Weisbjerg, A.L.F. Hellwing, A. Bannink, and P. Lund. Methane production and diurnal variation measured in dairy cows and predicted from fermentation pattern and nutrient or carbon flow. *Animal*, 9:1795–1806, 2015.

R. Brun, P. Reichert, and H.R. Künsch. Practical identifiability analysis of large environmental simulation models. *Water Resources Research*, 37:1015–1030, 2001.

M.P. Bryant and N. Small. Characteristics of two new genera of anaerobic curved rods isolated from the rumen of cattle. *Journal of Bacteriology*, 72:22, 1956.

W. Buckel and R.K. Thauer. Energy conservation via electron bifurcating ferredoxin reduction and proton/Na^+ translocating ferredoxin oxidation. *Biochimica et Biophysica Acta*, 1827:94–113, 2013.

J.G. Caporaso, J. Kuczynski, J. Stombaugh, K. Bittinger, F.D. Bushman, E.K. Costello, N. Fierer, A.G. Pena, J.K. Goodrich, J.I. Gordon, G.A. Huttley, S.T. Kelley, D. Knights, J.E. Koenig, R.E. Ley, C.A. Lozupone, D. McDonald, B.D. Muegge, M. Pirrung, J. Reeder, J.R. Sevinsky, P.J. Turnbaugh, W.A. Walters, J. Widmann, T. Yatsunenko, J. Zaneveld, and R. Knight. QIIME allows analysis of high-throughput community sequencing data. *Nature Methods*, 7:335–336, 2010.

J. Castro Montoya, A.M. Bhagwat, N. Peiren, S. De Campeneere, B. De Baets, and V. Fievez. Relationships between odd-and branched-chain fatty acid profiles in milk and calculated enteric methane proportion for lactating dairy cattle. *Animal Feed Science and Technology*, 166:596–602, 2011.

J.M. Castro-Montoya, N. Peiren, J. Veneman, B. De Baets, S. De Campeneere, and V. Fievez. Predictions of methane emission levels and categories based on milk fatty acid profiles from dairy cows. *Animal*, page In press, 2017.

Y. Chilliard, F. Glasser, A. Ferlay, L. Bernard, J. Rouel, and M. Doreau. Diet, rumen biohydrogenation and nutritional quality of cow and goat milk fat. *European Journal of Lipid Science and Technology*, 109:828–855, 2007.

Y. Chilliard, C. Martin, J. Rouel, and M. Doreau. Milk fatty acids in dairy cows fed whole crude linseed, extruded linseed, or linseed oil, and their relationship with methane output. *Journal of Dairy Science*, 92:5199–5211, 2009.

J.L. Clapperton and J.W. Czerkawski. Methane production and soluble carbohydrates in the rumen of sheep in relation to the time of feeding and the effects of short-term intraruminal infusions of unsaturated fatty acids. *British Journal of Nutrition*, 23: 813–826, 1969.

P.W.H.G. Coenen, C.W.M. van der Maas, P.J. Zijlema, E.J.M.M. Arets, K. Baas, A.C.W.M. Van den Berghe, M.M. Nijkamp, E.P. Van Huis, G. Geilenkirchen, C.W. Versluijs, R. Te Molder, R. Dröge, J.A. Montfoort, C.J. Peek, and J. Vonk. Greenhouse gas emissions in the Netherlands 1990-2014: National Inventory Report 2016. *RIVM rapport 2016-0047*, 2016.

J. Cohen. *Statistical power analysis for the behavioral sciencies, 2nd edition.* Hillsdale, NJ: Lawrence Erlbaum Associates, 1988.

E. Colman, B.M. Tas, W. Waegeman, B. De Baets, and V. Fievez. The logistic curve as a tool to describe the daily ruminal pH pattern and its link with milk fatty acids. *Journal of Dairy Science*, 95:5845–5865, 2012.

A.R. Conn, N.I.M. Gould, and Ph.L. Toint. Convergence of quasi-Newton matrices generated by the symmetric rank one update. *Mathematical Programming*, 50: 177–195, 1991.

G.H.M. Counotte and R.A. Prins. Regulation of lactate metabolism in the rumen. *Veterinary Research Communications*, 5:101–115, 1981.

L.A. Crompton, J.A.N. Mills, and C.K. Reynolds. Effect of feeding frequency and replacing calcium salts of palm oil with crushed rapeseed or coconut oil on methane emissions in lactating dairy cows. *Proceedings of the Nutrition Society*, 69:E329, 2010a.

L.A. Crompton, J.A.N. Mills, C.K. Reynolds, and J. France. Fluctuations in methane emission in response to feeding pattern in lactating dairy cows. In *Modelling nutrient digestion and utilisation in farm animals*, pages 176–180. Wageningen Academic Publishers, 2010b.

L.A. Crompton, J.A.N. Mills, K.E. Kliem, and C.K. Reynolds. Effect of milled rapeseed on methane emissions and milk quality in lactating dairy cows. *Advances in Animal Biosciences*, 2:75, 2011.

J.W. Czerkawski. *An introduction to rumen studies*. Pergamon Press, 1986.

F.A.M. de Bok, A.J.M. Stams, C. Dijkema, and D.R. Boone. Pathway of propionate oxidation by a syntrophic culture of *Smithella propionica* and *Methanospirillum hungatei*. *Applied and Environmental Microbiology*, 67:1800–1804, 2001.

S. De Kok, J. Meijer, M.C.M. van Loosdrecht, and R. Kleerebezem. Impact of dissolved hydrogen partial pressure on mixed culture fermentations. *Applied Microbiology and Biotechnology*, 97:2617–2625, 2013.

K. Dieho, J. Dijkstra, J.T. Schonewille, and A. Bannink. Changes in ruminal volatile fatty acid production and absorption rate during the dry period and early lactation as affected by rate of increase of concentrate allowance. *Journal of Dairy Science*, 99:5370–5384, 2016.

J. Dijkstra, H.D.St.C. Neal, D.E. Beever, and J. France. Simulation of nutrient digestion, absorption and outflow in the rumen: model description. *Journal of Nutrition*, 122:2239–2256, 1992.

J. Dijkstra, H. Boer, J. Van Bruchem, M. Bruining, and S. Tamminga. Absorption of volatile fatty acids from the rumen of lactating dairy cows as influenced by volatile fatty acid concentration, pH and rumen liquid volume. *British Journal of Nutrition*, 69:385–396, 1993.

J. Dijkstra, J. France, H.D.St.C. Neal, A.G. Assis, L.J.M. Aroeira, and O.F. Campos. Simulation of digestion in cattle fed sugarcane: model development. *Journal of Agricultural Science*, 127:231–246, 1996.

J. Dijkstra, E. Kebreab, J.A.N. Mills, W.F. Pellikaan, S. Lopez, A. Bannink, and J. France. Predicting the profile of nutrients available for absorption: from nutrient requirement to animal response and environmental impact. *Animal*, 1:99–111, 2007.

J. Dijkstra, S.M. Van Zijderveld, J.A. Apajalahti, A. Bannink, W.J.J. Gerrits, J.R. Newbold, H.B. Perdok, and H. Berends. Relationships between methane production

and milk fatty acid profiles in dairy cattle. *Animal Feed Science and Technology*, 166:590–595, 2011.

J. Dijkstra, S. Van Gastelen, E.C. Antunes-Fernandes, D. Warner, B. Hatew, G. Klop, S.C. Podesta, H.J. Van Lingen, K.A. Hettinga, and A. Bannink. Relationships between milk fatty acid profiles and enteric methane production in dairy cattle fed grass-or grass silage-based diets. *Animal Production Science*, 56:541–548, 2016.

F. Dohme, A. Machmüller, A. Wasserfallen, and M. Kreuzer. Comparative efficiency of various fats rich in medium-chain fatty acids to suppress ruminal methanogenesis as measured with rusitec. *Canadian Journal of Animal Science*, 80:473–484, 2000.

M.A. Dojka, P. Hugenholtz, S.K. Haack, and N.R. Pace. Microbial diversity in a hydrocarbon-and chlorinated-solvent-contaminated aquifer undergoing intrinsic bioremediation. *Applied and Environmental Microbiology*, 64:3869–3877, 1998.

J. Dolfing. Syntrophic propionate oxidation via butyrate: a novel window of opportunity under methanogenic conditions. *Applied and Environmental Microbiology*, 79:4515–4516, 2013.

H. Dong, J. Mangino, T.A. McAllister, J.L. Hatfield, D.E. Johnson, K.R. Lassey, M. Aperacida de Lima, and A. Romanovskaya. Emissions from livestock and manure management. In *2006 IPCC Guidelines for National Greenhouse Gas Inventories*, volume 4. Intergovernmental Panel on Climate Change, 2006.

A. Dumas, J. Dijkstra, and J. France. Mathematical modelling in animal nutrition: a centenary review. *Journal of Agricultural Science*, 146:123–142, 2008.

S.M. Duval, C.J. Newbold, N.R. McEwan, R.C. Graham, and R.J. Wallace. Effect of a specific blend of essential oils on the colonization of substrates by rumen microorganisms. *Reproductive Nutrition Development*, 44:35, 2004.

J.L. Ellis, E. Kebreab, N.E. Odongo, B.W. McBride, E.K. Okine, and J. France. Prediction of methane production from dairy and beef cattle. *Journal of Dairy Science*, 90:3456–3466, 2007.

J.L. Ellis, J. Dijkstra, E. Kebreab, A. Bannink, N.E. Odongo, B.W. McBride, and J. France. Aspects of rumen microbiology central to mechanistic modelling of methane production in cattle. *Journal of Agricultural Science*, 146:213–233, 2008.

J.L. Ellis, A. Bannink, J. France, E. Kebreab, and J. Dijkstra. Evaluation of enteric methane prediction equations for dairy cows used in whole farm models. *Global Change Biology*, 16:3246–3256, 2010.

P.C. Elwood, J.E. Pickering, D.I. Givens, and J.E. Gallacher. The consumption of milk and dairy foods and the incidence of vascular disease and diabetes: an overview of the evidence. *Lipids*, 45:925–939, 2010.

T. Fenchel and B.J. Finlay. Free-living protozoa with endosymbiotic methanogens. In J. Fagerberg, D.C. Mowery, and R.R. Nelson, editors, *(Endo) symbiotic Methanogenic Archaea*, pages 1–11. Springer Berlin Heidelberg, 2010.

V. Fievez, E. Colman, J.M. Castro-Montoya, I. Stefanov, and B. Vlaeminck. Milk odd-and branched-chain fatty acids as biomarkers of rumen function - an update. *Animal Feed Science and Technology*, 172:51–65, 2012.

M.A. Fischbach and J.L. Sonnenburg. Eating for two: how metabolism establishes interspecies interactions in the gut. *Cell host & Microbe*, 10:336–347, 2011.

R.A. Fisher. On the "probable error" of a coefficient of correlation deduced from a small sample. *Metron*, 1:1–32, 1921.

P. Forster, V. Ramaswamy, P. Artaxo, T. Berntsen, R. Betts, D.W. Fahey, J. Haywood, J. Lean, D.C. Lowe, G. Myhre, J. Nganga, R. Prinn, G. Raga, M. Schulz, and R. Van Dorland. Changes in atmospheric constituents and in radiative forcing. *Climate Change 2007: The Physical Science Basis. Contribution of Working Group I to the Fourth Assessment Report of the Intergovernmental Panel of Climate Change*, 20, 2007.

E.A. French, S.J. Bertics, and L.E. Armentano. Rumen and milk odd-and branched-chain fatty acid proportions are minimally influenced by ruminal volatile fatty acid infusions. *Journal of Dairy Science*, 95:2015–2026, 2012.

E.J. Gagen, Stuart E. Denman, J. Padmanabha, S. Zadbuke, R. Al Jassim, M. Morrison, and C.S. McSweeney. Functional gene analysis suggests different acetogen populations in the bovine rumen and tammar wallaby forestomach. *Applied and Environmental Microbiology*, 76:7785–7795, 2010.

P.J. Gerber, H. Steinfeld, B. Henderson, A. Mottet, C. Opio, J. Dijkman, A. Falcucci, and G. Tempio. *Tackling climate change through livestock: a global assessment of emissions and mitigation opportunities.* Food and Agriculture Organization of the United Nations (FAO), Rome, 2013.

P.J. Gerber, A. Mottet, C.I. Opio, A. Falcucci, and F. Teillard. Environmental impacts of beef production: Review of challenges and perspectives for durability. *Meat Science*, 109:2–12, 2015.

S. Ghimire, P. Gregorini, and M.D. Hanigan. Evaluation of predictions of volatile fatty acid production rates by the Molly cow model. *Journal of Dairy Science*, 97: 354–362, 2014.

T.L. Glass, M.P. Bryant, and M.J. Wolin. Partial purification of ferredoxin from *Ruminococcus albus* and its role in pyruvate metabolism and reduction of nicotinamide adenine dinucleotide by H_2. *Journal of Bacteriology*, 131:463–472, 1977.

F. Glasser, P. Schmidely, D. Sauvant, and M. Doreau. Digestion of fatty acids in ruminants: a meta-analysis of flows and variation factors. 2. C18 fatty acids. *Animal*, 2:691–704, 2008.

D.H. Gould, B.A. Cummings, and D.W. Hamar. *In vivo* indicators of pathologic ruminal sulfide production in steers with diet-induced polioencephalomalacia. *Journal of Veterinary Diagnostic Investigation*, 9:72–76, 1997.

C. Grainger and K.A. Beauchemin. Can enteric methane emissions from ruminants be lowered without lowering their production? *Animal Feed Science and Technology*, 166:308–320, 2011.

P. Gregorini, P.C. Beukes, M.D. Hanigan, G. Waghorn, S. Muetzel, and J.P. McNamara. Comparison of updates to the Molly cow model to predict methane production from dairy cows fed pasture. *Journal of Dairy Science*, 96:5046–5052, 2013.

K.E. Griswold, W.H. Hoover, T.K. Miller, and W.V. Thayne. Effect of form of nitrogen on growth of ruminal microbes in continuous culture. *Journal of Animal Science*, 74:483–491, 1996.

J.F. Gross, H.A. van Dorland, R.M. Bruckmaier, and F.J. Schwarz. Milk fatty acid profile related to energy balance in dairy cows. *Journal of Dairy Research*, 78: 479–488, 2011.

T.J. Hackmann and J.L. Firkins. Electron transport phosphorylation in rumen Butyrivibrios: unprecedented ATP yield for glucose fermentation to butyrate. *Frontiers in Microbiology*, 6:622, 2015.

H. Hafez, M.H.El. Naggar, and G. Nakhla. Steady-state and dynamic modeling of biohydrogen production in an integrated biohydrogen reactor clarifier system. *International Journal of Hydrogen Energy*, 35:6634–6645, 2010.

K.J. Hammond, L.A. Crompton, A. Bannink, J. Dijkstra, D.R. Yáñez-Ruiz, P. O'Kiely, E. Kebreab, M.A. Eugenè, Z. Yu, K.J. Shingfield, A. Schwarm, A.N. Hristov, and C.K. Reynolds. Review of current *in vivo* measurement techniques for quantifying enteric methane emission from ruminants. *Animal Feed Science and Technology*, 219:13–30, 2016.

B. Hatew, S.C. Podesta, H. Van Laar, W.F. Pellikaan, J.L. Ellis, J. Dijkstra, and A. Bannink. Effects of dietary starch content and rate of fermentation on methane production in lactating dairy cows. *Journal of Dairy Science*, 98:486–499, 2015.

J.M.L. Heck, H.J. van Valenberg, H. Bovenhuis, J. Dijkstra, and T.C. van Hooijdonk. Characterization of milk fatty acids based on genetic and herd parameters. *Journal of Dairy Research*, 79:39–46, 2012.

L.V. Hedges and I. Olkin. *Statistical methods for meta-analysis*. Orlando, FL: Academic Press, 1985.

R.S. Hegarty. Reducing rumen methane emissions through elimination of rumen protozoa. *Crop and Pasture Science*, 50:1321–1328, 1999.

R.S. Hegarty and R. Gerdes. Hydrogen production and transfer in the rumen. *Recent Advances in Animal Nutrition in Australia*, 12:37–44, 1999.

G. Henderson, F. Cox, S. Ganesh, A. Jonker, W. Young, Global Rumen Census Collaborators, and P.H. Janssen. Rumen microbial community composition varies with diet and host, but a core microbiome is found across a wide geographical range. *Scientific Reports*, 5:14567, 2015.

J.P.T. Higgins, S.G. Thompson, J.J. Deeks, and D.G. Altman. Measuring inconsistency in meta-analyses. *British Medical Journal*, 327:557–560, 2003.

T. Hino and J.B. Russell. Effect of reducing-equivalent disposal and NADH/NAD on deamination of amino acids by intact rumen microorganisms and their cell extracts. *Applied and Environmental Microbiology*, 50:1368–1374, 1985.

R.D. Hoelzle, B. Virdis, and D.J. Batstone. Regulation mechanisms in mixed and pure culture microbial fermentation. *Biotechnology and Bioengineering*, 111:2139–2154, 2014.

A.E.M. Hofmeister and W. Buckel. (R)-Lactyl-CoA dehydratase from *Clostridium propionicum*. *European Journal of Biochemistry*, 206, 1992.

T. Hothorn, F. Bretz, and P. Westfall. Simultaneous inference in general parametric models. *Biometrical Journal*, 50:346–363, 2008.

A.N. Hristov, J. Oh, J.L. Firkins, J. Dijkstra, E. Kebreab, G. Waghorn, H.P.S. Makkar, A.T. Adesogan, W. Yang, C. Lee, P.J. Gerber, B. Henderson, and J.M. Tricarico. Mitigation of methane and nitrous oxide emissions from animal operations: I. A review of enteric methane mitigation options. *Journal of Animal Science*, 91:5045–5069, 2013a.

A.N. Hristov, J. Oh, C. Lee, R. Meinen, F. Montes, T. Ott, J. Firkins, A. Rotz, C. Dell, A. Adesogan, W. Yang, J. Tricarico, E. Kebreab, G. Waghorn, J. Dijkstra, and S. Oosting. Mitigation of greenhouse gas emissions in livestock production. a review of technical options for non-CO_2 emissions. FAO Animal Production and Health Paper No. 177. FAO, Rome, Italy., 2013b.

A.N. Hristov, T. Ott, J. Tricarico, A. Rotz, G. Waghorn, A. Adesogan, J. Dijkstra, F. Montes, J. Oh, E. Kebreab, S.J. Oosting, P.J. Gerber, B. Henderson, H.P.S. Makkar, and J.L. Firkins. Mitigation of methane and nitrous oxide emissions from animal operations: III. A review of animal management mitigation options. *Journal of Animal Science*, 91:5095–5113, 2013c.

P. Huhtanen, M. Ramin, and P. Udén. Nordic dairy cow model Karoline in predicting methane emissions: 1. Model description and sensitivity analysis. *Livestock Science*, 178:71–80, 2015.

R.E. Hungate. Chapter 2, The rumen and its microbes. In *The Rumen and its Microbes.*, pages 8–90. Academic Press, Inc., New York: London, 1966.

P.J. Huth, D.B. DiRienzo, and G.D. Miller. Major scientific advances with dairy foods in nutrition and health. *Journal of Dairy Science*, 89:1207–1221, 2006.

S.A. Huws, J.E. Edwards, C.J. Creevey, P.R. Stevens, W. Lin, S.E. Girdwood, J.A. Pachebat, and A.H. Kingston-Smith. Temporal dynamics of the metabolically active rumen bacteria colonizing fresh perennial ryegrass. *FEMS Microbiology Ecology*, 92:fiv137, 2016.

ISO 1735. *Animal Feeding Stuffs. Determination of Fat Content.* International Organization for Standardization, Geneva, Switzerland, 2004.

B.E. Jackson and M.J. McInerney. Anaerobic microbial metabolism can proceed close to thermodynamic limits. *Nature*, 415:454–456, 2002.

A.A.A. Jacobs, J. Van Baal, M.A. Smits, H.Z.H. Taweel, W.H. Hendriks, A.M. Van Vuuren, and J. Dijkstra. Effects of feeding rapeseed oil, soybean oil, or linseed oil on stearoyl-CoA desaturase expression in the mammary gland of dairy cows. *Journal of Dairy Science*, 94:874–887, 2011.

M.J.W. Jansen, W.A.H. Rossing, and R.A. Daamen. Monte Carlo estimation of uncertainty contributions from several independent multivariate sources. In J. Grasman and G. Van Straten, editors, *Predictability and Nonlinear Modelling in Natural Sciences and Economics*, pages 334–343. Springer Netherlands, 1994.

P.H. Janssen. Influence of hydrogen on rumen methane formation and fermentation balances through microbial growth kinetics and fermentation thermodynamics. *Animal Feed Science and Technology*, 160:1–22, 2010.

P.H. Janssen and M. Kirs. Structure of the archaeal community of the rumen. *Applied and Environmental Microbiology*, 74:3619–3625, 2008.

R.G. Jensen. The composition of bovine milk lipids: January 1995 to december 2000. *Journal of Dairy Science*, 85:295–350, 2002.

Q. Jin and C.M. Bethke. The thermodynamics and kinetics of microbial metabolism. *American Journal of Science*, 307:643–677, 2007.

N. Jo, J. Kim, and S. Seo. Comparison of models for estimating methane emission factor for enteric fermentation of growing-finishing Hanwoo steers. *SpringerPlus*, 5: 1212, 2016.

K.A. Johnson, R.L. Kincaid, H.H. Westberg, C.T. Gaskins, B.K. Lamb, and J.D. Cronrath. The effect of oilseeds in diets of lactating cows on milk production and methane emissions. *Journal of Dairy Science*, 85:1509–1515, 2002.

D.L. Jones. *The Fathom Toolbox for MATLAB: software for multivariate ecological and oceanographic data analysis.* College of Marine Science, University of South Florida, St. Petersburg, FL, USA, 2015. URL `http://www.marine.usf.edu/user/djones/`.

J.P. Jouany, B. Lassalas, M. Doreau, and F. Glasser. Dynamic features of the rumen metabolism of linoleic acid, linolenic acid and linseed oil measured in vitro. *Lipids*, 42:351–360, 2007.

C. Kaewpila and K. Sommart. Development of methane conversion factor models for Zebu beef cattle fed low-quality crop residues and by-products in tropical regions. *Ecology and Evolution*, 6:7422–7432, 2016.

F. Karadagli and B.E. Rittmann. Kinetic characterization of *Methanobacterium bryantii* M.o.H. *Environmental Science & Technology*, 39:4900–4905, 2005.

H. Kettle, P. Louis, G. Holtrop, S.H. Duncan, and H.J. Flint. Modelling the emergent dynamics and major metabolites of the human colonic microbiota. *Environmental Microbiology*, 17:1615–1630, 2015.

S. Kittelmann, H. Seedorf, W.A. Walters, J.C. Clemente, R. Knight, J.I. Gordon, and P.H. Janssen. Simultaneous amplicon sequencing to explore co-occurrence patterns of bacterial, archaeal and eukaryotic microorganisms in rumen microbial communities. *PloS ONE*, 8:e47879, 2013.

R. Kleerebezem, J. Rodriguez, M.F. Temudo, and M.C.M. van Loosdrecht. Modeling mixed culture fermentations; the role of different electron carriers. *Water Science and Technology*, 57:493–498, 2008.

K.E. Kliem, R. Morgan, D.J. Humphries, K.J. Shingfield, and D.I. Givens. Effect of replacing grass silage with maize silage in the diet on bovine milk fatty acid composition. *Animal*, 2:1850–1858, 2008.

K.E. Kliem, P.C. Aikman, D.J. Humphries, R. Morgan, K.J. Shingfield, and D.I. Givens. Effect of replacing calcium salts of palm oil distillate with extruded linseeds on milk fatty acid composition in Jersey and Holstein cows. *Animal*, 3:1754–1762, 2009.

G. Klop, S. Van Laar-van Schuppen, W.F. Pellikaan, W.H. Hendriks, A. Bannink, and J. Dijkstra. Changes in *in vitro* gas and methane production from rumen fluid from dairy cows during adaptation to feed additives in vivo. *Animal*, 2017.

J.R. Knapp, G.L. Laur, P.A. Vadas, W.P. Weiss, and J.M. Tricarico. Invited review: Enteric methane in dairy cattle production: Quantifying the opportunities and impact of reducing emissions. *Journal of Dairy Science*, 97:3231–3261, 2014.

R.A. Kohn and T.F. Dunlap. Calculation of the buffering capacity of bicarbonate in the rumen and *in vitro*. *Journal of Animal Science*, 76:1702–1709, 1998.

J. Kopečnỳ, M. Zorec, J. Mrazek, Y. Kobayashi, and R. Marinšek-Logar. *Butyrivibrio hungatei* sp. nov. and *Pseudobutyrivibrio xylanivorans* sp. nov., butyrate-producing bacteria from the rumen. *International Journal of Systematic and Evolutionary Microbiology*, 53:201–209, 2003.

J.B. Kouazounde, J.D. Gbenou, S. Babatounde, N. Srivastava, S.H. Eggleston, C. Antwi, J. Baah, and T.A. McAllister. Development of methane emission factors for enteric fermentation in cattle from benin using IPCC Tier 2 methodology. *Animal*, 9:526–533, 2015.

J.T. Kraemer and D.M. Bagley. Supersaturation of dissolved H_2 and CO_2 during fermentative hydrogen production with N_2 sparging. *Biotechnology Letters*, 28: 1485–1491, 2006.

M. Kriss. Quantitative relations of the dry matter of the food consumed, the heat production, the gaseous outgo, and the insensible loss in body weight of cattle. *Journal of Agricultural Research*, 40:283–295, 1930.

H.J. Laanbroek, T. Abee, and I.L. Voogd. Alcohol conversion by desulfobulbus propionicus lindhorst in the presence and absence of sulfate and hydrogen. *Archives of Microbiology*, 133:178–184, 1982.

D.J. Lane. 16S/23S rRNA sequencing. *Nucleic Acid Techniques in Bacterial Systematics*, pages 125–175, 1991.

K. Lang, J. Schuldes, A. Klingl, A. Poehlein, R. Daniel, and A. Brune. New mode of energy metabolism in the seventh order of methanogens as revealed by comparative genome analysis of "candidatus methanoplasma termitum". *Applied and Environmental Microbiology*, 81:1338–1352, 2015.

T.D. Le Van, J.A. Robinson, J. Ralph, R.C. Greening, W.J. Smolenski, J.A.Z. Leedle, and D.M. Schaefer. Assessment of reductive acetogenesis with indigenous ruminal bacterium populations and acetitomaculum ruminis. *Applied and Environmental Microbiology*, 64:3429–3436, 1998.

J.A. Leedle, M.P. Bryant, and R.B. Hespell. Diurnal variations in bacterial numbers and fluid parameters in ruminal contents of animals fed low-or high-forage diets. *Applied and Environmental Microbiology*, 44:402–412, 1982.

J.A.Z. Leedle, K. Barsuhn, and R.B. Hespell. Postprandial trends in estimated ruminal digesta polysaccharides and their relation to changes in bacterial groups and ruminal fluid characteristics. *Journal of Animal Science*, 62:789–803, 1986.

R.A. Leng. Interactions between microbial consortia in biofilms: a paradigm shift in rumen microbial ecology and enteric methane mitigation. *Animal Production Science*, 54:519–543, 2014.

X.Z. Li, B.K. Park, J.S. Shin, S.H. Choi, S.B. Smith, and C.G. Yan. Effects of dietary linseed oil and propionate precursors on ruminal microbial community, composition, and diversity in yanbian yellow cattle. *PloS ONE*, 10:e0126473, 2015.

Y. Liu, D.L. Balkwill, H.C. Aldrich, G.R. Drake, and D.R. Boone. Characterization of the anaerobic propionate-degrading syntrophs *Smithella propionica* gen. nov., sp.

nov. and *Syntrophobacter wolinii*. *International Journal of Systematic Bacteriology*, 49:545–556, 1999.

K.M. Livingstone, D.J. Humphries, P. Kirton, K.E. Kliem, D.I. Givens, and C.K. Reynolds. Effects of forage type and extruded linseed supplementation on methane production and milk fatty acid composition of lactating dairy cows. *Journal of Dairy Science*, 98:4000–4011, 2015.

J.J. Loor, K. Ueda, A. Ferlay, Y. Chilliard, and M. Doreau. Biohydrogenation, duodenal flow, and intestinal digestibility of trans fatty acids and conjugated linoleic acids in response to dietary forage: Concentrate ratio and linseed oil in dairy cows. *Journal of Dairy Science*, 87:2472–2485, 2004.

P. Louis and H.J. Flint. Diversity, metabolism and microbial ecology of butyrate-producing bacteria from the human large intestine. *FEMS Microbiology Letters*, 294:1–8, 2009.

M. Lourenço, E. Ramos-Morales, and R.J. Wallace. The role of microbes in rumen lipolysis and biohydrogenation and their manipulation. *Animal*, 4:1008–1023, 2010.

M.R.G. Maia, L.C. Chaudhary, L. Figueres, and R.J. Wallace. Metabolism of polyunsaturated fatty acids and their toxicity to the microflora of the rumen. *Antonie van Leeuwenhoek*, 91:303–314, 2007.

M. Manes, L.J.E. Hofer, and S. Weller. Classical thermodynamics and reaction rates close to equilibrium. *The Journal of Chemical Physics*, 18:1355–1361, 1950.

M. Marounek, K. Fliegrova, and S. Bartos. Metabolism and some characteristics of ruminal strains of *Megasphaera elsdenii*. *Applied and Environmental Microbiology*, 55:1570–1573, 1989.

C. Martin, E. Devillard, and B. Michalet-Doreau. Influence of sampling site on concentrations and carbohydrate-degrading enzyme activities of protozoa and bacteria in the rumen. *Journal of Animal Science*, 77:979–987, 1999.

C. Martin, A. Ferlay, P. Mosoni, Y. Rochette, Y. Chilliard, and M. Doreau. Increasing linseed supply in dairy cow diets based on hay or corn silage: Effect on enteric methane emission, rumen microbial fermentation, and digestion. *Journal of Dairy Science*, 99:3445–3456, 2016.

T.A. McAllister, H.D. Bae, G.A. Jones, and K.J. Cheng. Microbial attachment and feed digestion in the rumen. *Journal of Animal Science*, 72:3004–3018, 1994.

M.J. McInerney, C.G. Struchtemeyer, J. Sieber, H. Mouttaki, A.J.M. Stams, B. Schink, L. Rohlin, and R.P. Gunsalus. Physiology, ecology, phylogeny, and genomics of microorganisms capable of syntrophic metabolism. *Annals of the New York Academy of Sciences*, 1125:58–72, 2008.

C.S. McSweeney, R.I. Mackie, and B.A. White. Transport and intracellular metabolism of major feed compounds by ruminal bacteria: the potential for metabolic manipulation. *Australian Journal of Agricultural Research*, 45:731–756, 1994.

R.R. Meier, I.H. Kwon, I.K. Cann, and R.I. Mackie. Interspecies hydrogen transfer and its effects on global transcript abundance in *Ruminococcus albus*, a predominant fiber-degrading species in the rumen.

S.B. Melville, T.A. Michel, and J.M. Macy. Pathway and sites for energy conservation in the metabolism of glucose by *Selenomonas ruminantium*. *Journal of Bacteriology*, 170:5298–5304, 1988.

T.A. Michel and J.M. Macy. Purification of an enzyme responsible for acetate formation from acetyl coenzyme A in *Selenomonas ruminatium*. *FEMS Microbiology Letters*, 68:189–194, 1990.

T.L. Miller. The pathway of formation of acetate and succinate from pyruvate by *Bacteroides succinogenes*. *Archives of Microbiology*, 117:145–152, 1978.

T.L. Miller and S.E. Jenesel. Enzymology of butyrate formation by *Butyrivibrio fibrisolvens*. *Journal of Bacteriology*, 138:99–104, 1979.

J.A.N. Mills, J. Dijkstra, A. Bannink, S.B. Cammell, E. Kebreab, and J. France. A mechanistic model of whole-tract digestion and methanogenesis in the lactating dairy cow: model development, evaluation, and application. *Journal of Animal Science*, 79:1584–1597, 2001.

J.A.N. Mills, E. Kebreab, C.M. Yates, L.A. Crompton, S.B. Cammell, M.S. Dhanoa, R.E. Agnew, and J. France. Alternative approaches to predicting methane emissions from dairy cows. *Journal of Animal Science*, 81:3141–3150, 2003.

P.J. Moate, T. Clarke, L.H. Davis, and R.H. Laby. Rumen gases and bloat in grazing dairy cows. *Journal of Agricultural Science*, 129:459–469, 1997.

P.W. Moe and H.F. Tyrrell. Methane production in dairy cows. *Journal of Dairy Science*, 62:1583–1586, 1979.

R. Mohammed, S.M. McGinn, and K.A. Beauchemin. Prediction of enteric methane output from milk fatty acid concentrations and rumen fermentation parameters in dairy cows fed sunflower, flax, or canola seeds. *Journal of Dairy Science*, 94: 6057–6068, 2011.

F. Montes, R. Meinen, C. Dell, A. Rotz, A.N. Hristov, J. Oh, G. Waghorn, P.J. Gerber, B. Henderson, H.P.S. Makkar, and Dijkstra J. Mitigation of methane and nitrous oxide emissions from animal operations: II. A review of manure management mitigation options. *Journal of Animal Science*, 91:5070–5094, 2013.

L.E. Moraes, A.B. Strathe, J.G. Fadel, D.P. Casper, and E. Kebreab. Prediction of enteric methane emissions from cattle. *Global Change Biology*, 20:2140–2148, 2014.

D.P. Morgavi, E. Forano, C. Martin, and C.J. Newbold. Microbial ecosystem and methanogenesis in ruminants. *Animal*, 4:1024–1036, 2010.

Y. Morvay, A. Bannink, J. France, E. Kebreab, and J. Dijkstra. Evaluation of models to predict the stoichiometry of volatile fatty acid profiles in rumen fluid of lactating holstein cows. *Journal of Dairy Science*, 94:3063–3080, 2011.

F.E. Mosey. Mathematical modelling of the anaerobic digestion process: regulatory mechanisms for the formation of short-chain volatile acids from glucose. *Water Science and Technology*, 15:209–232, 1983.

V. Müller. *Bacterial Fermentation.* In: Encyclopedia of Life Sciences. John Wiley & Sons Ltd, Chichester, 2008.

M.R. Murphy, R.L. Baldwin, and L.J. Koong. Estimation of stoichiometric parameters for rumen fermentation of roughage and concentrate diets. *Journal of Animal Science*, 55:411–421, 1982.

G. Myhre, D. Shindell, F.-M. Bréon, W. Collins, J. Fuglestvedt, J. Huang, D. Koch, J.-F. Lamarque, D. Lee, B. Mendoza, T. Nakajima, A. Robock, G. Stephens, T. Takemura, Zhang, and H. Anthropogenic and natural radiative forcing. In *Climate Change 2013: The Physical Science Basis. Contribution of Working Group I to the Fifth Assessment Report of the Intergovernmental Panel on Climate Change*. Cambridge University Press, 2013.

H.D.St.C. Neal, J. Dijkstra, and M. Gill. Simulation of nutrient digestion, absorption and outflow in the rumen: model evaluation. *Journal of Nutrition*, 122:2257–2272, 1992.

C.J. Newbold, G. de la Fuente, A. Belanche, E. Ramos-Morales, and N.R. McEwan. The role of ciliate protozoa in the rumen. *Frontiers in Microbiology*, 6:1313, 2015.

P. Nozière, I. Ortigues-Marty, C. Loncke, and D. Sauvant. Carbohydrate quantitative digestion and absorption in ruminants: from feed starch and fibre to nutrients available for tissues. *Animal*, 4:1057–1074, 2010.

P. Nozière, F. Glasser, and D. Sauvant. *In vivo* production and molar percentages of volatile fatty acids in the rumen: a quantitative review by an empirical approach. *Animal*, 5:403–414, 2011.

M. Oba. Review: Effects of feeding sugars on productivity of lactating dairy cows. *Canadian Journal of Animal Science*, 91:37–46, 2011.

N.E. Odongo, M.M. Or-Rashid, E. Kebreab, J. France, and B.W. McBride. Effect of supplementing myristic acid in dairy cow rations on ruminal methanogenesis and fatty acid profile in milk. *Journal of Dairy Science*, 90:1851–1858, 2007.

A. Offner and D. Sauvant. Thermodynamic modeling of ruminal fermentations. *Animal Research*, 55:343–365, 2006.

D.W. Olijhoek, A.L.F. Hellwing, M. Brask, M.R. Weisbjerg, O. Højberg, M.K. Larsen, J. Dijkstra, E.J. Erlandsen, and P. Lund. Effect of dietary nitrate level on enteric methane production, hydrogen emission, rumen fermentation, and nutrient digestibility in dairy cows. *Journal of Dairy Science*, 99:6191–6205, 2016.

M. Patel, E. Wredle, and J. Bertilsson. Effect of dietary proportion of grass silage on milk fat with emphasis on odd-and branched-chain fatty acids in dairy cows. *Journal of Dairy Science*, 96:390–397, 2013.

A.K. Patra. The effect of dietary fats on methane emissions, and its other effects on digestibility, rumen fermentation and lactation performance in cattle: A meta-analysis. *Livestock Science*, 155:244–254, 2013.

S.G. Pavlostathis, T.L. Miller, and M.J. Wolin. Cellulose fermentation by continuous cultures of *Ruminococcus albus* and *Methanobrevibacter smithii. Applied Microbiology and Biotechnology*, 33:109–116, 1990.

J.W. Peters, G.J. Schut, E.S. Boyd, D.W. Mulder, E.M. Shepard, J.B. Broderick, P.W. King, and M.W.W. Adams. [FeFe]-and [NiFe]-hydrogenase diversity, mechanism, and maturation. *Biochimica et Biophysica Acta*, 1853:1350–1369, 2015.

L. Petzold. Automatic selection of methods for solving stiff and nonstiff systems of ordinary differential equations. *SIAM Journal on Scientific and Statistical Computing*, 4:136–148, 1983.

J. Pinheiro and D. Bates. *Mixed-effects models in S and S-PLUS*. Springer Verlag New York, Inc., 2000.

L.S. Piperova, B.B. Teter, I. Bruckental, J. Sampugna, S.E. Mills, M.P. Yurawecz, J. Fritsche, K. Ku, and R.A. Erdman. Mammary lipogenic enzyme activity, trans fatty acids and conjugated linoleic acids are altered in lactating dairy cows fed a milk fat–depressing diet. *Journal of Nutrition*, 130:2568–2574, 2000.

A. Popp, H. Lotze-Campen, and B. Bodirsky. Food consumption, diet shifts and associated non-CO_2 greenhouse gases from agricultural production. *Global Environmental Change*, 20:451–462, 2010.

S.E. Pryde, S.H. Duncan, G.L. Hold, C.S. Stewart, and H.J. Flint. The microbiology of butyrate formation in the human colon. *FEMS Microbiology Letters*, 217:133–139, 2002.

C. Quast, E. Pruesse, P. Yilmaz, J. Gerken, T. Schweer, P. Yarza, J. Peplies, and F.O. Glöckner. The SILVA ribosomal RNA gene database project: improved data processing and web-based tools. *Nucleic Acids Research*, 41:D590–D596, 2013.

R Core Team. *R: A Language and Environment for Statistical Computing*. R Foundation for Statistical Computing, Vienna, Austria, 2016. URL `https://www.R-project.org/`.

M. Ramin and G.B. Arhonditsis. Bayesian calibration of mathematical models: Optimization of model structure and examination of the role of process error covariance. *Ecological Informatics*, 18:107–116, 2013.

M. Ramin and P. Huhtanen. Nordic dairy cow model Karoline in predicting methane emissions: 2. Model evaluation. *Livestock Science*, 178:81–93, 2015.

J. Ramiro-Garcia, G.D.A. Hermes, C. Giatsis, D. Sipkema, E.G. Zoetendal, P.J. Schaap, and H. Smidt. NG-tax, a highly accurate and validated pipeline for analysis of 16S rRNA amplicons from complex biomes. *F1000Research*, 5:1791, 2016.

K.F. Reed, G.B. Arhonditsis, J. France, and E. Kebreab. Technical note: Bayesian calibration of dynamic ruminant nutrition models. *Journal of Dairy Science*, 99: 6362–6370, 2016.

A.E. Relling, L.A. Crompton, S.C. Loerch, and C.K. Reynolds. Short communication: Plasma concentration of glucose-dependent insulinotropic polypeptide may regulate milk energy production in lactating dairy cows. *Journal of Dairy Science*, 97: 2440–2443, 2014.

N. Ren, B. Wang, and J.C. Huang. Ethanol-type fermentation from carbohydrate in high rate acidogenic reactor. *Biotechnology and Bioengineering*, 54:428–433, 1997.

C. K. Reynolds, D.J. Humphries, P. Kirton, L.A. Crompton, J.A.N. Mills, and D.I. Givens. Methane production by lactating dairy cows fed diets containing allicin, glycerol or naked oats. In *Proceedings of the 4th International Greenhouse Gases Animal Agriculture Conference, Banff, Canada*, page 120, 2010.

C.K. Reynolds, D.J. Humphries, P. Kirton, M. Kindermann, S. Duval, and W. Steinberg. Effects of 3-nitrooxypropanol on methane emission, digestion, and energy and nitrogen balance of lactating dairy cows. *Journal of Dairy Science*, 97: 3777–3789, 2014.

J. Rodríguez, R. Kleerebezem, J.M. Lema, and M.C.M. van Loosdrecht. Modeling product formation in anaerobic mixed culture fermentations. *Biotechnology and Bioengineering*, 93:592–606, 2006.

M. Rogosa. Transfer of *Peptostreptococcus elsdenii* Gutierrez et al. to a new genus, *Megasphaera* [*M. elsdenii* (Gutierrez et al.) comb. nov.]. *International Journal of Systematic Bacteriology*, 21:187–189, 1971.

J.A. Rooke, R.J. Wallace, C.A. Duthie, N. McKain, S.M. de Souza, J.J. Hyslop, D.W. Ross, T. Waterhouse, and R. Roehe. Hydrogen and methane emissions from beef cattle and their rumen microbial community vary with diet, time after feeding and genotype. *British Journal of Nutrition*, 112:398–407, 2014.

J.B. Russell. Effect of extracellular pH on growth and proton motive force of *Bacteroides succinogenes*, a cellulolytic ruminal bacterium. *Applied and Environmental Microbiology*, 53:2379–2383, 1987.

J.B. Russell and R.L. Baldwin. Substrate preferences in rumen bacteria: evidence of catabolite regulatory mechanisms. *Applied and Environmental Microbiology*, 36: 319–329, 1978.

J.B. Russell and R.J. Wallace. Energy-yielding and energy-consuming reactions. In P.N. Hobson and C.S. Stewart, editors, *The Rumen Microbial Ecosystem*, pages 246–282. Blackie Academic & Professional, London, 1997.

M.J.M. Rutten, H. Bovenhuis, K.A. Hettinga, H.J.F. van Valenberg, and J.A.M. Van Arendonk. Predicting bovine milk fat composition using infrared spectroscopy based on milk samples collected in winter and summer. *Journal of Dairy Science*, 92:6202–6209, 2009.

J.E. Salem, G.M. Saidel, W.C. Stanley, and M.E. Cabrera. Mechanistic model of myocardial energy metabolism under normal and ischemic conditions. *Annals of Biomedical Engineering*, 30:202–216, 2002.

A. Salonen, J. Nikkilä, J. Jalanka-Tuovinen, O. Immonen, M. Rajilić-Stojanović, R.A. Kekkonen, A. Palva, and W.M. de Vos. Comparative analysis of fecal DNA extraction methods with phylogenetic microarray: effective recovery of bacterial and archaeal DNA using mechanical cell lysis. *Journal of Microbiological Methods*, 81:127–134, 2010.

F.D. Sauer, V. Fellner, R. Kinsman, J.K. Kramer, H.A. Jackson, A.J. Lee, and S. Chen. Methane output and lactation response in Holstein cattle with monensin or unsaturated fat added to the diet. *Journal of Animal Science*, 76:906–914, 1998.

B. Schink. Energetics of syntrophic cooperation in methanogenic degradation. *Microbiology and Molecular Biology Reviews*, 61:262–280, 1997.

K. Schlegel, V. Leone, J.D. Faraldo-Gómez, and V. Müller. Promiscuous archaeal ATP synthase concurrently coupled to Na^+ and H^+ translocation. *Proceedings of the National Academy of Sciences*, 109:947–952, 2012.

G.J. Schut and M.W.W. Adams. The iron-hydrogenase of *Thermotoga maritima* utilizes ferredoxin and NADH synergistically: a new perspective on anaerobic hydrogen production. *Journal of Bacteriology*, 191:4451–4457, 2009.

E.C. Shin, B.R. Choi, W.J. Lim, S.Y. Hong, C.L. An, K.M. Cho, Y.K. Kim, J.M. An, J.M. Kang, S.S. Lee, H. Kim, and H.D. Yun. Phylogenetic analysis of archaea in three fractions of cow rumen based on the 16S rDNA sequence. *Anaerobe*, 10: 313–319, 2004.

K.J. Shingfield, S. Ahvenjarvi, V. Toivonen, A. Vanhatalo, P. Huhtanen, and J.M. Griinari. Effect of incremental levels of sunflower-seed oil in the diet on ruminal lipid metabolism in lactating cows. *British Journal of Nutrition*, 99:971–983, 2008.

K.J. Shingfield, L. Bernard, C. Leroux, and Y. Chilliard. Role of trans fatty acids in the nutritional regulation of mammary lipogenesis in ruminants. *Animal*, 4: 1140–1166, 2010.

P. Šmilauer and J. Lepš. *Multivariate analysis of ecological data using CANOCO 5*. Cambridge University Press, 2014.

W.J. Smolenski and J.A. Robinson. *In situ* rumen hydrogen concentrations in steers fed eight times daily, measured using a mercury reduction detector. *FEMS Microbiology Ecology*, 4:95–100, 1988.

K. Soetaert and T. Petzoldt. Inverse modelling, sensitivity and Monte Carlo analysis in R using package FME. *Journal of Statistical Software*, 33:1–28, 2010.

N. Song, M.T. Zhang, R.A. Binstead, Z. Fang, and T.J. Meyer. Multiple pathways in the oxidation of a NADH analogue. *Inorganic chemistry*, 53:4100–4105, 2014.

H. Soyeurt, F. Dehareng, P. Mayeres, C. Bertozzi, and N. Gengler. Variation of δ9-desaturase activity in dairy cattle. *Journal of Dairy Science*, 91:3211–3224, 2008.

H. Soyeurt, F. Dehareng, N. Gengler, S. McParland, E.P.B.D. Wall, D.P. Berry, M. Coffey, and P. Dardenne. Mid-infrared prediction of bovine milk fatty acids across multiple breeds, production systems, and countries. *Journal of Dairy Science*, 94:1657–1667, 2011.

J.W. Spek, J. Dijkstra, G. Van Duinkerken, and A. Bannink. A review of factors influencing milk urea concentration and its relationship with urinary urea excretion in lactating dairy cattle. *Journal of Agricultural Science*, 151:407–423, 2013.

N.R. St-Pierre. Invited review: Integrating quantitative findings from multiple studies using mixed model methodology. *Journal of Dairy Science*, 84:741–755, 2001.

S.M. Staerfl, S.L. Amelchanka, T. Kälber, C.R. Soliva, M. Kreuzer, and J.O. Zeitz. Effect of feeding dried high-sugar ryegrass ('abermagic') on methane and urinary nitrogen emissions of primiparous cows. *Livestock Science*, 150:293–301, 2012.

A.J.M. Stams and C.M. Plugge. Electron transfer in syntrophic communities of anaerobic bacteria and archaea. *Nature Reviews Microbiology*, 7:568–577, 2009.

A.J.M. Stams, D.R. Kremer, K. Nicolay, G.H. Weenk, and T.A. Hansen. Pathway of propionate formation in desulfobulbus propionicus. *Archives of Microbiology*, 139: 167–173, 1984.

A. Sterk, B.. Vlaeminck, A.M. van Vuuren, W.H. Hendriks, and J. Dijkstra. Effects of feeding different linseed sources on omasal fatty acid flows and fatty acid profiles of plasma and milk fat in lactating dairy cows. *Journal of Dairy Science*, 95: 3149–3165, 2012.

C.S. Stewart, H.J. Flint, and M.P. Bryant. The rumen bacteria. In P.N. Hobson and C.S. Stewart, editors, *The Rumen Microbial Ecosystem, 2nd edition*, pages 10–72. Springer Netherlands, 1997.

W.M. Stoop, H. Bovenhuis, J.M.L. Heck, and J.A.M. Van Arendonk. Effect of lactation stage and energy status on milk fat composition of Holstein-Friesian cows. *Journal of Dairy Science*, 92:1469–1478, 2009.

I.M.L.D. Storm, A.L.F. Hellwing, N.I. Nielsen, and J. Madsen. Methods for measuring and estimating methane emission from ruminants. *Animals*, 2:160–183, 2012.

J.D. Sutton, M.S. Dhanoa, S.V. Morant, J. France, D.J. Napper, and E. Schuller. Rates of production of acetate, propionate, and butyrate in the rumen of lactating dairy cows given normal and low-roughage diets. *Journal of Dairy Science*, 86: 3620–3633, 2003.

M.T. Suzuki, L.T. Taylor, and E.F. DeLong. Quantitative analysis of small-subunit rRNA genes in mixed microbial populations via 5'-nuclease assays. *Applied and Environmental Microbiology*, 66:4605–4614, 2000.

R. Takahashi and K. Nakamura. Concentrations of free sugars in sheep rumen fluids. *Agricultural and Biological Chemistry*, 33:619–621, 1969.

S. Tamminga and A.M. Van Vuuren. Formation and utilization of end products of lignocellulose degradation in ruminants. *Animal Feed Science and Technology*, 21: 141–159, 1988.

R.J. Tempelman. Experimental design and statistical methods for classical and bioequivalence hypothesis testing with an application to dairy nutrition studies. *Journal of Animal Science*, 82:E162–E172, 2004.

R.K. Thauer, A.K. Kaster, H. Seedorf, W. Buckel, and R. Hedderich. Methanogenic archaea: ecologically relevant differences in energy conservation. *Nature Reviews Microbiology*, 6:579–591, 2008.

L. Tian, J. Scholte, K. Borewicz, B. Bogert, H. Smidt, A.J.W. Scheurink, H. Gruppen, and H.A. Schols. Effects of pectin supplementation on the fermentation patterns of different structural carbohydrates in rats. *Molecular Nutrition & Food Research*, 60:2256–2266, 2016.

S.M. Troy, C.A. Duthie, J.J. Hyslop, R. Roehe, D.W. Ross, R.J. Wallace, A. Waterhouse, and J.A. Rooke. Effectiveness of nitrate addition and increased oil content as methane mitigation strategies for beef cattle fed two contrasting basal diets. *Journal of Animal Science*, 93:1815–1823, 2015.

E.M. Ungerfeld. A theoretical comparison between two ruminal electron sinks. *Frontiers in Microbiology*, 4:1–15, 2013.

E.M. Ungerfeld and R.A. Kohn. The role of thermodynamics in the control of ruminal fermentation. In T. Hvelplund K. Sejrsen and M.O. Nielsen, editors, *Ruminant Physiology: Digestion, Metabolism and Impact of Nutrition on Gene Expression, Immunology and Stress*, pages 55–85. Wageningen Academic Publishers, Wageningen, the Netherlands, 2006.

S. Van Gastelen and J. Dijkstra. Prediction of methane emission from lactating dairy cows using milk fatty acids and mid-infrared spectroscopy. *Journal of the Science of Food and Agriculture*, 96:3963–3968, 2016.

S. Van Gastelen, E.C. Antunes-Fernandes, K.A. Hettinga, G. Klop, S.J.J. Alferink, W.H. Hendriks, and J. Dijkstra. Enteric methane production, rumen volatile fatty acid concentrations, and milk fatty acid composition in lactating Holstein-Friesian cows fed grass silage- or corn silage-based diets. *Journal of Dairy Science*, 98: 1915–1927, 2015.

S.W. Van Ginkel and B. Logan. Increased biological hydrogen production with reduced organic loading. *Water Research*, 39:3819–3826, 2005.

A.T.M. Van Knegsel, H. Van den Brand, J. Dijkstra, W.M. Van Straalen, M.J.W. Heetkamp, S. Tamminga, and B. Kemp. Dietary energy source in dairy cows in early lactation: energy partitioning and milk composition. *Journal of Dairy Science*, 90:1467–1476, 2007.

H.J. Van Lingen, C.M. Plugge, J.G. Fadel, E. Kebreab, A. Bannink, and J. Dijkstra. Thermodynamic driving force of hydrogen on rumen microbial metabolism: A theoretical investigation. *PLoS ONE*, 11:e0161362, 2016.

S.M. Van Zijderveld, W.J.J. Gerrits, J.A. Apajalahti, J.R. Newbold, J. Dijkstra, R.A. Leng, and H.B. Perdok. Nitrate and sulfate: Effective alternative hydrogen sinks for mitigation of ruminal methane production in sheep. *Journal of Dairy Science*, 93:5856–5866, 2010.

S.M. Van Zijderveld, J. Dijkstra, H.B. Perdok, J.R. Newbold, and W.J.J. Gerrits. Dietary inclusion of diallyl disulfide, yucca powder, calcium fumarate, an extruded linseed product, or medium-chain fatty acids does not affect methane production in lactating dairy cows. *Journal of Dairy Science*, 94:3094–3104, 2011a.

S.M. Van Zijderveld, B. Fonken, J. Dijkstra, W.J.J. Gerrits, H.B. Perdok, W. Fokkink, and J.R. Newbold. Effects of a combination of feed additives on methane

production, diet digestibility, and animal performance in lactating dairy cows. *Journal of Dairy Science*, 94:1445–1454, 2011b.

S.M. Van Zijderveld, W.J.J. Gerrits, J. Dijkstra, J.R. Newbold, R.B.A. Hulshof, and H.B. Perdok. Persistency of methane mitigation by dietary nitrate supplementation in dairy cows. *Journal of Dairy Science*, 94:4028–4038, 2011c.

V.A. Vavilin, L.Y. Lokshina, X. Flotats, and I. Angelidaki. Anaerobic digestion of solid material: Multidimensional modeling of continuous-flow reactor with non-uniform influent concentration distributions. *Biotechnology and Bioengineering*, 97:354–366, 2007.

J.B. Veneman, St. Muetzel, K.J. Hart, C.L. Faulkner, J.M. Moorby, H.B. Perdok, and C.J. Newbold. Does dietary mitigation of enteric methane production affect rumen function and animal productivity in dairy cows? *PLoS ONE*, 10:e0140282, 2015.

W. Viechtbauer. Conducting meta-analyses in R with the metafor package. *Journal of Statistical Software*, 36:1–48, 2010.

B. Vlaeminck, V. Fievez, S. Tamminga, R.J. Dewhurst, A. Van Vuuren, D. De Brabander, and D. Demeyer. Milk odd-and branched-chain fatty acids in relation to the rumen fermentation pattern. *Journal of Dairy Science*, 89:3954–3964, 2006a.

V. Vlaeminck, B. Fievez, A.R.J. Cabrita, A.J.M. Fonseca, and R.J. Dewhurst. Factors affecting odd-and branched-chain fatty acids in milk: a review. *Animal Feed Science and Technology*, 131:389–417, 2006b.

R.J. Wallace, L.C. Chaudhary, E. Miyagawa, N. McKain, and N.D. Walker. Metabolic properties of *Eubacterium pyruvativorans*, a ruminal 'hyper-ammonia-producing' anaerobe with metabolic properties analogous to those of *Clostridium kluyveri*. *Microbiology*, 150:2921–2930, 2004.

R.J. Wallace, N. McKain, K.J. Shingfield, and E. Devillard. Isomers of conjugated linoleic acids are synthesized via different mechanisms in ruminal digesta and bacteria. *Journal of Lipid Research*, 48:2247–2254, 2007.

R.J. Wallace, Jo.A. Rooke, C.A. Duthie, J.J. Hyslop, D.W. Ross, N. McKain, S.M. de Souza, T.J. Snelling, A. Waterhouse, and R. Roehe. Archaeal abundance in post-mortem ruminal digesta may help predict methane emissions from beef cattle. *Scientific Reports*, 4:5892, 2014.

W. Walters, E.R. Hyde, D. Berg-Lyons, G. Ackermann, G. Humphrey, A. Parada, J.A. Gilbert, J.K. Jansson, J.G. Caporaso, J.A. Fuhrman, A. Apprill, and R. Knight. Improved bacterial 16S rRNA Gene (V4 and V4-5) and fungal internal transcribed spacer marker gene primers for microbial community surveys. *mSystems*, 1: e00009–15, 2015.

M. Wang, R. Wang, P.H. Janssen, X.M. Zhang, X.Z. Sun, D. Pacheco, and Z.L. Tan. Sampling procedure for the measurement of dissolved hydrogen and volatile fatty acids in the rumen of dairy cows. *Journal of Animal Science*, 94:1159–1169, 2016a.

M. Wang, R. Wang, T.Y. Xie, P.H. Janssen, X.Z. Sun, K.A. Beauchemin, Z.L. Tan, and M. Gao. Shifts in rumen fermentation and microbiota are associated with dissolved ruminal hydrogen concentrations in lactating dairy cows fed different types of carbohydrates. *Journal of Nutrition*, 146:1714–1721, 2016b.

D. Warner, S.C. Podesta, B. Hatew, G. Klop, H. Van Laar, A. Bannink, and J. Dijkstra. Effect of nitrogen fertilization rate and regrowth interval of grass herbage on methane emission of zero-grazing lactating dairy cows. *Journal of Dairy Science*, 98:3383–3393, 2015.

M.R. Weisbjerg, T. Hvelplund, and B.M. Bibby. Hydrolysis and fermentation rate of glucose, sucrose and lactose in the rumen. *Acta Agriculturae Scandinavica A - Animal Sciences*, 48:12–18, 1998.

K. Willquist, S.S. Pawar, and E.W.J. Van Niel. Reassessment of hydrogen tolerance in *Caldicellulosiruptor saccharolyticus*. *Microbial Cell Factories*, 10:111, 2011.

M.J. Wolin. The rumen fermentation: a model for microbial interactions in anaerobic ecosystems. *Advances in Microbial Ecology*, 3:49–77, 1979.

M.J. Wolin, T.L. Miller, and C.S. Stewart. Microbe-microbe interactions. In P.N. Hobson and C.S. Stewart, editors, *The Rumen Microbial Ecosystem*, pages 467–491. Springer Netherlands, 1997.

S.L. Yang, D.P. Bu, J.Q. Wang, Z.Y. Hu, D. Li, H.Y. Wei, L.Y. Zhou, and J.J. Loor. Soybean oil and linseed oil supplementation affect profiles of ruminal microorganisms in dairy cows. *Animal*, 3:1562–1569, 2009.

L. Yu, P.C. Wensel, J. Ma, and S. Chen. Mathematical modeling in anaerobic digestion (AD). *Journal of Bioremediation & Biodegradation*, S4:003, 2013.

Y. Yu, Ch. Lee, J. Kim, and S. Hwang. Group-specific primer and probe sets to detect methanogenic communities using quantitative real-time polymerase chain reaction. *Biotechnology and Bioengineering*, 89:670–679, 2005.

F. Zhang, Y. Zhang, M. Chen, M.C.M. van Loosdrecht, and R.J. Zeng. A modified metabolic model for mixed culture fermentation with energy conserving electron bifurcation reaction and metabolite transport energy. *Biotechnology and Bioengineering*, 110:1884–1894, 2013.

Y. Zheng, J. Kahnt, I.H. Kwon, R.I. Mackie, and R.K. Thauer. Hydrogen formation and its regulation in *Ruminococcus albus*: involvement of an electron-bifurcating [FeFe]-hydrogenase, of a non-electron-bifurcating [FeFe]-hydrogenase, and of a putative hydrogen-sensing [FeFe]-hydrogenase. *Journal of Bacteriology*, 196: 3840–3852, 2014.

E.G. Zoetendal, C.C.G.M. Booijink, E.S. Klaassens, H.G.H.J. Heilig, M. Kleerebezem, H. Smidt, and W.M. De Vos. Isolation of RNA from bacterial samples of the human gastrointestinal tract. *Nature Protocols*, 1:954–959, 2006.

S.S. Zumdahl. *Chemical Principles, 5th edition.* Houghton Mifflin Company, 2005.

Summary

Methane (CH_4) is a greenhouse gas (GHG) with a global warming potential of 28 CO_2 equivalents. The livestock sector was estimated to emit 7.1 gigatonnes of CO_2 equivalents, which is approximately 14.5% of total global anthropogenic GHG emissions. Enteric CH_4 production is the main source of GHG emissions from dairy cattle, representing 46% of the global GHG emissions in dairy supply chains. Dairy production has great value in view of the ability of ruminants to effectively turn human inedible biomass into human edible food and to produce food from non-arable land. Consequently, there is an urgent need to develop strategies to decrease dairy cattle enteric CH_4 emission. Evaluation of these strategies requires meticulous quantification and increased understanding of anaerobic fermentation and methanogenesis in the rumen ecosystem. The overall aim of this PhD research was, therefore, to quantitatively evaluate enteric CH_4 emission from dairy cows as affected by feeding and rumen microbial metabolism.

In Chapter 2, a meta-analysis was performed to quantify relationships between enteric CH_4 yield (per unit of feed and unit of milk) and milk FA profile in dairy cattle and to develop equations to predict CH_4 yield based on milk FA profile of cows fed a wide variety of diets. Data from eight experiments encompassing 30 different dietary treatments and 146 observations were included. Milk FA concentrations of C6:0, C8:0, C10:0, C16:0 and C16:0-*iso* were significantly or tended to be positively related to CH_4 yield per unit of feed. Concentrations of *trans*-6+7+8+9-C18:1, *trans*-10+11-C18:1, *cis*-11-C18:1, *cis*-12-C18:1, *cis*-13-C18:1, *trans*-16+*cis*-14-C18:1 and *cis*-9,12-C18:2 in milk fat were significantly or tended to be negatively related to CH_4 yield per unit feed. Milk FA concentrations of C10:0, C12:0, C14:0-*iso*, C14:0, *cis*-9-C14:1, C15:0 and C16:0 were significantly or tended to be positively related to CH_4 yield per unit of milk. Concentrations of C4:0, C18:0, *trans*-10+11-C18:1, *cis*-9-C18:1, *cis*-11-C18:1, and *cis*-9,12-C18:2 in milk fat were significantly or tended to be negatively related to CH_4 yield per unit of milk. Mixed model multiple regression was applied to predict CH_4 yield with milk FA as input (g/100 g FA) resulted in: CH_4 (g/kg DMI) =

23.39 + 9.74 × C16:0-*iso* – 1.06 × *trans*-10+11-C18:1 – 1.75 × *cis*-9,12-C18:2 (R^2 = 0.54), and CH_4 (g/kg FPCM) = 21.13 – 1.38 × C4:0 + 8.53 × C16:0-*iso* – 0.22 × *cis*-9-C18:1 – 0.59 × *trans*-10+11-C18:1 (R^2 = 0.47). This indicated milk FA profile to have a moderate potential for predicting CH_4 yield per unit of feed and a slightly lower potential for predicting CH_4 yield per unit of milk.

In Chapter 3, the thermodynamic control of p_{H_2} on reaction rates of specific fermentation pathways, NADH oxidation and methanogenesis in rumen microbes was quantitatively explored. This control was determined using the thermodynamic potential factor (F_T), which is a dimensionless factor that corrects a predicted kinetic reaction rate for the thermodynamic control exerted. Unity F_T was calculated for all glucose fermentation pathways considered, indicating no inhibition of p_{H_2} on the production of a specific type of VFA (e.g., acetate, propionate and butyrate) in the rumen. For NADH oxidation without ferredoxin oxidation, increasing p_{H_2} within the rumen physiological range decreased F_T from unity to zero for different NAD^+ to NADH ratios and pH of 6.2 and 7.0, which indicates thermodynamic control of p_{H_2}. For NADH oxidation with ferredoxin oxidation, increasing p_{H_2} within the rumen physiological range decreased F_T from unity at pH of 7.0 only. For methanogenesis by archaea without cytochromes, F_T differed from unity only below the rumen range of p_{H_2}, indicating no thermodynamic control. The thermodynamic feasibility of these microbial conversions shows that the control of p_{H_2} on individual VFA produced and associated yield of H_2 and CH_4 cannot be explained without considering NADH oxidation.

In Chapter 4, diurnal patterns of gaseous and dissolved metabolite concentrations in the bovine rumen, H_2 and CH_4 emitted, and the rumen microbiota were monitored. In addition, the effect of dietary inclusion of linseed oil on these patterns was assessed. An *in vivo* experiment with rumen cannulated dairy cows was performed to study the anaerobic metabolism and the microbiota composition in the rumen. A 100-fold increase in p_{H_2} in the rumen headspace was observed at 0.5 h after feeding, followed by a decline. Qualitatively similar patterns after feeding were observed for H_2 and CH_4 emission, ethanol and lactate concentrations, and propionate molar proportion, whereas an opposite pattern was seen for acetate molar proportion. Associated with these patterns, a temporal biphasic change in the microbial composition was observed as based on 16S ribosomal RNA with certain taxa specifically associated with each phase. Bacterial concentrations were affected by time and increased by linseed oil supplementation. Archaeal concentrations tended to be affected by time and were not affected by diet, despite linseed oil supplementation tending to decrease the partial pressure and emission of CH_4 and tending to increase propionate molar proportion. The various diurnal profiles that were monitored support the key role of the redox

state of NAD in rumen fermentation and the importance of diurnal dynamics when understanding VFA, H_2 and CH_4 production.

In Chapter 5, a dynamic mechanistic model was developed that represents the thermodynamic control of p_{H_2} on VFA fermentation pathways, and methanogenesis in the bovine rumen. The model represents substrate degradation, microbial fermentation and methanogenesis in the rumen, with the type of VFA formed is controlled by the NAD^+ to NADH ratio, which in turn is controlled by p_{H_2}. Feed composition and feed intake rate (twice daily feeding regime) were used as model input. Model parameters were estimated to experimental data using a Bayesian calibration procedure, after which the uncertainty of the parameter distribution on the model output was assessed. The model predicted a marked peak in p_{H_2} after feeding that rapidly declined in time. This peak in p_{H_2} caused a decrease in NAD^+ to NADH ratio followed by an increased propionate molar proportion at the expense of acetate molar proportion. In response to feeding, the model predicted an increase in CH_4 production that steadily decreased in time. The pattern of CH_4 emission rate followed the patterns of p_{H_2} and H_2 emission rate, but its magnitude of increase in response to feeding was less pronounced. A global sensitivity analysis was performed to determine the impact of parameters on daily CH_4 production. The parameter that determines the NADH oxidation rate explained 41% of the variation of predicted daily CH_4 emission. Model evaluation indicated under-prediction of experimental total CH_4 emission with a root mean square prediction error of 15%. The modeling effort provides the integration of more detailed knowledge than in previous rumen fermentation models and enables assessment of diurnal dynamics of rumen metabolic pathways yielding VFA, H_2 and CH_4.

In Chapter 6, the coherence of the previous chapters and the overall value of this thesis is examined. The potential for predicting enteric CH_4 emission from dairy cattle based on milk FA profile was discussed in the light of several recently published studies and compared with empirical modeling of enteric CH_4 based on feed input. Moreover, the concept of NAD-controlled fermentation was considered in a more general perspective. For example, the rumen ecosystem system was compared with bioreactors. Furthermore, the feasibility of the developed models as alternative IPCC tiered approaches was explored. In conclusion, the research reported in this thesis has contributed to increased understanding of rumen fermentation and microbial metabolism, and has provided a basis to further improve prediction models of enteric CH_4 emissions from dairy cattle.

Samenvatting

Methaan (CH_4) is een broeikasgas met een opwarmingspotentieel die 28 keer zo groot is als die van CO_2. De schatting is dat de broeikasgasuitstoot van de veehouderijsector ongeveer 7.1 gigaton CO_2 equivalenten bedraagt. Deze hoeveelheid komt overeen met ongeveer 14.5% van de totale antropogene broeikasgasuitstoot op aarde. Enterische CH_4-productie is de belangrijkste bron van broeikasgassen van melkvee, goed voor 46% van de mondiale broeikasgasuitstoot van de zuivelketen. Zuivelproductie is waardevol vanwege de mogelijkheid van herkauwers om biomassa die niet bruikbaar is voor mensen om te zetten in humaan consumeerbaar voedsel. Tevens kunnen herkauwers voedsel produceren op land dat niet bebouwbaar is voor gewastelers. Gezien deze potentie van herkauwers is het van urgent belang om strategieën te ontwikkelen die leiden tot een afname van de enterische methaanuitstoot door melkvee. Het evalueren van deze strategieën vereist een nauwkeurige kwantificatie en een goed begrip van anaerobe fermentatie en methanogenese van het ecosysteem in de pens. Het overkoepelende doel van dit promotieonderzoek is daarom het kwantitatief evalueren van enterische methaanuitstoot van melkvee beïnvloed door het voeraanbod en het microbieel metabolisme in de pens.

In hoofdstuk 2 is een meta-analyse uitgevoerd voor de kwantificatie van de relatie tussen de enterische methaanopbrengst (per eenheid voer en melk) en het melkvetzuurprofiel in melkvee, en voor de ontwikkeling van voorspellingsvergelijkingen van de methaanopbrengst gebaseerd op melkvetzuurconcentraties. Hiervoor werd een dataset gebruikt die was gebaseerd op een grote variëteit aan rantsoenen. Deze dataset omvatte 8 experimenten, 30 rantsoenbehandelingen en 146 observaties. De concentraties van de vetzuren C6:0, C8:0, C10:0, C16:0 en C16:0-*iso* in melkvet hadden een significant positieve relatie of tendeerden een positieve relatie te hebben met methaanuitstoot per eenheid voer. De concentraties van *trans*-6+7+8+9-C18:1, *trans*-10+11-C18:1, *cis*-11-C18:1, *cis*-12-C18:1, *cis*-13-C18:1, *trans*-16+*cis*-14-C18:1 en *cis*-9,12-C18:2 in melkvet hadden een significant negatieve relatie of tendeerden een negatieve relatie te hebben met CH_4-opbrengst per eenheid voer. De

melkvetzuurconcentraties van C10:0, C12:0, C14:0-*iso*, C14:0, *cis*-9-C14:1, C15:0 en C16:0 waren significant positief gerelateerd of tendeerden positief gerelateerd te zijn aan CH_4-opbrengst per eenheid melk. De concentraties van C4:0, C18:0, *trans*-10+11-C18:1, *cis*-9-C18:1, *cis*-11-C18:1, en *cis*-9,12-C18:2 in melkvet waren significant negatief gerelateerd of tendeerden negatief gecorreleerd te zijn met de CH_4-opbrengst per eenheid melk. Mengmodel meervoudige regressie werd toegepast voor het voorspellen van CH_4-opbrengst met melkvetzuurconcentraties (g/100 g vet) als invoer en resulteerde in: CH_4 (g/kg DS) = 23.39 + 9.74 × C16:0-*iso* – 1.06 × *trans*-10+11-C18:1 – 1.75 × *cis*-9,12-C18:2 (R^2 = 0.54), en CH_4 (g/kg VECM) = 21.13 – 1.38 × C4:0 + 8.53 × C16:0-*iso* – 0.22 × *cis*-9-C18:1 – 0.59 × *trans*-10+11-C18:1 (R^2 = 0.47). Dit impliceert een matige potentie voor het voorspellen van CH_4-opbrengst per eenheid voer, en een iets lagere potentie voor het voorspellen van de CH_4-opbrengst per eenheid melk.

In Hoofdstuk 3 is de thermodynamische controle van de partiële gasdruk van H_2 (p_{H_2}) op reactiesnelheden van specifieke fermentatiepaden, NADH-oxidatie en methanogenese in pensmicroben kwantitatief onderzocht Deze controle werd in kaart gebracht met behulp van de thermodynamische potentie factor (F_T), een dimensieloze grootheid die een voorspelde kinetische reactiesnelheid corrigeert voor de uitgeoefende thermodynamische controle. De F_T benaderde de waarde van één voor alle geëvalueerde fermentatiepaden van glucose, en suggereert dat er geen sprake is van inhibitie van p_{H_2} op the productie van specifieke vluchtige vetzuren (afgekort VVZ; voorbeelden zijn azijnzuur, propionzuur en boterzuur) in de pens. Voor NADH-oxidatie zonder ferredoxine-oxidatie resulteerden hogere p_{H_2}-waarden binnen het fysiologische bereik in de pens in een afname van F_T van één naar nul voor verschillende NAD^+/NADH-verhoudingen en voor pH-waarden van 6,2 en 7,0; dit duidt op thermodynamische controle van p_{H_2}. Voor NADH-oxidatie gekoppeld aan ferredoxine-oxidatie resulteerden hogere p_{H_2}-waarden binnen het fysiologische bereik in de pens alleen in F_T-waarden kleiner dan één voor pH-waarde gelijk aan 7,0. Voor methanogenese door archaea zonder cytochromen nam F_T alleen waarden kleiner dan één aan voor p_{H_2} buiten het fysiologische bereik, hetgeen suggereert dat er geen thermodynamische controle plaatsvindt. De thermodynamische potentie van deze microbiële conversies laat zien dat de controle van p_{H_2} op de productie van individuele VVZ en de daarmee geassocieerde opbrengst van H_2 en CH_4 niet kan worden uitgelegd zonder het meewegen van NADH-oxidatie.

In Hoofdstuk 4 zijn de dagpatronen van de concentraties van gasvormige en wateroplosbare metabolieten in de runderpens, en van de hoeveelheden geëmitteerde H_2 en CH_4 en de pensmicrobiota in kaart gebracht. Tevens werd het effect van de rantsoensupplementatie met lijnzaadolie op deze patronen onderzocht. Een *in*

vivo experiment met pensfistelkoeien werd uitgevoerd om het anaerobe metabolisme en de samenstelling van de pensmicrobiota te bestuderen. Een verhonderdvoudigde p_{H_2} in de gaslaag van de pens werd een half uur na het voeren geobserveerd. Na deze scherpe toename volgde een afname. Ten opzichte van het voertijdstip werden vergelijkbare patronen waargenomen voor H_2- en CH_4-emissie, de concentraties van ethanol en melkzuur, en de molaire proportie van propionzuur, terwijl een tegengesteld patroon werd waargenomen voor de molaire proportie van azijnzuur. Gerelateerd aan deze patronen werd een tweefasige verandering in de microbiële samenstelling waargenomen op basis van 16S ribosomaal RNA, waarbij bepaalde taxa gecorreleerd waren aan een specifieke fase. Bacterieconcentraties werden niet beïnvloed door tijd en namen toe door lijnzaadoliesupplementatie. Archaeaconcentraties tendeerden beïnvloed te zijn door tijd, maar werden niet beïnvloed door het rantsoen, ondanks het feit dat lijnzaadoliesupplementatie de partiële gasdruk en emissie van CH_4 tendeerde te verlagen, en een tendens voor een toename in de molaire proportie van propionzuur. De dagprofielen die in kaart zijn gebracht sluiten aan bij de centrale rol van de redoxtoestand van NAD in pensfermentatie en het belang van binnendagdynamiek voor het begrijpen van variatie in de productie van VVZ, H_2 en CH_4.

In hoofdstuk 5 wordt een dynamisch mechanistisch model beschreven met een weergave van de thermodynamische controle van p_{H_2} op VVZ-fermentatiepaden en methanogenese in the runderpens is beschreven. In dit model worden substraatafbraak, microbiële fementatie en methanogenese in de pens mathematische beschreven, waarbij het type VVZ-productie wordt gecontroleerd door de NAD^+/NADH verhouding, die vervolgens wordt gecontroleerd door p_{H_2}. De voersamenstelling en de -opnamesnelheid (gebruikmakend van een regime van het experiment beschreven in hoofdstuk 4 waarin twee keer per dag werd gevoerd) werd gebruikt als modelinvoer. Modelparameters werden geschat op experimentele data door middel van een Bayesiaanse kalibratieprocedure, waarna de onzekerheid van modeluitvoer op basis van de parameterdistributie in kaart werd gebracht. Het model simuleerde een duidelijke piek in p_{H_2} na het voeren, gevolgd door een snelle afname in de tijd. De piek in p_{H_2} veroorzaakte een afname in de NAD^+/NADH-verhouding, gevolgd door een toename in de molaire proportie van propionzuur ten koste van de molaire proportie azijnzuur. Als reactie op de voeropname voorspelde het model een toename in CH_4-productie die gestaag afnam in de tijd. Het patroon van de CH_4-emissiesnelheid volgde het patroon van de p_{H_2} en de H_2-emissiesnelheid, hoewel de omvang van de toename van de CH_4-emissiesnelheid als reactie op de voeropname veel kleiner was. Een globale gevoeligheidsanalyse werd uitgevoerd om de invloed van de verschillende parameters op de dagsom van de CH_4-productie te determineren. De parameter die de NADH-oxidatiesnelheid bepaalt, verklaarde

41% van de variatie van de berekende dagelijkse CH_4-emissie. Een modelevaluatie liet zien dat de CH_4-emissie 15% werd onderschat op basis van de wortel van de gekwadrateerde voorspellingsfout. Deze modelleerexercitie verstrekt de integratie van een meer gedetailleerde mechanistische aanpak dan eerder pensfermentatiemodellen. Tevens biedt dit de mogelijkheid tot simuleren van binnendagdynamiek van metabole paden in de pens die resulteren in VVZ, H_2 en CH_4.

In Hoofdstuk 6 werden de coherentie van de eerdere hoofdstukken en de algehele waarde van dit proefschrift bediscussieerd. De potentie voor het voorspellen van enterische methaanuitstoot door melkvee gebaseerd op het melkvetzuurprofiel werd bediscussieerd in het licht van verschillende recent gepubliceerde studies en vergeleken met empirische modellen van enterische methaanuitstoot met voersamenstelling als invoer. Vervolgens werd het concept van NAD-gecontroleerde fermentatie in een breder perspectief bediscussieerd. Het ecosysteem in de pens werd bijvoorbeeld vergeleken met bioreactoren. Daarna werd de potentie van de ontwikkelde modellen voor alternatieve IPCC-benaderingen nagegaan. Concluderend kan worden opgemerkt dat het onderzoek dat is beschreven in dit proefschrift heeft bijgedragen aan het begrip van pensfermentatie en het microbieel metabolisme. Dit kan als basis dienen voor het verder ontwikkelen van voorspellingsmodellen van enterische methaanuitstoot van melkvee.

Dankwoord/Acknowledgments

Het uitvoeren van promotieonderzoek is minder een solistische aangelegenheid dan promoveren en daarom zou ik graag een aantal mensen bedanken. Allereerst wil ik prof. Wouter Hendriks bedanken voor zijn bereidheid om op te treden als promotor. Wouter, hoewel je geen nadrukkelijke rol had als begeleider heb ik je bijdrage-vanuit-de-wandelgangen zeker kunnen waarderen. Als tweede wil ik dr. Jan Dijkstra hartelijk danken voor zijn inbreng en bijdrage als hoofdbegeleider. Jan, het was indrukwekkend hoe nauwgezet jij alle conceptteksten doornam! Vervolgens wil ik dr. (André) Bannink bedanken. André, hartelijk dank voor je toegankelijk manier van werken en je amicale instelling. Het was vanuit mentaal oogpunt vaak heel verfrissend om 's avonds na zes uur nog even bij je binnen te lopen. Dr. Caroline Plugge wil ik bedanken als vierde begeleider. Caroline, naarmate mijn onderzoek vorderde werd het contact intensiever en dat heeft geresulteerd in twee mooie publicaties. Dank je wel voor je interesse in mijn ideeën en je bereidheid om als microbioloog een bijdrage te leveren.

Omdat dit onderzoek is uitgevoerd binnen het TI Food and Nutrition project "Reduced methane emission of dairy cows" wil ik, naast Jan en Caroline, alle mensen die daarbinnen participeerden ook bedanken. Sanne, wat fijn dat je ook bij diervoeding zat! Joan, it's been a real pleasure to work with you! Jueeli, thank you for performing many GC and HPLC analyses together! Vervolgens dank ik Henk Bovenhuis die Johan van Arendonk opvolgde als projectleider, Marleen Visker die als assistent-projectleider fungeerde, Sabine van Engelen, Kasper Hettinga, Elsa Antunes Fernandes, Tom van den Bogert, Bastian Hornung en Hauke Smidt. Edoardo, you are not part of the TI Food and Nutrition group but you certainly had your contribution; thanks for performing the PERMANOVA. En in dit rijtje kan ik er ook niet omheen Ton van Gelder hartelijk te bedanken voor zijn hulp bij de laboratoriumanalyses bij microbiologie.

I thank prof. Ermias Kebreab for hosting my 4-month stay at the University of California, Davis in 2014. Ermias, the period I spent in your modeling lab has

been very valuable for the qualitative progress of my PhD research. I acknowledge prof. James G. Fadel for proactively challenging me to discover new and unknown areas. Apart from the scientific ideas that were born, this made me understand what the difference is between MSc and PhD level. Many other people that I met at UC Davis, such as Luis, Kristan, Ranga, Pedro, Mutian, Holland, Katie, Mitch, Tekeste, Diogo, Lydia and Kara, thank you very much for contributing to such a wonderful period! Two other international collaborators from the University of Reading, prof. Chris Reynolds and Dr. Les Crompton, are also greatly acknowledged for providing data and their contribution to Chapter 2 of this thesis.

Ook binnen diervoeding zijn er de nodige mensen om te bedanken. Sanne en Kasper, dank dat jullie paranimfen willen zijn! Sanne, dank je wel voor het becommentariëren van de algemene discussie van dit proefschrift. Kasper, dank voor je aanbod de layout van de leesversie van commentaar te voorzien, ik heb er graag gebruik van gemaakt! Walter, als iemand geïnteresseerd was in mijn onderzoek dan was jij het wel, waarvoor veel dank! Het is ook zeker fijn om nu met jou te werken. Betty en Yvon, het is een cliché, maar de leerstoelgroep zou wellicht niet functioneren zonder jullie. My (former) roommates Arie and Genet, thanks a lot for many enjoyable chats. Bayissa, dear friend, there have been numerous unforgettable moments. Geronda, Sabrina, Yvonne, Tetske, Sandra, Hsuan, Myrthe, Wouter S, Lotte, Harma, Myrthe, Sergio, Huyen, Daniel, Mubarak, Felicidade, Pierre, Nazri, Eli, Lei, Yuan, Kazeem, Kelly, Marijke, Bianca, Sholeha, Rik, Miranda, Chantal, Wilbert, René, John, Guido, Thomas, Martin, Sonja, Sven, Tamme, Saskia, Leon, Michel, Jane, Erika, Xuan-Huong, Francine en Milou, dank voor de goede sfeer en collegialiteit bij ANU! Van het personeel van Carus wil ik de namen van Ries, Teus en Willem niet onvermeld laten. I also thank the WIAS Science Day 2015 committee members for the nice time we spent together.

Vanuit de kennissenkring wil ik prof. em. dr. Guus J. Borger hartelijk bedanken voor zijn interesse in mijn persoon en onderzoek. Er was niemand eerder geweest die mij uitdaagde te beginnen aan een promotietraject. Veel familie en vrienden kan ik bedanken voor veel fijne momenten in het leven buiten de universiteit. Mijn ouders wil ik in het bijzonder bedanken voor het feit dat zij mij altijd hebben gestimuleerd om te studeren. Na het bedanken van veel mensen sluit ik af met een Soli Deo Gloria.

Henk

About the author

Henk van Lingen was born on September 11, 1986 in Krimpen aan den IJssel, The Netherlands. He obtained his VWO-diploma (pre-university high school education) in 2005. Thereafter, he studied Chemistry at the Vrije Universiteit in Amsterdam. His MSc thesis was entitled "Kinetics and fidelity of the replication of the hereditory information". During his MSc, he also spent a three-month period at the Computational Chemistry group of the Universidad de Guanajuato (Mexico). Furthermore, as a part of his MSc, Henk took extracurricular courses in Animal Nutrition at Wageningen University. Immediately after his MSc graduation in 2012, he started as a PhD candidate at Wageningen University and joined the cross-disciplinary "Reduced methane emission of dairy cows" project. To strengthen his modeling skills, Henk had a four-month stay at the University of California, Davis as a visiting scholar. For this stay, Henk received a WIAS PhD-scholarship. Henk is currently employed as a researcher on "Modeling post-absorptive metabolism in calves" at Wageningen University & Research and will start as a postdoctoral research fellow at the University of California, Davis in June 2017.

Publications

List of publications

- H.J. van Lingen, A. Bannink, and J. Dijkstra. Methane production and dynamics of hydrogen and volatile fatty acids in the bovine rumen: modeling cofactor controlled microbial metabolism. In preparation.
- B. Hornung, J.E. Edwards, H.J. van Lingen, V.A.P. Martins dos Santos, C.M. Plugge, P.J. Schaap, J. Dijkstra, and H. Smidt. Influence of diurnal dynamics and inclusion of dietary linseed oil on the rumen metatranscriptome. In preparation.
- H.J. van Lingen, J.E. Edwards, J.D. Vaidya, S. van Gastelen, B. van den Bogert, E. Saccenti, A. Bannink C.M. Plugge, H. Smidt, and J. Dijkstra. 2017. Diurnal patterns of headspace gas and dissolved metabolite concentrations and microbiome composition in the bovine rumen. *Frontiers in Microbiology* 8:425.
- A. Bannink, H.J. van Lingen, J.L. Ellis, J. France and J. Dijkstra. 2016. The contribution of mathematical modelling to the understanding of rumen metabolism. *Frontiers in Microbiology*, 7:1820.
- H.J. van Lingen, C.M. Plugge, J.G. Fadel, E. Kebreab, A. Bannink, and J. Dijkstra. 2016. Thermodynamic driving force of hydrogen on rumen microbial metabolism: A theoretical investigation, *PLoS ONE*, 11 (10): e0161362.
- J. Dijkstra, S. van Gastelen, E.C. Antunes-Fernandes, D. Warner, B. Hatew, G. Klop, S.C. Podesta, H.J. van Lingen, K.A. Hettinga, and A. Bannink. 2016. Relationships between milk fatty acid profiles and enteric methane production in dairy cattle fed grass- or grass silage-based diets. *Animal Production Science*, 56:541.
- H.J. van Lingen, L.A. Crompton, W.H. Hendriks, C.K. Reynolds, and J. Dijkstra. 2014. Meta-analysis of relationships between enteric methane

emissions and milk fatty acid profile in dairy cows. *Journal of Dairy Science*, 97:7115. (Web of Sciences top 0.1% cited paper in the Agricultural Sciences field)

- P. Tecmer, H.J. van Lingen, A.S.P. Gomes, and L. Visscher. 2012. The electronic spectrum of CUONg4 (Ng= Ne, Ar, Kr, Xe): New insights in the interaction of the CUO molecule with noble gas matrices. *The Journal of Chemical Physics*, 137:084308.

Abstracts in Conference proceedings

- J. Dijkstra, S. van Gastelen, E.C. Antunes Fernandes, D. Warner, B. Hatew, G. Klop, S.C. Podesta, H.J. van Lingen, K.A. Hettinga, and A. Bannink. Relationships between milk fatty acid profiles and enteric methane production in dairy cattle fed grass- or grass silage-based diets. 6th Greenhouse Gas and Animal Agriculture Conference, February 14 - 18, 2016, Melbourne, Australia. (oral)

- J.E. Edwards, H.J. van Lingen, J.D. Vaidya, S. van Gastelen, B. van den Bogert, A. Bannink, C.M. Plugge, J. Dijkstra, and H. Smidt. Diurnal dynamics of metabolites and microbes in the bovine rumen: implications for the control of fermentation pathways. 10th Joint Symposium INRA-Rowett, June 20-23, 2016, Clermont-Ferrand, France. (poster)

- H.J. van Lingen, L.A. Crompton, C.K. Reynolds, and J. Dijkstra. Meta-analysis of relationships between enteric methane output and milk fatty acid composition in dairy cows. 39th Animal Nutrition Research Forum, April 3, 2014, Utrecht, the Netherlands. (oral)

- H.J. van Lingen, L.A. Crompton, C.K. Reynolds, and J. Dijkstra. Relationships between enteric methane production and milk fatty acid profile in dairy cattle: a meta-analysis. Joint ISNH/ISRP International Conference, September 8-12, 2014, Canberra, Australia. (poster)

- H.J. van Lingen, A. Bannink, E. Kebreab, and J. Dijkstra. Methane production and hydrogen dynamics in dairy cattle: a model of rumen metabolic pathways. 8th International Workshop Modelling Nutrient Digestion and Utilization in Farm Animals, September 15 - 17, 2014, Cairns, Australia. (oral)

- H.J. van Lingen, J.D. Vaidya, S. van Gastelen, B. van den Bogert, A. Bannink, C.M. Plugge, H. Smidt, and J. Dijkstra. Daily patterns of hydrogen and volatile fatty acid concentrations in relation to thermodynamic control on fermentation

in the bovine rumen. Joint Annual Meeting of the American Dairy Science Association & American Society of Animal Science, July 12 - 16, 2015, Orlando, USA. (oral)

- H.J. van Lingen, J.D. Vaidya, J.E. Edwards, S. van Gastelen, B. van den Bogert, A. Bannink, H. Smidt, C.M. Plugge, and J. Dijkstra. Metabolic sequences of fermentation products in and from the bovine rumen. 41th Animal Nutrition Research Forum, April 15, 2016, Wageningen, the Netherlands. (oral)

Training and Supervision plan

Basic package (3 ECTS)	**Year**
WIAS Introduction Course	2013
Course on philosophy of science and/or ethics	2013
International conferences (5 ECTS)	
Greenhouse Gas and Animal Agriculture conference (including pre-conference workshop), Dublin (Ireland)	2013
International symposium on Ruminant Physiology, Canberra (Australia)	2014
International workshop Modeling Nutrient Digestion Utilization in Farm Animals, Cairns (Australia)	2014
Joint annual meeting ADSA-ASAS + mixed models workshop	2015
Seminars and workshops (2 ECTS)	
WIAS Science Day 3×	2013-2015
Animal Nutrition Research Forum 2×	2014, 2016
International Symposium on Dairy Cattle Nutrition, Wageningen	2012-2014
Presentations (5 ECTS)	
International symposium on Ruminant Physiology, Canberra (Australia); poster	2014
International workshop Modeling Nutrient Digestion Utilization in Farm Animals, Cairns (Australia); oral	2014
Animal Nutrition Research forum, Utrecht; oral	2014
Animal Nutrition Research forum, Wageningen; oral	2016
Joint annual meeting ADSA-ASAS, Orlando (USA); oral	2015

In-depth studies (11 ECTS)	
Fatty acids in dairy cattle in relation to product quality and health (Ghent University), Ghent	2012
Postgraduate Cursus Rundveevoeding (Wageningen Business School), Wageningen	2012
Meta Analysis course (PE&RC)	2012
Ecological Modeling in R (Wageningen University, MSc course)	2012
Statistical Uncertainty Analysis of Dynamic Models course (PE&RC), Wageningen	2015
Professional Skills Support Courses (5 ECTS)	
IP Workshop (TI Food and Nutrition), Wageningen	2013
Presentation skills	2014
Scientific writing	2014
How to get the right message across (TI Food and Nutrition)	2014
Writing Grant Proposals	2016
Research skills training (4 ECTS)	
Preparing own PhD research proposal (maximum 6 credits)	2012
4-month external training period at the University of California, Davis	2014
Didactic skills training (10 ECTS)	
Supervision of simulation practicals of Nutrient Dynamics MSc course	2013-2016
BSc thesis supervision	2013
Management Skills Training (2 ECTS)	
Membership of WIAS Science Day Committee	2015
Education and Training Total:	**47 ECTS**

Colophon

The studies presented in this thesis were performed within the framework of TI Food and Nutrition.

Cover design: Chris-Jan de Leeuw
Layout: Henk van Lingen
Printed by: Digiforce